APPENDIX B
REEVALUATION OF CONSTRAINTS ON GROUNDWATER FLOW USING GEOCHEMICAL AND ISOTOPIC DATA FROM NYE COUNTY EARLY WARNING DRILLING PROGRAM WELLS

B1. PURPOSE

The purpose of this appendix is to provide an analysis of flow directions and velocities, and mixing proportions of water from different source areas based on groundwater geochemical and isotopic data. The analysis of hydrochemical and isotopic data is intended to provide a basis for evaluating the hydrologic system at Yucca Mountain independently of evaluations that are based purely on hydraulic arguments. In this way, this appendix is intended as an independent corroboration of the saturated zone flow model presented in the main text of this report.

This appendix provides a focused update of *Appendix A—Geochemical and Isotopic Constraints on Groundwater Flow* in *Saturated Zone Site-Scale Model* (BSC 2004 [DIRS 170037). Since the issuance of *Saturated Zone Site-Scale Flow Model* (BSC 2004 [DIRS 170037], Appendix A), several new boreholes have been drilled, and groundwater samples from these boreholes have been analyzed for hydrochemical and isotopic constituents. In addition, new hydrochemical data have also been obtained from several of the previously existing boreholes. This update primarily involves the incorporation of new data on major ion chemistry, $^{234}U/^{238}U$ activity ratios, and ^{14}C available as of September 2006. These new hydrochemical data are evaluated to determine their impacts on inferences about groundwater flowpaths and travel times from beneath the repository established in Appendix A. In so doing, this appendix also addresses condition report (CR) 6767, which asked if any new hydrochemical and isotopic data from Nye County wells, particularly ^{14}C activities and $^{234}U/^{238}U$ activity ratios, suggested trends counter to the conclusions and interpretations of groundwater flowpaths and travel times as documented in Appendix A of this report. This appendix analyzes the latest hydrochemical and isotopic data and confirms that none of it contradicts the conclusions and analyses in Appendix A.

Addressing these and related issues will help in determining the performance of the saturated zone as a natural barrier to radionuclide migration. The physical and hydrochemical parameters summarized in Appendix A and augmented by this appendix are important controls on the transport of dissolved and colloidal species in the saturated zone. This information can be used in the SZ site-scale flow and SZ transport models to simulate the transport of radionuclides as breakthrough curves. These breakthrough curves are then used as input in the TSPA-LA calculations.

This report is governed by the Office of Civilian Radioactive Waste Management *Technical Work Plan for Saturated Zone Flow and Transport Modeling* (BSC 2006 [DIRS 177375]). Activities listed in the TWP (BSC 2006 [DIRS 177375], Sections 1.2.2 and 1.2.7) that are appropriate to this appendix are documented in this report.

B2. QUALITY ASSURANCE

Planning and preparation of this appendix was initiated under the Bechtel SAIC Company (BSC) Quality Assurance Program. Therefore, forms and associated documentation prepared prior to October 2, 2006, the date this work transitioned to the Lead Laboratory, were completed in accordance with BSC procedures. Forms and associated documentation executed on or after October 2, 2006, were prepared in accordance with Lead Laboratory procedures.

Development of this appendix is subject to the Office of Civilian Radioactive Waste Management quality assurance program as indicated in the TWP (BSC 2006 [DIRS 177375]. Approved quality assurance procedures identified in Section 4 of the TWP (BSC 2006 [DIRS 177375]) have been used to conduct and document the activities described in this appendix:

- LP-7.5Q-OCRWM, *Establishing Deliverable Acceptance Criteria and Submitting and Reviewing Deliverables*
- DM-PRO-002, *Records Management*
- IT-PRO-0011, *Software Management*
- LS-PRO-001, *Technical Reports*
- SCI-PRO-003, *Document Review*
- SCI-PRO-004, *Managing Technical Product Inputs*
- SCI-PRO-006, *Models*
- TST-PRO-001, *Submittal and Incorporation of Data to the Technical Data Management System.*

These procedures are a deviation from the TWP (BSC 2006 [DIRS 177375]) and reflect the change to corresponding Sandia National Laboratories Lead Laboratory procedures. Section 8 of the TWP (BSC 2006 [DIRS 177375]) also identifies the methods used to control the electronic management of data.

B3. USE OF SOFTWARE

YMP-qualified software (CORPSCON V.5.11.08, STN: 10547-5.11.08-00 [DIRS 155082]) was used to convert borehole survey results from Nevada State Plane coordinates to UTM coordinates in NAD-27 (see Appendix F). The converted coordinates are reported in the following DTN:

- Output DTN: LA0612RR150304.001, UTM Coordinates for Selected Nye County Early Warning Drilling Program Boreholes: NC-EWDP-7SC and Phases III and IV.

Commercial, off-the-shelf software used in support of this analysis to create data plots is exempt from the qualification requirements of IM-PRO-003, but meets the acceptance criteria of being able to correctly produce plots of acceptable graphic quality in formats suitable for incorporation into this report.

- *EXCEL 2003* was used to preprocess data from DTNs to obtain representative average values. The calculation of basic statistics was used with standard functions only.

- *Adobe Illustrator CS2* was used to visualize and illustrate data to create flowpath maps.

- *AqQA* V3.7, was used to create trilinear diagrams showing proportions of major ions in groundwater and *x-y* scatter plots.

Outputs from *EXCEL*, *Adobe Illustrator*, and *AqQA* were visually checked for correctness. The data used to produce the outputs can be found in the Technical Data Management System (TDMS) within data packages that have been assigned data tracking numbers (DTN). The DTNs are identified in appropriate places throughout this appendix to allow the independent reviewer to reproduce or verify results by visual inspection or hand calculation.

B4. INPUTS

This appendix summarizes hydrochemistry data to ultimately derive hydrochemically inferred flow pathways. The data evaluations, including the derived flow pathways, are used to corroborate information put forth in the main body of this report. As such, this appendix does not require direct inputs nor does it produce qualified technical outputs. Output developed within this appendix is considered unqualified intermediary output.

Newly available geochemical and isotopic data are presented in Tables B4-1 through B4-9. These data inputs are listed below in three general categories: (a) geographic and depth-related data for new NC-EWDP wells (Table B4-1), (b) geochemical and isotopic data for these new wells (Tables B4-2 and B4-3), and (c) geochemical and isotopic data that fill data gaps for existing well locations from Appendix A (Tables B4-4 to B4-9). The new geochemical and isotopic data that were obtained from the TDMS were acquired primarily by the U.S. Geological Survey (USGS), the NC-EWDP, and the Nevada System of Higher Education through its cooperative agreement with the U.S. Department of Energy Yucca Mountain Site Characterization Office. The latter data source is signified by the use of UCC (shortened acronym for the University and Community College System of Nevada) in the source DTN identifiers listed below. Additional acquired data not found in the TDMS were extracted from the Underground Test Area (UGTA) Program's publicly available geochemical database (intermediary output DTN: LA0612RR150304.003). The relevant data in this database were acquired by the USGS, the Nye County Nuclear Waste Repository Program (NWRPO), the Harry Reid Center for Environmental Studies, the Desert Research Institute, and Lawrence Livermore National Laboratory.

Geographic coordinates, screen depths, and lithologies for the new Nye County wells and samples are listed in Table B4-1, which was compiled from the following DTNs:

- Output DTN (developed in Appendix F): LA0612RR150304.001, UTM Coordinates for Selected Nye County Early Warning Drilling Program Boreholes: NC-EWDP-7SC and Phases III and IV

- GS010908312332.002 [DIRS 163555], Borehole Data from Water-Level Data Analysis for the Saturated Zone Site-Scale Flow and Transport Model

- GS011008314211.001 [DIRS 158690], Interpretation of the Lithostratigraphy in Deep Boreholes NC-EWDP-19D1 and NC-EWDP-2DB Nye County Early Warning Drilling Program
- GS020108314211.001 [DIRS 174112], Interpretation of the Lithostratigraphy in Deep Boreholes, NC-EWDP-7SC and NC-EWDP-15D, Nye County Early Warning Drilling Program
- GS030108314211.001 [DIRS 163483], Interpretation of the Lithostratigraphy in Deep Boreholes NC-EWDP-18P, NC-EWDP-22SA, NC-EWDP-10SA, NC-EWDP-23P, NC-EWDP-19IM1A, and NC-EWDP-19IM2A, Nye County Early Warning Drilling Program, Phase III
- GS031108314211.004 [DIRS 174113], Interpretation of the Lithostratigraphy in Deep Boreholes NC-EWDP-16P, NC-EWDP-27P, and NC-EWDP-28P, Nye County Early Warning Drilling Program, Phase IV A
- GS040908314211.001 [DIRS 174114], Interpretation of the Lithostratigraphy in Deep Boreholes NC-EWDP-24P and NC-EWDP-29P, Nye County Early Warning Drilling Program, Phase IV B
- GS050708314211.001 [DIRS 179435], Description and Interpretation of Core Samples from Alluvial Core Holes NC-EWDP-19PB and NC-EWDP-22PC, Nye County Early Warning Drilling Program
- MO0112DQRWLNYE.014 [DIRS 157184], Well Completion Diagram for Borehole NC-EWDP-19P
- MO0112DQRWLNYE.018 [DIRS 157187], Well Completion Diagram for Borehole NC-EWDP-19D
- MO0110NYE03848.087 [DIRS 179436], NC-EWDP-Washburn-1X Well Completion Diagram
- MO0206NYE04926.119 [DIRS 179372], NC-EWDP-7SC Well Completion Diagram
- MO0306NYE05259.165 [DIRS 165876], Revised NC-EWDP-19IM1 Well Completion Diagram
- MO0306NYE05260.166 [DIRS 165877], Revised NC-EWDP-19IM2 Well Completion Diagram
- MO0306NYE05261.167 [DIRS 179373], Revised NC-EWDP-10S Well Completion Diagram
- MO0306NYE05262.168 [DIRS 179374], Revised NC-EWDP-10P Well Completion Diagram

- MO0306NYE05263.169 [DIRS 179375], Revised NC-EWDP-18P Well Completion Diagram
- MO0306NYE05264.170 [DIRS 179376], Revised NC-EWDP-22S Well Completion Diagram
- MO0306NYE05265.171 [DIRS 179377], Revised NC-EWDP-22PA Well Completion Diagram
- MO0306NYE05266.172 [DIRS 179378], Revised NC-EWDP-22PB Well Completion Diagram
- MO0306NYE05267.173 [DIRS 179379], Revised NC-EWDP-23P Well Completion Diagram
- MO0312NYE05716.204 [DIRS 179380], NC-EWDP-27P Well Completion Diagram
- MO0312NYE05718.202 [DIRS 179381], NC-EWDP-28P Well Completion Diagram
- MO0409NYE06093.241 [DIRS 179382], NC-EWDP-29P Well Completion Diagram
- MO0409NYE06096.242 [DIRS 179383], NC-EWDP-24P Well Completion Diagram
- MO0409NYE06101.246 [DIRS 179384], NC-EWDP-19PB Well Completion Diagram
- MO0702NYE05714.375 [DIRS 179443], NC-EWDP-16P Well Completion Diagram.

Geochemical and isotopic compositions for the new Nye County wells (Tables B4-2 and B4-3) derive from a large number of DTNs as well as from sources outside the YMP. The source data are compiled, evaluated, developed and averaged in the following intermediary output DTNs:

- LA0612RR150304.002, Hydrochemical Data Obtained from the Underground Test Area (UGTA) Program's Geochem05 Database
- LA0612RR150304.003, Geochemical and Isotopic Data for Selected NC-EWDP Wells, Phases II, III, and IV
- LA0612RR150304.005, Uranium Activity Ratios Calculated from Isotopic Ratios Reported for Nye County EWDP Boreholes and McCracken Well by Geochron Laboratories, for Samples Collected between November 1999 and June 2000.

Some new geochemical and isotopic data were considered inappropriate for use in this analysis. Reasons for considering data inappropriate include water samples collected prior to well completion, samples with problems noted during collection, samples with inadequate specification of the sampled depth interval in the source DTN, and outliers. These reasons and other considerations are documented in the supporting documentation for the above DTNs.

New geochemical and isotopic data for existing wells (Tables B4-4 to B4-9, Figure B6-14) are taken from the following acquired and developed DTNs:

- GS010608315215.002 [DIRS 156187], Uranium and Thorium Isotope Data for Waters Analyzed between January 18, 1994 and September 14, 1996
- GS031208312322.004 [DIRS 179431], Dissolved Organic Carbon-14 (DOC-14) Hydrochronology Data for Groundwater from Wells in the Yucca Mountain Area for Samples Analyzed through 1/30/2003
- GS040108312322.001 [DIRS 179422], Field and Chemical Data Collected between 10/4/01 and 10/3/02 and Isotope Data Collected between 5/19/00 and 5/22/03 from Wells in the Yucca Mountain Area, Nye County, Nevada
- GS040708312322.004 [DIRS 179432], Strontium Isotope Ratios and Strontium Concentrations on Groundwater Samples from Springs in the Area of Amargosa Valley and Desert
- GS040808312322.005 [DIRS 179433], Strontium Isotope Ratios and Strontium Concentrations on Groundwater Samples in Support of Nye Co. Early Warning Drilling Program (EWDP) and the Alluvial Tracer Complex (ATC)
- GS040808312322.006 [DIRS 179434], Field, Chemical, and Isotope Data for Spring and Well Samples Collected between 03/01/01 and 05/12/04 in the Yucca Mountain Area, Nye County, Nevada
- Output DTN: LA0612RR150304.002, Hydrochemical Data Obtained from the Underground Test Area (UGTA) Program's Geochem05 Database
- Output DTN: LA0612RR150304.005, Uranium Activity Ratios Calculated from Isotopic Ratios Reported for Nye County EWDP Boreholes and McCracken Well by Geochron Laboratories, for Samples Collected between November 1999 and June 2000
- MO0310UCC008IF.003 [DIRS 179440], Major Cation, Major Anion, and Trace Element Concentrations in Groundwater Collected from the October 2000 Sampling of Phase II and III Wells of the Nye County Early Warning Drilling Program (NC-EWDP)
- MO0311UCC008IF.007 [DIRS 179441], Major Cation, Major Anion, and Trace Element Concentrations in Groundwater Collected during the May 2000 Sampling of Phase I and II Wells of the Nye County Early Warning Drilling Program (NC-EWDP)
- UN0010SPA008KS.001 [DIRS 179442], Major Cation, Major Anion, and Trace Element Concentrations in Groundwaters Collected from Bond Gold Well, SD-6ST1, and the May 99 Sampling of the Phase I Wells of the Nye County Early Warning Drilling Program (EWDP).

Table B4-1. Geographic and Geologic Data Sources for New Nye County Boreholes and Zones

Well Identifier[a]	Assigned Sample ID[a]	UTM-X[b] (m)	UTM-Y[b] (m)	Area[c]	Interval Sampled	Geologic Unit[d]	DTN References for Sampled Depth and Geologic Unit
NC-EWDP-07SC Zone 1	203	539632	4064317	CF-SW Crater Flat—Southwest	80.0 to 90.0 ft 24.4 to 27.4 m (screen)	QTu	MO0206NYE04926.119 [DIRS 179372] GS020108314211.001 [DIRS 174112]
NC-EWDP-07SC Zone 2	204	539632	4064317	CF-SW Crater Flat—Southwest	180.0 to 210.0 ft 54.9 to 64.0 m (screen)	QTu	
NC-EWDP-07SC Zone 3	205	539632	4064317	CF-SW Crater Flat—Southwest	270.0 to 370.0 ft 82.3 to 112.8 m (screen)	Tmr	
NC-EWDP-07SC Zone 4	206	539632	4064317	CF-SW Crater Flat—Southwest	429.8 to 449.8 ft 131.0 to 137.1 m (screen)	Tmr	
NC-EWDP-07SC Zone 5	207	539632	4064317	CF-SW Crater Flat—Southwest	470.0 to 778.5 ft 143.2 to 237.3 m (bottom of borehole, filled with natural fill and drill cuttings)	Tmr, Tpt, Tcp, Tcb	
NC-EWDP-10P Zone 1	208	553149	4064916	FMW-N Fortymile Wash—North	660.1 to 699.3 ft 201.2 to 213.1 m (screen)	QTu[e]	MO0306NYE05262.168 [DIRS 179374] GS030108314211.001 [DIRS 163483]
NC-EWDP-10P Zone 2	209	553149	4064916	FMW-N Fortymile Wash—North	801.2 to 860.0 ft 244.2 to 262.1 m (screen)	Tab[e]	
NC-EWDP-10S composite	210	553140	4064899	FMW-N Fortymile Wash—North	660.0 to 860.0 ft 201.2 to 262.1 m (screen)	QTu, Tab	MO0306NYE05261.167 [DIRS 179373] GS030108314211.001 [DIRS 163483]
NC-EWDP-10S Zone 1	211	553140	4064899	FMW-N Fortymile Wash—North	660.0 to 700.0 ft 201.2 to 213.3 m (screen)	QTu	
NC-EWDP-10S Zone 2	212	553140	4064899	FMW-N Fortymile Wash—North	800.0 to 860.0 ft 243.8 to 262.1 m (screen)	Tab	

Table B4-1. Geographic and Geologic Data Sources for New Nye County Boreholes and Zones (Continued)

Well Identifier[a]	Assigned Sample ID[a]	UTM-X[b] (m)	UTM-Y[b] (m)	Area[c]	Interval Sampled[a]	Geologic Unit[d]	DTN References for Sampled Depth and Geologic Unit
NC-EWDP-16P composite	213	545665	4064263	YM-S Yucca Mountain—South	489.4 to 549.4 ft 149.2 to 167.4 m (screen)	Tmr	MO0702NYE05714.375 [DIRS 179443] GS031108314211.004 [DIRS 174113]
NC-EWDP-18P composite	214	549416	4067233	YM-S Yucca Mountain--South	835.8 to 885.0 ft 254.7 to 269.7 m (screen)	Tpts	MO0306NYE05263.169 [DIRS 179375] GS030108314211.001 [DIRS 163483]
NC-EWDP-19D Zones 5-7	215	549317	4058270	YM-S Yucca Mountain—South	882.2 to 980.3 ft 268.9 to 298.8 m 1122.1 to 1219.6 ft 342.0 to 371.6 m 1296.7 to 1379.7 ft 395.2 to 420.5 m (3 screens)	Tpt, Tpts, Tge	MO0112DQRWLNYE.018 [DIRS 157187] GS011008314211.001 [DIRS 158690]
NC-EWDP-19IM1 Composite	216	549317	4058291	YM-S Yucca Mountain—South	Not reported	QTu, Tpt	MO0306NYE05259.165 [DIRS 165876] GS030108314211.001 [DIRS 163483]
NC-EWDP-19IM1 Zone 1	217	549317	4058291	YM-S Yucca Mountain—South	410.0 to 430.0 ft 125.0 to 131.1 m (screen)	QTu	
NC-EWDP-19IM1 Zone 2	218	549317	4058291	YM-S Yucca Mountain—South	515.0 to 535.0 ft 157.0 to 163.1 m (screen)	QTu	
NC-EWDP-19IM1 Zone 3	219	549317	4058291	YM-S Yucca Mountain—South	574.9 to 674.9 ft 175.2 to 205.7 m (screen)	QTu	
NC-EWDP-19IM1 Zone 4	220	549317	4058291	YM-S Yucca Mountain—South	724.9 to 784.8 ft 220.9 to 239.2 m (screen)	QTu	
NC-EWDP-19IM1 Zone 5	221	549317	4058291	YM-S Yucca Mountain—South	849.5 to 949.3 ft 258.9 to 289.3 m (screen)	Tpt	
NC-EWDP-19IM2 Composite	222	549337	4058291	YM-S Yucca Mountain—South	Not reported	QTu, Tpt	MO0306NYE05260.166 [DIRS 165877] GS030108314211.001 [DIRS 163483]

Table B4-1. Geographic and Geologic Data Sources for New Nye County Boreholes and Zones (Continued)

Well Identifier[a]	Assigned Sample ID[a]	UTM-X[b] (m)	UTM-Y[b] (m)	Area[c]	Interval Sampled[a]	Geologic Unit[d]	DTN References for Sampled Depth and Geologic Unit
NC-EWDP-19P	223	549329	4058292	YM-S Yucca Mountain—South	359.2 to 458.6 ft 109.5 to 139.8 m (screen)	QTu[f]	MO0112DQRWLNYE.014 [DIRS 157184] GS011008314211.001 [DIRS 158690]
NC-EWDP-19PB Zone 1	224	549337	4058316	YM-S Yucca Mountain—South	375.0 to 395.0 ft 114.3 to 120.4 m (screen)	QTu	MO0409NYE06101.246 [DIRS 179384] GS050708314211.001 [DIRS 179435]
NC-EWDP-19PB Zone 2	225	549337	4058316	YM-S Yucca Mountain—South	514.7 to 534.7 ft 156.9 to 163.0 m (screen)	QTu	
NC-EWDP-22PA Zone 1	226	552020	4062038	FMW-N Fortymile Wash—North	520.7 to 579.7 ft 158.7 to 176.7 m (screen)	QTu[g]	MO0306NYE05265.171 [DIRS 179377] GS030108314211.001 [DIRS 163483]
NC-EWDP-22PA Zone 2	227	552020	4062038	FMW-N Fortymile Wash—North	661.5 to 759.8 ft 201.6 to 231.6 m (screen)	QTu[g]	
NC-EWDP-22PB Zone 1	228	552038	4062037	FMW-N Fortymile Wash—North	881.3 to 979.7 ft 268.8 to 298.6 m (screen)	QTu[g]	MO0306NYE05266.172 [DIRS 179378] GS030108314211.001 [DIRS 163483]
NC-EWDP-22PB Zone 2	229	552038	4062037	FMW-N Fortymile Wash—North	1,140.3 to 1,179.7 ft 347.5 to 359.6 m (screen)	QTu[g]	
NC-EWDP-22S Zone 1	230	552019	4062020	FMW-N Fortymile Wash—North	521.5 to 581.3 ft 159.1 to 176.7 m (screen)	QTu	MO0306NYE05264.170 [DIRS 179376] GS030108314211.001 [DIRS 163483]

Table B4-1. Geographic and Geologic Data Sources for New Nye County Boreholes and Zones (Continued)

Well Identifier[a]	Assigned Sample ID[a]	UTM-X[b] (m)	UTM-Y[b] (m)	Area[c]	Interval Sampled[a]	Geologic Unit[d]	DTN References for Sampled Depth and Geologic Unit
NC-EWDP-22S Zone 2	231	552019	4062020	FMW-N Fortymile Wash—North	661.2 to 760.6 ft 201.8 to 231.5 m (screen)	QTu	
NC-EWDP-22S Zone 3	232	552019	4062020	FMW-N Fortymile Wash—North	880.2 to 980.0 ft 268.8 to 298.5 m (screen)	QTu	
NC-EWDP-22S Zone 4	233	552019	4062020	FMW-N Fortymile Wash—North	1,140.0 to 1,180.0 ft 348.1 to 359.5 m (screen)	Tab	
NC-EWDP-23P Zone 1	234	553924	4059875	LW Amargosa Valley	460.9 to 519.9 ft 140.2 to 158.5 m (screen)	QTu	MO0306NYE05267.173 [DIRS 179379] GS030108314211.001 [DIRS 163483]
NC-EWDP-23P Zone 2	235	553924	4059875	LW Amargosa Valley	650.5 to 689.8 ft 198.1 to 210.3 m (screen)	QTu	
NC-EWDP-24P	236	549386	4062055	YM-S Yucca Mountain—South	400.0 to 440.0 ft 121.9 to 134.1 m (screen)	Tcb	MO0409NYE06096.242 [DIRS 179383] GS040908314211.001 [DIRS 174114]
NC-EWDP-27P	237	544935	4065276	YM-S Yucca Mountain—South	580.7 to 620.6 ft 177.0 to 189.1 m (screen)	Tpt	MO0312NYE05716.204 [DIRS 179380] GS031108314211.004 [DIRS 174113]
NC-EWDP-28P	238	545746	4062393	YM-S Yucca Mountain—South	370.0 to 449.0 ft 112.8 to 136.8 m (screen)	Tma, Tmabt	MO0312NYE05718.202 [DIRS 179381] GS031108314211.004 [DIRS 174113]

Table B4-1. Geographic and Geologic Data Sources for New Nye County Boreholes and Zones (Continued)

Well Identifier[a]	Assigned Sample ID[a]	UTM-X[b] (m)	UTM-Y[b] (m)	Area[c]	Interval Sampled[a]	Geologic Unit[d]	DTN References for Sampled Depth and Geologic Unit
NC-EWDP-29P	239	549396	4059606	YM-S Yucca Mountain—South	340.0 to 390.0 ft 103.6 to 118.9 m (screen)	Tpc, Tpbt4	MO0409NYE06093.241 [DIRS 179382] GS040908314211.001 [DIRS 174114]
NC-EWDP-Washburn-1X[h] Zone 2	240	551465	4057563	FMW-N Fortymile Wash—North	420.0 to 480.0 ft 128.0 to 146.3 m (screen)	unknown	MO0110NYE03848.087 [DIRS 179436] NA

UTM = Universal Transverse Mercator.

[a] The well identifier includes the designator "Zone" to indicate that the sample derives from a discrete portion of the borehole length, usually a screened interval. The borehole interval included in a specified zone is defined in the table column labeled "Interval Sampled." Sample IDs are assigned to these new samples sequentially, starting with the number immediately following the last one assigned in Table A4-3. Sample locations are labeled with their assigned sample identifiers in Figure B6-1.

[b] Data source for UTM coordinates: DTN: GS010908312332.002 [DIRS 163555] for NC-EWDP-19D, NC-EWDP-19P and NC-EWDP-Washburn-1X; Output DTN: LA0612RR150304.001 for all others (developed in Appendix F). Throughout this appendix, UTM-X is used to refer to UTM-Easting, and UTM-Y refers to UTM-Northing.

[c] See Figure A6-5 and Section A6.7.2 for a definition of these subareas, or hydrochemical groups, in the vicinity of Yucca Mountain. Section B6.2 describes the basis used to assign each new groundwater sample to one of these subareas.

[d] Geologic units: QTu, Quaternary and Tertiary alluvium (undivided); Tab Tertiary sedimentary rocks; Tge Pre-volcanic Tertiary sedimentary rocks; Tma Ammonia Tanks Tuff; Tmabt, Pre-Ammonia Tanks Tuff bedded tuff; Tmr Rainier Mesa Tuff; Tpbt4 Pre-Tiva Canyon Tuff; Tpc Tiva Canyon Tuff; Tpt Topopah Spring Tuff; Tpts Pre-Topopah Spring Sedimentary Rocks.

[e] The identification of geologic units for zones 1 and 2 in NC-EWDP-10P is extrapolated from those reported for these depths in the nearby borehole NC-EWDP-10SA in DTN: GS030108314211.001 [DIRS 163483].

[f] The identification of geologic units for NC-EWDP-19P is extrapolated from those reported for these depths in the nearby borehole NC-EWDP-19D1 in DTN: GS011008314211.001 [DIRS 158690].

[g] The identification of geologic units for zones 1 and 2 in NC-EWDP-22PA and zones 1 and 2 in NC-EWDP-22PB is extrapolated from those reported for these depths in the nearby borehole NC-EWDP-22SA in DTN: GS030108314211.001 [DIRS 163483].

[h] DTNs are inconsistent in the use of a hole name for NC-EWDP-Washburn-1X with or without "EWDP." In this appendix, it was judged best to maintain a uniform usage of the inclusion of "EWDP" in the identifier.

Table B4-2. Field Parameters and Average Major Ion Compositions for New Wells

Well Identifier	Sample ID Assigned in Table B4-1	Sample Temperature (°C)	pH	Ca^{2+} (mg/L)	Mg^{2+} (mg/L)	Na^{+} (mg/L)	K^{+} (mg/L)	Cl^{-} (mg/L)	SO_4^{2-} (mg/L)	HCO_3^{-} (mg/L)	CO_3^{2-} (mg/L)	F^{-} (mg/L)	SiO_2 (mg/L)
NC-EWDP-07SC Zone 1	203	19, 33	7.5	76	37	84	5.9	15.1	151	418	0	0.8	22
NC-EWDP-07SC Zone 2	204	14, 23	7.3	77	37	84	6.0	15.2	153	438	0	0.8	22
NC-EWDP-07SC Zone 3	205	20, 23	7.7	69	37	87	7.3	16.7	146	435	0	0.8	27
NC-EWDP-07SC Zone 4	206	—	8.2	28	28	85	8.6	15.9	128	288	0	0.8	28
NC-EWDP-07SC Zone 5	207	—	—	—	—	—	—	—	—	—	—	—	—
NC-EWDP-10P Zone 1	208	26	7.6	14	2.2	44	5.8	6.6	20	134	0	2.1	58
NC-EWDP-10P Zone 2	209	22, 30	7.6	15	2.3	41	5.7	6.3	19	130	0	2.1	60
NC-EWDP-10S composite	210	28	7.8	15	2.4	41	5.8	6.3	20	126	0	1.9	59
NC-EWDP-10S Zone 1	211	22, 30	7.8	14	2.4	42	5.9	6.6	19	135	0	2.1	59
NC-EWDP-10S Zone 2	212	22, 31	7.9	11	1.7	51	5.4	6.7	20	147	0	2.0	54
NC-EWDP-16P composite	213	—	8.5	0.8	0.08	106	1.7	8.5	55	190	5	2.7	44
NC-EWDP-18P composite	214	27, 34	8.1	9.8	0.1	68	1.8	7.0	21	174	0	2.5	48
NC-EWDP-19D Zones 5-7	215	31	9.0	0.6	0.03	113	3.5	5.5	20	224	22	2.2	60
NC-EWDP-19IM1 composite[a]	216	—	8.7	2.9	0.2	96	3.3	6.3	26	206	6	2.0	57
NC-EWDP-19IM1 Zone 1	217	18	8.7	2.1	0.3	95	3.2	5.3	17	216	10	2.2	58
NC-EWDP-19IM1 Zone 2[a]	218	29	8.5	5.9	0.5	77	3.3	6.0	22	193	4	2.0	56
NC-EWDP-19IM1 Zone 3[a]	219	30	8.6	1.1	0.03	101	3.4	6.2	25	218	9	2.0	57
NC-EWDP-19IM1 Zone 4[a]	220	31	9.1	0.7	0.02	107	3.2	5.5	17	209	23	2.3	59
NC-EWDP-19IM1 Zone 5	221	31	8.8	0.5	0.04	98	2.9	5.2	16	206	16	2.1	62
NC-EWDP-19IM2 composite	222	32	8.8	0.3	0.02	100	3.1	5.2	16	217	12	2.1	62
NC-EWDP-19P	223	—	7.7	18	1.5	45	3.8	6.4	20	143	0	1.7	53
NC-EWDP-19PB Zone 1	224	—	8.3	14	1.4	56	3.9	6.5	29	149	0	1.7	47
NC-EWDP-19PB Zone 2	225	—	8.4	7.8	0.6	80	3.1	5.7	23	203	1	1.5	56
NC-EWDP-22PA Zone 1	226	28	7.5	15	2.5	43	5.4	6.4	19	126	0	2.0	53
NC-EWDP-22PA Zone 2	227	24, 28	7.4	20	2.9	37	5.1	6.5	21	131	0	1.6	58
NC-EWDP-22PB Zone 1	228	29	7.9	25	3.3	39	5.6	6.3	22	157	0	1.0	56
NC-EWDP-22PB Zone 2	229	28	7.9	23	3.0	46	5.0	6.1	27	157	0	0.9	44

Table B4-2. Field Parameters and Average Major Ion Compositions for New Wells (Continued)

Well Identifier	Sample ID assigned in Table B4-1	Sample Temperature (°C)	pH	Ca^{2+} (mg/L)	Mg^{2+} (mg/L)	Na^{+} (mg/L)	K^{+} (mg/L)	Cl^{-} (mg/L)	SO_4^{2-} (mg/L)	HCO_3^{-} (mg/L)	CO_3^{2-} (mg/L)	F^{-} (mg/L)	SiO_2 (mg/L)
NC-EWDP-22S Zone 1	230	28	7.6	15	2.6	39	5.3	6.3	18	124	0	1.7	54
NC-EWDP-22S Zone 2	231	28	7.8	18	2.8	37	5.2	6.4	21	138	0	1.4	48
NC-EWDP-22S Zone 3	232	28	7.9	22	3.1	37	5.5	6.4	19	141	0	1.1	52
NC-EWDP-22S Zone 4	233	29	8.0	20	2.6	41	5.1	5.9	20	142	0	1.0	51
NC-EWDP-23P Zone 1	234	25	7.9	25	5.2	90	8.2	13.6	127	173	0	1.4	41
NC-EWDP-23P Zone 2	235	25	8.4	16	0.9	119	4.2	10.8	155	149	4	1.1	35
NC-EWDP-24P	236	32	7.9	15	0.9	53	3.1	6.7	24	164	—	2.2	38[b]
NC-EWDP-27P	237	—	8.4	5.0	1.0	102	3.7	9.0	39	222	5	3.7	39
NC-EWDP-28P	238	29	8.6	3.7	0.4	101	4.2	7.6	32	213	10	2.1	67
NC-EWDP-29P	239	26	8.1	16	1.2	52	4.3	6.3	21	151	—	2.1	60[b]
NC-EWDP-Washburn-1X Zone 2	240	—	7.7	20	2.7	37	4.8	6.9	27	127	0	1.4	55

Source: Output DTN: LA0612RR150304.003.

[a] The only water-quality sample available for this interval was collected less than 3 months after well completion, and may not be representative of undisturbed chemistry.

[b] Analyses for this analyte are only available for a sample that was collected less than 3 months after well completion, and may not be representative of undisturbed chemistry.

Table B4-3. Average Isotope and Trace Element Compositions for New Wells

Well Identifier	Sample ID assigned in Table B4-1	δ^{13}C-DIC (per mil)	^{14}C-DIC (pmc)	δD (per mil)	δ^{18}O (per mil)	δ^{34}S (per mil)	U (µg/L)	^{234}U/^{238}U Activity Ratio	Sr^{2+} (µg/L)	^{87}Sr/^{86}Sr (ratio)	δ^{87}Sr (per mil)
NC-EWDP-07SC Zone 1	203	−4.8	5.6	−98.8	−13.3	14.3	5.5	—	510	0.71351	6.1
NC-EWDP-07SC Zone 2	204	−4.7	5.5	−98.3	−13.3	14.3	5.5	—	522	0.71334	5.8
NC-EWDP-07SC Zone 3	205	−4.8	6.0	−98.0	−13.3	16.1	3.0	—	549	0.71287	5.2
NC-EWDP-07SC Zone 4	206	−5.7	6.9	−97.8	−13.4	21.7	0.2	—	365	0.71229	4.4
NC-EWDP-07SC Zone 5	207	—	—	—	—	—	—	—	—	—	—
NC-EWDP-10P Zone 1	208	−10.2	24.7	−98.5	−13.1	9.6	0.9	—	62	0.71122	2.8
NC-EWDP-10P Zone 2	209	−10.0	24.1	−96.8	−13.2	9.7	0.9	—	60	0.71122	2.8
NC-EWDP-10S composite	210	−8.8	26.2	−100.0	−12.7	9.7	0.7	—	53	—	—
NC-EWDP-10S Zone 1	211	−9.1	24.3	−99.5	−13.1	9.9	0.7	—	62	0.71103	2.6
NC-EWDP-10S Zone 2	212	−8.4	24.4	−97.3	−13.2	9.2	0.9	—	55	0.71047	1.8
NC-EWDP-16P composite	213	−8.5	16.8	−99.5	−13.6	4.7	3.9	—	8.8	—	—
NC-EWDP-18P composite	214	−8.1	21.0	−102.3	−13.7	12.2	2.5	—	25	0.70931	0.2
NC-EWDP-19D Zones 5-7	215	−7.1	9.2	−106.0	−13.2	9.6	2.6	—	1.1	0.71025	1.5
NC-EWDP-19IM1 composite [a]	216	−8.9	—	−104.5	−13.4	9.3	1.7	—	8.2	0.71081	2.3
NC-EWDP-19IM1 Zone 1 [a]	217	−6.0	12.5	−105.0	−14.0	11.2	2.8	—	17	0.70970	0.7
NC-EWDP-19IM1 Zone 2 [a]	218	−9.5	14.9	−100.0	−11.8	9.2	2.0	—	18	0.71069	2.1
NC-EWDP-19IM1 Zone 3 [a]	219	−7.0	11.4	−103.0	−13.0	9.8	1.9	—	2.0	0.71043	1.7
NC-EWDP-19IM1 Zone 4 [a]	220	−7.5	9.0	−101.5	−12.1	11.2	1.6	—	1.4	0.70990	1.0
NC-EWDP-19IM1 Zone 5 [a]	221	−6.8	6.4	−104.5	−13.8	11.6	2.0	—	1.9	0.71000	1.1
NC-EWDP-19IM2 composite	222	−7.0	5.9	−104.5	−13.9	11.9	2.2	—	1.0	0.71117	2.8
NC-EWDP-19P	223	−7.9	20.3	−100.0	−13.5	11.3	0.8	5.1	61	0.71143	3.1
NC-EWDP-19PB Zone 1	224	−8.4	20.6	—	—	8.0	2.0	—	81	0.71007	1.2
NC-EWDP-19PB Zone 2	225	−6.8	10.9	—	—	9.8	3.1	—	36	0.71002	1.2
NC-EWDP-22PA Zone 1	226	−10.5	24.1	−99.0	−13.1	8.2	0.9	—	65	0.71090	2.4
NC-EWDP-22PA Zone 2	227	−10.0	21.7	−97.5	−13.3	9.5	0.5	—	70	0.71060	2.0
NC-EWDP-22PB Zone 1	228	−9.5	20.3	−97.8	−13.2	9.1	1.1	—	101	0.71036	1.6
NC-EWDP-22PB Zone 2	229	−10.7	21.8	−96.8	−13.1	8.3	1.6	—	79	0.71059	2.0
NC-EWDP-22S Zone 1	230	−9.1	22.7	−98.3	−13.1	9.5	0.4	—	59	0.71093	2.4
NC-EWDP-22S Zone 2	231	−7.6	20.9	−98.4	−13.1	9.9	0.5	—	73	0.71047	1.8

Table B4-3. Average Isotope and Trace Element Compositions for New Wells (Continued)

Well Name	Sample ID assigned in Table B4-1	δ^{13}C-DIC (per mil)	^{14}C-DIC (pmc)	δD (per mil)	δ^{18}O (per mil)	δ^{34}S (per mil)	U (µg/L)	^{234}U/^{238}U Activity Ratio	Sr^{2+} (µg/L)	^{87}Sr/^{86}Sr (ratio)	δ^{87}Sr (per mil)
NC-EWDP-22S Zone 3	232	−8.1	19.6	−98.8	−13.1	9.9	0.7	—	92	0.71044	1.8
NC-EWDP-22S Zone 4	233	−8.8	20.2	−98.5	−13.0	8.9	0.7	—	78	0.71038	1.7
NC-EWDP-23P Zone 1	234	−10.5	23.6	−101.0	−13.1	5.1	5.9	—	132	0.71054	1.9
NC-EWDP-23P Zone 2	235	−10.6	20.8	−104.3	−13.3	2.1	3.7	—	134	0.70944	0.3
NC-EWDP-24P [a]	236	−8.1	17.2	−104.0	−13.6	12.3	0.8	—	68	—	—
NC-EWDP-27P	237	−7.3	12.4	−102.0	−13.6	11.1	4.4	—	45	—	—
NC-EWDP-28P	238	−11.6	16.0	−101.5	−13.5	8.9	4.7	—	33	—	—
NC-EWDP-29P [a]	239	−8.8	20.2	−102.0	−13.3	10.2	1.0	—	70	0.71040	1.7
NC-EWDP-Washburn-1X Zone 2	240	−9.4	21.3	−101.3	−13.2	9.3	0.7	—	70	0.71009	1.3

Sources: Output DTNs: LA0612RR150304.002, LA0612RR150304.003, LA0612RR150304.005.

DIC = dissolved inorganic carbon; pmc = percent modern carbon.

[a] The only water-quality sample available for this well was collected less than 3 months after well completion, and may not be representative of undisturbed chemistry.

Table B4-4. Additional Data on Field Parameters and Major Ion Compositions for Well Cited in Appendix A

Well Identifier	Sample ID on Figure A6-5	Temperature (°C)	pH	Ca^{2+} (mg/L)	Mg^{2+} (mg/L)	Na^{+} (mg/L)	K^{+} (mg/L)	Cl^{-} (mg/L)	SO_4^{2-} (mg/L)	HCO_3^{-} (mg/L)	CO_3^{2-} (mg/L)	F^{-} (mg/L)	SiO_2 (mg/L)
U.S. Ecology MR-3 (Bond Gold Mining Well #12 (BGMW12)) (16-Aug-89, 18-May-99)	18	—	7.7[a]	47.5	18	161	10.5	80	195	325.0[a]	0.0[a]	3.2	67.5

Source: Output DTN: LA0612RR150304.002.

[a] Value from Table A6-1.

Table B4-5. Additional Data on Strontium Isotopic Compositions for Wells Cited in Appendix A

Well Identifier	Sample ID on Figure A6-5	Sr^{2+} (µg/L)	$^{87}Sr/^{86}Sr$ (ratio)	$\delta\ ^{87}Sr$ (per mil)[a]	Source DTN[a]
ER-EC-08	1	2.2	0.70864[c]	−0.8	LA0612RR150304.002 (Output DTN)
Bond Gold Mining #1 (BGMW1)[d]	14	157	0.71028	1.5	GS040708312322.004 [DIRS 179432]
US Ecology MW-313	15	398	0.71197	3.9	GS040708312322.004 [DIRS 179432]
US Ecology MW-600[b]	16	363	0.71202	4.0	GS040708312322.004 [DIRS 179432]
U.S. Ecology MR-3 (Bond Gold Mining Well #12 (BGMW12))[d]	18	390	0.71196	3.9	GS040708312322.004 [DIRS 179432]
USW SD-6	50	0.4	0.71106	2.6	LA0612RR150304.002 (Output DTN) UN0010SPA008KS.001 [DIRS 179442]
J-11	67	264[c]	0.70935	0.2	LA0612RR150304.002 (Output DTN)
NC-EWDP-07S	71	641	0.71322	5.7	GS040808312322.005 [DIRS 179433]
NC-EWDP-07SC[b,e]	72	562	0.71329	5.8	GS040808312322.005 [DIRS 179433]
NC-EWDP-01DX (borehole)	73	510[c]	0.71280	5.1	LA0612RR150304.002 (Output DTN)
NC-EWDP-01S[b,e]	77	557[c]	0.71288	5.2	GS040808312322.005 [DIRS 179433]
NC-EWDP-03D (SMF Barcode 537190)[b]	86	2.5	0.71016	1.4	GS040808312322.005 [DIRS 179433]
NC-EWDP-02D	91	53.0[c]	0.71161	3.4	GS040808312322.005 [DIRS 179433]
NC-EWDP-19D (alluvial; Zones 1 to 4)[b,e]	94	7.5[c]	0.71100	2.5	GS040808312322.005 [DIRS 179433]
NC-EWDP-19D (Zone 1) (SMF Barcode 571011)[b]	95	34	0.71129	3.0	GS040808312322.005 [DIRS 179433]
NC-EWDP-19D (Zone 2) (SMF Barcode 554583)[b]	96	39	0.71120	2.8	GS040808312322.005 [DIRS 179433]
NC-EWDP-19D (Zone 3) (SMF Barcode 554543)[b]	97	2.2	0.71052	1.9	GS040808312322.005 [DIRS 179433]
NC-EWDP-19D (Zone 4) (SMF Barcode 553974)[b]	98	2.2	0.71107	2.6	GS040808312322.005 [DIRS 179433]
Desert Farms Garlic Plot (DFGP)[d]	101	144[c]	0.70973	0.8	GS040708312322.004 [DIRS 179432]
Airport Well[b]	106	24.0[c]	0.70984	0.9	GS040708312322.004 [DIRS 179432]
Barrachman Domestic / Irrigation	116	473[c]	0.71770	12.0	GS040708312322.004 [DIRS 179432]
Selbach Domestic	121	217[c]	0.71472	7.8	GS040708312322.004 [DIRS 179432]
Funeral Mountain Ranch Irrig	126	114[c]	0.71664	10.5	GS040708312322.004 [DIRS 179432]
DeLee Large Irrigation	133	110[c]	0.71169	3.5	GS040708312322.004 [DIRS 179432]
Bray Domestic	136	101[c]	0.71163	3.4	GS040708312322.004 [DIRS 179432]
Amargosa Estates #2[d]	137	129[c]	0.71286	5.2	GS040708312322.004 [DIRS 179432]
O'Neill Domestic	145	109[c]	0.71136	3.0	GS040708312322.004 [DIRS 179432]
Ponderosa Dairy	149	248[c]	0.71216	4.2	GS040708312322.004 [DIRS 179432]
M. Gilgan Well[d]	152	155[c]	0.71287	5.2	GS040708312322.004 [DIRS 179432]
Nelson Domestic	157	830[c]	0.71309	5.5	GS040708312322.004 [DIRS 179432]

Table B4-5. Additional Data on Strontium Isotopic Compositions for Wells Cited in Appendix A (Continued)

Well Identifier	Sample ID on Figure A6-5	Sr^{2+} (µg/L)	$^{87}Sr/^{86}Sr$ (ratio)	$\delta^{87}Sr$ (per mil)[a]	Source DTN [a]
Lowe Domestic	159	724[c]	0.71305	5.4	GS040708312322.004 [DIRS 179432]
Anvil Ranch Irrigation	161	319[c]	0.71191	3.8	GS040708312322.004 [DIRS 179432]
Payton Domestic	164	1,069[c]	0.71327	5.7	GS040708312322.004 [DIRS 179432]
Oettinger Well	167	915[c]	0.71325	5.7	GS040708312322.004 [DIRS 179432]
Amargosa Motel (B)	168	954[c]	0.71316	5.6	GS040708312322.004 [DIRS 179432]
Crane Domestic	178	674[c]	0.71835	12.9	GS040708312322.004 [DIRS 179432]
IMV on Windjammer [b]	180	430[c]	0.71668	10.5	GS040708312322.004 [DIRS 179432]
Moms Place	184	346[c]	0.71652	10.3	GS040708312322.004 [DIRS 179432]

NOTE: Unless noted otherwise, data presented here are limited to those for samples collected at least 3 months following well completion.

[a] With the exception of Output DTN: LA0612RR150304.002, the cited DTNs that report $^{87}Sr/^{86}Sr$ ratios do not report $\delta^{87}Sr$ values. In these cases, the $\delta^{87}Sr$ values shown in this table were calculated by the equation: $[(R_x / 0.70920) - 1] \times 1{,}000$, in which R_x is the sample's $^{87}Sr/^{86}Sr$ ratio and 0.70920 is the present-day strontium isotopic ratio assumed for the USGS seawater standard EN1 (Futa et al. 2006 [DIRS 178742], p. 302).

[b] When more than one analysis was reported for a particular location (other than the NC-EWDP wells), then the results shown above are averages of the available data; such is the case for sample IDs 16, 106, and 180. For NC-EWDP wells, because these were drilled and completed so recently, the values reported in the table above are either for the most recent sample collected (sample IDs 86 and 95 to 98, SMF barcode is listed next to the well's identifier), or an average of results from all sampling events reported in the source DTN (sample IDs 72, 77 and 94). Although sampling dates are not included in DTNs: GS040708312232.004 [DIRS 179432] and GS040808312322.005 [DIRS 179433], these dates are documented in sample collection reports that are traceable through SMF barcode numbers reported in these DTNs. Sample collection dates for the NC-EWDP samples in this table are reported on the sample collection forms (YMP 2001 [DIRS 179430], pp. 18 to 20, 34, 42, 44, 46, 53, 55, 57, 63, 69, 72, 75, and 78).

[c] Data from Table A6-2.

[d] The source DTNs show minor inconsistencies in the well identifier used for this location. In this appendix, it was judged best to maintain a uniform usage with the identifier used in Table A4-3.

[e] The only strontium isotopic data available for this interval are for samples collected less than 3 months after well completion, and may not be representative of undisturbed chemistry.

SMF = Sample Management Facility.

Table B4-6. Additional Data on Uranium Isotope Values for Wells Cited in Appendix A

Well Identifier	Sample ID in Figure A6-5	U (µg/L)[a]	$^{234}U/^{238}U$ Activity Ratio[a]	Source DTN [b]
ER-EC-08	1	4.8	5.1	LA0612RR150304.002 (Output DTN)—U, AR
ER-30-1 (upper)	28	1.9	2.0	LA0612RR150304.002 (Output DTN)—U, AR
ER-30-1 (lower)	29	1.6	2.5	LA0612RR150304.002 (Output DTN)—U, AR
USW UZ-14 (pump test #4) [c]	46	0.02	7.4	GS010608315215.002 [DIRS 156187]—U, AR
UE-25c #1 HTH	58	0.6	5.7	LA0612RR150304.002 (Output DTN)—U, AR
NC-EWDP-07S (24-Oct-00)	71	6.2	—	MO0310UCC008IF.003 [DIRS 179440]—U
NC-EWDP-12PA	78	1.1	7.5	LA0612RR150304.002 (Output DTN)—U LA0612RR150304.005 (Output DTN)—AR MO0310UCC008IF.003 [DIRS 179440]—U MO0311UCC008IF.007 [DIRS 179441]—U
NC-EWDP-12PB	79	0.95	6.5	LA0612RR150304.002 (Output DTN)—U LA0612RR150304.005 (Output DTN)—AR MO0310UCC008IF.003 [DIRS 179440]—U MO0311UCC008IF.007 [DIRS 179441]—U
NC-EWDP-12PC	80	9.0	4.4	LA0612RR150304.002 (Output DTN)—U LA0612RR150304.005 (Output DTN)—AR MO0310UCC008IF.003 [DIRS 179440]—U MO0311UCC008IF.007 [DIRS 179441]—U
NC-EWDP-15P	90	3.3	5.2	LA0612RR150304.002 (Output DTN) —U LA0612RR150304.005 (Output DTN)—AR MO0310UCC008IF.003 [DIRS 179440]—U MO0311UCC008IF.007 [DIRS 179441]—U
NC-EWDP-19D (open hole; 7 zones)	92	1.8	3.6	LA0612RR150304.002 (Output DTN)—U LA0612RR150304.005 (Output DTN)—AR
NC-EWDP-19P	93	—	5.1	LA0612RR150304.005 (Output DTN)—AR
NC-EWDP-19D (alluvial; Zones 1 to 4)	94	1.7	—	LA0612RR150304.002 (Output DTN)—U
NC-EWDP-19D (Zone 1)	95	1.5	—	LA0612RR150304.002 (Output DTN)—U
NC-EWDP-19D (Zone 2)	96	1.2	—	LA0612RR150304.002 (Output DTN)—U
NC-EWDP-19D (Zone 3)	97	1.7	—	LA0612RR150304.002 (Output DTN)—U
NC-EWDP-19D (Zone 4)	98	1.7	—	LA0612RR150304.002 (Output DTN)—U
NC-EWDP-04PB	99	0.5	2.5	LA0612RR150304.002 (Output DTN)—U LA0612RR150304.005 (Output DTN)—AR MO0310UCC008IF.003 [DIRS 179440]—U MO0311UCC008IF.007 [DIRS 179441]—U GS040808312322.006 [DIRS 179434]—U

Table B4-6. Additional Data on Uranium Isotope Values for Wells Cited in Appendix A (Continued)

Well Identifier	Sample ID in Figure A6-5	U (µg/L)[a]	$^{234}U/^{238}U$ Activity Ratio[a]	Source DTN [b]
NC-EWDP-04PA	100	0.8	2.7	LA0612RR150304.002 (Output DTN)—U LA0612RR150304.005 (Output DTN)—AR
NC-EWDP-05SB	155	0.15	4.1	LA0612RR150304.002 (Output DTN)—U LA0612RR150304.005 (Output DTN)—AR MO0310UCC008IF.003 [DIRS 179440]—U

[a] When more than one analysis was reported for a particular location, then the results shown above are averages of the available data.

[b] Each source DTN is identified as a source of uranium concentrations (U) and/or activity ratios (AR) in the last column.

[c] Average values for the last 6 samples collected from pump test #4, on August 25 to 27, 1993. (Note: The date is embedded in the sample name listed for this sampling event in DTN: GS010608315215.002 [DIRS 156187], in the format YrMoDy (Year-Month-Day).) Based on the variably elevated uranium concentrations observed for earlier samples, these later samples are considered more likely to be representative of the perched water at this location.

Table B4-7. Additional Data on Sulfur Isotope Values for Wells Cited in Appendix A

Well Identifier	Sample ID in Figure A6-5	$\delta^{34}S$ (per mil)[a]
J-13	35	10.5
VH-2	70	14.7
VH-1	69	13.0
NC-EWDP-07SC (composite, 28/29-Mar-01)	72	13.5

Source: DTN: GS040108312322.001 [DIRS 179422].

[a] When more than one analysis was reported for a particular location, then the results shown above are averages of the available data. This was the case for J-13, VH-1 and NC-EWDP-07SC.

Table B4-8. Additional Data on Carbon Isotope Values for Wells Cited in Appendix A

Well name	Sample ID in Figure A6-5	$\delta^{13}C$ (per mil)	^{14}C (pmc)	Source DTN
U.S. Ecology MR-3 (Bond Gold Mining Well #12 (BGMW12)), 16-Aug-89	18	−6.7	26.2	LA0612RR150304.002 (Output DTN)
ER-30-1 (upper)	28	−8.1	33.9	LA0612RR150304.002 (Output DTN)
ER-30-1 (lower)	29	−8.2	43.6	LA0612RR150304.002 (Output DTN)
USW SD-6	50	−9.4 [a]	15.0	LA0612RR150304.002 (Output DTN)
VH-1	69	−7.3 [b]	14.5 [b]	GS040108312322.001 [DIRS 179422] GS040808312322.006 [DIRS 179434]

Table B4-8. Additional Data on Carbon Isotope Values for Wells Cited in Appendix A (Continued)

Well name	Sample ID in Figure A6-5	$\delta^{13}C$ (per mil)	^{14}C (pmc)	Source DTN
VH-2	70	−4.8	7.0	GS040108312322.001 [DIRS 179422]
NC-EWDP-07SC	72	−4.9	6.5	GS040108312322.001 [DIRS 179422]
NC-EWDP-03S	87	−8.4[a]	61.2	GS040808312322.006 [DIRS 179434]
NC-EWDP-19D	95	−7.0[a]	19.4	GS040108312322.001 [DIRS 179422]
NC-EWDP-04PB	99	−10.0[a]	8.7	GS040808312322.006 [DIRS 179434]
NC-EWDP-05SB	155	−1.0	1.48	GS040108312322.001 [DIRS 179422]

[a] Data from Table A6-2.

[b] Values reported for VH-1 are averages of data from two different sampling events at this location. Equal weight is given to each sampling event by "averaging the averages" from each event.

pmc = percent modern carbon.

Table B4-9. Additional Data on Stable Hydrogen and Oxygen Isotope Values for Wells Cited in Appendix A

Well Name	Sample ID in Figure A6-5	δD (per mil)	$\delta^{18}O$ (per mil)	Source DTN
NEC well a	17	−107.7	−14.0	LA0612RR150304.002 (Output DTN)
Test Well #1	26	−110.3	−14.7[b]	LA0612RR150304.002 (Output DTN)
VH-2	70	−105.0	−13.6	GS040108312322.001 [DIRS 179422]
NC-EWDP-07SC	72	−100.0[c]	−13.5[c]	GS040108312322.001 [DIRS 179422]

[a] DTNs are slightly inconsistent in the use of a unique well identifier for this location. In this appendix, it was judged best to maintain a uniform usage with the identifier used in Table A4-3.

[b] Data from Table A6-2.

[c] The reported value represents the average of several analyses reported for this well in the source DTN.

B5. ASSUMPTIONS

A list of the assumptions used in Sections B6 and B7 is provided in Section A5 of Appendix A, and is augmented by the following additional assumptions:

1. Borehole coordinates used in this analysis are sufficiently accurate for the intended purpose of delineating regional flowpaths based on areal distributions of hydrochemical and isotopic species. The rationale for this assumption is presented in Section 6.2.1 of *Water-Level Data Analysis for the Saturated Zone Site-Scale Flow and Transport Model* (BSC 2004 [DIRS 170009]).

2. Averaged hydrochemical and isotopic analyses provide values representative of natural, steady-state conditions in the flow system. In general, groundwater samples were collected from boreholes from which many borehole volumes of groundwater had been pumped prior to sampling. In many cases, data were available from sampling events at different times, such that the dataset could be evaluated for outliers and/or temporal trends to determine the validity of this assumption. Because these data are used in this report to define broad regional patterns, geochemical anomalies that may be due to

violations of this assumption can be distinguished from regional trends and are not used to define regional geochemical patterns and flow pathways. Anomalous values are excluded for reasons provided in the supporting documentation for the source DTNs, and in table footnotes.

3. Hydrochemical and isotopic compositions from the uppermost open interval of each borehole represent the uppermost part of the saturated zone (i.e., the water table). The rationale for this assumption is presented in Section 6.2.1 of *Water-Level Data Analysis for the Saturated Zone Site-Scale Flow and Transport Model* (BSC 2004 [DIRS 170009]).

B6. ANALYSIS OF NEW HYDROCHEMICAL AND ISOTOPIC DATA

B6.1 OBJECTIVES

The specific objectives of this appendix as outlined in *Technical Work Plan for Saturated Zone Flow and Transport Modeling* (BSC 2006 [DIRS 177375], Section 1.2.2, p. 7) are to incorporate new data on major ion chemistry, uranium series and ^{14}C and to evaluate the impact of these data on inferred groundwater flow pathways and travel times. Appendix A is a compilation and interpretation performed by the YMP of hydrochemical and isotopic data, for data that were available through 2003. Since then, several new boreholes have been drilled, and data from these boreholes as well as new data from existing boreholes have become available. This appendix presents and evaluates new data that were available as of September 2006.

New analytical methods have been used to obtain some of the ^{14}C data evaluated herein. These methods involve the measurement of ^{14}C on the organic fraction of carbon present in the groundwater. This method was not employed to collect data reported in Appendix A, and therefore a brief description of methodology is presented in Section B6.5.

B6.2 New Nye County EWDP Wells

Locations of 19 boreholes with 35 sampled intervals or zones cited in this appendix are shown in Figure B6-1. The new wells are located south of the Yucca Mountain repository, partially filling the previous gap in borehole distribution between the cluster of wells in central and northern Yucca Mountain, and the line of wells along U.S. Highway 95.

In Appendix A, each groundwater sample was assigned to one of 22 different hydrochemical groups. This convention is continued for the new groundwater samples presented in this update, with each new borehole being assigned to one of the existing groups; no new hydrochemical groupings are necessary to categorize the new data. Each group is identified by a unique symbol and color, which are then used in plots throughout Appendices A and B. Groupings are based largely on geographic distribution or common physiographic feature, as well as on hydrochemical similarities and/or trends. A brief geographic and hydrochemical description of the groups to which the new EWDP wells have been assigned follows. Hydrochemical trends of the new EWDP well samples are shown on trilinear (Piper) plots (Figure B6-2). The group assignments for the new wells are listed in Table B4-1 and shown in Figure B6-3. Sections B6.3 and B6.4 incorporate these new data into updated maps showing areal distributions of individual chemical species and in updated scatter plots addressing the implications of the new data for

groundwater mixing relationships. Throughout this appendix, borehole designations may be shortened by dropping the Nye County prefixes. For example, most Nye County boreholes identified by NC-EWDP-xxx are shortened to read -xxx. Each borehole identifier is followed by the sample number(s) assigned to it in Table B4-1, and as shown in Figure B6-1.

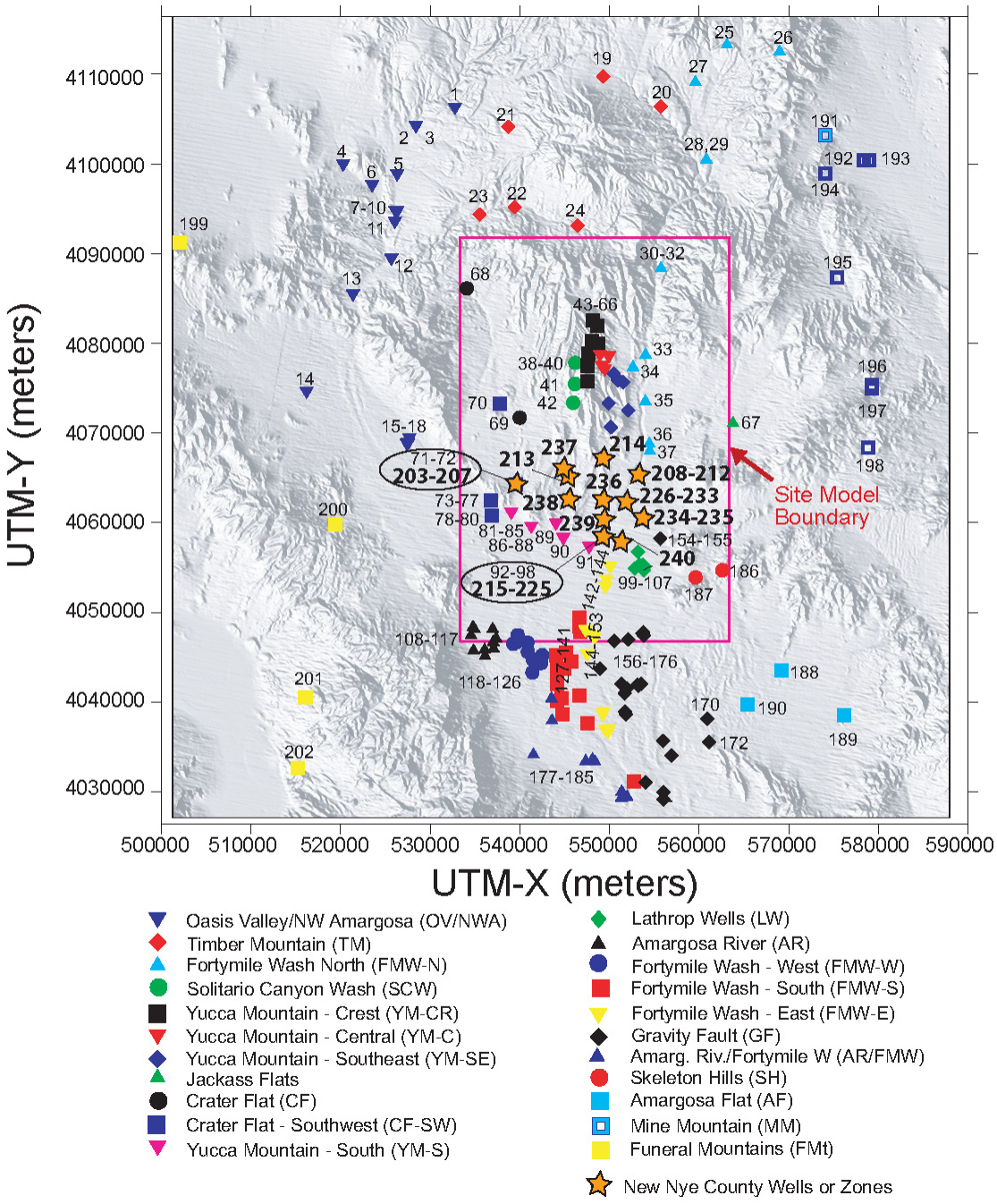

Sources: Figure A6-5, Tables A4-3 and B4-1.

NOTES: This figure has color-coded data points and should not be read in a black and white version.

UTM-X = UTM-Easting; UTM-Y = UTM-Northing; UTM = Universal Transverse Mercator.

The new borehole locations, 203 through 240, are defined in Table B4-1, which is a continuation of the sample number sequence listed in Table A4-3.

Figure B6-1. Map Showing Locations of New Nye County Boreholes in the Vicinity of the Northern Amargosa Desert

Borehole NC-EWDP-7SC (samples 203 to 207) was drilled proximal to borehole NC-EWDP-7S (sample 71). Borehole -7SC contains four screens. The chemistry of the upper three zones of -7SC is very similar to that of -7S, with these four samples plotting nearly on top of one another on the trilinear diagram in Figure B6-2, as well as to data previously presented for the composite sample of -7SC (sample 72). Both -7S and -07SC were assigned to the Crater Flat—Southwest (CF-SW) hydrochemical group in Appendix A. Accordingly, borehole -7SC is also assigned to the CF-SW group.

Hydrochemistry data are available for several boreholes drilled in new locations in the region between the repository and U.S. Highway 95. These include boreholes NC-EWDP-16P, -18P, -24P, -27P, -28P, and -29P (samples 213, 214, 236, 237, 238, and 239, respectively). In addition to these six new boreholes, new hydrochemistry data have become available for five boreholes at the NC-EWDP-19 complex (-19D, -19IM1, -19IM2, -19P, and -19PB; samples 215–225). All of these boreholes are provisionally assigned to the Yucca Mountain—South (YM-S) hydrochemical grouping, primarily on the basis of geographic distribution although this assignment is also supported by the general similarity between their geochemical signatures and those of other boreholes in the YM-S group (Figure B6-2). Patterson and Striffler (2006 [DIRS 178743], Figure 1) assigned three of these boreholes (-16P, -27P, and -28P) to their Western hydrochemical facies, distinguishing these from boreholes to the east, which were assigned to their Eastern hydrochemical facies. The grouping presented here is strictly for convenience, and is not meant to connote genetic relationships among different groundwaters or to guide interpretation of flow pathways. As more boreholes become available in this region and as additional hydrochemical data are made available for evaluation, the YM-S group may warrant finer subdivision.

Multiple new boreholes were drilled at two new locations along Fortymile Wash. Hydrochemical data are available for two new boreholes at the NC-EWDP-10 location (-10P and -10S; samples 208 to 212), and for three new boreholes at the NC-EWDP-22 location (-22PA, -22PB, and -22S; samples 226 to 233). These boreholes contain multiple screened intervals, some of which show chemical characteristics that differ slightly from those in other zones of the same borehole (Figure B6-2). Nonetheless, the general hydrochemistry of these boreholes and most of their individual zones is sufficiently consistent to justify assigning all of them to a single group, the Fortymile Wash—North (FMW-N) grouping.

As pointed out by Patterson and Striffler (2006 [DIRS 178743], p. 393) and by Futa et al. (2006 [DIRS 178742], p. 305), geochemical data for groundwater from NC-EWDP-19PB and -22S show evidence supporting the possibility of vertical stratification in this part of the flow system. This interpretation is based mostly on chemical and isotopic data obtained from a detailed vertical sampling of groundwater extracted from aquifer material collected during drilling. The main conclusion of these studies is that groundwater derived primarily from recharge along Fortymile Wash may overlie older groundwater derived from regions to the north, closer to the repository footprint.

Borehole Washburn-1X (sample 240) is located due south of NC-EWDP-22 (assigned to the FMW-N group), and midway between boreholes of the NC-EWDP-19 complex (assigned to the YM-S group) and boreholes of the NC-EWDP-4PA, -4PA, and -4PC complex (assigned to the Amargosa Valley group (LW, reflecting that this area was formerly called Lathrop Wells). The chemistry of Washburn-1X is not distinctly different from any of these three locations, but most closely resembles groundwater in the FMW-N grouping (Figure B6-2), to which it is therefore assigned.

Groundwater from borehole NC-EWDP-23P (samples 234 and 235) has a fairly distinctive chemistry with relatively high SO_4, low $\delta^{34}S$, and other geochemical characteristics most similar to those of groundwater from well J-11 (sample 67) in Jackass Flats (Figure B6-2). Borehole -23P also lies along Flow Path 3 (Figure A6-62, updated in Section B6.6), which originates at well J-11 and passes through other boreholes assigned to the Amargosa Valley (LW, Lathrop Wells) grouping. Accordingly, borehole -23P is also assigned to the LW group.

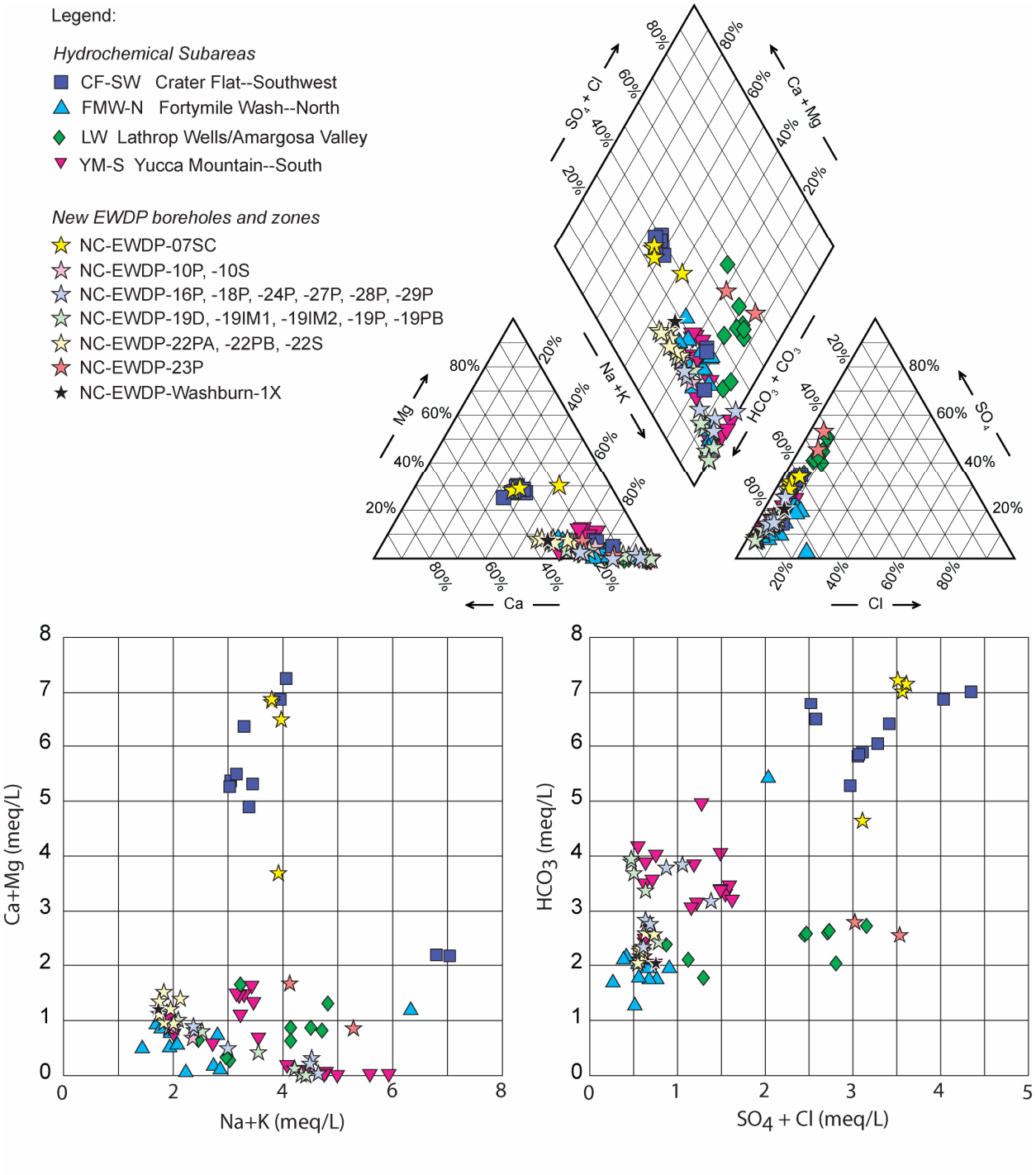

Sources: Tables A6-1 and B4-2.

NOTES: Units for the trilinear plot are percent milliequivalents (meq) per liter.

Figure B6-2. Trilinear and Scatter plots for New Nye County Boreholes and Zones

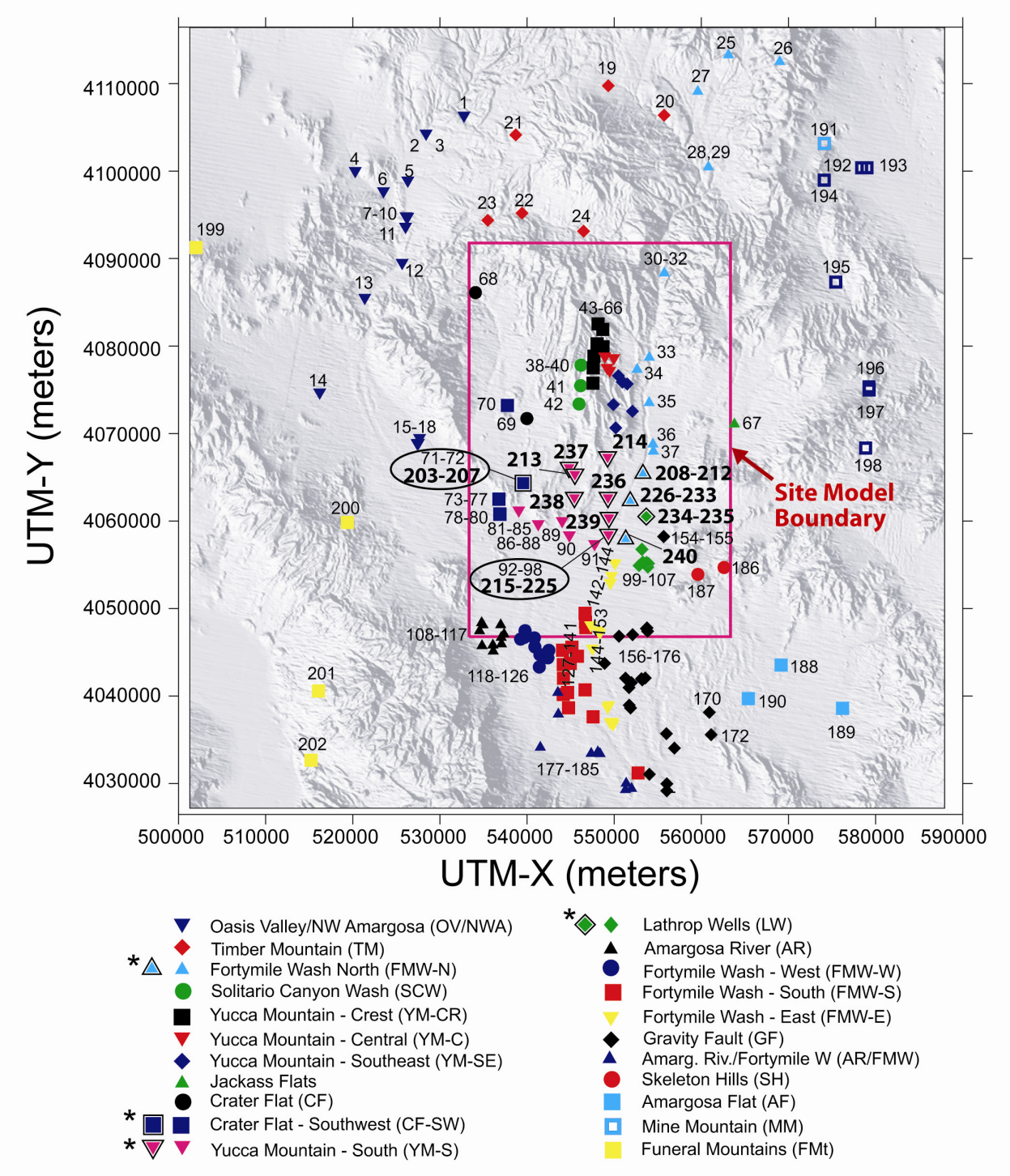

NOTES: This figure has color-coded data points and should not be read in a black and white version.

A black and white border around a plotted symbol (such as those marked with an asterisk in the legend) identifies new Nye County boreholes and zones, which are overlaid on the map from Figure A6-5. The numbers assigned to these new locations, 203 through 240, are defined in Table B4-1, which is a continuation of the sample number sequence listed in Table A4-3.

UTM-X = UTM-Easting; UTM-Y = UTM-Northing; UTM = Universal Transverse Mercator.

Figure B6-3. Map Showing Assignment of New Nye County Boreholes to Hydrochemical Groupings

B6.3 ANALYSIS OF AREAL DISTRIBUTIONS OF NEW HYDROCHEMICAL AND ISOTOPIC DATA

Maps showing the areal distributions of selected chemical species are presented in this section. Selection of these chemical species follows that in the TWP (BSC 2006 [DIRS 177375], Section 2.1.2.2) and is supported by the following rationale. Chloride, sulfate and bicarbonate are plotted because they are major groundwater constituents and because chloride and sulfate, in particular, tend to behave as conservative species and therefore are potentially very informative for tracing groundwater flow pathways. Calcium is plotted to illustrate the distribution of this major divalent cation, and sodium is plotted as the major monovalent cation. One of the objectives of this appendix, as established in the TWP (BSC 2006 [DIRS 177375], Section 2.1.2.2), is to qualitatively evaluate new carbon isotope data with respect to their implications for transport velocities. As described in Section A6.3.1.2.2, interpretation of ^{14}C groundwater ages is aided by knowledge of $\delta^{13}C$ as well as the ^{14}C values. Accordingly, spatial distributions are shown for both stable and radioactive carbon isotopes.

The following maps of areal distributions plot the new data with distinctive white and black outlines surrounding the symbols coded by shape and color to represent different concentration ranges. Many locations have multiple boreholes, as well as multiple sampled zones for a single borehole. It is difficult in these two-dimensional maps to illustrate ranges of values. Therefore, the presentation of data in this section follows the practice described in Section A6.3.4, by selecting one or in some cases two values considered to best represent the average groundwater composition at each mapped location. Data from uppermost intervals are given slightly more weight than those from deeper intervals because the higher zones are considered more likely to describe the transport flowpaths from the repository (with the possible exception of boreholes in the Fortymile Wash area, as discussed in the previous section). As described in Section A6.3.4, vertical heterogeneity is recognized as being present and undoubtedly complicates this two-dimensional evaluation of flow pathways.

A number of the new samples in this appendix are from one of the boreholes that had previously produced a sample (from a different interval than the new one) that was included in Appendix A. A sample in this appendix is plotted as “new data” as described above only if its concentration differs significantly from that of the previous sample from this borehole. For example, borehole NC-EWDP-7SC was completed with four screened intervals after Appendix A was prepared in 2003. The chemistry of the upper three zones of -7SC is very similar to that of -7S as well as to data previously presented for the composite interval of -7SC. No changes to the symbols used for this location in Appendix A are required for many solutes and therefore only new data that differ significantly from older data are shown as “new” in the following plots. Interpretations based on data presented for borehole -7SC in Appendix A are not affected by the new data. The borehole complex at NC-EWDP-19 contains three new boreholes, most with multiple sampled intervals. These new data were examined for consistency with data presented in Appendix A, with emphasis placed on data from upper intervals in these new wells. The symbols plotted at the -19 location were modified only for those few cases in which the new data extended the range of values previously displayed. Consistent values were not changed. The new data do not affect this two-dimensional analysis, although they do further define the range of vertical anisotropy at this site.

B6.3.1 Areal Distribution of Chloride in Groundwater (Figure B6-4)

Chloride concentration data are shown in Figure B6-4. Most new samples in the YM-S and FMW-N groupings show low chloride concentrations (< 7 mg/L) typical of this region and of boreholes further north near the repository footprint. Exceptions to this trend are boreholes NC-EWDP-16P, -27P, and -28P (samples 213, 237, and 238), with slightly higher chloride concentrations (8.5 mg/L, 9.0 mg/L, and 7.6 mg/L, respectively). This slight increase may reflect small amounts of flow contributed from the west or northwest. Borehole Washburn-1X (sample 240) has a low chloride value (6.9 mg/L) typical of surrounding groundwater. The two screens in borehole -23P (samples 234 and 235) have significantly higher chloride values (10.8 mg/L and 13.6 mg/L), which likely reflect addition of groundwater from the northeast as discussed in the next section.

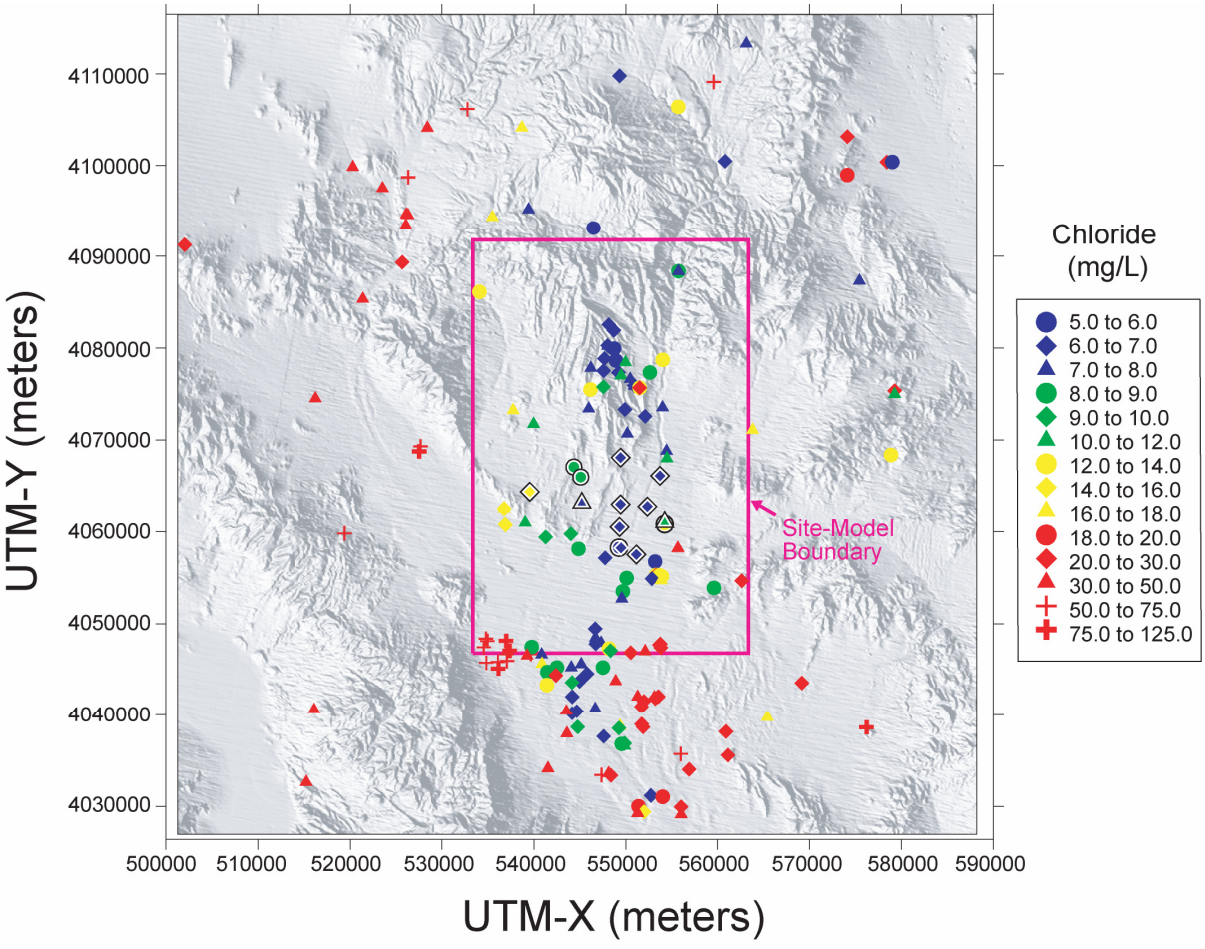

Sources: Tables A6-1 and B4-2.

NOTES: This figure has color-coded data points and should not be read in a black and white version.

A black and white border around a plotted symbol (such as those marked with an asterisk in the legend) identifies new Nye County boreholes and zones, as well as any existing locations for which new data support reassignment to a different concentration category than was used in Figure A6-15.

UTM-X = UTM-Easting; UTM-Y = UTM-Northing; UTM = Universal Transverse Mercator.

Figure B6-4. Areal Distribution of Chloride in Groundwater

B6.3.2 Areal Distribution of Sulfate in Groundwater (Figure B6-5)

Sulfate concentrations are shown in Figure B6-5. Samples NC-EWDP-18P, -24, -29 (samples 214, 236, and 239) as well as those from new boreholes along Fortymile Wash (-10 complex, samples 208 to 212; -22 complex, samples 226 to 233) have consistent sulfate concentrations (19 mg/L to 27 mg/L) that are typical of groundwater to the north. Boreholes -16P, -27P, and -28P (samples 213, 237, and 238) have slightly elevated sulfate concentrations (55 mg/L, 39 mg/L, and 32 mg/L, respectively) that, similar to the interpretation of the chloride values, may indicate contribution of groundwater from the northwest or west in Crater Flat, which have consistently higher sulfate concentrations compared to boreholes nearer the repository footprint to the north. Sulfate concentrations in borehole -23P (samples 234 and 235) are relatively high (127 mg/L and 155 mg/L), which is likely to reflect flow from the northeast or east. Washburn-1X (sample 240) has a sulfate concentration (27 mg/L) that is intermediate between sulfate concentrations of boreholes located to the north and west and those located to the east. This intermediate sulfate concentration may indicate flow of groundwater from the northeast or east through the Washburn-1X locality.

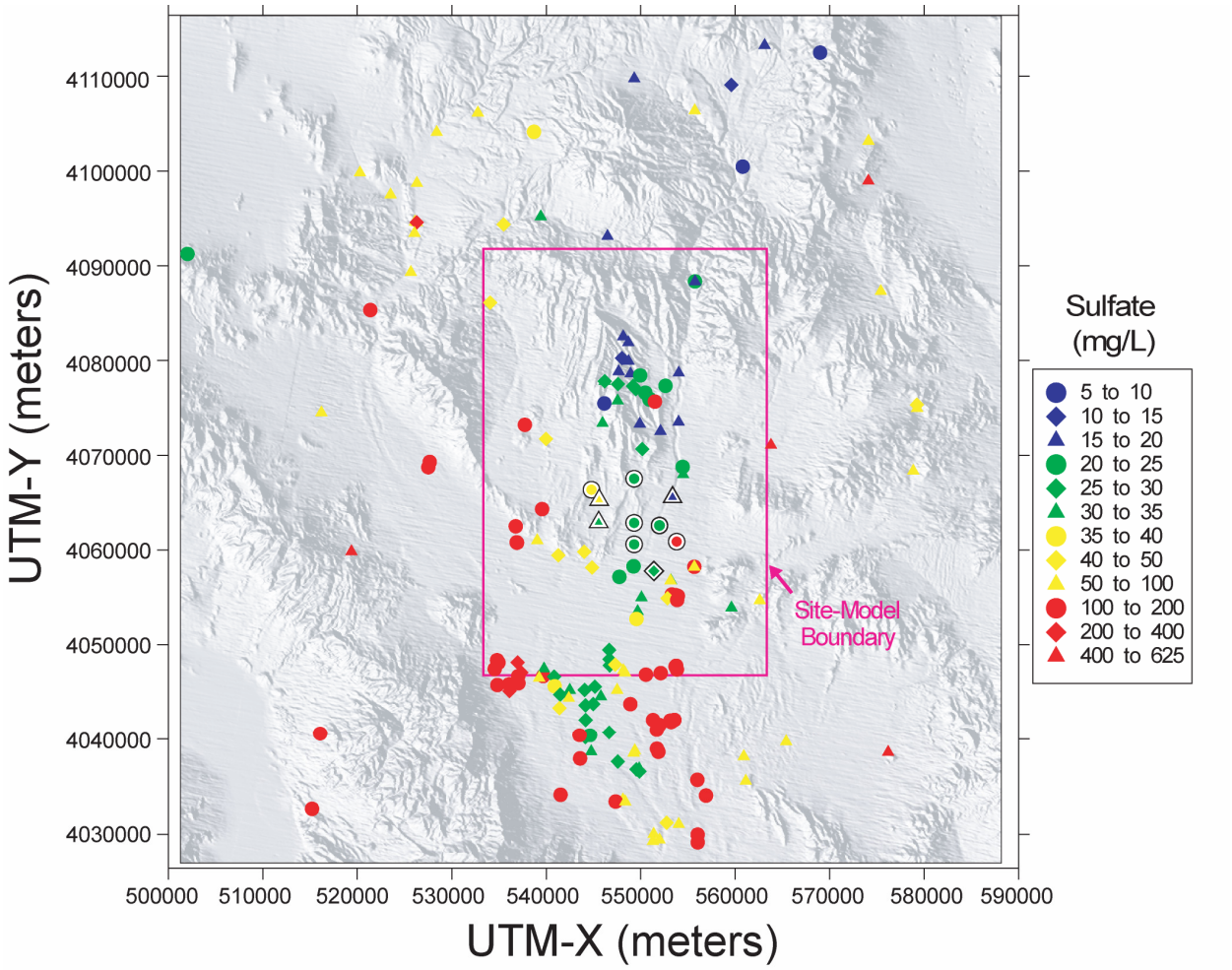

Sources: Tables A6-1 and B4-2.

NOTES: This figure has color-coded data points and should not be read in a black and white version.

A black and white border around a plotted symbol identifies new Nye County boreholes and zones, as well as any existing locations for which new data support reassignment to a different concentration category than was used in Figure A6-16.

UTM-X = UTM-Easting; UTM-Y = UTM-Northing; UTM = Universal Transverse Mercator.

Figure B6-5. Areal Distribution of Sulfate in Groundwater

B6.3.3 Areal Distribution of Bicarbonate in Groundwater (Figure B6-6)

Bicarbonate concentrations are shown in Figure B6-6. Samples NC-EWDP-16P, -27P, and -28P (samples 213, 237, and 238) have bicarbonate concentrations (190, 222, and 213 mg/L) that are higher relative to samples to the east, but which are typical of samples to the north and west. The rest of the samples from the new Nye County boreholes have slightly variable bicarbonate concentrations ranging between 125 to 173 mg/L. This concentration range is within the range of samples to the north.

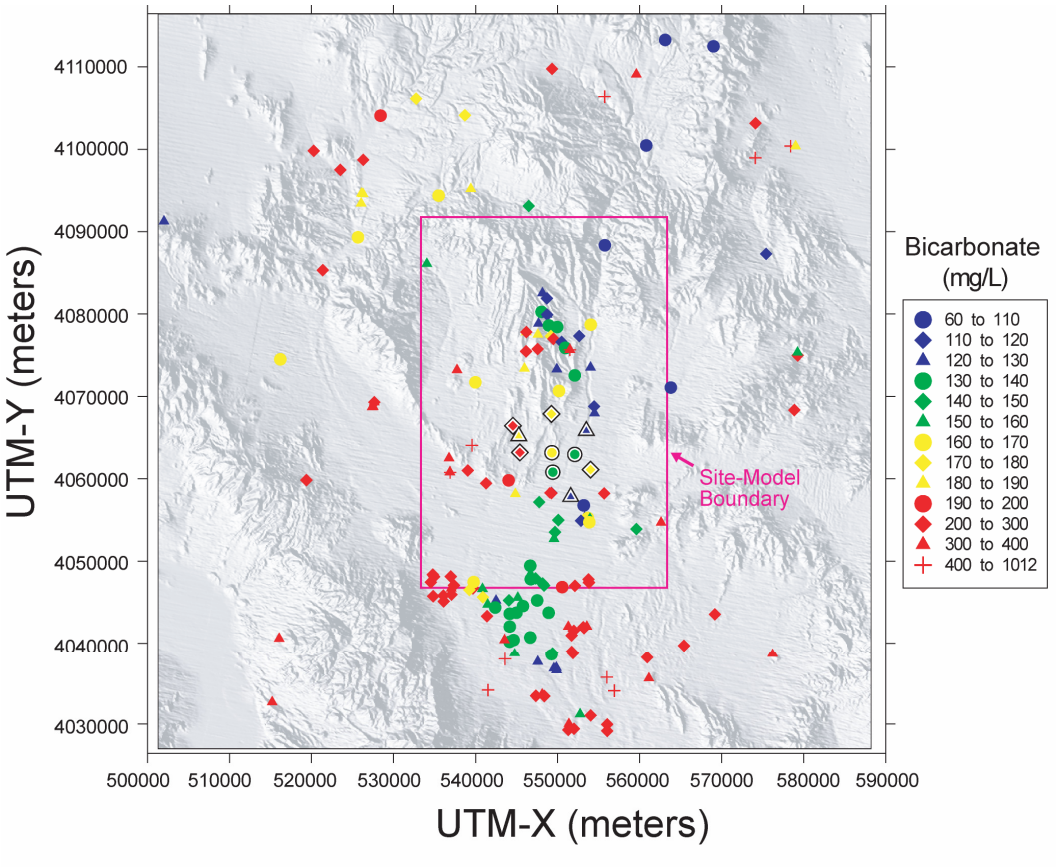

Sources: Tables A6-1 and B4-2.

NOTES: This figure has color-coded data points and should not be read in a black and white version.

A black and white border around a plotted symbol identifies new Nye County boreholes and zones, as well as any existing locations for which new data support reassignment to a different concentration category than was used in Figure A6-17.

UTM-X = UTM-Easting; UTM-Y = UTM-Northing; UTM = Universal Transverse Mercator.

Figure B6-6. Areal Distribution of Bicarbonate in Groundwater

B6.3.4 Areal Distribution of Calcium in Groundwater (Figure B6-7)

Calcium concentrations are shown in Figure B6-7. Samples -16P, -27P, and -28P (samples 213, 237, and 238) have low calcium concentrations (≤ 5 mg/L), similar to samples from the Solitario Canyon Wash and Yucca Crest groupings to the north. Samples -23P (samples 234 and 235) and Washburn-1X (sample 240) have calcium concentrations (16 to 25 mg/L) that are higher relative to most samples to the west and north. The only upgradient location in the region with higher calcium concentrations than these two boreholes is borehole J-11 (sample 67 in Table A6-1, 76.5 mg/L). The remaining samples have low to intermediate calcium concentrations (mostly < 20 mg/L) typical of locations to the north.

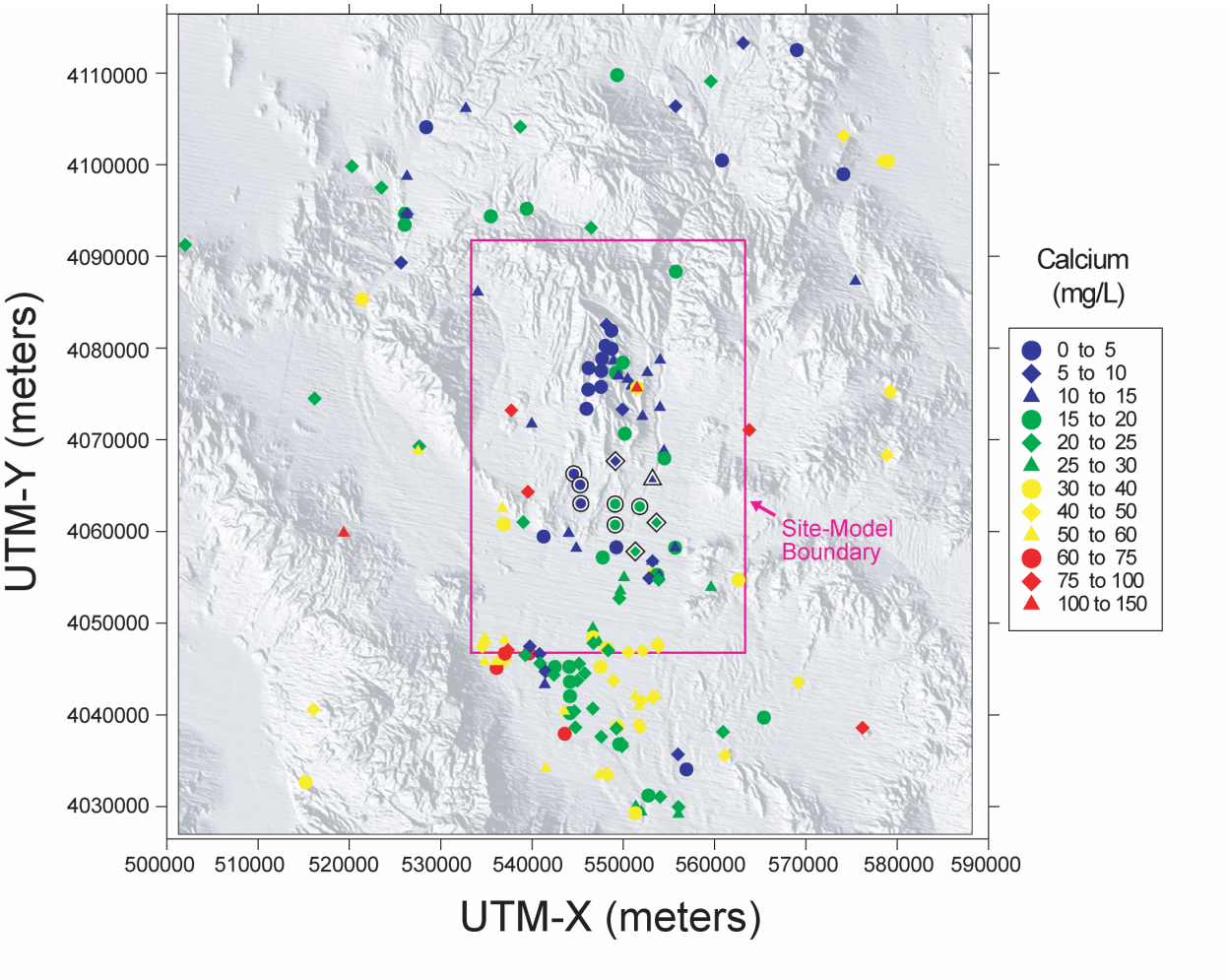

Sources: Tables A6-1 and B4-2.

NOTES: This figure has color-coded data points and should not be read in a black and white version.

A black and white border around a plotted symbol identifies new Nye County boreholes and zones, as well as any existing locations for which new data support reassignment to a different concentration category than was used in Figure A6-20.

UTM-X = UTM-Easting; UTM-Y = UTM-Northing; UTM = Universal Transverse Mercator.

Figure B6-7. Areal Distribution of Calcium in Groundwater

B6.3.5 Areal Distribution of Sodium in Groundwater (Figure B6-8)

Sodium concentrations are shown in Figure B6-8. Sodium concentrations in samples -16P, -27P, and -28P (samples 213, 237, and 238; 101 mg/L to 106 mg/L) are higher relative to most samples to the northwest; however, they are similar to some boreholes in the Solitario Canyon Wash and Yucca Crest groupings. Sodium concentrations in sample -23P (samples 234 and 235, 90 and 119 mg/L) are intermediate between that for sample J-11 (154 mg/L, sample 67 in Table A6-1) and samples to the north. The remaining samples have low sodium concentrations mostly within a range of 37 to 80 mg/L, typical of samples to the north.

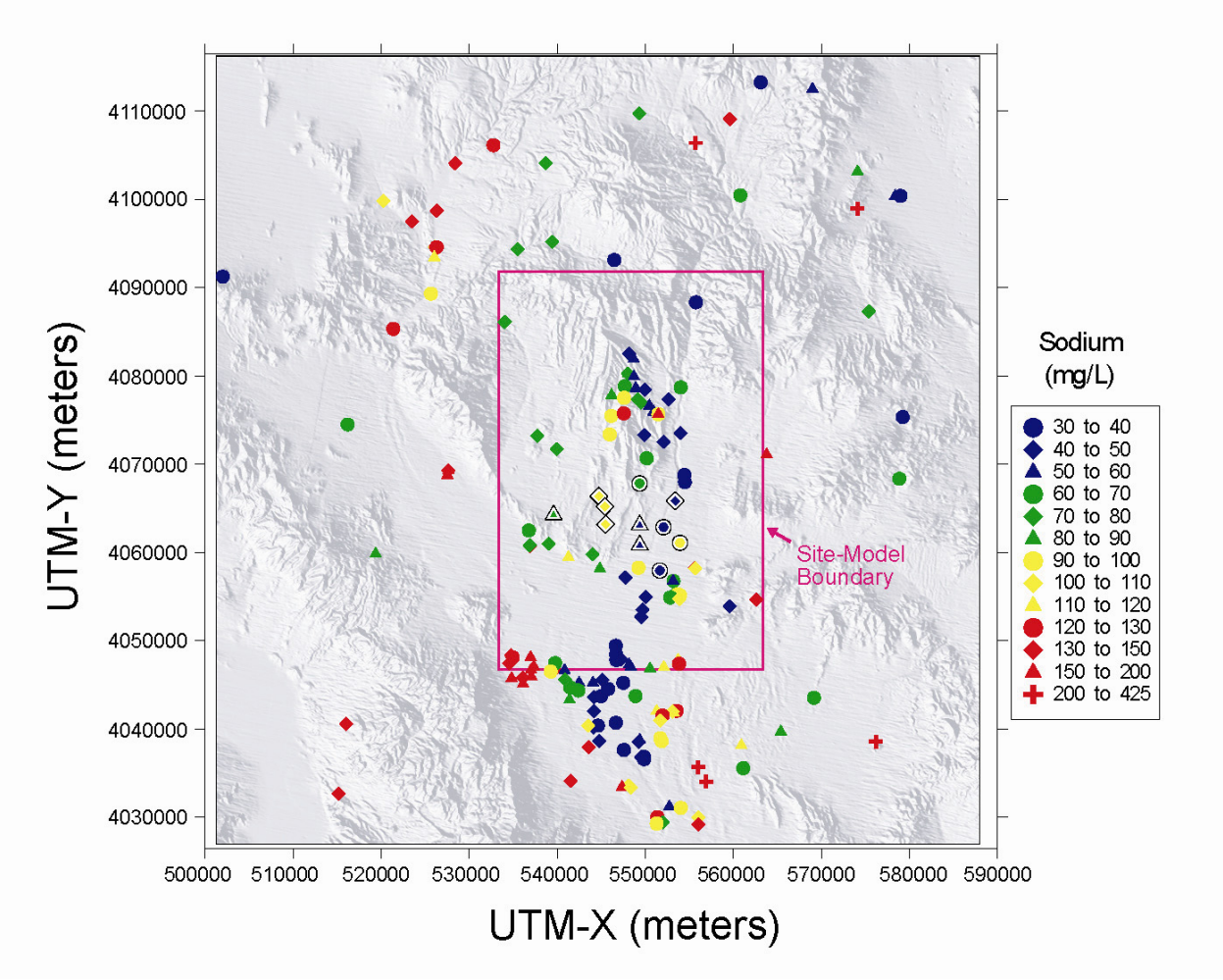

Sources: Tables A6-1 and B4-2.

NOTES: This figure has color-coded data points and should not be read in a black and white version.

A black and white border around a plotted symbol identifies new Nye County boreholes and zones, as well as any existing locations for which new data support reassignment to a different concentration category than was used in Figure A6-22.

UTM-X = UTM-Easting; UTM-Y = UTM-Northing; UTM = Universal Transverse Mercator.

Figure B6-8. Areal Distribution of Sodium in Groundwater

B6.3.6 Areal Distribution of Delta ^{13}C in Groundwater (Figure B6-9)

The areal distribution of $\delta^{13}C$ values is shown in Figure B6-9. The new samples show a range of values that is generally typical of values documented in upgradient areas to the north. The shallowmost sample from each of the new boreholes located adjacent to Fortymile Wash (-10P Zone 1, -10S Zone 1, -22PA Zone 1, -22PB Zone 1, -22S Zone 1, and Washburn-1X; samples 208, 211, 226, 228, 230, and 240, respectively), have slightly lighter (more negative) values (−9.1 to −10.5 per mil, Table B4-3) compared to deeper samples from the same boreholes or samples from wells immediately to the north (−7.9 and −8.6 per mil for J-12 and JF#3, samples 36 and 37 in Table A6-2). This lighter isotopic signal has been cited as evidence for more recent recharge of water via Fortymile Wash (Patterson and Striffler 2006 [DIRS 178743], p. 392). To

the east of Fortymile Wash, sample -23P also has light $\delta^{13}C$ values (–10.5 and –10.6 per mil, samples 234 and 235 in Table B4-3) that are similar to those for borehole J-11 (–11.0 per mil, sample 67 in Table A6-2) and the Amargosa Valley (LW, Lathrop Wells) grouping (–9.1 to –10.5 per mil, samples 99, 100, 101, and 106 in Table A6-2).

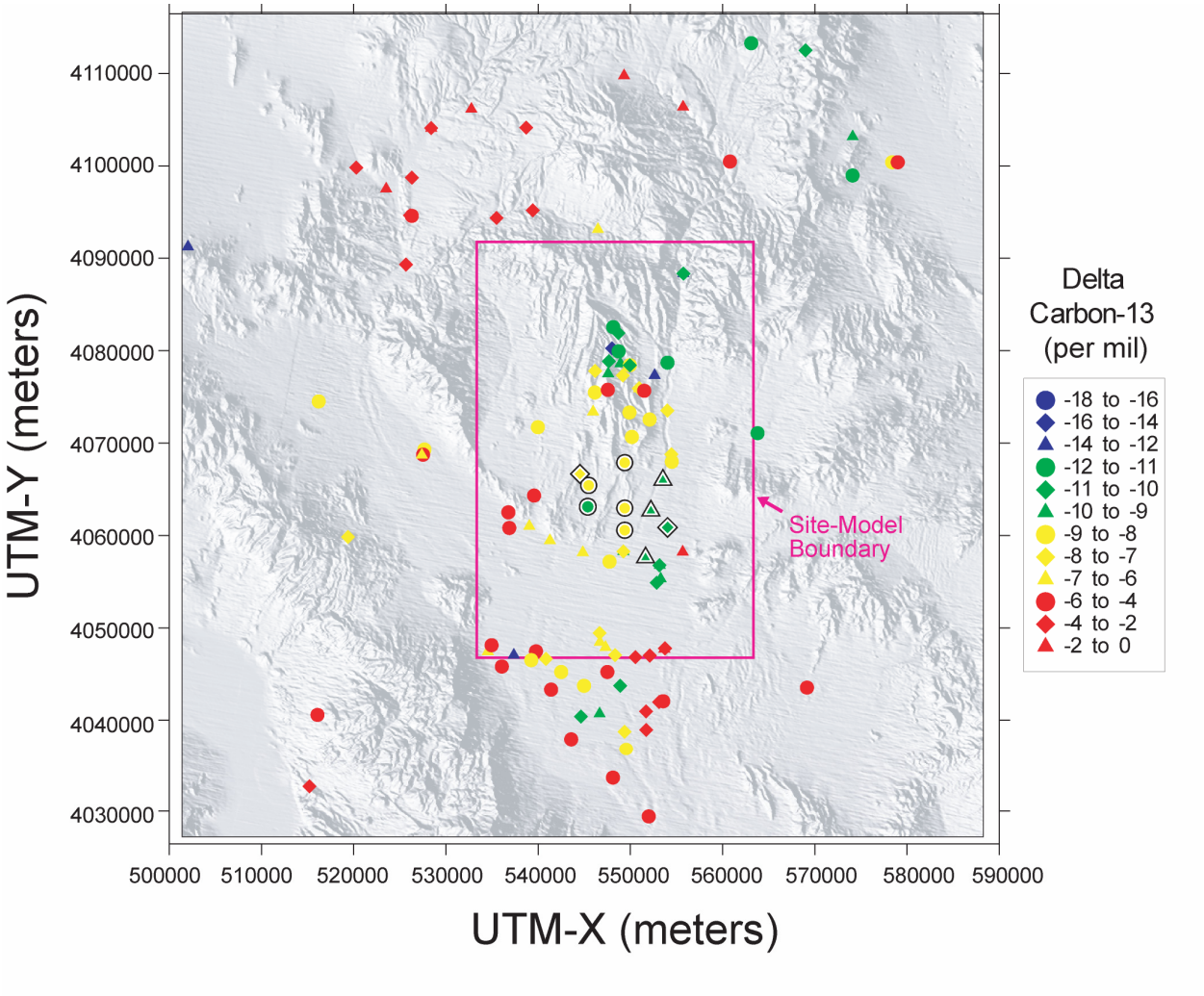

Sources: Tables A6-2 and B4-3.

NOTES: This figure has color-coded data points and should not be read in a black and white version.

A black and white border around a plotted symbol identifies new Nye County boreholes and zones, as well as any existing locations for which new data support reassignment to a different isotopic category than was used in Figure A6-27.

UTM-X = UTM-Easting; UTM-Y = UTM-Northing; UTM = Universal Transverse Mercator.

Figure B6-9. Areal Distribution of Delta ^{13}C in Groundwater

B6.3.7 Areal Distribution of ^{14}C in Groundwater (Figure B6-10)

The areal distribution of ^{14}C activities is shown in Figure B6-10. Data from new samples show a trend that is generally consistent with that of previously reported samples. The new samples show a general increase in ^{14}C activity from west to east. Samples -16P, -27P, and -28P (samples 213, 237, and 238) have ^{14}C activities between 12 and 17 pmc, values that are common

to the north and west. A central group of samples (-18P, -24P, and -29P) have slightly higher activities between 17 and 21 pmc (samples 214, 236, and 239 in Table B4-3). Samples along Fortymile Wash from -10, -22, and Washburn-1X have values generally between 20 and 25 pmc. The ^{14}C activity for borehole VH-2 (7.0 pmc, sample 70 in Table B4-8), which had not previously been included in Appendix A, is also plotted. This value is consistent with other values for the CF-SW grouping.

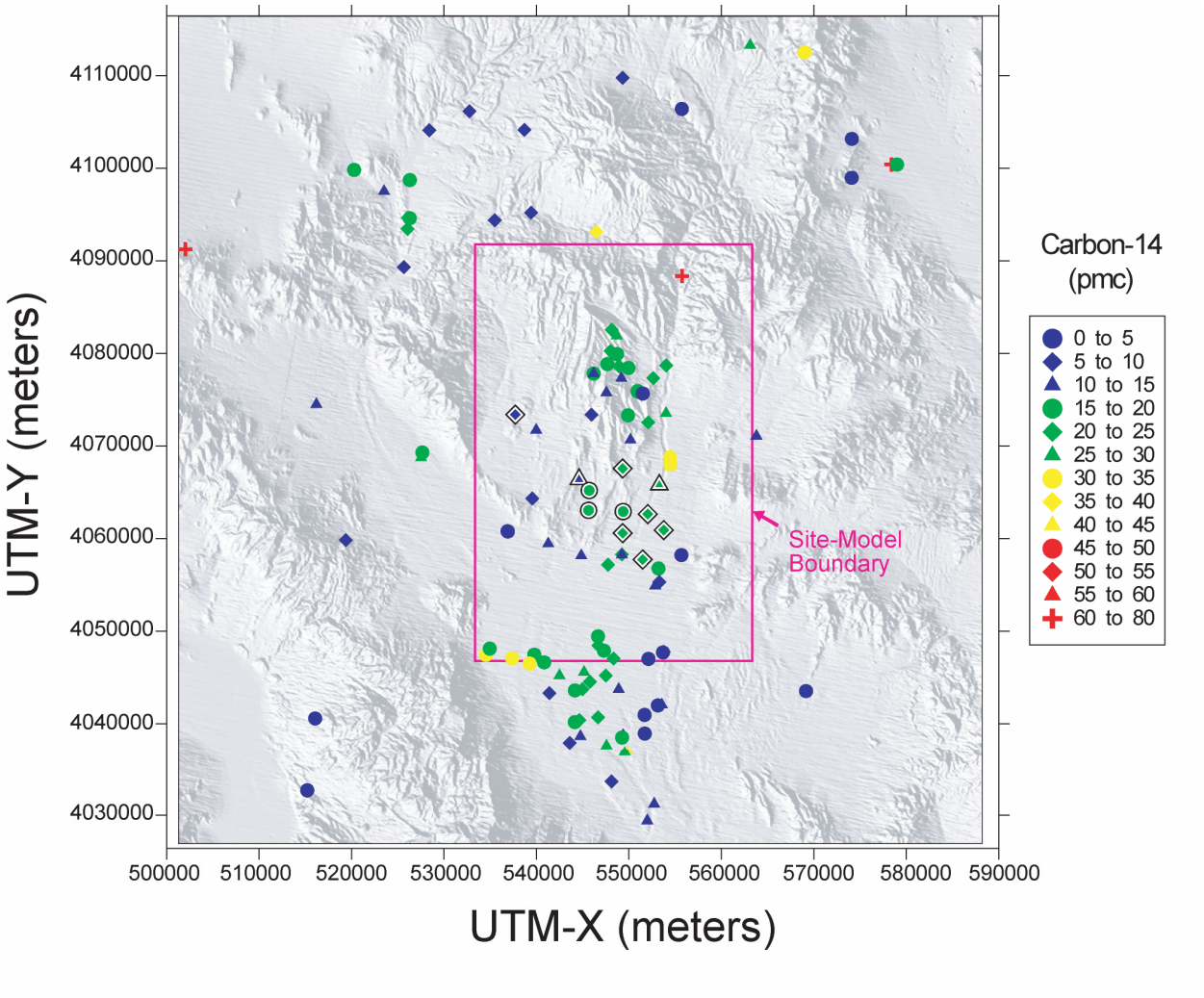

Sources: Tables A6-2 and B4-3.

NOTES: This figure has color-coded data points and should not be read in a black and white version.

A black and white border around a plotted symbol identifies new Nye County boreholes and zones, as well as any existing locations for which new data support reassignment to a different radiocarbon activity category than was used in Figure A6-28.

UTM-X = UTM-Easting; UTM-Y = UTM-Northing; UTM = Universal Transverse Mercator.

Figure B6-10. Areal Distribution of ^{14}C in Groundwater

B6.3.8 Areal Distribution of $^{234}U/^{238}U$ Activity Ratios in Groundwater (No Figure)

Few new uranium isotopic data have become available since production of Appendix A. New uranium isotopic data are presented in Table B4-6. Taken as a whole, the dataset helps to better define regional variations in uranium activity ratios. Activity ratios for groundwater to the north of Yucca Mountain (ER-EC-08, ER-30-1 upper and lower; 5.1, 2.0, and 2.5, respectively; Table B4-6) plot within the range of ratios previously observed in those respective regions. The activity ratio in groundwater from perched water in USW-UZ-14 (7.3, Table B4-6) is typical of values in the Yucca Mountain potential repository area. The ratio for UE-25c#1 (5.7) is lower than the only other value reported for that well complex in Appendix A (8.1 for UE-25c#3, sample 60 in Table A6-2). This result indicates greater variation in uranium activity ratios in this area than was previously recognized. Data from boreholes to the south of Yucca Mountain are generally consistent with values previously reported for the region with a few exceptions. The activity ratio of 7.5 for borehole NC-EWDP-12PA is larger than previously observed for this grouping (CF-SW). The activity ratio reported for borehole NC-EWDP-05SB (4.1, sample 155, Table B4-6) is less than that measured in adjacent borehole -5S (6.7, sample 154, Table A6-2). Activity ratios determined for closely spaced boreholes -12PA, -12PB, and -12PC (7.5, 6.5, 4.4, respectively, Table B4-6) differ significantly and indicate vertical heterogeneity in this borehole.

B6.4 ANALYSIS OF NEW EVIDENCE FOR MIXING RELATIONS BETWEEN WATER OF DIFFERENT SOURCES

Examination of areal distribution Figures B6-4 to B6-10 reveals some consistent patterns. For example, samples from boreholes -16P, -27P, and -28P share similar chemical and isotopic characteristics that are also similar to some samples to the north and/or west, but notably dissimilar to samples to the northeast and east. The chemical and isotopic characteristics of samples from borehole -23P are generally unique when compared to those of the most proximal boreholes, but show similarities to borehole J-11 located to the northeast. In the following section these patterns are analyzed to evaluate mixing of different groundwater. This information is then integrated into the delineation of groundwater flow pathways.

As discussed in Section A6.3.7.1, most solute concentrations in groundwater in the YM-S grouping increase to the west, from low values typical of the dilute groundwater near Fortymile Wash and regions to the north, to higher values more typical of the CF-SW grouping to the west. This same general geochemical pattern is also demonstrated with boreholes -16P, -27P, and -28P, which typically have solute concentrations that are intermediate between those of groundwater to the east and those to the west. On a plot of sulfate vs. chloride concentrations (Figure B6-11), these three boreholes plot along a mixing line between samples from the Solitario Canyon Wash grouping and groundwater from either the CF-SW grouping or the CF grouping (borehole VH-1). The trend defined by samples -27P, -28P, and VH-1 (Figure B6-11) suggests mixing with Crater Flat-type water in this area. However, comparison of chloride vs δD (Figure B6-11) as well as of chloride and bicarbonate values suggests that groundwater similar to that of CF-SW grouping is the more likely candidate for mixing. Although an unambiguous distinction cannot be made with the available data, the new data for boreholes -16P, -27P, and -28P increase confidence in the hypothesis that groundwater similar to that of the Solitario Canyon Wash grouping to the north mixes with groundwater derived from the northwest or west in this region.

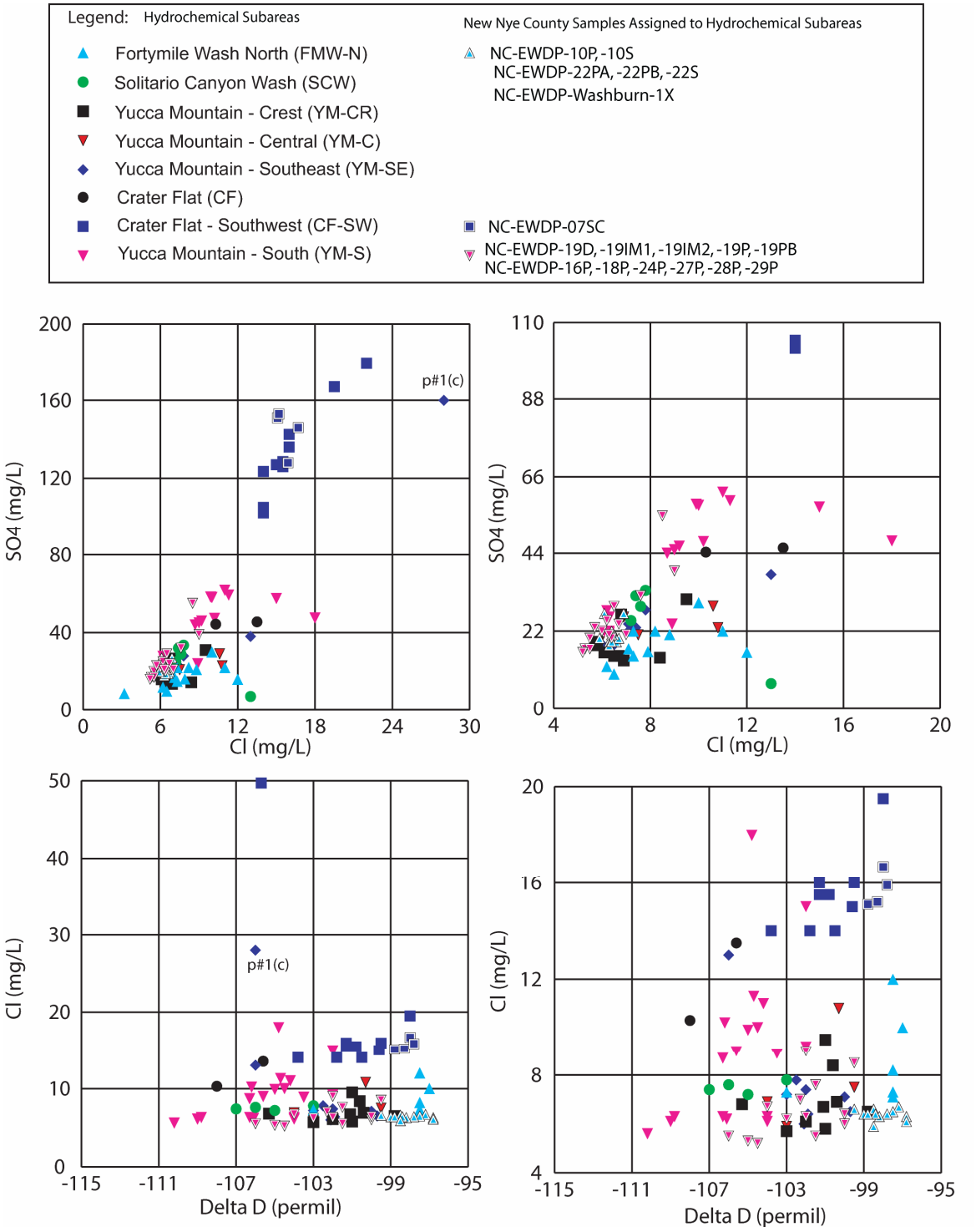

Sources: Tables A6-1, A6-2, B4-2, and B4-3.

NOTE: The plots on the right side of this figure have expanded scale compared to similar plots directly to their left to better display details in the tightly clustered data.

Figure B6-11. Scatter Plots Showing Mixing in Southern Yucca Mountain

In contrast with Figure B6-11, Figure B6-12 focuses specifically on the use of sulfate and chloride concentrations for evaluating mixing endmembers for groundwaters within the site model boundaries, and only to the south and east of Yucca Mountain (i.e. this figure excludes data for groundwater samples to the west or further south). Compared to its nearest neighbors (-27 and -28), groundwater from borehole -16P has an elevated sulfate concentration (55 mg/L, Table B4-2) and plots distinctly above the mixing trend defined by samples -27P and -28P in Figure B6-12, despite the fact that -16P is located roughly halfway between these two wells. This sample also has an anomalously low $\delta^{34}S$ value (4.7 per mil, Table B4-3) (Figure B6-13). Taken together, these data indicate that groundwater in this borehole has a different sulfate source compared to adjacent boreholes.

Groundwater from borehole -23P, which lies east of Fortymile Wash and due north of Amargosa Valley (formerly Lathrop Wells), typically has solute concentrations and isotopic values that are intermediate between proximal samples to the west and south (i.e., samples in the Yucca Mountain—South and Fortymile Wash—East hydrochemical subareas) and those of groundwater from borehole J-11 to the northeast (Figure B6-12). As shown on Figure B6-12, groundwater from Zone 2 of borehole -23P (10.8 mg/L Cl and 155 mg/L SO_4, Table B4-2) plots near the mixing line between dilute samples to the south and west and borehole J-11. Groundwater from Zone 1 (13.6 mg/L Cl and 127 mg/L SO_4, Table B4-2) plots off of this trend and towards the mixing lines formed between the dilute end-member and samples in the Amargosa Valley (Lathrop Wells) group and/or the Gravity Fault Group, suggesting a possible contribution from the east. As shown on Figure B6-13, the source of some of the sulfate in samples from -23P has a lower $\delta^{34}S$ value compared to that from any other borehole plotted on this figure, including the potential upgradient end-member, borehole J-11 (8.8 per mil). As for the case of -16P, these trends also indicate that groundwater in this borehole has a different sulfate source compared to other boreholes in the regional flow system.

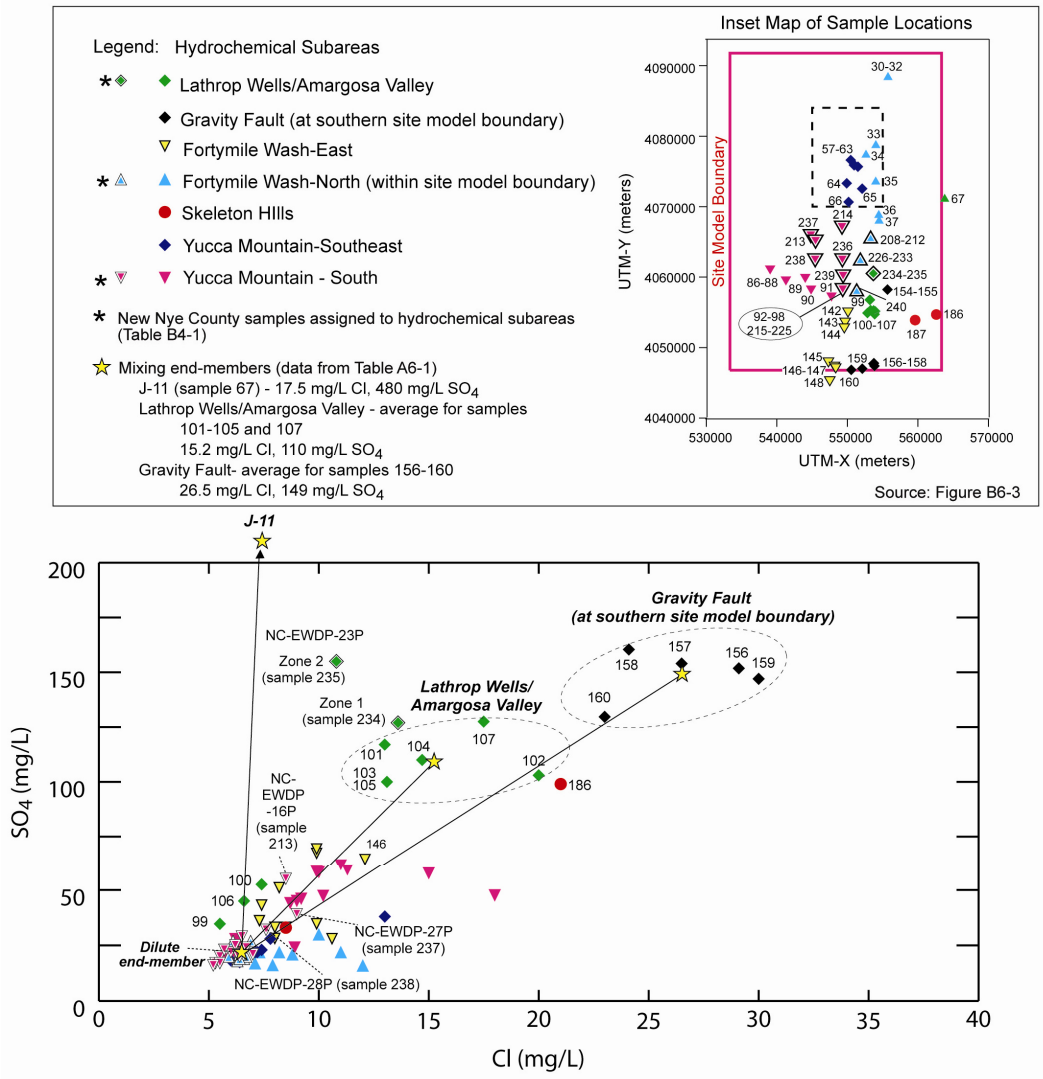

Sources: Tables A6-1 and B4-3.

NOTE: The dilute endmember for all three mixing lines is 6.5 mg/L Cl^- and 22 mg/L SO_4^{2-} and the compositions of the upper endmembers are listed in the legend.

Figure B6-12. Cross Correlation Plot of Sulfate versus Chloride for Groundwaters within the Boundaries of the Site Model, and South and East of Yucca Mountain

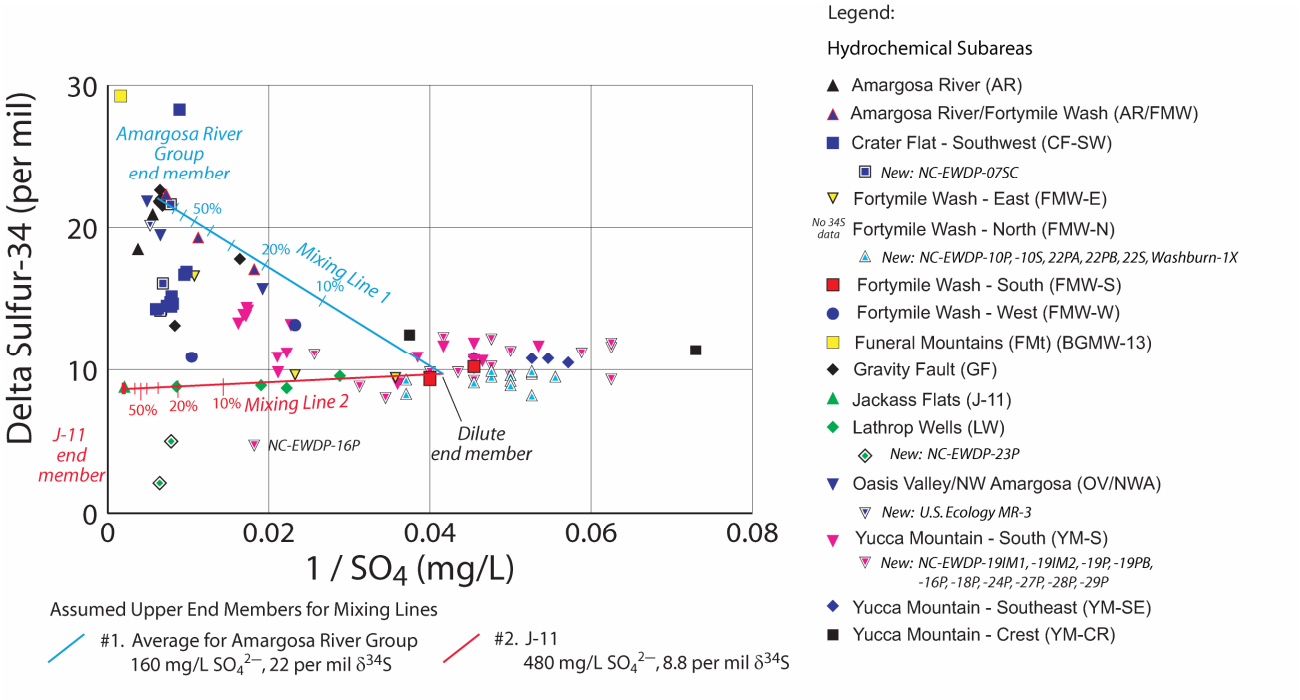

Sources: Tables A6-1, A6-2, B4-2, and B4-3.

NOTE: In this diagram, a mixture plots as a straight line. Mixing lines show tic marks at 10% increments. The dilute endmember for both mixing lines is 24 mg/L SO_4^{2-} and 9.65 per mil $\delta^{34}S$. The compositions of the upper endmembers are listed in the legend. Mixing lines are drawn by plotting calculated values for SO_4^{2-} and $\delta^{34}S$ obtained using the mixing equation: $[\delta^{34}S]_{mix} = \{F \bullet [SO_4^{2-}]_A + (1-F) \bullet [SO_4^{2-}]_B$, where F is the fraction of component A in the mix. $\delta^{34}S$ is determined by: $[\delta^{34}S]_{mix} = \{F \bullet [SO_4^{2-}]_A \bullet \delta^{34}S_A + (1-F) \bullet [SO_4^{2-}]_B \bullet \delta^{34}S_B) / [SO_4^{2-}]_{mix}$.

Figure B6-13. Scatter Plot of $\delta^{34}S$ versus Inverse Sulfur for Samples in the Vicinity of Yucca Mountain and the Amargosa Desert Region

B6.5 ANALYSIS OF NEW EVIDENCE FOR GROUNDWATER TRAVEL TIMES BASED ON ^{14}C

Groundwater travel times based on ^{14}C activities in dissolved inorganic carbon (DIC) can be calculated based on the extent of decrease in ^{14}C activities along a flowpath. However, some proportion of the radiocarbon reduction (expressed as a percentage) may be attributable to its dilution by inorganic carbon sources along the flowpath that contain no measurable ^{14}C activity ("dead" carbon). The result is that the radiocarbon-based travel times may be longer than the actual travel times. A variety of models exist for estimating and correcting for such dilution, based on shifts in stable carbon isotope ratios and in DIC concentrations. These models were reviewed in Section A6.3.9. An alternative approach proposed for obtaining more reliable groundwater travel time estimates is to measure ^{14}C activities in fractions of dissolved organic carbon (DOC). As precipitation infiltrates through the soil zone, it acquires much or most of its carbon (including ^{14}C) from the soil zone. This carbon will be a mixture of "old" carbon, for example from dissolution or exchange with carbonate minerals, and contemporary carbon in the form of decaying organic matter. In this case, the calculated "age" based solely on ^{14}C measurements for DOC fractions will theoretically reflect the actual time of infiltration of the

groundwater. In contrast, "ages" based on total inorganic carbon may require corrections based on assumed models of water-rock interaction (Patterson and Thomas 2005 [DIRS 179459]).

New data that bear on groundwater travel times including ^{14}C, ^{13}C, and DIC values are available for most of the new Nye County Wells. DIC and DOC radiocarbon measurements in groundwater from the Yucca Mountain vicinity are also presented by Patterson and Thomas (2005 [DIRS 179459], Figure 3). These new data are summarized in Figure B6-14 and discussed below.

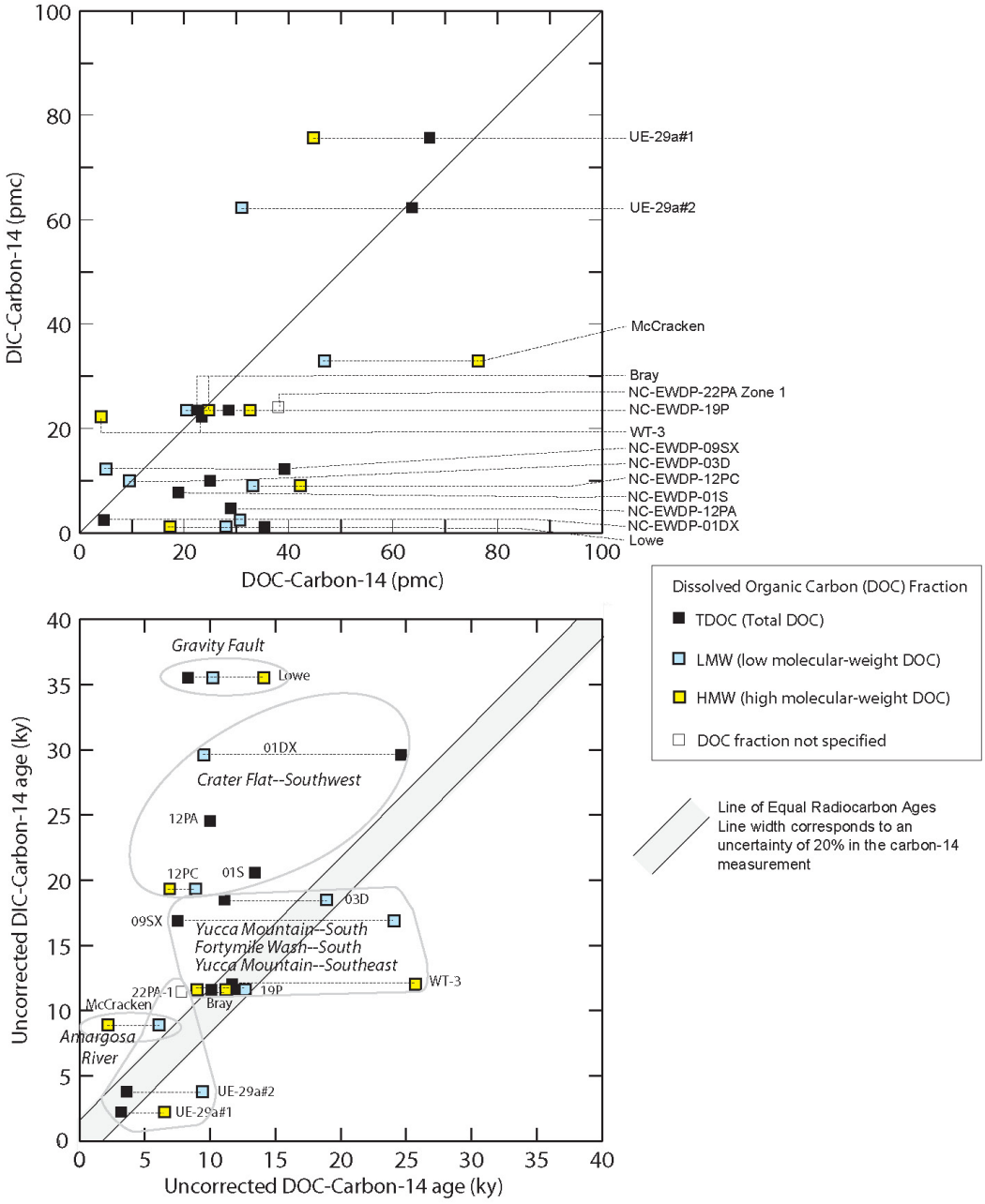

Sources: Tables A6-2 and B6-4, for DIC-14; DTN: GS031208312322.004 [DIRS 179431], for DOC-14.

Figure B6-14. Comparison of Radiocarbon Measurements of Inorganic and Organic Dissolved ^{14}C in Groundwater Samples from the Yucca Mountain Vicinity

Areal distributions of bicarbonate (as a surrogate for DIC), $\delta^{13}C$, and ^{14}C (measured on the DIC fraction) are shown in Figures B6-6, B6-9, and B6-10, respectively. These new inorganic-carbon data are generally consistent with data presented in Appendix A. Although these new data do not show consistent north to south trends, there is a general west to east increase in ^{14}C activity among the new Nye County boreholes (Figure B6-10). This shift corresponds to a decrease in bicarbonate concentration and decrease in $\delta^{13}C$ values. These data are consistent with a greater component of carbonate-derived groundwater in the west compared to the east and a greater component of more recently recharged water along Fortymile Wash.

Preliminary results of uncorrected radiocarbon ages based on ^{14}C activities measured for the total DOC fraction of several groundwaters are reported in DTN: GS031208312322.004 [DIRS 179431]. Figure B6-14 compares these uncorrected ^{14}C-TDOC ages, along with uncorrected radiocarbon ages calculated from separate analyses of the light and heavy molecular-weight DOC fractions, to uncorrected ^{14}C-DIC ages.

^{14}C ages determined from ^{14}C activities in DIC and TDOC fractions are in reasonable agreement for samples UE-29a#1, UE-29a#2, -22PA-1 (although the DOC fraction used for the -22PA-1 age estimate was not specified), -19P, and WT-3, all of which are located near Fortymile Wash. However, ^{14}C ages for these same samples determined from the low or high molecular weight fractions are in poor agreement with ages determined using ^{14}C-DIC. These data plot in fields that indicate a smaller percentage of ^{14}C activity (relative to that in modern carbon) in the DOC fraction relative to that in the DIC fraction and correspondingly older ^{14}C ages. The reason for this shift is unknown at this time. Several other samples plot in fields indicating smaller DIC percentages compared to those of TDOC, which yield older uncorrected ^{14}C ages based on DIC. Many of these samples (-1DX, -12PA, -12PC, and -9SX) are located in the CF-SW region, which hosts groundwater with a distinct carbonate signature. The age relationship noted is consistent with addition of dead carbon as inorganic carbon.

B6.6 REGIONAL FLOWPATHS INFERRED FROM HYDROCHEMICAL DATA

Hydrochemical data from the new boreholes presented above validate many of the flow pathways presented previously (Figure A6-62) and also allow minor refinements of that figure. The new boreholes are located in the region bounded between Flow Path 4 and Flow Path 3. A slightly modified version of the regional flowpath figure (Figure A6-62) is presented in Figure B6-15. The rationale underlying each modification is described below.

New hydrochemical data from -23P further validate Flow Path 3. In particular, sulfate/chloride ratios and high sulfate concentrations in -23P are similar to those from borehole J-11 (Jackass Flat grouping), strengthening the argument that water from Jackass Flat flows southwesterly to this region. Boreholes -23P and Washburn-1X constrain the position of Flow Path 3. Only minor adjustments were made to this flowpath. Based on interpretation of new data from -23P, mixing zone C was extended slightly to the north, and an additional arrow indicating eastward flow of Flow Path 8 was added.

New hydrochemical data from boreholes -27P, -16P, and -28P confirm a southerly flow from the Solitario Canyon Wash (Grouping SCW) area along Flow Path 6. Slightly elevated sulfate and chloride values in two samples suggest that groundwater from regions to the northwest and/or

west are added along this flowpath. The exact source of these groundwaters is not well constrained by the available data. Accordingly, Flow Path 4 was shortened to allow the possibility that groundwater from the CF-SW group, or from the direction of VH-1, or possibly a mix of these waters, flows southeast to the region of the -27P, -16P, and -28P boreholes.

New hydrochemical data from boreholes in and immediately west of Fortymile Wash are generally dilute, consistent with groundwater to the north. No changes to Flow Paths 2 or 7 are required by the data.

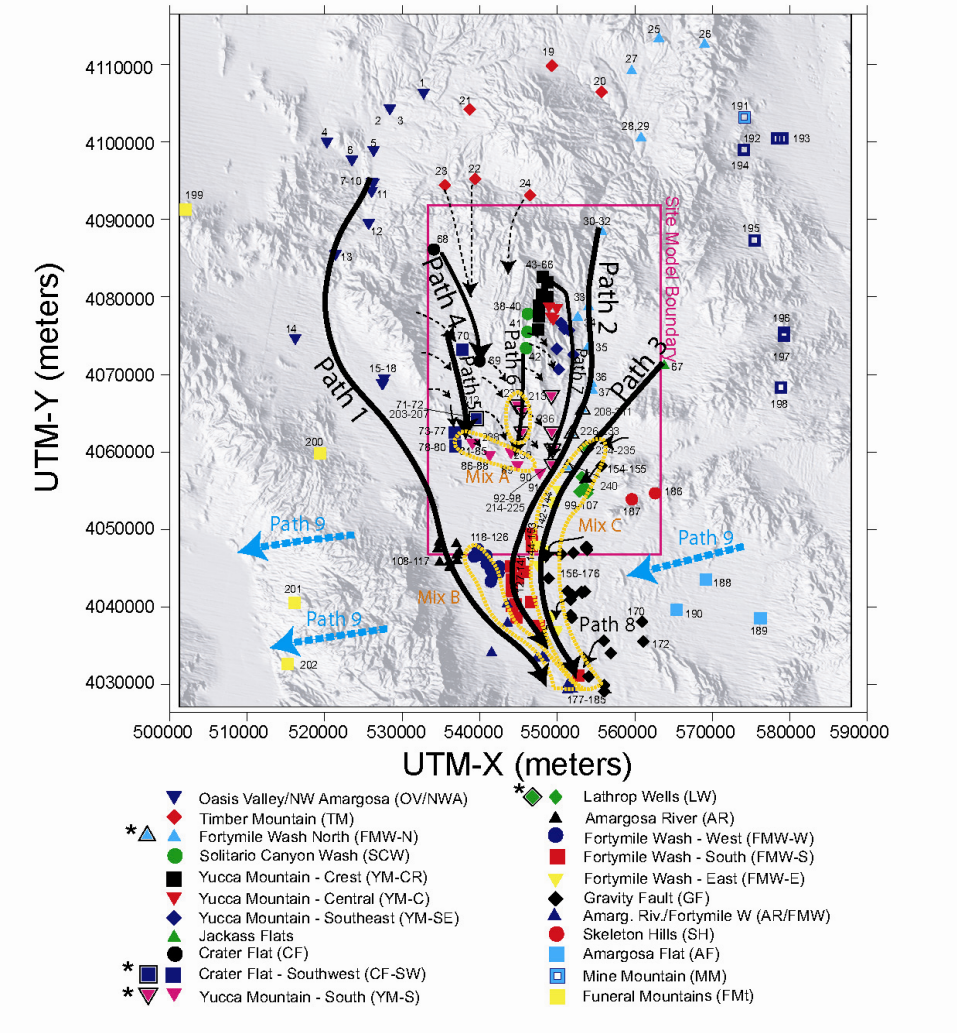

Output DTN: LA0612RR150304.004.

NOTES: This figure has color-coded data points and should not be read in a black and white version.

Solid lines indicate a relatively high degree of confidence in the interpretations; dashed flow paths indicate relatively less confidence. Base map shows borehole designators and inserts; see Figure A6-5 and Table A4-3. A black and white border around a plotted symbol (such as those marked with an asterisk in the legend) identifies new Nye County boreholes and zones, which are overlaid on the map from Figure A6-5. The numbers assigned to these new locations, 203 through 240, are defined in Table B4-1, which is a continuation of the sample number sequence listed in Table A4-3.

UTM-X = UTM-Easting; UTM-Y = UTM-Northing; UTM = Universal Transverse Mercator.

Figure B6-15. Regional Flow Paths Inferred from Hydrochemical and Isotopic Data

B7. CONCLUSIONS

Analysis of new hydrochemical data largely confirm and strengthen hypotheses presented previously in Appendix A. The probable flow pathway from the repository remains dominantly to the south. New carbon isotope data do not contradict calculations of travel times performed in Appendix A. In fact, these new carbon isotope data strengthen suggestions that dilutions in original ^{14}C activity can be reasonably accounted for by correction using dissolved inorganic carbon as outlined in Appendix A. The sparse new uranium isotopic data are in general agreement with data previously reported. These new uranium data do not require any modifications to the previously proposed flowpaths.

APPENDIX C
DATA SUITABILITY EVALUATION – THE 2004 DEATH VALLEY REGIONAL GROUNDWATER FLOW SYSTEM MODEL

C1. INTRODUCTION

SCI-PRO-006 establishes the process for documenting performance assessment modeling activities. It states in Section 6.2.1(L) that:

> "Data obtained from external sources that are not established fact must be qualified for intended use either in accordance with SCI-PRO-001 or within the specific model by doing the following:
>
> 1. Plan and document the qualification process in the model report. Documentation will include:
>
>   - Description of unqualified external source data evaluated
>   - Data qualification method(s) used (as specified in Attachment 3 of SCI-PRO-001) and rationale for selection of method(s)
>   - Acceptance criteria used to determine if the data are qualified (as related to the attributes in Attachment 4 of SCI-PRO-001)
>   - The decision as to the qualification of the data
>
> 2. If relevant data from external sources are evaluated against any of the above factors and determined not to meet a criterion, describe the basis for this conclusion. Also document whether the data were justified using an alternative factor (i.e., acceptance criteria) and included as direct input to the technical product, or excluded from the technical product."

The plan for this appendix is to demonstrate (based on the above-mentioned criteria) that inputs to and outputs of the DVRFS model (Belcher 2004 [DIRS 173179]) are suitable for use in the SZ site-scale flow model with emphasis on the recharge input data and flux output data. To facilitate this plan, this appendix uses technical assessment methods, as discussed in SCI-PRO-001 to evaluate the appropriateness of unqualified DVRFS data, the applicable portions of the data are qualified for intended use in this report in accordance with the requirements of SCI-PRO-006. While selected methodologies of SCI-PRO-001 were incorporated because they provide a sound, well established framework for demonstrating suitability of the DVRFS data for their intended use, SCI-PRO-006 is the governing procedure used to qualify the data for use within this technical product only. The data will remain unqualified for all other uses unless it is separately qualified outside this report.

The DVRFS model was prepared by the USGS and has been published as a Scientific Investigations Report. Inputs to the regional model were used to identify recharge to the upper surface of the SZ site-scale flow and transport model, and outputs from the regional model were used to identify flux targets across the lateral boundaries of the site-scale model. Specifically, the data to be evaluated for suitability (*cbcf.asc*) are found in DTN: MO0602SPAMODAR.000 [DIRS 177371], which contains all the input and output files from the DVRFS (Belcher 2004 [DIRS 173179]). The SZ flow model boundary data extracted from the DVRFS model are the

subject of Output DTN: SN0612T0510106.003. These data include information from several input files related to recharge (infiltration) and the output cell-by-cell flux file. The extracted flux data are used to calibrate the SZ flow model lateral boundaries fluxes (see Sections 6.3.1.6 and 6.3.1.7). This appendix demonstrates the suitability of these data for use in this model using arguments supporting the data reliability, qualifications of the organization, and prior uses of the data.

Executive Summary

The Evaluation Team found the DVRFS model database to be well researched, the model to be appropriately constructed, and the resulting output to provide a reasonable simulation of regional flow. The net infiltration model, INFILV3 (Hevesi et al. 2003 [DIRS 169681]), was calibrated to available surface water flow measurements and constrained by prior estimates of recharge and discharge. The INFILV3 model simulated a mean annual potential recharge to the model domain of about 125×10^6 m^3 for the period 1950 to 1999 (Belcher 2004 [DIRS 173179], p. 132). Within the area of the SZ site-scale model, the recharge fluxes from the regional model are consistent with similar-magnitude fluxes independently estimated from the unsaturated zone flow model and from focused recharge through Fortymile Wash. The INFILV3 model and method are used and accepted by the technical community and it is appropriate for use with the regional model.

The simulated hydraulic heads of the final calibrated transient model fit observed heads reasonably well (residuals with absolute values less than 10 m) with two exceptions: in most areas of nearly flat hydraulic gradient the fit is considered moderate (residuals with absolute values of 10 to 20 m), and in areas of steep hydraulic gradient, such as Indian Springs, western Yucca Flat, and the southern part of the Bullfrog Hills, the fit is poor (residuals with absolute values greater than 20 m, Belcher 2004 [DIRS 173179], pp. 1 and 334).

The Evaluation Team considers this overall goodness-of-fit to be acceptable for use in this report. Because the goodness-of-fit is a measure of the model's accuracy, a degree of uncertainty must be associated with the regional model outputs used to identify lateral flux boundary conditions for the site-scale model. These uncertainties were adequately addressed by using the regional model fluxes not as absolute values, but as target boundary conditions during site-scale model calibration. Specifying the fluxes absolutely would also over-constrain the site-scale model and interferes with its calibration.

The Evaluation Team has concluded that the DVRFS model provides a suitable source of data for establishing recharge and lateral flux boundary conditions for the SZ site-scale flow and transport model. In accordance with SCI-PRO-006, this finding qualifies these data only for their intended uses in this report. The regional model source DTN: MO0602SPAMODAR.000 [DIRS 177371] will remain unqualified.

C1.1 PURPOSE

This appendix evaluates the appropriateness of unqualified data from the USGS flow model of the DVRFS for use in the SZ site-scale flow model. The regional flow model was developed in part to support site-scale modeling for the YMP. Inputs to the regional model were used in this

report to identify recharge across the upper surface of the site-scale model and outputs from the regional model were used to identify flow targets across the lateral boundaries of the site-scale model. This evaluation was performed in accordance with the data requirements of SCI-PRO-006, Section 6.2.1(L). A finding that the regional model is suitable for this specific application means that it is qualified to support the license application, but only for the uses made in this report. The appropriateness and limitations of the data with respect to intended use are addressed in this appendix.

C1.2 SCOPE

This data suitability evaluation identifies one data tracking number (DTN) containing unqualified, developed hydrogeological data associated with the DVRFS model. These data were collected by the USGS and are cited in a USGS Scientific Investigations Report by Belcher (2004 [DIRS 173179]). The data evaluated in the plan are presented in DTN: MO0602SPAMODAR.000 [DIRS 177371], "Model Archives from USGS Special Investigations Report 2004-5204, Death Valley Regional Ground-Water Flow System, Nevada and California – Hydrogeologic Framework and Transient Ground-Water Flow Model."

The aforementioned DTN is unqualified because it summarizes a study performed for the YMP and contains data collected by non-YMP personnel. MODFLOW-2000 (Harbaugh et al. 2000 [DIRS 155197]) had not been qualified as of the writing of this report. In addition to the recharge and lateral flow data used in this report, the data set contains other information that was not directly used here and is not within the scope of this evaluation activity. However, the larger body of data is used in the DVRFS model and must also be evaluated for the model outputs to be considered suitable for use in the SZ site-scale flow model. This appendix focuses on the specific data selected to support the SZ site-scale flow model. To the extent that only subsets of data within this DTN were used (e.g., cell-by-cell fluxes were extracted from the 2004 DVRFS model at positions corresponding to the boundaries of the SZ site-scale flow model), only those data are evaluated for suitability.

C1.3 DATA EVALUATION TEAM

The Chairperson for this data evaluation is Scott C. James.

The team member for this data evaluation is David K. Rudeen.

C1.4 BACKGROUND

C1.4.1 DVRFS

In the early 1990s, two numerical models of the DVRFS were developed by the DOE to support investigations at the Nevada Test Site (NTS), where nuclear tests were conducted from 1951 to 1992, and at Yucca Mountain. In general, the two models were based on the same hydrologic data set. However, the models differed in the details of their implementation and calibration techniques. These differences yielded somewhat different flowpaths and flux results between the two models.

An earlier version of the DVRFS was used to provide boundary conditions for the previous revision of the SZ site-scale flow model (BSC 2004 [DIRS 170015], Appendix B). Much of the justification used is still relevant even though some methods, data interpretations, software and inputs have changed. Many of these changes are due to expanded input databases, better interpretation methods, and model refinements rather than corrections to erroneous or faulty data and models. Therefore, evaluations here are expansions on the justifications presented earlier (BSC 2004 [DIRS 170015], Appendix B).

In 1998, the DOE requested that the USGS begin a 5-year project to develop an improved model of the DVRFS to support NNSA/NSO and YMP programs. This work was performed by the USGS in cooperation with the DOE under Interagency Agreements. Newly available data and modeling tools were used and the data and results of the previous regional-scale model were built upon. During this effort, the USGS cooperated with other Federal, State, and local entities in the region, including the National Park Service, the Fish and Wildlife Service, the Bureau of Land Management, and county governments in Nevada and California to benefit from their expertise. The ultimate objective of the DVRFS model project is the construction and calibration of a model that simulates the transient flow conditions throughout the model domain.

The hydrogeology, conceptual hydrologic model, and the hydrologic system inputs and outputs were used to construct a regional hydrogeologic framework model (HFM) and a transient numerical flow model. The flow model simulates transient conditions from 1913 through 1998 using the modular code, MODFLOW-2000 (Harbaugh et al. 2000 [DIRS 155197]) and yields the simulated steady-state head distribution representing prepumping conditions. Transient stresses imposed on the regional groundwater flow system include pumpage that occurred from 1913 through 1998, and flows from springs affected by pumping. Simulated areal recharge was held constant at average annual values.

The DVRFS model domain encompasses approximately 100,000 km^2 in Nevada and California and is bounded by latitudes 35°00'N and 38°15'N and by longitudes 115°00'W and 118°00'W (Belcher 2004 [DIRS 173179], p. 9).

C1.4.2 SZ Site-Scale Flow

The data from DTN: MO0602SPAMODAR.000 [DIRS 177371] are presented in *Death Valley Regional Ground-Water Flow System, Nevada and California – Hydrogeologic Framework and Transient Ground-Water Flow Model* (SIR 2004-5205) (Belcher 2004 [DIRS 173179]). Although that report is unqualified, the model was developed and reviewed in accordance with USGS policy and the model results were formally published in a Scientific Investigations Report after receiving USGS Director approval.

The domain of the SZ site-scale flow and transport model lies entirely within the larger domain of the regional-scale flow model. Three sources are used to develop estimates of recharge across the upper surface of the SZ site-scale model: (1) distributed recharge as used in the 2004 DVRFS, (2) flux at the bottom boundary of the 2003 UZ site-scale flow model (DTN: LB03023DSSCP9I.001 [DIRS 163044]), (3) and data from infiltration through Fortymile Wash (Savard 1998 [DIRS 102213]). Only the first of these data sources, the 2004 DVRFS model, is addressed in this appendix. Outflow from the UZ model is technical product output,

and the estimates of recharge from Fortymile Wash have been separately qualified (Wilson 2001 [DIRS 155614]; DTN: MO0102DQRGWREC.001 [DIRS 155523]).

Output from the regional model was used to develop estimates of flow across the lateral boundaries of the base-case SZ site-scale flow model. The SZ site-scale flow model uses a nested modeling approach, where uncertainties in boundary conditions for the smaller model are reduced by developing them from internal flow patterns calculated within a larger model. The increased precision and accuracy required in a site-specific study requires fine grid resolution, which is computationally expensive. To increase computational efficiency, the SZ flow model domain is reduced in size (area of model footprint) with the consequence that the model boundaries are often not optimally located where flow conditions are well understood. Thus, it is common to develop the boundary conditions from a larger, lower-resolution model that has optimally located boundaries (e.g., at groundwater divides). This is the process followed when using the regional model to develop boundary conditions for the SZ site-scale model.

C2. SUITABILITY EVALUATION APPROACH

C2.1 SUITABILITY EVALUATION METHODS

The regional model is unqualified because its input data and software are unqualified. The regional hydrologic and geologic data required for the model were collected outside the YMP. However, model construction and review were performed in accordance with accepted YMP quality assurance procedures and USGS policy (Belcher 2004 [DIRS 173179]). In view of these conditions and the unique status of the model in depicting regional flow, the data evaluation was guided by Method 5, *Technical Assessment*, of SCI-PRO-001, Attachment 3*, Considerations for Determining Qualification Methods*. This methodology was used as a guideline because of it provides well established framework for the suitability evaluation.

The Evaluation Team evaluated the appropriateness and accuracy of the methods used by the USGS to develop the regional model inputs and outputs. Technical assessments focused on the methodology used to prepare the model inputs and perform the modeling. The assessments also considered the appropriateness of the model results for the applied uses in this report and the accuracy requirements associated with those uses. Because the modeling was performed on a regional basis in an area with unevenly distributed data and complex hydrogeology, the modeling results are necessarily approximate. Such results can be appropriately used so long as consideration is given to limitations on their accuracy, precision, and representativeness for intended use.

C2.2 PLAN FOR QUALIFYING THE DATA

A technical assessment of the data will be undertaken in this data qualification process. It will be demonstrated that the processes used to generate the data were generated by qualified professionals, are reliable, and that there are prior uses of these type of data.

Evaluation Criteria: The unqualified data were evaluated for use in this report based on consideration of the following criteria. These criteria were selected to incorporate the

considerations in SCI-PRO-001, *Attachment 3, Considerations for Determining Qualification Methods*, and *Attachment 4, Qualification Process Attributes*.

1. Are the methods used to develop the regional-scale model reasonable and generally accepted by the technical community?

2. Are the methods used to develop boundary conditions for the SZ site-scale model from the regional-scale flow model results reasonable and generally accepted by the technical community?

3. Are there more appropriate sources of information for developing the SZ site-scale model boundary conditions?

4. Are the boundary condition data and their associated uncertainties acceptable for their intended use by the SZ site-scale flow model?

Other considerations:

1. Appropriateness of data acquisition and subsequent data development relative to intended use

2. Similar application or uses of data, model, or results

3. The qualifications of personnel and organization performing the work

4. The quality and reliability of the measurement control program

5. Peer and/or professional reviews of the data, model and results

6. Extent and reliability of the documentation.

Recommendation Criteria: A recommendation for suitability is based on the satisfactory resolution of the evaluation criteria. Although these criteria are considered in determining whether the data are appropriate for their intended use in the SZ site-scale flow model, the final conclusions of the Evaluation Team are based on expert judgment, and not all of the evaluation criteria may be applied.

C3. EVALUATION RESULTS

A technical assessment of the DVRFS model (Belcher 2004 [DIRS 173179]) was performed by evaluating the approach used to develop the model's input database, the code selection and model development processes, and the assessment of the model output. Each of these elements of the review is discussed in the following sections of this appendix. These sections summarize the data evaluated by the evaluation team, demonstrate the depth of data sources used and/or developed by the USGS and demonstrate the effort and diligence the USGS (Belcher 2004 [DIRS 173179]) put into the development of the DVRFS model.

C3.1 INPUT DATABASE

The methods used to compile the regional model's input database were reviewed with special emphasis on the recharge data that were directly used as the boundary condition at the water table in the SZ site-scale flow model. The model was constructed using methods that have been widely accepted within the technical community. The model was based primarily on existing data, accompanied by extensive analysis and synthesis. In compiling the input database, heavy reliance was placed on the USGS National Water Information System database and on formal USGS publications, such as professional papers, water resources (or scientific) investigations reports, and water supply papers. Because the USGS uses standard scientific work practices and rigorous procedural controls for data collection, these data sources are considered to be reliable. New methods of storage, retrieval, and analysis of the complex input database were used that take advantage of recent advances in the technology of Geoscientific Information Systems (GSIS). Emphasis on the input database focused on identifying regional discharge, recharge, the regional hydrogeologic framework, and the regional patterns of groundwater movement.

The USGS (Belcher 2004 [DIRS 173179], p. 103) conducted a series of studies to reassess previous estimates of the major flow components and hydraulic properties of the DVRFS region to improve the data for the conceptual model and for model calibration as part of the DVRFS investigation. These studies focused on refining estimates of natural groundwater discharge by developing local estimates of evapotranspiration, and compiling and making additional spring-flow measurements; compiling groundwater pumpage information to estimate the history of groundwater development; estimating groundwater recharge from numerical simulations of net infiltration; estimating boundary inflow and outflow by using regional hydraulic gradients and water budgets of areas adjacent to the DVRFS model domain; estimating hydraulic properties from available literature and aquifer-test data; and evaluating available water-level data to estimate representative pre- and post-pumping hydraulic head information. In general, existing and newly acquired data were evaluated using current technology and concepts, analyses were refined or new algorithms were implemented for making interpretations, and values appropriate for the regional extent and scale of the model were estimated.

C3.1.1 Discharge Component

Estimates of natural groundwater discharge were evaluated for Death Valley, Oasis Valley, and the other major discharge areas in the DVRFS model domain by the USGS (Belcher 2004 [DIRS 173179], p. 132). Natural groundwater discharge was estimated from evaporation from open water and moist, bare soil and from transpiration by the phreatophytes growing in the discharge area. Discharge from the many regional springs in these discharge areas was accounted for because most spring flow eventually is evapotranspired. In Pahrump and Penoyer Valleys, where groundwater is discharged both naturally and by pumping, natural discharge estimates were based on published sources and were assumed to vary with local pumping. In discharge areas not affected by pumping, rates of natural groundwater discharge were assumed to remain fairly constant, presuming no major changes in climate. Mean annual discharge from evapotranspiration for the model domain is estimated at about 115.5×10^6 m^3 (Belcher 2004 [DIRS 173179], p. 132).

The evapotranspiration investigations did not account for spring flow where springs supported narrow bands of riparian habitat along the valley margins or where local pumping had decreased spring flow. Previously published spring-discharge rates and some additional measurements of discharge from selected springs were compiled. Annual natural discharge from springs not accounted for in evapotranspiration studies is estimated at about 16.8×10^6 m^3 (Belcher 2004 [DIRS 173179], p. 132).

The local pumping of groundwater for large-scale agricultural use in Pahrump Valley caused Bennetts Spring to stop flowing in 1959 and Manse Spring to stop flowing around 1977. A history of groundwater use for the DVRFS (1913 to 1998) was developed by compiling available information and using various estimation methods to fill gaps where data were missing. In 1913, groundwater used to support agriculture in Pahrump Valley was estimated at less than 5×10^6 m^3. Groundwater pumping remained relatively constant through 1944 and thereafter increased steadily in response to agricultural expansion. The estimated total volume of groundwater pumped from the DVRFS model domain from 1913 to 1998 is about 3.276×10^6 m^3 and in 1998 about 93.5×10^6 m^3. These estimates are not adjusted for water potentially returned to the groundwater flow system (Belcher 2004 [DIRS 173179], p. 132).

C3.1.2 Recharge Component

Groundwater recharge is defined as water that infiltrates downward through the unsaturated zone into the water table. Most of the groundwater recharge originates from precipitation that falls on mountainous areas throughout the DVRFS. The distribution and quantification of recharge for basins in the DVRFS were evaluated by the USGS using empirical, water-balance, chloride mass-balance, and distributed-parameter methods (Belcher 2004 [DIRS 173179], p. 115).

Recharge in the DVRFS was estimated from net infiltration using a distributed-parameter, deterministic watershed model, INFILv3, documented in the USGS Water Resources Investigations Report 03-4090 (Hevesi et al. 2003 [DIRS 169681]). The INFILv3 model was developed by the USGS specifically for estimating the magnitude and the spatial and temporal distribution of net infiltration in the Death Valley region. In the INFILv3 model, net infiltration equals the sum of snowmelt, precipitation, and infiltrating surface flow minus the sum of evapotranspiration, runoff, and changes in root-zone storage. The approach simulated daily climate changes and numerous near surface processes controlling infiltration. The INFILv3 model was calibrated to available surface-water flow measurements and constrained by prior estimates of recharge and discharge. The INFILv3 model simulated a mean annual potential recharge to the model domain of about 125×10^6 m^3 from 1950 to 1999 (Belcher 2004 [DIRS 173179], p. 132).

The recharge fluxes from the regional model are consistent with similar magnitude fluxes independently estimated from the 2003 UZ site-scale flow model (DTN: LB03023DSSCP9I.001 [DIRS 163044]) and from the focused recharge through Fortymile Wash (Savard 1998 [DIRS 102213]). The correlation between topography and recharge is similar in the regional and the UZ models, both of which show decreasing recharge with decreasing elevations to the south. The magnitudes of recharge are also similar, ranging from near zero to 1,262 mm/yr beneath a stream channel with an average net recharge over the entire model domain of 2.8 mm/yr (Belcher 2004 [DIRS 173179], p. 115). In addition, the more refined UZ site-scale flow model

and Fortymile Wash analysis supplement the coarser, regional-scale analysis. The regional model focus is on broad topographical and vegetal considerations. It does not account for the refined topography of Yucca Mountain captured in the UZ site-scale flow model, nor does it specifically account for localized recharge from runoff in Fortymile Wash. Although residual uncertainties affect the recharge data, the total recharge mass fluxes of about 61.2 kg/s into the site scale SZ flow model from the 2004 DVRFS is small compared to the total lateral mass influx of about 617 kg/s calculated for the lateral boundaries of the model. Residual uncertainties in the recharge will therefore have relatively little impact on the overall modeling results. However, it is noted that beneath the repository site, where vertical seepage may be an important transport mechanism for migrating radionuclides, the recharge is comprehensively defined and integrated into the upper boundary of the SZ site-scale flow and transport model.

C3.1.2.1 Lateral Flow

Areas of potential inflow and outflow, or lateral flow, along the DVRFS model boundary were defined for prepumped conditions. Hydraulic gradients determined from a regional potentiometric map indicate that one boundary segment has no flow and that flow occurs across 11 of 12 lateral boundary segments of the model domain—8 boundary segments have inflow and 3 have outflow (Belcher 2004 [DIRS 173179], p. 118).

Lateral flow across the boundary of the DVRFS model domain was estimated. Flows from water-budget studies were compared to Darcy calculations by using hydraulic gradients obtained from a regional potentiometric surface map (Belcher 2004 [DIRS 173179], Appendix 1) and estimated hydraulic conductivities of the hydrogeologic units (HGUs) along the model boundary. The estimated mean annual groundwater flow into the model domain is about 18.4×10^6 m^3 and out of the model domain is about 9.5×10^6 m^3 (Belcher 2004 [DIRS 173179], pp. 118 and 132).

C3.1.2.2 Balance of Components

A water budget is used to assess the significance of individual flow components in the groundwater system and to evaluate the balance between inflows and outflows.

A water budget for the prepumping period (before 1913) computed for the DVRFS model domain was balanced to within about 7%. For prepumped conditions, annual recharge accounted for about 87% of the total inflow and natural discharge (evapotranspiration and spring flow) accounted for about 93% of the total outflow. Although natural discharge by evapotranspiration was assumed to represent prepumped conditions, actual discharge may have been reduced by local pumpage. The remainder of the inflow and outflow is accounted for by lateral flows into and out of the model domain (Belcher 2004 [DIRS 173179], p. 132).

The water budget for pumped conditions for the DVRFS model domain is incomplete because accurate estimates for the major hydrologic components are not available. Pumpage in 1998 was about 70% of the total outflow estimated for prepumped conditions. A likely source of most of the water being pumped from the DVRFS region is groundwater in storage. This water, when removed from the flow system, decreases the hydraulic head within aquifers and decreases natural discharge through evapotranspiration and from spring flow. These decreases are partly

reflected by declining water-level measurements in areas of pumping and by estimates showing declining spring discharge in Pahrump Valley (Belcher 2004 [DIRS 173179], p. 132).

C3.1.2.3 Hydraulic Properties

Previously developed reasonable ranges of hydraulic properties, primarily horizontal hydraulic conductivity, were used for the major HGUs of the DVRFS. Fracturing appears to have the greatest influence on the permeability of bedrock HGUs; the greater the degree of fracturing, the greater the permeability. In the Cenozoic volcanic rocks, alteration decreases hydraulic conductivity and welding forms brittle rocks that fracture more easily and increase hydraulic conductivity. Storage coefficients from the literature were used because field data necessary to develop HGU-specific values were extremely limited (Belcher 2004 [DIRS 173179], p. 133).

The average depth for hydraulic-conductivity estimates within the model domain is 700 m with a maximum depth of 3,600 m. Using these limited data, hydraulic conductivity decreased with depth. A rigorous quantification of a depth-decay function was prevented by the variability in available hydraulic-conductivity data (Belcher 2004 [DIRS 173179], p. 133).

C3.1.2.4 Hydraulic Head

Nearly 40,000 water levels measured since 1907 in about 2,100 wells were evaluated as part of the DVRFS investigation. Almost 100 wells in the DVRFS model domain have a record of 20 years or longer. Head observations representing steady-state, prepumped conditions were computed from about 12,000 water levels averaged at 700 wells in the DVRFS model domain. Head observations range from about 2,500 m above sea level in the Spring Mountains to nearly 100 m below sea level in Death Valley. Transient, pumped conditions were represented by head observations computed from nearly 15,000 water levels measured in about 350 wells. Water-level records for individual wells spanned periods from 1 to about 50 years. Each head observation was assigned an uncertainty based on potential errors related to uncertainties in the altitude measurement of a water level and fluctuations introduced by climate variations or any other non-simulated transient stress (Belcher 2004 [DIRS 173179], p. 133).

C3.1.3 Regional Hydrogeologic Framework

The regional HFM accounts for the influences of stratigraphy and geologic structure on groundwater movement, the hydrologic properties of the HGU, and the regional potentiometric surface. The framework is a geometrical configuration of the regional hydrogeologic structure designed to support the regional model. A regional digital elevation model was combined with geologic maps to provide a three-dimensional series of points locating the outcrops of individual geologic formations, geologic cross sections, and borehole lithologic logs. The surface and subsurface data were then interpolated to define the tops of HGUs.

A three-dimensional digital HFM was constructed to interpret the regional hydrogeology of the DVRFS. The HFM integrates existing and new geologic information developed in the DVRFS and describes the geometry and extent of the HGUs that control groundwater flow. It is a required information source for the DVRFS numerical groundwater flow model. The primary data sources used to develop the HFM are: digital elevation models, geologic maps, borehole

lithologic logs, geologic and hydrogeologic cross sections, local three-dimensional hydrogeologic framework models, and hydrostructural information. The geologic data from geologic maps, cross sections, and borehole lithologic logs were correlated into 27 HGUs. Gridded surfaces from other three-dimensional HFMs constructed for the NTS and Yucca Mountain were also used. The HFM defines regional-scale hydrogeology and structures to a depth of 4,000 m below sea level. The model has 1,500-m horizontal resolution and variable vertical thickness for the HGUs. The faults thought to be hydrologically significant were used for offsetting HGUs in the three-dimensional model (Belcher 2004 [DIRS 173179], p. 253).

The HFM was evaluated for accuracy by visual inspection and by analysis of the gridded surfaces for HGU extent and thickness. The HFM was compared to the known extent of HGUs, input cross sections, and other three-dimensional framework models. Evaluations of the HFM show that it generally portrays the regional hydrogeology. During flow-model calibration, in some locations the HFM did not allow accurate simulations. In such locations, the HFM was examined and the uncertainty in the existing interpretations considered; where alternative interpretations were appropriate and deemed necessary, the HFM was modified (Belcher 2004 [DIRS 173179], pp. 184 and 253).

C3.1.4 Discussion

The Evaluation Team found that the regional model's input database was diligently compiled using appropriate methodologies that take into account the difficulties of handling large amounts of data for a large and complex region, as well as the uncertainties that are present in much of the developed information. Data collection methods were based on standard scientific work practices using USGS procedures.

Discharges from evapotranspiration, playa evaporation, spring flow, and pumping were well researched, particularly the evapotranspiration component, which constituted the largest single source of discharge. Recharge was dominated by infiltration of precipitation, which remained somewhat uncertain despite significant efforts to quantify it. The average estimated regional recharge from infiltration of 125×10^6 m^3/yr (Belcher 2004 [DIRS 173179], pp. 132 to 133) amounts to over 87 percent of the total regional inflow. Although the general magnitude of the simulated net-infiltration volume was consistent with prior discharge and recharge estimates for the DVRFS region, substantial differences were observed in some local basins. Nonetheless, the spatial distribution of estimated net infiltration was considered a reasonable indication of the spatial distribution of the potential recharge across the model domain under current climate conditions (Belcher 2004 [DIRS 173179], p. 118).

C3.2 CODE SELECTION AND MODEL DEVELOPMENT

As of November 2006, *MODFLOW-2000* (Hill et al. 2000 [DIRS 158753]; Harbaugh et al. 2001 [DIRS 155197]) was used to simulate the DVRFS. This code is currently being added to the YMP software baseline and is expected to be available for use in qualified calculations. *MODFLOW-2000* incorporates a nonlinear least squares regression technique that is used to estimate aquifer parameters that yield the best fit to measured heads and discharges (Belcher 2004 [DIRS 173179], p. 346). Although more refined interim databases were developed, the final model was constructed with 16 layers with $1,500 \times 1,500$-m^2 grid spacing,

consisting of 27 HGUs through which groundwater flows (Belcher 2004 [DIRS 173179], p. 349). Belcher (2004 [DIRS 173179], p. 350) found this configuration appropriate for evaluation of regional-scale processes. These include the assessment of boundary conditions of local-scale models, the evaluation of alternative conceptual models, the approximation of aspects of regional-scale advective transport of contaminants, and the analysis of the consequences of changed system stresses, such as those that would be imposed on the system by increased pumping.

C3.2.1 Model Construction

The three-dimensional hydrogeologic data sets for the DVRFS described previously were discretized to develop the input arrays required for the model. Because the data sets were developed at grid cell resolutions ranging from 100 to 1,500 m, their discretization to a common, larger grid cell resolution inevitably results in further simplification of the flow-system conceptual model and HFM. This resampling and simplification of the three-dimensional hydrogeologic data sets were apparent in definition of the model grid, assignment of boundary conditions, and definition of model parameters (Belcher 2004 [DIRS 173179], p. 265).

A GSIS was used to ensure accurate spatial control of physical features and the finite-difference model grid. GSIS also was used during calibration to manipulate and compare model input data sets with model output (Belcher 2004 [DIRS 173179], p. 265).

C3.2.2 Hydraulic Properties

HGUs are the basis for assigning horizontal hydraulic conductivity, vertical anisotropy, depth decay of hydraulic conductivity, and storage characteristics to model grid. Model input arrays also were used to account for variations in the hydraulic properties within HGUs by zonation (Belcher 2004 [DIRS 173179], pp. 266 to 268).

To incorporate the hypothesis that hydraulic conductivity decreases with depth, exponential decay was implemented to yield HGUs that are relatively impermeable at depth and relatively permeable near the land surface (Belcher 2004 [DIRS 173179], p. 268).

Vertical anisotropy (the ratio of horizontal to vertical hydraulic conductivity) is defined for each HGU. Because of their layered nature, basin-fill sediments are likely to have significant vertical anisotropy. The assumed presence of solution features in carbonate rocks would indicate that these rocks have relatively small vertical anisotropy. The vertical anisotropy of other rocks and sediments would be expected to fall somewhere between these two extremes (Belcher 2004 [DIRS 173179], p. 268).

Model layers were simulated as confined, and the storage consequences of water-table changes over time were simulated using a storage coefficient in the top model layer that was equivalent to a specific yield. The top model layer was defined as the simulated potentiometric surface in the unconfined part of the system (Belcher 2004 [DIRS 173179], p. 268).

C3.2.3 Observations Used In Model Calibration

Poorly quantified or unquantified characteristics of the system can be constrained on the basis of observations. Observations used to calibrate the DVRFS model were those of hydraulic heads (water levels), changes in head over time due to pumpage, and discharge by evapotranspiration and spring flow. Estimated boundary flows (simulated as constant-head boundaries) were treated like observations but are less accurate than other observation types and were given less weight in the simulation (Belcher 2004 [DIRS 173179], p. 279).

For the prepumped, steady-state stress period, all observations were considered representative of steady-state conditions. For the pumped, transient stress periods, some hydraulic-head and discharge observations are not influenced by pumping and thus were also considered representative of long-term steady-state conditions. Hydraulic-head observations influenced by pumping were treated as head-change observations. Natural discharge from evapotranspiration and springs was considered to be constant and not influenced by pumping, with some exceptions. It was assumed that constant-head observations used to simulate flow into and out of the model boundary were not influenced by pumping (Belcher 2004 [DIRS 173179], p. 279).

C3.2.4 Hydraulic Head

Water levels measured in boreholes and wells located within the model domain were used to develop hydraulic-head and head-change observations for calibration of the regional flow model. Only those water levels considered representative of regional groundwater conditions were used to calculate head observations (Belcher 2004 [DIRS 173179], p. 279).

C3.2.5 Groundwater Discharge Observations and Errors

Discharge observations were developed primarily from discharge estimates that were derived from evapotranspiration estimates and spring-flow measurements discussed above. Uncertainty in the discharge from each area was also estimated (Belcher 2004 [DIRS 173179], p. 283).

C3.2.6 Boundary Flow Observations and Errors

The boundary flow observations were obtained from Belcher (2004 [DIRS 173179], Appendix 2) that estimates potential flow through 7 segments of the boundary of the DVRFS model domain. These values have a great deal of uncertainty associated with them, but were used as observations during calibration (Belcher 2004 [DIRS 173179], p. 283).

C3.2.7 Model Calibration

Model calibration is the process of changing model input values in an attempt to match simulated and actual conditions. Models typically are calibrated either by trial and error or by using formal parameter-estimation methods. Calibration of parameter values of the DVRFS model primarily relied on the parameter-estimation techniques available in MODFLOW-2000 and was achieved using a two-step process. First, the model was calibrated to prepumped (steady-state) flow conditions. Once calibrated, this model formed the initial condition for the transient flow model. The model was calibrated again to simulate transient flow conditions for 1913 to 1998 (Belcher 2004 [DIRS 173179], p. 283).

Sensitivity analyses were used to evaluate the information provided by the observations for the estimation of all defined parameters, and nonlinear regression was used to estimate parameter values that produced the best fit to observed hydraulic heads and discharges. For the DVRFS model, 100 parameters are used and more than 90 were estimated at some point during the modeling process. The maximum number of parameters estimated by nonlinear regression peaked at around 30 (Belcher 2004 [DIRS 173179], p. 283).

Uncertain aspects of the hydrogeology were evaluated by constructing models with different hydraulic property distributions and different methods to simulate evapotranspiration, spring flow, recharge, and the boundary conditions. These models were evaluated through sensitivity analyses and nonlinear regression methods. Also discussed was how model errors were detected when estimated parameter values were found to be unreasonable (Belcher 2004 [DIRS 173179], p. 283).

C3.2.8 Conceptual Model Variations

During calibration, a number of conceptual models were evaluated using regression methods within *MODFLOW-2000*. A best fit to hydraulic head, groundwater discharge, and boundary-flow observations was calculated for each conceptual model. Evidence of model errors or data problems was investigated after each model run. These analyses were used in conjunction with hydrogeologic data to modify and improve the existing conceptual model, observation data sets, and weighting (Belcher 2004 [DIRS 173179], p. 287). Model parameters that were varied include: horizontal hydraulic conductivity depth of decay of hydraulic conductivity, vertical anisotropy, storage properties hydrogeologic structures, recharge and discharge.

C3.2.9 Discussion

The Evaluation Team considers use of *MODFLOW-2000* to be appropriate. *MODFLOW* has been the industry standard for simulating flow. The advantages of *MODFLOW-2000* in simplifying the parameter estimation and calibration process and evaluation of the model results are clearly explained (Belcher 2004 [DIRS 173179], pp. 283 to 327). No model modifications were made without supporting hydrogeologic criteria. Also, hydraulic parameter values were maintained within reasonable bounds.

C3.3 MODEL EVALUATION

The final calibration was evaluated to assess the accuracy of simulated results by comparing measured and expected values to simulated values. The fit of simulated heads to observed hydraulic heads is generally good (residuals with absolute values less than 10 m) in most areas of nearly flat hydraulic gradients, and moderate (residuals with absolute values of 10 to 20 m) in the remainder of the areas of nearly flat hydraulic gradients. The poorest fit of simulated heads to observed hydraulic heads (residuals with absolute values greater than 20 m) is in steep hydraulic-gradient areas in the vicinity of Indian Springs, western Yucca Flat, and the southern Bullfrog Hills. Most of these inaccuracies can be attributed to: (1) insufficient representation of the hydrogeology in the HFM, (2) misinterpretation of water levels, and (3) model error associated with grid cell size (Belcher 2004 [DIRS 173179], p. 349).

Groundwater discharge residuals are fairly random, with as many areas in which simulated discharges are less than observed discharges as areas in which simulated discharges are greater than observed. The largest unweighted groundwater discharge residuals are in Death Valley and Sarcobatus Flat (northeastern area). The two major discharge areas that contribute the largest volumetric error to the model are the Shoshone/Tecopa area and Death Valley. Positive weighted residuals were computed in transient simulations of the Pahrump Valley that may indicate a poor definition of hydraulic properties and discharge estimates, especially near Bennetts Spring (Belcher 2004 [DIRS 173179], p. 349).

Parameter values estimated by the regression analyses were within the range of expected values. As with any model, uncertainties and errors remain, but this model is considered an improvement on previous representations of the flow system (Belcher 2004 [DIRS 173179], p. 350).

Inherent limitations result from uncertainty in three basic aspects of the model inadequacies or inaccuracies: in observations used to calibrate the model, in the representation of geologic complexity in the HFM, and in representation of the groundwater flow system in the flow model. It is important to understand how these characteristics limit the use of the model. These basic aspects of the model are represented at a regional scale, and the use of the model to address regional-scale issues or questions is the most appropriate use of the model (Belcher 2004 [DIRS 173179], p. 350).

C3.4 DISCUSSION

The Evaluation Team concurs with Belcher (2004 [DIRS 173179], p. 349) that this model provides a generally good simulation of the DVRFS. Considering the large size of the region, the hydrogeologic complexity, and the sparse data, achieving any better overall validation accuracy would have been surprising. The team found that the DVRFS model database was well researched, the model was appropriately constructed, and the resulting output provides a reasonable simulation of regional flow. Fitting techniques used by Belcher (2004 [DIRS 173179]) were considered state-of-the-art when the report was published. The calibration process and the uncertain aspects of the hydrogeology that were evaluated through the sensitivity analyses and nonlinear regression methods are well described (Belcher 2004 [DIRS 173179], pp. 283 to 327). Uncertainties in the model output are of potential concern to the Evaluation Team because the simulated fluxes along the boundaries of the SZ site-scale flow models account for most of the flow through this model. Fluxes are dependent on the adopted hydraulic properties and the DVRFS adopted hydraulic properties are technically reasonable for the given units and rock types. The model assumption that conductivity decreases with respect to depth is reasonable for the given rock type. In the SZ site-scale flow model, the fluxes in the 16 regional model layers are combined to provide total flow across the boundary for vertical panels of various widths extending from the water table to a depth of 4,000 m below the water table. Uncertainties are incorporated into the SZ site-scale models by treating the fluxes as target values during model calibration. Fixed-head boundary conditions were assigned to the perimeter of the SZ site-scale models from regional water level and head data, where heads were varied laterally along the model perimeter but were held constant in the vertical direction. Other targets were also considered during base-case SZ site-scale flow model calibration that affect fluxes, including rock permeabilities and specific discharge estimates given by the Expert Elicitation Panel (see Section 6.5.1.3). A comparison of the resulting calibrated boundary fluxes of the

site-scale model with those determined from the regional model shows a reasonable matching of total boundary fluxes but greater differences, some on the order of 100%, for individual boundary segments (Section 6.5.2.2). The reasons for these differences are primarily attributed to the increased resolution of the site-scale model. In addition, the pumping wells modeled in the 2004 DVRFS are not considered in the SZ site-scale flow model. These discharges are effectively replaced by additional flux through the southern boundary of the SZ site-scale flow model because constant head boundary conditions reflect drawdown due to pumping. Use of the regional model flux data as target rather than absolute values in the site-scale model is appropriate considering the uncertainties inherent in those data and the fact that DVRFS model does not necessarily match estimated regional recharge/discharge fluxes.

Upon review of the alternative models (e.g., Waddell 1982 [DIRS 101062]; Rice 1984 [DIRS 101284]), the DVRFS model was found to be the most appropriate source of information for both distributed recharge and lateral flow boundary conditions for the SZ site-scale flow and transport model.

C3.5 SUMMARY OF EVALUATION RESULTS

The Evaluation Team found the DVRFS model database to be well researched, the model to be appropriately constructed, and the resulting output to provide a reasonable simulation of regional flow. Sound methodologies were used during the calibration process, in that, the model was not modified without supporting hydrogeologic criteria and hydraulic parameter values were maintained within reasonable bounds.

Quantification of the recharge component of flow was reviewed in particular detail because of the direct use of those data in the SZ site-scale flow model. Recharge in the DVRFS region was estimated from net infiltration using a deterministic mass-balance method. The approach, using INFIL V3, simulated daily climate changes and numerous near surface processes controlling infiltration. As expected, recharge was dominated by infiltration of precipitation. Within the domain of the SZ site-scale flow and transport model, the recharge fluxes from the regional model are consistent with estimates from the 2003 UZ site-scale flow model and with focused recharge from Fortymile Wash. Discharges from evapotranspiration, playa evaporation, spring flow, and pumping were well researched, particularly the evapotranspiration component, which constituted the largest single source of discharge. The Evaluation Team considers use of the *MODFLOW-2000* code in constructing the model to be appropriate. The MODFLOW codes have become industry standards and the advantages of the *MODFLOW-2000* adaptation in simplifying the calibration process and evaluating the model results were important.

The simulated hydraulic heads of the final calibrated transient model generally fit observed heads reasonably well (residuals with absolute values less than 10 m) with two exceptions: in most areas of nearly flat hydraulic gradient the fit is considered moderate (residuals with absolute values of 10 to 20 m), and in areas of steep hydraulic gradient, the fit is poor (residuals with absolute values greater than 20 m). The Evaluation Team considers the overall goodness-of-fit of the regional model to be good, although in some cases a significant degree of uncertainty is associated with the model outputs. Nevertheless, the output from the 2004 DVRFS model is relevant and appropriate for its intended use.

Uncertainties in the simulated fluxes along the lateral boundaries of the SZ site-scale flow model are potentially significant because these fluxes constitute the greatest sources of flow through the SZ site-scale model and they are not independently corroborated. However, these uncertainties were recognized in calibrating the site-scale model by using the regional model fluxes along with other data sources in a generalized manner as calibration targets rather than as fixed model inputs. Actual boundary conditions in the site-scale model were defined by fixed heads, which are better known than the boundary fluxes. This approach made the fluxes largely a function of the calibrated model permeabilities. A comparison of the resulting calibrated regional and site-scale model boundary fluxes shows reasonable matching of total fluxes but greater differences, some on the order of 100%, for individual boundary segments. These observations indicate that the use of the regional model flux data in the site-scale model is appropriately generalized considering the uncertainties inherent in those data.

C4. EVALUATION CONCLUSIONS

The conclusions of the Evaluation Team review of the regional model are presented below in terms of the primary evaluation criteria presented in Section C2.2.

1. *Are the methods used to develop the regional-scale model reasonable and generally accepted by the technical community?*

   The methods used to develop the database, the choice of models, the methods of calibration, and the analysis of the results are all reasonable and generally accepted by the technical community. The use of GSIS to store, manipulate, and analyze the data is also accepted by the technical community.

2. *Are the methods used to develop boundary conditions for the SZ site-scale model from the regional-scale flow model results reasonable and generally accepted by the technical community?*

   The nested model approach for obtaining lateral flux boundary conditions for smaller models is well established and accepted by the technical community. The recharge boundary for the regional model was obtained from a net-infiltration model, INFIL V3, which was calibrated to available surface-water flow measurements and constrained by prior estimates of recharge and discharge. The model and method are also well established and accepted by the technical community.

3. *Are there more appropriate sources of information for developing the SZ site-scale model boundary conditions?*

   Other sources of similar information are older and less well developed than the 2004 DVRFS model. The regional model was developed in part to support site-scale modeling. It provides a reasonable and comprehensive simulation of regional flow, and is an appropriate source of information for developing hydrologic boundary conditions for the SZ site-scale model.

4. *Are the boundary condition data and their associated uncertainties acceptable for their intended use by the SZ site-scale flow model?*

   Uncertainties in the lateral boundary condition data have been appropriately addressed by using them as target values for SZ site-scale flow model calibration. The calibration has been successfully completed using this approach, indicating that the boundary condition data have been successfully used and are therefore appropriate for their intended use. In addition, much of the source data for the regional model are YMP-accepted data, the *MODFLOW-2000* code is currently being qualified for project use, the regional model has been validated and residual uncertainties have been identified, and the modeling effort was adequately reviewed and documented. Furthermore, it should be noted that differences between the 1997 DVRFS (D'Agnese et al. 1997 [DIRS 100131]) and the 2001 DVRFS (D'Agnese et al. 2002 [DIRS 158876]) models, while not extraordinary, can largely be attributed to the fact that the 1997 DVRFS model simulates conditions found in the early 1990s (includes pumping) and the 2001 DVRFS model simulates predevelopment conditions (no pumping). The 2004 DVRFS, with extensive modeling enhancements, combines both the predevelopment condition in the initial steady state step and groundwater pumping in subsequent transient steps.

C5. RECOMMENDATIONS

The Evaluation Team has concluded that the Death Valley regional flow model database was well researched, the model was appropriately constructed, and the resulting output provides a reasonable simulation of regional flow based on application of all evaluation criteria. At the time of publication of this report, this model was the most recent and best-supported SZ flow model of the Yucca Mountain region. It incorporates updated geological and hydrogeological data, it benefits from contemporary geological and hydrogeological conceptual models, and it provides a three-dimensional representation of the region. Upon review of the alternatives, the DVRFS model was found to be an appropriate source of information for both recharge and lateral flux boundary conditions for the SZ site-scale flow and transport model.

Based on the foregoing evaluation, the Evaluation Team has concluded that the 2004 DVRFS model provides a suitable source of data for establishing recharge and lateral flux boundary conditions for the SZ site-scale flow and transport model. In accordance with SCI-PRO-006, this finding qualifies these data only for their intended uses in this report. The source DTN: MO0602SPAMODAR.000 [DIRS 177371] will remain unqualified for other uses.

APPENDIX D
DATA SUITABILITY EVALUATION – NYE COUNTY EARLY WARNING DRILLING PROGRAM (NC-EWDP) WELL DATA

D1. INTRODUCTION

SCI-PRO-006, Section 6.2.1(L), establishes the process for documenting performance assessment modeling activities:

> "Data obtained from external sources that are not established fact must be qualified for intended use either in accordance with SCI-PRO-001 or within the specific model by doing the following:
>
> 1. Plan and document the qualification process in the model report. Documentation will include:
>
>   - Description of unqualified external source data evaluated
>
>   - Data qualification method(s) used (as specified in Attachment 3 of SCI-PRO-001) and rationale for selection of method(s)
>
>   - Acceptance criteria used to determine if the data are qualified (as related to the attributes in Attachment 4 of SCI-PRO-001)
>
>   - The decision as to the qualification of the data
>
> 2. If relevant data from external sources are evaluated against any of the above factors and determined not to meet a criterion, describe the basis for this conclusion. Also document whether the data were justified using an alternative factor (i.e., acceptance criteria) and included as direct input to the technical product, or excluded from the technical product."

D1.1 PURPOSE

The plan for this appendix is to evaluate the suitability (based on the above-mentioned criteria) of unqualified Nye County well data for use in the SZ site-scale flow model. The well data are used in developing the potentiometric surface and to calibrate and validate the SZ site-scale flow model. Specifically, these data are the coordinates of the well head (UTM), average depths of the open intervals, and measured water levels. The well data were developed from the NC-EWDP, which is considered an outside source and they are not established fact and, therefore, the data are considered unqualified.

To facilitate this plan, this evaluation uses the methodologies of SCI-PRO-001 as a guideline to qualify applicable portions of a dataset for intended use in this report in accordance with the requirements of SCI-PRO-006, Section 6.2.1(L) (see above). Some of the methodologies of SCI-PRO-001 were incorporated because they provide a sound, well established framework for demonstrating suitability of the NC-EWDP well data for intended use within this product only. However, SCI-PRO-006 is the governing procedure used to qualify the data for use within this technical product only. The data will remain unqualified for all other uses, unless it is separately qualified outside of this report. A finding that the data from Nye County wells are suitable for

intended use means that they are qualified to support the license application, but only for the uses made in this report. The appropriateness and limitations of the data with respect to intended use are addressed in this appendix. This appendix demonstrates the suitability of these data for use in this model using arguments supporting the data reliability, qualifications of the organization, and prior uses of the data.

D1.2 SCOPE

This appendix identifies one DTN containing unqualified data associated with the Nye County well dataset. These data were collected by the Early Warning Drilling Program. The data also reside in the TDMS for use by the YMP. The data evaluated in this appendix consisting of dozens of DTNs, were obtained from TDMS and consolidated into a single model Output DTN: SN0702T0510106.007. The consolidated DTN consists of acquired survey data in geographic (latitude-longitude) coordinates, water-level measurement open-intervals, water-level histories and time averaged water-levels for wells 7SC, 10P, 10S, 16P, 18P, 19IM1, 19IM2, 19PB, 22PA, 22PB, 22S, 23P, 24P, 27P, 28P, and 29P, and Phase V wells 13P, 22PC, 24PB, 32P, and 33P. Well locations in terms of UTM coordinates for 7SC through 29P are provided in Output DTN: LA0612RR150304.001 and are discussed in Appendix F. Well locations for Phase V wells are developed in Output DTN: SN0702T0510106.007. The aforementioned DTN is unqualified because it contains data collected by non-YMP personnel under QA procedures that are different than YMP QA procedures. This qualification report focuses on the specific data selected to support the SZ site-scale flow model. To the extent that only subsets of data within this DTN were used, only those data are evaluated for suitability (see Table D-2).

D1.3 DATA EVALUATION TEAM

The chairperson for this evaluation is Scott C. James, SNL, Department 8757.

The team member for this evaluation is David K. Rudeen, RHYM,Inc. (SNL, Department 6781).

D2. EVAUATION APPROACH

D2.1 EVAUATION METHODS

The Nye County well data are unqualified because they were collected outside the YMP. However, these data were evaluated for use in this report because the data source is considered reliable, the data have been used in previous revision of this report, and there are available corroborating data from qualified sources (proximally located qualified water levels). Also, Nye County has a rigorous Quality Assurance Program (QAP). In view of these conditions the data were evaluated for their intended use using a combination of Method 1, *Equivalent QA Program*, and Method 2, *Corroborating Data,* from SCI-PRO-001, Attachment 3, *Considerations for Determining Qualification Methods*, as a guide. SCI-PRO-001 methodologies are only used as framework for the suitability evaluation because, they are sound and well established.

D2.2 PLAN FOR QUALIFYING THE DATA

A technical assessment of the data will be undertaken in this data qualification process. It will be demonstrated that the processes used to generate the data were generated by qualified professionals, are reliable and there is available corroborating data.

The NC-EWDP data were evaluated for use in this report based on consideration of the following evaluation criteria. These criteria were selected to incorporate the considerations in SCI-PRO-001, Attachment 3*, Considerations for Determining Qualification Methods* and Attachment 4*, Qualification Process Attributes*.

1. Is there functional equivalence of the data-gathering process to applicable QARD concepts (qualification of personnel, technical adequacy of equipment and procedures, quality and reliability of measurement control and audits)?

2. Is the data addressed in this appendix consistent with corroborating data?

3. Are the methods used to incorporate the data into the SZ site-scale model reasonable and generally accepted by the technical community?

4. Are there more appropriate sources of the required SZ site-scale model data?

5. Are the associated uncertainties acceptable for their intended use by the SZ site-scale flow model?

A recommendation of suitable for intended use is based on the satisfactory resolution of the evaluation criteria. Although these criteria are considered in determining whether the data are appropriate for their intended use in the SZ site-scale flow model, the final conclusions of the Evaluation Team are based on expert judgment, and not all of the evaluation criteria may be applied.

D3. EVALUATION RESULTS

The data from several Nye County wells will be used to develop the potentiometric surface and to calibrate and validate the SZ site-scale flow model. As such, the wells need to be located with an accuracy on the order of 10 m and water levels and open interval should be measured to the nearest 1 m. Nye County well data meet these criteria. The suitability of these data is, therefore, justified for this specific application. These data are considered acceptable for use in this report because the personnel (Nye County geologists) and organization (the Early Warning Drilling Program, EWDP) collecting the data are qualified to do so, the data have been used in previous revisions of this report, and there are available corroborating data from qualified sources (proximally located qualified water levels). Most importantly, Nye County has a rigorous Quality Assurance Program that governs the development and implementation of procedures used for sample collection and data production and, while it is not necessarily equivalent to the Yucca Mountain Quality Assurance Program, it meets the highest standard required under their Quality Assurance Program, which adds confidence to the initial quality of the data.

D3.1 QA PROGRAM

The NWRPO QAP provides assurance that data gathered from Nye County nuclear waste oversight and investigation programs are of the highest quality. The QA program ensures that NWRPO scientific activities proceed in a systematic and technically sound manner. The QAP uses documented instructions and procedures to ensure the validity, integrity, preservation and retrievability of all data generated by NWRPO programs. Comprehensiveness of the Nye County QAP is illustrated by the index shown in Figure D-1.

Nye County policy requires the NWRPO to establish and maintain a documented Quality Assurance Program for the purpose of ensuring the NWRPO will continually achieve quality of performance in all areas of its responsibilities, through the application of effective management systems and in conformance with its mission. The NWRPO QAP meets the requirements of ANSI/ASME NQA-1 [DIRS 176399] and the criteria at 10 CFR Part 50 [DIRS 176567], Appendix B.

All NWRPO personnel and contractors or subcontractors who perform or manage quality-affecting functions, work under the procedures outlined in the QAP. The NWRPO Project Manager is responsible for assuring all work performed under his or her direction complies with the requirements of the QAP. The YMP Quality Assurance Officer is responsible for establishing, implementing and verifying the QAP complies with this policy.

The QAP provides assurance that data derived from NWRPO oversight and investigation programs are of the highest quality. The QAP ensures NWRPO scientific activities proceed in a systematic manner, using documented instructions and procedures that ensure the validity, integrity, preservation, and retrievability of data generated.

Revision 11, 03-31-04

NYE COUNTY NUCLEAR WASTE REPOSITORY PROJECT OFFICE
QUALITY ASSURANCE NUMERICAL INDEX

Number	Title	Revision	Date	Change Notices
	Policy Documents			
QAPP	Quality Assurance Program Plan	4	6-15-03	
	Quality Administrative Procedures			
QAP-3.1	Independent Technical Review	1	3-31-04	
QAP-3.2	Documentation of Technical Investigations	2	3-31-04	
QAP-5.1	Preparation of Quality Administrative Procedures	1	3-31-04	
QAP 5.2	Preparation of Work Plans, Test Plans, and Technical Procedures	2	3-31-04	
QAP-6.1	Issue and Control of Quality Assurance Documents	1	3-31-04	
QAP-7.1	Procurement of Items and Services	1	3-31-04	
QAP-8.1	Sample Management	1	3-31-04	
QAP-12.1	Control of Measuring and Test Equipment	2	3-31-04	
QAP-15.1	Control of Nonconforming Items or Activities	1	3-31-04	
QAP-16.1	Corrective Action	1	3-31-04	
QAP-17.1	Records Management	2	3-31-04	
QAP-18.1	Audits and Surveillances	1	3-31-04	

Figure D-1. Snapshot of Index Nye County QAP

The NWRPO QAP is based on the interpretation of Federal requirements (ANSI/ASME NQA-1 [DIRS 176399]), 10 CFR Part 50, Appendix B [DIRS 176567]) for nuclear power plants, adapted for waste repository research. The program also establishes procedures for controlling activities that ultimately affect the final product of NWRPO oversight and investigation. The extent to which this QAP deals with quality assurance and the responsibilities outlined within the range of NWRPO activities, is consistent with the importance of individual tasks. NWRPO QA program components include: (1) impact monitoring and assessment, (2) suitability evaluation and compliance, (3) employment and procurement outreach, and (4) public involvement and education.

The current NWRPO QAP was reinitiated in March of 1997 after being in hiatus since October of 1996. The program focuses on the establishment of fundamental elements of the quality assurance program, including creation of a measuring and test equipment control system and refinement of a quality assurance records management system.

The primary issue facing the NWRPO QAP is ensuring the traceability and validity of data gathered by the program. The QA applied to the gathering and analysis of data must be sufficient to ensure their conformance to regulatory controls. In addition, as NWRPO technical activity increases, QA audits, surveillance, and evaluation actions also increase. As additional technical and administrative staff is added, it is necessary to communicate relevant. QA responsibilities and provide proper training to enable project participants to perform appropriate QA.

D3.2 CORROBORATING DATA

Unqualified Nye County well data is compared with existing qualified Nye County and private well data in Table D-1. Well locations used for comparison are sometimes hundreds to thousands of meters separated, so exact comparisons are not expected. The comparison is made with nearest qualified well or a well that is expected to be in a comparable head region given the understood head gradient in the region. Differences tend to be well within the range of residuals seen from the calibration and consistent regions of flat gradients (lower residuals) just south of the repository and high gradients (higher residuals) in the region hear U.S. Highway 95 Fault. The largest difference (–37.8) is for the deepest open interval (Z4) at well NC-EWDP-7SC for which the qualified well did not have a corresponding open interval. Overall the new Nye County EWDP well data is very consistent with existing qualified data and is deemed appropriate for use as calibration targets and development of the potentiometric surface.

Table D-1. Comparison of New Nye County Well Data with Corroborating Data

Well ID	X-UTM (m)	Y-UTM (m)	Elevation (m)	Measured Head (m)	Qualified Well ID	X-UTM (m)	Y-UTM (m)	Qualified Head (m)	Difference (m)
NC-EWDP-7SC	539632	4064317	704.5	828.5	NC-EWDP-7S	539638	4064323	830.3	–1.8
NC-EWDP-7SC-Z1	539632	4064317	812.6	830.3	NC-EWDP-7S	539638	4064323	830.3	0
NC-EWDP-7SC-Z2	539632	4064317	779.1	830.4	NC-EWDP-7S	539638	4064323	830.3	0.1
NC-EWDP-7SC-Z3	539632	4064317	741	821.7	NC-EWDP-7S	539638	4064323	830.3	–8.6
NC-EWDP-7SC-Z4	539632	4064316	704.5	792.5	NC-EWDP-7S	539638	4064323	830.3	–37.8
NC-EWDP-10P Deep	553149	4064916	650.4	726.9	UE-25 J-12	554444	4068774	727.9	–1.0
NC-EWDP-10P Shallow	553149	4064916	696.4	726.9	UE-25 J-12	554444	4068774	727.9	–1.0
NC-EWDP-10S-Z1	553140	4064899	696	727	UE-25 J-12	554444	4068774	727.9	–0.9
NC-EWDP-10S-Z2	553140	4064899	650.3	727.5	UE-25 J-12	554444	4068774	727.9	–0.4
NC-EWDP-18P	549416	4067233	702.3	711.2	NC-EWDP-2DB	547800	4057196	712.6	–1.4
NC-EWDP-19IM1-Z1	549317	4058291	691.1	711.9	NC-EWDP-19D	549317	4058271	711.8	0.1
NC-EWDP-19IM1-Z2	549317	4058291	659.1	712.1	NC-EWDP-19D	549317	4058271	711.8	0.3
NC_EWDP-19IM1-Z3	549317	4058291	628.6	712.5	NC-EWDP-19D	549317	4058271	711.8	0.7
NC_EWDP-19IM1-Z4	549317	4058291	589	713.3	NC-EWDP-19D	549317	4058271	711.8	1.5
NC_EWDP-19IM1-Z5	549317	4058291	545	711.8	NC-EWDP-19D	549317	4058271	711.8	0.0
NC_EWDP-19IM2	549337	4058291	599.2	723.3	NC-EWDP-19D	549317	4058271	711.8	11.5
NC_EWDP-22PA Deep	552020	4062038	652	724.8	NC-EWDP-4PB	553281	4056774	723.5	1.3
NC_EWDP-22PA Shallow	552020	4062038	700.9	724.8	NC-EWDP-4PB	553281	4056774	723.5	1.3
NC_EWDP-22PB Deep	552038	4062037	514.9	724.8	NC-EWDP-4PB	553281	4056774	723.5	1.3
NC_EWDP-22PB Shallow	552038	4062037	584.9	724.8	NC-EWDP-4PB	553281	4056774	723.5	1.3
NC_EWDP-22S-Z1	552019	4062020	700.3	724.9	NC-EWDP-4PB	553281	4056774	723.5	1.4
NC_EWDP-22S-Z2	552019	4062020	651.7	724.9	NC-EWDP-4PB	553281	4056774	723.5	1.4
NC_EWDP-22S-Z3	552019	4062020	584.9	724.9	NC-EWDP-4PB	553281	4056774	723.5	1.4
NC_EWDP-22S-Z4	552019	4062020	514.8	724.9	NC-EWDP-4PB	553281	4056774	723.5	1.4
NC_EWDP-23P Deep	553923	4059875	649.2	724.3	NC-EWDP-4PB	553281	4056774	723.5	0.8

Table D-1. Comparison of New Nye County Well Data with Corroborating Data (Continued)

Well ID	X-UTM (m)	Y-UTM (m)	Elevation (m)	Measured Head (m)	Qualified Well ID	X-UTM (m)	Y-UTM (m)	Qualified Head (m)	Difference (m)
NC_EWDP-23P Shallow	553923	4059875	704	724.2	NC-EWDP-4PB	553281	4056774	723.5	0.7
NC_EWDP-16P	545665	4064263	722.3	729.4	Cind-R-Lite Well	544027	4059809	729.8	–0.4
NC_EWDP-19PB Deep	549337	4058316	659.5	707.9	NC-EWDP-19D	549317	4058271	711.8	–3.9
NC_EWDP-19PB Shallow	549337	4058316	702.1	707.4	NC-EWDP-19D	549317	4058271	711.8	–4.4
NC_EWDP-24P	549386	4062055	786.4	727.1	USW WT-11	547542	4070428	730.7	–3.6
NC_EWDP-27P	544935	4065276	728.2	728.6	Cind-R-Lite Well	544027	4059809	729.8	–1.2
NC_EWDP-28P	545746	4062393	718.7	729.3	Cind-R-Lite Well	544027	4059809	729.8	–0.5
NC_EWDP-29P	549396	4059606	719.2	724.8	NC-EWDP-15P	544927	4058163	722.4	2.4
13P	543471	4066433	759.5	764.4	NC-EWDP-9SX,P1	539118	4061010	766.4	–2.0
22PC-Z1	552037	4062019	702.3	724.9	NC-EWDP-4PB	553281	4056774	723.5	1.4
22PC-Z2	552037	4062019	651.8	724.9	NC-EWDP-4PB	553281	4056774	723.5	1.4
24PB	549387	4062025	621.6	727.2	USW WT-11	547542	4070428	730.7	–3.6
32P-Z1	546184	4054789	697.1	701.7	NC-EWDP-2D	547823	4057170	706.1	–4.4
32P-Z2	546184	4054789	631.5	701.0	NC-EWDP-2D	547823	4057170	706.1	–5.1
32P-Z3	546184	4054789	558.2	701.1	NC-EWDP-2D	547823	4057170	706.1	–5.0
33P-Z1	545117	4057146	713.1	720.8	NC-EWDP 15P	544927	4058163	722.4	–1.6
33P-Z2	545117	4057146	629.7	721.9	NC-EWDP 15P	544927	4058163	722.4	–0.5
33P-Z3	545117	4057146	594.2	721.8	NC-EWDP 15P	544927	4058163	722.4	–0.6

Sources: DTNs: GS010908312332.002 [DIRS 163555], Output DTNs: LA0612RR150304.001, see Appendix F; SN0702T0510106.007. See Table D-2 for well to DTN mapping.

D4. EVALUATION CONCLUSIONS

The conclusions of the Evaluation Team review of the Nye County well data are presented below in terms of the evaluation criteria presented in Section D2.2.

1. *Is there functional equivalence of the data-gathering process to applicable QARD concepts (qualification of personnel, technical adequacy of equipment and procedures, quality and reliability of measurement control and audits)?*

The evaluation in Section D3 found the Nye County QAP (index shown in Figure D-1) to be functionally equivalent to applicable QARD concepts. The Nye Count QA program ensures NWRPO scientific programs, including the EWDP, proceed in a systematic and technically sound manner. The documented instructions and procedures ensure the qualification of personnel, the technical adequacy of equipment and testing procedures and the validity, integrity, preservation and retrievability of data generated by the NWRPO programs.

2. *Are the data addressed in this appendix consistent with corroborating data?*

The data addressed in this appendix is consistent with the corroborating data presented above. Measurements from wells in close proximity and in same formations agree to within expectations and requirements of the intended use.

3. *Are the methods used to incorporate the data into the SZ site-scale model reasonable and generally accepted by the technical community?*

The use of well data in both the construction of the potentiometric surface and as calibration targets in the SZ site-scale flow model is well established and accepted by the technical community.

4. *Are there more appropriate sources of the required SZ site-scale model data?*

Other sources of similar information are older and less well developed than the recently obtained well data. The Nye County well data was obtained in part to support YMP ground flow monitoring and modeling. It provides a reasonable and most comprehensive source of head data and is an appropriate source of information for developing hydrologic data for the SZ site-scale model.

5. *Are the associated uncertainties acceptable for their intended use by the SZ site-scale flow model?*

Uncertainties in the well data have been appropriately addressed by using them as target values for SZ site-scale flow model calibration. The calibration has been successfully completed using this approach, indicating that the well data have been successfully used and are therefore appropriate for their intended use.

Based on the assessment of the NWRPO QAP and corroborating data presented above, the Nye County well data are considered suitable for use in both the construction of the potentiometric surface and as calibration targets for the SZ site-scale flow model. In accordance with criteria established in Section D2.2, this finding qualifies these data only for their intended uses in this report. The Output DTN: SN0702T0510106.007 will remain unqualified for other uses.

D6. DATA SOURCE AND DEVELOPMENT

This section describes the data sources compiled into Output DTN: SN0702T0510106.007 as well as documents the qualified software and basic MS-Excel spreadsheet calculations used to convert the NC-EWDP well data into a form suitable for use in the SZ site-scale flow model.

A list of Nye County wells with data to be qualified in this appendix and their corresponding DTNs are presented in Table D-2. YMP qualified software (CORPSCON V.5.11.08, STN: 10547-5.11.08-00 [DIRS 155082]) was used to convert the GPS latitude and longitude coordinates into UTM (m) coordinates for modeling purposes in Output DTN: LA0612RR150304.001 (see Appendix F) and for Phase V wells in Output DTN: SN0702T0510106.007. These data are summarized in Table D-3. To calibrate the SZ site-scale flow model, in addition to the UTM coordinates of the well and water level, the measurement point is also needed. This measurement point corresponds to the midpoint of the open interval of the well screen. The land surface elevations, distances to the tops and bottoms of the open interval well screens and measurement points are presented in Table D-4. Water-level data are provided in Tables D-5 and D-6. The measurement point elevations (or reference elevations) listed in Table D-5 are different than the ground surface elevations presented in Table D-3 and the open interval measurement points listed in Table D-4.

The data listed in Tables D-3 through D-6 were developed as follows:

DTNs (Table D-2) are available for GPS survey summary reports and well completion reports for most of the NC-EWDP wells discussed in this appendix. Data discussed in this appendix were developed from the reports as follows:

- Well locations in UTM coordinates consistent with the SZ Flow model were calculated from longitude/latitude geographic coordinates obtained from the DTNs listed in Table D-2. UTM coordinates for calibration wells NC-EWDP-7SC through -29P were provided by Output DTN: LA0612RR150304.001, which is discussed in Appendix F. The Phase V UTM well locations used in validation were calculated using CORPSCON V.5.11.08 (STN: 10547-5.11.08-00 [DIRS 155082]) and are included in Output DTN: SN0702T0510106.007.

- Screened intervals used in water level measurements were obtained from the well completion reports listed in Table D-2. The screened intervals were converted from feet relative to a surface marker to elevations (amsl) in meters using basic MS Excel spreadsheet functions. The midpoint elevation (m) for each screened interval was also calculated and is used as the measurement location. The spreadsheet calculations are included in Output DTN: SN0702T0510106.007. For water level measurements that fell below the top of the screened interval, new measurement locations were calculated

as the midpoint between the water level elevation and the bottom elevation of the interval.

- Time-averaged water-level data were developed from the water level DTNs shown in Table D-2 also using a MS Excel spreadsheet. There are two different water level DTNs representing the two different time frames of the SZ Flow model development. The well data used for SZ Flow model calibration includes well data through February 2005; the second is well data used for validation that did not become available until December 2006, which includes water-level data through November 2006. Generally, variability of measured water levels with time falls within expected values (< 1 m).

All developed data and sources, including the MS Excel workbook, have been stored under Output DTN: SN0702T0510106.007.

Table D-2. Nye County Wells with Data to Be Evaluated and Corresponding Data Sources

Well	Phase	Summary GPS Survey DTN	Well Completion Report DTN
Phase II, III, and IV Wells used in SZ Flow Calibration			
7SC	II	MO0206GSC02074.000 [DIRS 168378]	MO0206NYE04926.119 [DIRS 179372]
10P	III	MO0206GSC02074.000 [DIRS 168378]	MO0306NYE05262.168 [DIRS 179374]
10S	III	MO0203GSC02034.000 [DIRS 168375]	MO0306NYE05261.167 [DIRS 179373]
16P	IV	MO0307GSC03094.000 [DIRS 170556]	MO0702NYE05714.375 [DIRS 179443]
18P	III	MO0203GSC02034.000 [DIRS 168375]	MO0306NYE05263.169 [DIRS 179375]
19IM1	III	MO0206GSC02074.000 [DIRS 168378]	MO0306NYE05259.165 [DIRS 165876]
19IM2	III	MO0206GSC02074.000 [DIRS 168378]	MO0306NYE05260.166 [DIRS 165877]
19PB	IV	MO0408GSC04123.000 [DIRS 174102]	MO0409NYE06101.246 [DIRS 179384]
22PA	III	MO0206GSC02074.000 [DIRS 168378]	MO0306NYE05265.171 [DIRS 179377]
22PB	III	MO0206GSC02074.000 [DIRS 168378]	MO0306NYE05266.172 [DIRS 179378]
22S	III	MO0203GSC02034.000 [DIRS 168375]	MO0306NYE05264.170 [DIRS 179376]
23P	III	MO0206GSC02074.000 [DIRS 168378]	MO0306NYE05267.173 [DIRS 179379]
24P	IV	MO0312GSC03180.000 [DIRS 174103]	MO0409NYE06096.242 [DIRS 179383]
27P	IV	MO0307GSC03094.000 [DIRS 170556]	MO0312NYE05716.204 [DIRS 179380]
28P	IV	MO0307GSC03094.000 [DIRS 170556]	MO0312NYE05718.202 [DIRS 179381]
29P	IV	MO0312GSC03180.000 [DIRS 174103]	MO0409NYE06093.241 [DIRS 179382]
Phase V Wells used for SZ Flow Validation			
13P	V	MO0606ABLNCPVB.000 [DIRS 180020]	MO0611NYE06947.344 [DIRS 180022]
22PC	V	MO0503GSC05025.000 [DIRS 175275]	MO0505NYE06464.314 [DIRS 179599]
24PB	V	MO0608ABEWDPPV.000 [DIRS 180021]	MO0606NYE06949.340 [DIRS 180023]
32P	V	MO0608ABEWDPPV.000 [DIRS 180021]	MO0612NYE07008.366 [DIRS 179486]
33P	V	MO0608ABEWDPPV.000 [DIRS 180021]	MO0612NYE07011.368 [DIRS 179487]
Water-Level Data			
Calibration Wells	II-IV	MO0507NYE06631.323 [DIRS 177372]	
Validation wells	V	MO0612NYE07122.370 [DIRS 179337]	

Table D-3. Nye County Wells with GPS Locations

Well	NC-EWDP Phase	Latitude	Longitude	Northing (m)	Easting (m)
7SC	II	36° 43' 31.822"	116° 33' 25.425"	4064317	539632
10P	III	36° 43' 48.874"	116° 24' 20.362"	4064916	553149
10S	III	36° 43' 48.339"	116° 24' 20.725"	4064899	553140
16P	IV	36° 43' 29.089"	116° 29' 22.219"	4064263	545665
18P	III	36° 45' 04.797"	116° 25' 50.340"	4067233	549416
19IM1	III	36° 40' 14.615"	116° 26' 56.397"	4058291	549317
19IM2	III	36° 40' 14.614"	116° 26' 55.597"	4058291	549337
19PB	IV	36° 40' 15.440"	116° 26' 55.593"	4058316	549337
22PA	III	36° 42' 15.712"	116° 25' 06.581"	4062038	552020
22PB	III	36° 42' 15.665"	116° 25' 05.863"	4062037	552038
22S	III	36° 42' 15.132"	116° 25' 06.636"	4062020	552019
23P	III	36° 41' 05.137"	116° 23' 50.412"	4059875	553923
24P	IV	36° 42' 16.775"	116° 26' 52.756"	4062055	549386
27P	IV	36° 44' 02.072"	116° 29' 51.436"	4065276	544935
28P	IV	36° 42' 28.386"	116° 29' 19.390"	4062393	545746
29P	IV	36° 40' 57.297"	116° 26' 52.884"	4059606	549396
13P	V	36° 44' 39.866"	116° 30' 50.235"	4066433	543471
22PC	V	36° 42' 15.090"	116° 25' 05.906"	4062019	552037
24PB	V	36° 42' 15.777"	116° 26' 52.692"	4062025	549387
32P	V	36° 38' 21.544"	116° 29' 03.381"	4054789	546184
33P	V	36° 39' 38.210"	116° 29' 45.814"	4057146	545117

Source : Output DTNs: LA0612RR150304.001 (see Appendix F) ; Phase V: SN0702T0510106.007.

Table D-4. Land Surface Elevation and the Top and Bottom of the Open Intervals for Nye County Wells

Well NC-EWDP	Elevation (ft)	Top (ft)	Bottom (ft)		Elevation (m)	Top (m)	Bottom (m)	Measurement Point (m)
7SC	2751.0	429.8	449.8		838.5	131.0	137.1	704.5
7SC-Z1	2751.0	80.0	90.0		838.5	24.4	27.4	812.6
7SC-Z2	2751.0	180.0	210.0		838.5	54.9	64.0	779.1
7SC-Z3	2751.0	270.0	370.0		838.5	82.3	112.8	741.0
7SC-Z4	2751.0	429.8	449.8		838.5	131.0	137.1	704.5
10P Shallow	2964.6	660.0	700.0		903.6	201.2	213.4	696.3
10P Deep	2964.6	800.0	860.0		903.6	243.8	262.1	650.6
10S-Z1	2963.5	660.1	699.3		903.3	201.2	213.1	696.1
10S-Z2	2963.5	801.2	860.0		903.3	244.2	262.1	650.1
16P	2889.1	489.4	549.4		880.6	149.2	167.5	722.3
18P	3164.5	835.8	885.0		964.5	254.8	269.7	702.3

Table D-4. Land Surface Elevation and the Top and Bottom of the Open Intervals for Nye County Wells (Continued)

Well NC-EWDP	Elevation (ft)	Top (ft)	Bottom (ft)		Elevation (m)	Top (m)	Bottom (m)	Measurement Point (m)
19IM1-Z1	2687.3	410.0	430.0		819.1	125.0	131.1	691.1
19IM1-Z2	2687.3	515.0	535.0		819.1	157.0	163.1	659.1
19IM1-Z3	2687.3	574.9	674.9		819.1	175.2	205.7	628.6
19IM1-Z4	2687.3	724.9	784.8		819.1	220.9	239.2	589.0
19IM1-Z5	2687.3	849.5	949.3		819.1	258.9	289.3	545.0
19IM2	2688.1	410.2	950.1		819.3	125.0	131.1	691.3
19PB Shallow	2688.7	375.0	395.0		819.5	114.3	120.4	702.2
19PB Deep	2688.7	514.7	534.7		819.5	156.9	163.0	659.6
22PA Shallow	2849.9	520.7	579.7		868.6	158.7	176.7	700.9
22PA Deep	2849.9	661.5	759.8		868.6	201.6	231.6	652.0
22PB Shallow	2849.3	881.3	979.7		868.5	268.6	298.6	584.9
22PB Deep	2849.3	1140.3	1179.7		868.5	347.6	359.6	514.9
22S-Z1	2849.0	521.5	581.3		868.4	159.0	177.2	700.3
22S-Z2	2849.0	661.2	760.6		868.4	201.5	231.8	651.7
22S-Z3	2849.0	880.2	980.0		868.4	268.3	298.7	584.9
22S-Z4	2849.0	1140.0	1180.0		868.4	347.5	359.7	514.8
23P Shallow	2800.2	460.9	519.9		853.5	140.5	158.5	704.0
23P Deep	2800.2	650.5	689.8		853.5	198.3	210.3	649.2
24P	2790.2	400.0	440.0		850.4	121.9	134.1	722.4
27P	2973.6	580.7	620.6		853.5	177.0	189.2	670.4
28P	2767.5	370.0	449.0		843.5	112.8	136.9	718.7
29P	2726.2	340.0	390.0		830.9	103.6	118.9	719.7
13P	2937.8	426.0	466.0		895.5	765.6	753.4	759.5
22PC-Z1	2848.9	510.0	579.8		868.3	712.9	691.6	702.3
22PC-Z2	2848.8	665.4	755.0		868.3	665.5	638.2	651.8
24PB	2788.8	729.2	769.9		850.0	627.8	615.4	621.6
32P-Z1	2545.3	238.7	277.9		775.8	703.1	691.1	697.1
32P-Z2	2545.3	463.7	483.3		775.8	634.5	628.5	631.5
32P-Z3	2545.3	697.9	730.0		775.8	563.1	553.3	558.2
33P-Z1	2570.1	210.8	249.9		783.4	719.1	707.2	713.1
33P-Z2	2570.1	484.5	523.6		783.4	635.7	623.8	629.7
33P-Z3	2570.1	600.9	640.0		783.4	600.2	588.3	594.2

Source: Output DTN: SN0702T0510106.007.

Table D-5. Nye County Water Level Measurements through 2/2005

Well NC-EWDP	Phase	Date	Time	Groundwater Elevation (ft amsl)	MP Elevation (ft amsl)	Depth to Water (ft)	Sounder
7SC	II	2/14/2001	9:00	2717.63	2749.68	32.05	NWRPO-500
7SC	II	2/21/2001	10:15	2713.88	2749.68	35.80	NWRPO-500
7SC	II	2/28/2001	11:40	2717.63	2749.68	32.05	NWRPO-500
7SC	II	3/26/2001	15:08	2711.97	2749.68	37.71	NWRPO-500
7SC	II	3/27/2001	14:18	2722.30	2749.68	27.38	NWRPO-500
7SC	II	3/30/2001	11:35	2721.97	2749.68	27.71	NWRPO-500
7SC	II	4/2/2001	10:15	2721.97	2749.68	27.71	NWRPO-500
7SC-Z1	II	3/19/2003	11:53	2724.29	2749.68	25.39	NWRPO-500-2
7SC-Z1	II	2/17/2004	11:54	2723.93	2749.68	25.75	NWRPO-1000-7
7SC-Z1	II	9/29/2004	14:36	2724.21	2749.68	25.47	NWRPO-500-8
7SC-Z2	II	9/13/2002	9:54	2724.27	2749.68	25.41	NWRPO-1000-4
7SC-Z2	II	9/13/2002	12:30	2724.1	2749.68	25.58	NWRPO-1000-4
7SC-Z2	II	3/19/2003	12:14	2724.32	2749.68	25.36	NWRPO-500-2
7SC-Z2	II	2/17/2004	12:28	2724.34	2749.68	25.34	NWRPO-1000-7
7SC-Z2	II	9/29/2004	15:06	2724.47	2749.68	25.21	NWRPO-500-8
7SC-Z3	II	9/12/2002	15:45	2695.40	2749.68	54.28	NWRPO-1000-4
7SC-Z3	II	9/13/2002	9:24	2694.61	2749.68	55.07	NWRPO-1000-4
7SC-Z3	II	3/21/2003	9:23	2696.82	2749.68	52.86	NWRPO-500-2
7SC-Z3	II	3/10/2004	9:17	2696.78	2749.68	52.90	NWRPO-500-1
7SC-Z4	II	3/28/2003	11:55	2613.73	2749.68	135.95	NWRPO-500-2
7SC-Z4	II	3/15/2004	10:42	2586.37	2749.68	163.31	NWRPO-500-1
10P Deep	III	1/28/2002	8:23	2384.93	2966.65	581.72	NWRPO-1000-4
10P Deep	III	2/5/2002	15:47	2384.83	2966.65	581.82	NWRPO-1000-4
10P Deep	III	2/11/2002	10:55	2384.75	2966.65	581.90	NWRPO-1000-4
10P Deep	III	3/25/2002	6:29	2384.69	2966.65	581.96	NWRPO-1000-4
10P Deep	III	4/25/2002	10:48	2384.88	2966.65	581.77	NWRPO-1000-4
10P Deep	III	5/21/2002	10:16	2384.68	2966.65	581.97	NWRPO-1000-4

Table D-5. Nye County Water Level Measurements through 2/2005 (Continued)

Well NC-EWDP	Phase	Date	Time	Groundwater Elevation (ft amsl)	MP Elevation (ft amsl)	Depth to Water (ft)	Sounder
10P Deep	III	6/27/2002	7:01	2384.83	2966.65	581.82	NWRPO-1000-4
10P Deep	III	7/24/2002	9:15	2384.67	2966.65	581.98	NWRPO-1000-5
10P Deep	III	7/25/2002	7:07	2384.81	2966.65	581.84	NWRPO-1000-4
10P Deep	III	8/22/2002	7:08	2384.77	2966.65	581.88	NWRPO-1000-4
10P Deep	III	8/22/2002	7:35	2384.70	2966.65	581.95	NWRPO-1000-5
10P Deep	III	8/27/2002	8:15	2384.97	2966.65	581.68	NWRPO-1000-4
10P Deep	III	8/27/2002	16:45	2385.05	2966.65	581.60	NWRPO-1000-4
10P Deep	III	9/25/2002	8:19	2384.98	2966.65	581.67	NWRPO-1000-4
10P Deep	III	10/16/2002		2384.98	2966.65	581.67	NWRPO-1000-5
10P Deep	III	11/18/2002	11:13	2384.63	2966.65	582.02	NWRPO-1000-5
10P Deep	III	12/23/2002	11:05	2384.85	2966.65	581.80	NWRPO-1000-5
10P Deep	III	1/30/2003	10:43	2384.72	2966.65	581.93	NWRPO-1000-5
10P Deep	III	2/24/2003	9:25	2385.09	2966.65	581.56	NWRPO-1000-5
10P Deep	III	3/12/2003	8:58	2384.86	2966.65	581.79	NWRPO-1000-5
10P Deep	III	4/17/2003	9:45	2385.08	2966.65	581.57	NWRPO-1000-4
10P Deep	III	4/17/2003	9:36	2384.96	2966.65	581.69	NWRPO-1000-5
10P Deep	III	4/17/2003	9:55	2384.99	2966.65	581.66	NWRPO-1000-6
10P Deep	III	5/15/2003	9:01	2384.84	2966.65	581.81	NWRPO-1000-5
10P Deep	III	6/16/2003	8:57	2384.83	2966.65	581.82	NWRPO-1000-5
10P Deep	III	7/17/2003	7:25	2384.79	2966.65	581.86	NWRPO-1000-5
10P Deep	III	8/18/2003	6:33	2384.94	2966.65	581.71	NWRPO-1000-5
10P Deep	III	9/15/2003	7:22	2384.88	2966.65	581.77	NWRPO-1000-5
10P Deep	III	10/21/2003	8:45	2384.72	2966.65	581.93	NWRPO-1000-5
10P Deep	III	11/13/2003	8:19	2384.79	2966.65	581.86	NWRPO-1000-5
10P Deep	III	1/19/2004	10:57	2384.87	2966.65	581.78	NWRPO-1000-5
10P Deep	III	2/15/2004	8:26	2384.90	2966.65	581.75	NWRPO-1000-5
10P Deep	III	2/25/2004	8:26	2384.72	2966.65	581.93	NWRPO-1000-5
10P Deep	III	3/25/2004	8:02	2384.84	2966.65	581.81	NWRPO-1000-5
10P Deep	III	5/17/2004	8:05	2384.93	2966.65	581.72	NWRPO-1000-5

Table D-5. Nye County Water Level Measurements through 2/2005 (Continued)

Well NC-EWDP	Phase	Date	Time	Groundwater Elevation (ft amsl)	MP Elevation (ft amsl)	Depth to Water (ft)	Sounder
10P Deep	III	6/28/2004	7:21	2384.86	2966.65	581.79	NWRPO-1000-5
10P Deep	III	7/26/2004	7:20	2384.85	2966.65	581.80	NWRPO-1000-5
10P Deep	III	8/23/2004	10:35	2384.93	2966.65	581.72	NWRPO-1000-5
10P Deep	III	9/20/2004	8:20	2384.65	2966.65	582.00	NWRPO-1000-5
10P Deep	III	10/11/2004	8:25	2384.81	2966.65	581.84	NWRPO-1000-5
10P Shallow	III	1/28/2002	8:14	2385.11	2966.65	581.54	NWRPO-1000-4
10P Shallow	III	2/5/2002	15:36	2384.96	2966.65	581.69	NWRPO-1000-4
10P Shallow	III	2/11/2002	11:05	2384.86	2966.65	581.79	NWRPO-1000-4
10P Shallow	III	3/25/2002	6:36	2384.86	2966.65	581.79	NWRPO-1000-4
10P Shallow	III	4/25/2002	10:38	2385.01	2966.65	581.64	NWRPO-1000-4
10P Shallow	III	5/21/2002	10:01	2384.82	2966.65	581.83	NWRPO-1000-4
10P Shallow	III	6/27/2002	6:52	2384.96	2966.65	581.69	NWRPO-1000-4
10P Shallow	III	7/24/2002	9:24	2384.82	2966.65	581.83	NWRPO-1000-5
10P Shallow	III	7/25/2002	6:57	2384.93	2966.65	581.72	NWRPO-1000-4
10P Shallow	III	8/22/2002	7:03	2384.88	2966.65	581.77	NWRPO-1000-4
10P Shallow	III	8/22/2002	7:21	2384.81	2966.65	581.84	NWRPO-1000-5
10P Shallow	III	8/26/2002	15:45	2385.18	2966.65	581.47	NWRPO-1000-4
10P Shallow	III	8/27/2002	10:45	2385.08	2966.65	581.57	NWRPO-1000-4
10P Shallow	III	9/25/2002	8:07	2385.13	2966.65	581.52	NWRPO-1000-4
10p Shallow	III	10/16/2002	11:35	2385.14	2966.65	581.51	NWRPO-1000-6
10p Shallow	III	10/16/2002	11:48	2385.24	2966.65	581.41	NWRPO-1000-4
10p Shallow	III	10/16/2002	11:58	2385.14	2966.65	581.51	NWRPO-1000-5
10p Shallow	III	11/18/2002	11:02	2384.77	2966.65	581.88	NWRPO-1000-5
10p Shallow	III	12/23/2002	10:54	2385.00	2966.65	581.65	NWRPO-1000-5
10P Shallow	III	1/30/2003	10:32	2384.85	2966.65	581.80	NWRPO-1000-5
10P Shallow	III	2/24/2003	9:13	2385.18	2966.65	581.47	NWRPO-1000-5
10P Shallow	III	3/12/2003	8:46	2385.01	2966.65	581.64	NWRPO-1000-5
10P Shallow	III	4/17/2003	9:24	2385.12	2966.65	581.53	NWRPO-1000-5
10P Shallow	III	5/15/2003	8:49	2385.02	2966.65	581.63	NWRPO-1000-5

Table D-5. Nye County Water Level Measurements through 2/2005 (Continued)

Well NC-EWDP	Phase	Date	Time	Groundwater Elevation (ft amsl)	MP Elevation (ft amsl)	Depth to Water (ft)	Sounder
10P Shallow	III	6/16/2003	8:46	2384.97	2966.65	581.68	NWRPO-1000-5
10P Shallow	III	7/17/2003	7:12	2384.94	2966.65	581.71	NWRPO-1000-5
10P Shallow	III	8/18/2003	6:33	2385.09	2966.65	581.56	NWRPO-1000-5
10P Shallow	III	9/15/2003	7:10	2385.00	2966.65	581.65	NWRPO-1000-5
10P Shallow	III	10/21/2003	8:34	2384.87	2966.65	581.78	NWRPO-1000-5
10P Shallow	III	11/13/2003	8:07	2384.95	2966.65	581.70	NWRPO-1000-5
10P Shallow	III	1/19/2004	10:46	2385.01	2966.65	581.64	NWRPO-1000-5
10P Shallow	III	2/25/2004	8:14	2384.87	2966.65	581.78	NWRPO-1000-5
10P Shallow	III	3/25/2004	7:50	2385.01	2966.65	581.64	NWRPO-1000-5
10P Shallow	III	5/17/2004	7:55	2385.11	2966.65	581.54	NWRPO-1000-5
10P Shallow	III	6/28/2004	7:10	2385.03	2966.65	581.62	NWRPO-1000-5
10P Shallow	III	7/26/2004	7:09	2385.00	2966.65	581.65	NWRPO-1000-5
10P Shallow	III	8/23/2004	10:20	2385.13	2966.65	581.52	NWRPO-1000-5
10P Shallow	III	9/20/2004	8:09	2384.84	2966.65	581.81	NWRPO-1000-5
10P Shallow	III	10/11/2004	8:15	2385.00	2966.65	581.65	NWRPO-1000-5
10P Shallow	III	2/14/2005	8:14	2385.04	2966.65	581.61	NWRPO-1000-5
10S-Z1	III	7/24/2002	11:24	2385.07	2966.27	581.20	NWRPO-1000-5
10S-Z1	III	9/12/2002	7:00	2385.28	2966.27	580.99	NWRPO-1000-4
10S-Z1	III	9/12/2002	10:25	2385.23	2966.27	581.04	NWRPO-1000-4
10S-Z1	III	6/10/2003	13:40	2385.32	2966.27	580.95	NWRPO-1000-5
10S-Z1	III	11/6/2003	8:34	2385.11	2966.27	581.16	NWRPO-1000-7
10S-Z1	III	6/29/2004	11:10	2385.32	2966.27	580.95	NWRPO-1000-7
10S-Z2	III	7/24/2002	9:36	2384.87	2966.27	581.40	NWRPO-1000-5
10S-Z2	III	9/11/2002	12:10	2385.10	2966.27	581.17	NWRPO-1000-4
10S-Z2	III	9/11/2002	16:25	2385.24	2966.27	581.03	NWRPO-1000-4
10S-Z2	III	6/10/2003	12:50	2385.07	2966.27	581.20	NWRPO-1000-5
10S-Z2	III	11/7/2003	16:35	2385.16	2966.27	581.11	NWRPO-1000-7
10S-Z2	III	6/29/2004	10:11	2385.09	2966.27	581.18	NWRPO-1000-7
18P	III	11/9/2001	9:50	2386.93	3166.56	779.63	NWRPO-1000-4

Table D-5. Nye County Water Level Measurements through 2/2005 (Continued)

Well NC-EWDP	Phase	Date	Time	Groundwater Elevation (ft amsl)	MP Elevation (ft amsl)	Depth to Water (ft)	Sounder
18P	III	1/2/2002	11:21	2386.96	3166.56	779.60	NWRPO-1000-4
18P	III	1/28/2002	7:35	2386.91	3166.56	779.65	NWRPO-1000-4
18P	III	2/25/2002	7:02	2386.79	3166.56	779.77	NWRPO-1000-4
18P	III	3/25/2002	7:07	2386.86	3166.56	779.70	NWRPO-1000-4
18P	III	5/21/2002	9:16	2386.82	3166.56	779.74	NWRPO-1000-4
18P	III	6/27/2002	8:05	2386.79	3166.56	779.77	NWRPO-1000-4
18P	III	7/25/2002	8:03	2386.95	3166.56	779.61	NWRPO-1000-4
18P	III	8/22/2002	8:23	2386.91	3166.56	779.65	NWRPO-1000-4
18P	III	8/22/2002	8:37	2386.81	3166.56	779.75	NWRPO-1000-5
18P	III	10/16/2002	9:38	2386.84	3166.56	779.72	NWRPO-1000-6
18P	III	10/16/2002	10:11	2386.92	3166.56	779.64	NWRPO-1000-5
18P	III	11/18/2002	11:52	2386.62	3166.56	779.94	NWRPO-1000-5
18P	III	12/23/2002	10:15	2386.79	3166.56	779.77	NWRPO-1000-5
18P	III	1/30/2003	11:48	2386.90	3166.56	779.66	NWRPO-1000-5
18P	III	2/24/2003	10:13	2387.16	3166.56	779.40	NWRPO-1000-5
18P	III	3/12/2003	9:42	2386.89	3166.56	779.67	NWRPO-1000-5
18P	III	4/17/2003	10:54	2387.09	3166.56	779.47	NWRPO-1000-4
18P	III	4/17/2003	10:42	2386.99	3166.56	779.57	NWRPO-1000-5
18P	III	4/17/2003	11:07	2387.01	3166.56	779.55	NWRPO-1000-6
18P	III	5/15/2003	9:45	2386.89	3166.56	779.67	NWRPO-1000-5
18P	III	6/16/2003	9:50	2386.95	3166.56	779.61	NWRPO-1000-5
18P	III	7/17/2003	8:15	2386.91	3166.56	779.65	NWRPO-1000-5
18P	III	8/18/2003	7:20	2386.95	3166.56	779.61	NWRPO-1000-5
18P	III	9/15/2003	8:06	2386.96	3166.56	779.60	NWRPO-1000-5
18P	III	10/21/2003	9:44	2386.92	3166.56	779.64	NWRPO-1000-4
18P	III	10/21/2003	9:30	2386.80	3166.56	779.76	NWRPO-1000-5
18P	III	10/21/2003	10:00	2386.85	3166.56	779.71	NWRPO-1000-6
18P	III	10/21/2003	10:17	2386.86	3166.56	779.70	NWRPO-1000-7
18P	III	11/13/2003	8:52	2386.76	3166.56	779.80	NWRPO-1000-5

Table D-5. Nye County Water Level Measurements through 2/2005 (Continued)

Well NC-EWDP	Phase	Date	Time	Groundwater Elevation (ft amsl)	MP Elevation (ft amsl)	Depth to Water (ft)	Sounder
18P	III	1/19/2004	11:33	2386.90	3166.56	779.66	NWRPO-1000-5
18P	III	2/25/2004	9:02	2386.81	3166.56	779.75	NWRPO-1000-5
18P	III	3/25/2004	8:36	2386.85	3166.56	779.71	NWRPO-1000-5
18P	III	5/17/2004	8:32	2386.92	3166.56	779.64	NWRPO-1000-5
18P	III	5/17/2004	8:46	2386.97	3166.56	779.59	NWRPO-1000-6
18P	III	5/17/2004	8:57	2386.99	3166.56	779.57	NWRPO-1000-7
18P	III	6/28/2004	8:07	2386.90	3166.56	779.66	NWRPO-1000-5
18P	III	8/23/2004	11:25	2386.95	3166.56	779.61	NWRPO-1000-5
18P	III	9/20/2004	8:50	2386.76	3166.56	779.80	NWRPO-1000-5
18P	III	10/11/2004	8:50	2386.85	3166.56	779.71	NWRPO-1000-5
18P	III	10/11/2004	9:00	2386.90	3166.56	779.66	NWRPO-1000-7
18P	III	10/11/2004	9:11	2386.89	3166.56	779.67	NWRPO-1000-6
18P	III	2/14/2005	7:40	2386.99	3166.56	779.57	NWRPO-1000-5
19IM1-Z1	III	11/14/2001	9:10	2321.09	2689.64	368.55	NWRPO-500-3
19IM1-Z1	III	1/23/2003	14:46	2322.9	2689.64	366.74	NWRPO-1000-5
19IM1-Z1	III	7/10/2003	11:35	2330	2689.64	359.64	NWRPO-1000-5
19IM1-Z1	III	2/17/2004	9:44	2332.17	2689.64	357.47	NWRPO-500-2
19IM1-Z1	III	9/20/2004	9:34	2333.17	2689.64	356.47	NWRPO-500-8
19IM1-Z2	III	11/14/2001	16:05	2321.36	2689.64	368.28	NWRPO-500-3
19IM1-Z2	III	1/23/2003	14:04	2327.18	2689.64	362.46	NWRPO-1000-5
19IM1-Z2	III	7/10/2003		2331.31	2689.64	358.33	NWRPO-1000-5
19IM1-Z2	III	2/17/2004	9:04	2333.95	2689.64	355.69	NWRPO-500-2
19IM1-Z2	III	9/16/2004	13:29	2335.67	2689.64	353.97	NWRPO-500-8
19IM1-Z3	III	11/14/2001	10:10	2328.96	2689.64	360.68	NWRPO-500-3
19IM1-Z3	III	1/23/2003	13:15	2329.24	2689.64	360.40	NWRPO-1000-5
19IM1-Z3	III	7/10/2003	9:50	2332.37	2689.64	357.27	NWRPO-1000-5
19IM1-Z3	III	2/12/2004	11:53	2334.25	2689.64	355.39	NWRPO-500-2
19IM1-Z3	III	9/16/2004	12:41	2336.25	2689.64	353.39	NWRPO-500-8
19IM1-Z4	III	11/14/2001	13:45	2329.61	2689.64	360.03	NWRPO-500-3

Table D-5. Nye County Water Level Measurements through 2/2005 (Continued)

Well NC-EWDP	Phase	Date	Time	Groundwater Elevation (ft amsl)	MP Elevation (ft amsl)	Depth to Water (ft)	Sounder
19IM1-Z4	III	1/23/2003	12:20	2332.63	2689.64	357.01	NWRPO-1000-5
19IM1-Z4	III	7/9/2003		2334.51	2689.64	355.13	NWRPO-1000-5
19IM1-Z4	III	2/12/2004	11:04	2335.41	2689.64	354.23	NWRPO-500-2
19IM1-Z4	III	9/16/2004	11:40	2337.63	2689.64	352.01	NWRPO-500-8
19IM1-Z5	III	11/14/2001	8:55	2337.18	2689.64	352.46	NWRPO-500-3
19IM1-Z5	III	1/23/2003	11:10	2336.63	2689.64	353.01	NWRPO-1000-5
19IM1-Z5	III	7/9/2003	12:35	2337.23	2689.64	352.41	NWRPO-1000-5
19IM1-Z5	III	2/12/2004	10:10	2337.42	2689.64	352.22	NWRPO-500-2
19IM1-Z5	III	9/8/2004	14:00	2340.36	2689.64	349.28	NWRPO-500-8
19IM1-Z5	III	9/9/2004	9:17	2340.30	2689.64	349.34	NWRPO-500-8
19IM2	III	1/29/2003	8:17	2333.85	2690.00	356.15	NWRPO-1000-5
19IM2	III	2/24/2003	7:31	2334.75	2690.00	355.25	NWRPO-1000-4
19IM2	III	3/11/2003	7:33	2334.72	2690.00	355.28	NWRPO-1000-5
19IM2	III	4/15/2003	9:20	2334.89	2690.00	355.11	NWRPO-1000-5
19IM2	III	5/14/2003	7:39	2334.83	2690.00	355.17	NWRPO-1000-5
19IM2	III	6/14/2003	6:36	2334.82	2690.00	355.18	NWRPO-1000-5
19IM2	III	7/17/2003	10:02	2335.38	2690.00	354.62	NWRPO-1000-5
19IM2	III	8/17/2003	7:17	2335.75	2690.00	354.25	NWRPO-1000-5
19IM2	III	9/13/2003	7:51	2335.87	2690.00	354.13	NWRPO-1000-5
19IM2	III	10/20/2003	12:14	2336.03	2690.00	353.97	NWRPO-1000-5
19IM2	III	11/14/2003	7:48	2336.13	2690.00	353.87	NWRPO-1000-5
19IM2	III	1/19/2004	8:27	2336.03	2690.00	353.97	NWRPO-1000-5
22PA Deep	III	2/11/2002	12:04	2377.75	2852.15	474.40	NWRPO-1000-4
22PA Deep	III	2/25/2002	7:43	2377.68	2852.15	474.47	NWRPO-1000-4
22PA Deep	III	3/25/2002	6:08	2377.73	2852.15	474.42	NWRPO-1000-4
22PA Deep	III	4/23/2002	6:44	2377.97	2852.15	474.18	NWRPO-500-3
22PA Deep	III	5/21/2002	10:55	2377.78	2852.15	474.37	NWRPO-500-3
22PA Deep	III	6/27/2002	6:07	2377.95	2852.15	474.20	NWRPO-500-3
22PA Deep	III	7/25/2002	6:10	2377.94	2852.15	474.21	NWRPO-500-3

Table D-5. Nye County Water Level Measurements through 2/2005 (Continued)

Well NC-EWDP	Phase	Date	Time	Groundwater Elevation (ft amsl)	MP Elevation (ft amsl)	Depth to Water (ft)	Sounder
22PA Deep	III	7/25/2002	9:35	2378.15	2852.15	474.00	NWRPO-1000-5
22PA Deep	III	8/22/2002	6:31	2377.86	2852.15	474.29	NWRPO-1000-4
22PA Deep	III	8/28/2002	6:30	2377.99	2852.15	474.16	NWRPO-500-3
22PA Deep	III	8/28/2002	13:00	2378.01	2852.15	474.14	NWRPO-500-3
22PA Deep	III	9/25/2002	7:26	2378.17	2852.15	473.98	NWRPO-1000-4
22PA Deep	III	10/16/2002	14:52	2378.30	2852.15	473.85	NWRPO-1000-5
22PA Deep	III	11/18/2002	10:17	2377.96	2852.15	474.19	NWRPO-1000-5
22PA Deep	III	12/23/2002	11:38	2378.15	2852.15	474.00	NWRPO-1000-5
22PA Deep	III	1/30/2003	9:45	2378.06	2852.15	474.09	NWRPO-1000-5
22PA Deep	III	2/24/2003	8:22	2378.25	2852.15	473.90	NWRPO-1000-5
22PA Deep	III	3/12/2003	7:53	2378.12	2852.15	474.03	NWRPO-1000-5
22PA Deep	III	4/17/2003	8:35	2378.28	2852.15	473.87	NWRPO-1000-5
22PA Deep	III	5/15/2003	7:46	2378.12	2852.15	474.03	NWRPO-1000-5
22PA Deep	III	6/16/2003	7:55	2378.15	2852.15	474.00	NWRPO-1000-5
22PA Deep	III	7/17/2003	6:20	2378.11	2852.15	474.04	NWRPO-1000-5
22PA Deep	III	7/31/2003	8:30	2378.08	2852.15	474.07	NWRPO-1000-5
22PA Deep	III	10/21/2003	7:45	2378.09	2852.15	474.06	NWRPO-1000-5
22PA Deep	III	11/13/2003	7:12	2378.12	2852.15	474.03	NWRPO-1000-5
22PA Deep	III	1/19/2004	9:56	2378.17	2852.15	473.98	NWRPO-1000-5
22PA Deep	III	2/25/2004	7:23	2378.11	2852.15	474.04	NWRPO-1000-5
22PA Deep	III	3/25/2004	7:01	2378.16	2852.15	473.99	NWRPO-1000-5
22PA Deep	III	5/17/2004	7:10	2378.20	2852.15	473.95	NWRPO-1000-5
22PA Deep	III	6/28/2004	6:27	2378.15	2852.15	474.00	NWRPO-1000-5
22PA Deep	III	7/26/2004	6:26	2378.16	2852.15	473.99	NWRPO-1000-5
22PA Deep	III	8/23/2004	9:25	2378.17	2852.15	473.98	NWRPO-1000-5
22PA Deep	III	9/20/2004	7:19	2377.92	2852.15	474.23	NWRPO-1000-5
22PA Deep	III	10/11/2004	7:33	2378.10	2852.15	474.05	NWRPO-1000-5
22PA Shallow	III	2/11/2002	12:12	2378.32	2852.15	473.83	NWRPO-1000-4
22PA Shallow	III	2/25/2002	7:52	2377.96	2852.15	474.19	NWRPO-1000-4

Table D-5. Nye County Water Level Measurements through 2/2005 (Continued)

Well NC-EWDP	Phase	Date	Time	Groundwater Elevation (ft amsl)	MP Elevation (ft amsl)	Depth to Water (ft)	Sounder
22PA Shallow	III	3/29/2002	6:06	2377.87	2852.15	474.28	NWRPO-1000-4
22PA Shallow	III	4/23/2002	6:38	2377.93	2852.15	474.22	NWRPO-500-3
22PA Shallow	III	5/21/2002	10:44	2377.73	2852.15	474.42	NWRPO-500-3
22PA Shallow	III	6/27/2002	5:59	2377.90	2852.15	474.25	NWRPO-500-3
22PA Shallow	III	7/25/2002	6:01	2377.91	2852.15	474.24	NWRPO-500-3
22PA Shallow	III	7/25/2002	9:47	2378.13	2852.15	474.02	NWRPO-1000-5
22PA Shallow	III	8/22/2002	6:26	2377.80	2852.15	474.35	NWRPO-1000-4
22PA Shallow	III	8/28/2002	11:53	2377.96	2852.15	474.19	NWRPO-500-3
22PA Shallow	III	8/28/2002	17:00	2377.97	2852.15	474.18	NWRPO-500-3
22PA Shallow	III	9/25/2002	7:18	2378.12	2852.15	474.03	NWRPO-1000-4
22PA Shallow	III	10/16/2002	14:41	2378.24	2852.15	473.91	NWRPO-1000-5
22PA Shallow	III	10/16/2002	14:41	2378.24	2852.15	473.91	NWRPO-1000-5
22PA Shallow	III	11/18/2002	10:08	2377.91	2852.15	474.24	NWRPO-1000-5
22PA Shallow	III	11/18/2002	10:08	2377.91	2852.15	474.24	NWRPO-1000-5
22PA Shallow	III	12/23/2002	11:29	2378.11	2852.15	474.04	NWRPO-1000-5
22PA Shallow	III	12/23/2002	11:29	2378.11	2852.15	474.04	NWRPO-1000-5
22PA Shallow	III	1/30/2003	9:34	2378.04	2852.15	474.11	NWRPO-1000-5
22PA Shallow	III	2/24/2003	8:22	2378.50	2852.15	473.65	NWRPO-1000-5
22PA Shallow	III	3/12/2003	8:07	2378.09	2852.15	474.06	NWRPO-1000-5
22PA Shallow	III	4/17/2003	8:25	2378.26	2852.15	473.89	NWRPO-1000-5
22PA Shallow	III	5/15/2003	7:56	2378.07	2852.15	474.08	NWRPO-1000-5
22PA Shallow	III	6/16/2003	7:44	2378.13	2852.15	474.02	NWRPO-1000-5
22PA Shallow	III	7/17/2003	6:08	2378.09	2852.15	474.06	NWRPO-1000-5
22PA Shallow	III	7/31/2003	8:45	2378.03	2852.15	474.12	NWRPO-1000-5
22PA Shallow	III	10/21/2003	8:07	2378.06	2852.15	474.09	NWRPO-1000-5
22PA Shallow	III	11/13/2003	6:59	2378.11	2852.15	474.04	NWRPO-1000-5
22PA Shallow	III	1/19/2004	9:46	2378.14	2852.15	474.01	NWRPO-1000-5
22PA Shallow	III	2/25/2004	7:12	2378.07	2852.15	474.08	NWRPO-1000-5
22PA Shallow	III	3/25/2004	6:50	2378.10	2852.15	474.05	NWRPO-1000-5

Table D-5. Nye County Water Level Measurements through 2/2005 (Continued)

Well NC-EWDP	Phase	Date	Time	Groundwater Elevation (ft amsl)	MP Elevation (ft amsl)	Depth to Water (ft)	Sounder
22PA Shallow	III	5/17/2004	7:02	2378.14	2852.15	474.01	NWRPO-1000-5
22PA Shallow	III	6/28/2004	6:20	2378.11	2852.15	474.04	NWRPO-1000-5
22PA Shallow	III	7/26/2004	6:18	2378.17	2852.15	473.98	NWRPO-1000-5
22PA Shallow	III	8/23/2004	9:10	2378.14	2852.15	474.01	NWRPO-1000-5
22PA Shallow	III	9/20/2004	7:08	2377.88	2852.15	474.27	NWRPO-1000-5
22PA Shallow	III	10/11/2004	7:23	2378.04	2852.15	474.11	NWRPO-1000-5
22PB Deep	III	3/29/2002	5:53	2377.71	2851.79	474.08	NWRPO-500-3
22PB Deep	III	4/23/2002	7:02	2377.76	2851.79	474.03	NWRPO-500-3
22PB Deep	III	5/21/2002	11:14	2377.60	2851.79	474.19	NWRPO-500-3
22PB Deep	III	6/27/2002	6:23	2377.76	2851.79	474.03	NWRPO-500-3
22PB Deep	III	7/25/2002	6:31	2377.75	2851.79	474.04	NWRPO-500-3
22PB Deep	III	7/25/2002	10:21	2377.94	2851.79	473.85	NWRPO-1000-5
22PB Deep	III	8/22/2002	6:42	2377.68	2851.79	474.11	NWRPO-1000-4
22PB Deep	III	8/29/2002	14:20	2377.69	2851.79	474.10	NWRPO-500-3
22PB Deep	III	8/30/2002	13:00	2378.09	2851.79	473.70	NWRPO-1000-4
22PB Deep	III	9/25/2002	7:42	2378.11	2851.79	473.68	NWRPO-1000-4
22PB Deep	III	10/16/2002	15:16	2378.11	2851.79	473.68	NWRPO-1000-5
22PB Deep	III	11/18/2002	10:35	2377.78	2851.79	474.01	NWRPO-1000-5
22PB Deep	III	12/23/2002	11:57	2377.99	2851.79	473.80	NWRPO-1000-5
22PB Deep	III	1/30/2003	10:06	2377.89	2851.79	473.90	NWRPO-1000-5
22PB Deep	III	2/24/2003	8:49	2378.08	2851.79	473.71	NWRPO-1000-5
22PB Deep	III	3/12/2003	7:53	2377.97	2851.79	473.82	NWRPO-1000-5
22PB Deep	III	4/17/2003	8:57	2378.10	2851.79	473.69	NWRPO-1000-5
22PB Deep	III	5/15/2003	8:19	2377.95	2851.79	473.84	NWRPO-1000-5
22PB Deep	III	6/16/2003	8:19	2378.00	2851.79	473.79	NWRPO-1000-5
22PB Deep	III	7/17/2003	6:45	2377.96	2851.79	473.83	NWRPO-1000-5
22PB Deep	III	7/31/2003	9:00	2377.92	2851.79	473.87	NWRPO-1000-5
22PB Deep	III	10/21/2003	7:57	2377.91	2851.79	473.88	NWRPO-1000-5
22PB Deep	III	11/13/2003	7:40	2377.98	2851.79	473.81	NWRPO-1000-5

Table D-5. Nye County Water Level Measurements through 2/2005 (Continued)

Well NC-EWDP	Phase	Date	Time	Groundwater Elevation (ft amsl)	MP Elevation (ft amsl)	Depth to Water (ft)	Sounder
22PB Deep	III	1/19/2004	10:21	2378.00	2851.79	473.79	NWRPO-1000-5
22PB Deep	III	2/25/2004	7:49	2377.94	2851.79	473.85	NWRPO-1000-5
22PB Deep	III	3/25/2004	7:25	2378.00	2851.79	473.79	NWRPO-1000-5
22PB Deep	III	5/17/2004	7:31	2378.04	2851.79	473.75	NWRPO-1000-5
22PB Deep	III	6/28/2004	6:44	2377.98	2851.79	473.81	NWRPO-1000-5
22PB Deep	III	7/26/2004	6:44	2377.98	2851.79	473.81	NWRPO-1000-5
22PB Deep	III	8/23/2004	9:50	2378.03	2851.79	473.76	NWRPO-1000-5
22PB Deep	III	9/20/2004	7:44	2377.81	2851.79	473.98	NWRPO-1000-5
22PB Deep	III	10/11/2004	7:52	2377.92	2851.79	473.87	NWRPO-1000-5
22PB Shallow	III	3/29/2002	5:58	2377.78	2851.79	474.01	NWRPO-500-3
22PB Shallow	III	4/23/2002	6:57	2377.85	2851.79	473.94	NWRPO-500-3
22PB Shallow	III	5/21/2002	11:04	2377.67	2851.79	474.12	NWRPO-500-3
22PB Shallow	III	6/27/2002	6:15	2377.84	2851.79	473.95	NWRPO-500-3
22PB Shallow	III	7/25/2002	6:22	2377.83	2851.79	473.96	NWRPO-500-3
22PB Shallow	III	7/25/2002	10:31	2377.99	2851.79	473.80	NWRPO-1000-5
22PB Shallow	III	8/22/2002	6:38	2377.74	2851.79	474.05	NWRPO-1000-4
22PB Shallow	III	8/28/2002	14:25	2377.89	2851.79	473.90	NWRPO-500-3
22PB Shallow	III	1/30/2003	9:57	2377.98	2851.79	473.81	NWRPO-1000-5
22PB Shallow	III	2/24/2003	8:40	2378.14	2851.79	473.65	NWRPO-1000-5
22PB Shallow	III	3/12/2003	8:07	2378.04	2851.79	473.75	NWRPO-1000-5
22PB Shallow	III	4/17/2003	8:47	2378.18	2851.79	473.61	NWRPO-1000-5
22PB Shallow	III	5/15/2003	8:08	2378.02	2851.79	473.77	NWRPO-1000-5
22PB Shallow	III	6/16/2003	8:08	2378.08	2851.79	473.71	NWRPO-1000-5
22PB Shallow	III	7/17/2003	6:33	2378.03	2851.79	473.76	NWRPO-1000-5
22PB Shallow	III	7/31/2003	9:10	2377.98	2851.79	473.81	NWRPO-1000-5
22PB Shallow	III	10/21/2003	8:07	2377.99	2851.79	473.80	NWRPO-1000-5
22PB Shallow	III	11/13/2003	7:29	2378.03	2851.79	473.76	NWRPO-1000-5
22PB Shallow	III	1/19/2004	10:11	2378.07	2851.79	473.72	NWRPO-1000-5
22PB Shallow	III	2/25/2004	7:37	2378.00	2851.79	473.79	NWRPO-1000-5

Table D-5. Nye County Water Level Measurements through 2/2005 (Continued)

Well NC-EWDP	Phase	Date	Time	Groundwater Elevation (ft amsl)	MP Elevation (ft amsl)	Depth to Water (ft)	Sounder
22PB Shallow	III	3/25/2004	7:14	2378.03	2851.79	473.76	NWRPO-1000-5
22PB Shallow	III	5/17/2004	7:21	2378.09	2851.79	473.70	NWRPO-1000-5
22PB Shallow	III	6/28/2004	6:37	2378.04	2851.79	473.75	NWRPO-1000-5
22PB Shallow	III	7/26/2004	6:36	2378.06	2851.79	473.73	NWRPO-1000-5
22PB Shallow	III	8/23/2004	9:40	2378.09	2851.79	473.70	NWRPO-1000-5
22PB Shallow	III	9/20/2004	7:32	2377.84	2851.79	473.95	NWRPO-1000-5
22PB Shallow	III	10/11/2004	7:44	2377.97	2851.79	473.82	NWRPO-1000-5
22S-Z1	III	7/25/2002	14:33	2378.30	2851.51	473.21	NWRPO-1000-5
22S-Z1	III	9/10/2002	16:20	2378.46	2851.51	473.05	NWRPO-1000-4
22S-Z1	III	9/11/2002	9:40	2378.31	2851.51	473.20	NWRPO-1000-4
22S-Z1	III	3/25/2003	14:48	2378.31	2851.51	473.20	NWRPO-500-2
22S-Z1	III	6/17/2003	13:35	2378.25	2851.51	473.26	NWRPO-1000-5
22S-Z1	III	7/31/2003	13:30	2378.16	2851.51	473.35	NWRPO-1000-5
22S-Z1	III	4/21/2004	14:29	2378.57	2851.51	472.94	NWRPO-1000-4
22S-Z2	III	7/25/2002	13:31	2378.27	2851.51	473.24	NWRPO-1000-5
22S-Z2	III	9/10/2002	11:20	2378.41	2851.51	473.10	NWRPO-1000-4
22S-Z2	III	9/10/2002	15:20	2378.52	2851.51	472.99	NWRPO-1000-4
22S-Z2	III	3/25/2003	14:00	2378.31	2851.51	473.20	NWRPO-500-2
22S-Z2	III	6/17/2003	12:45	2378.27	2851.51	473.24	NWRPO-1000-5
22S-Z2	III	8/7/2003	11:30	2378.24	2851.51	473.27	NWRPO-1000-5
22S-Z2	III	4/21/2004	13:36	2378.57	2851.51	472.94	NWRPO-1000-4
22S-Z3	III	7/25/2002	12:39	2378.24	2851.51	473.27	NWRPO-1000-5
22S-Z3	III	9/9/2002	16:15	2378.41	2851.51	473.10	NWRPO-1000-4
22S-Z3	III	9/10/2002	10:20	2378.41	2851.51	473.10	NWRPO-1000-4
22S-Z3	III	3/25/2003	12:58	2378.33	2851.51	473.18	NWRPO-500-2
22S-Z3	III	4/24/2003	9:15	2378.30	2851.51	473.21	NWRPO-1000-5
22S-Z3	III	6/17/2003	11:25	2378.30	2851.51	473.21	NWRPO-1000-5
22S-Z3	III	4/21/2004	12:16	2378.53	2851.51	472.98	NWRPO-1000-5
22S-Z4	III	7/25/2002	10:01	2378.21	2851.51	473.30	NWRPO-1000-5

Table D-5. Nye County Water Level Measurements through 2/2005 (Continued)

Well NC-EWDP	Phase	Date	Time	Groundwater Elevation (ft amsl)	MP Elevation (ft amsl)	Depth to Water (ft)	Sounder
22S-Z4	III	9/9/2002	14:40	2378.38	2851.51	473.13	NWRPO-1000-4
22S-Z4	III	3/25/2003	8:32	2378.18	2851.51	473.33	NWRPO-500-2
22S-Z4	III	4/23/2003	11:25	2378.11	2851.51	473.40	NWRPO-1000-5
22S-Z4	III	6/17/2003	10:25	2378.23	2851.51	473.28	NWRPO-1000-5
22S-Z4	III	4/21/2004	10:58	2378.43	2851.51	473.08	NWRPO-1000-7
23P Deep	III	4/23/2002	7:30	2375.66	2802.65	426.99	NWRPO-500-3
23P Deep	III	5/21/2002	8:20	2375.89	2802.65	426.76	NWRPO-1000-4
23P Deep	III	6/27/2002	5:41	2375.97	2802.65	426.68	NWRPO-1000-4
23P Deep	III	7/25/2002	5:42	2375.96	2802.65	426.69	NWRPO-1000-4
23P Deep	III	9/30/2002	7:50	2376.01	2802.65	426.64	NWRPO-1000-4
23P Deep	III	10/1/2002	10:25	2375.95	2802.65	426.70	NWRPO-1000-4
23P Deep	III	10/16/2002	13:52	2376.30	2802.65	426.35	NWRPO-1000-5
23P Deep	III	11/16/2002	9:28	2375.95	2802.65	426.70	NWRPO-1000-5
23P Deep	III	12/23/2002	12:25	2376.21	2802.65	426.44	NWRPO-1000-5
23P Deep	III	1/30/2003	9:12	2376.07	2802.65	426.58	NWRPO-1000-5
23P Deep	III	2/24/2003	8:04	2376.33	2802.65	426.32	NWRPO-1000-5
23P Deep	III	3/12/2003	7:19	2376.18	2802.65	426.47	NWRPO-1000-5
23P Deep	III	4/17/2003	7:42	2376.36	2802.65	426.29	NWRPO-500-1
23P Deep	III	4/17/2003	7:49	2376.36	2802.65	426.29	NWRPO-500-2
23P Deep	III	4/17/2003	7:57	2376.37	2802.65	426.28	NWRPO-1000-4
23P Deep	III	4/17/2003	7:34	2376.30	2802.65	426.35	NWRPO-1000-5
23P Deep	III	4/17/2003	8:04	2376.32	2802.65	426.33	NWRPO-1000-6
23P Deep	III	5/15/2003	7:08	2376.20	2802.65	426.45	NWRPO-1000-5
23P Deep	III	6/16/2003	7:17	2376.17	2802.65	426.48	NWRPO-1000-5
23P Deep	III	7/17/2003	5:42	2376.11	2802.65	426.54	NWRPO-1000-5
23P Deep	III	8/18/2003	5:57	2376.24	2802.65	426.41	NWRPO-1000-5
23P Deep	III	9/15/2003	6:36	2376.18	2802.65	426.47	NWRPO-1000-5
23P Deep	III	10/21/2003	6:50	2376.13	2802.65	426.52	NWRPO-500-1
23P Deep	III	10/21/2003	6:57	2376.13	2802.65	426.52	NWRPO-500-2

Table D-5. Nye County Water Level Measurements through 2/2005 (Continued)

Well NC-EWDP	Phase	Date	Time	Groundwater Elevation (ft amsl)	MP Elevation (ft amsl)	Depth to Water (ft)	Sounder
23P Deep	III	10/21/2003	7:04	2376.13	2802.65	426.52	NWRPO-1000-4
23P Deep	III	10/21/2003	6:42	2376.07	2802.65	426.58	NWRPO-1000-5
23P Deep	III	10/21/2003	7:11	2376.09	2802.65	426.56	NWRPO-1000-6
23P Deep	III	10/21/2003	7:17	2376.10	2802.65	426.55	NWRPO-1000-7
23P Deep	III	11/13/2003	6:29	2376.14	2802.65	426.51	NWRPO-1000-5
23P Deep	III	1/19/2004	9:17	2376.16	2802.65	426.49	NWRPO-1000-5
23P Deep	III	2/25/2004	6:44	2376.06	2802.65	426.59	NWRPO-1000-5
23P Deep	III	3/25/2004	6:24	2376.17	2802.65	426.48	NWRPO-1000-5
23P Deep	III	5/17/2004	6:20	2376.25	2802.65	426.40	NWRPO-1000-5
23P Deep	III	5/17/2004	6:27	2376.34	2802.65	426.31	NWRPO-500-2
23P Deep	III	5/17/2004	6:36	2376.35	2802.65	426.30	NWRPO-1000-6
23P Deep	III	5/17/2004	6:41	2376.30	2802.65	426.35	NWRPO-1000-7
23P Deep	III	6/28/2004	5:54	2376.16	2802.65	426.49	NWRPO-1000-5
23P Deep	III	7/26/2004	5:59	2376.13	2802.65	426.52	NWRPO-1000-5
23P Deep	III	8/23/2004	8:50	2376.19	2802.65	426.46	NWRPO-1000-5
23P Deep	III	9/20/2004	6:50	2375.99	2802.65	426.66	NWRPO-1000-5
23P Deep	III	10/11/2004	6:29	2376.12	2802.65	426.53	NWRPO-1000-5
23P Deep	III	10/11/2004	6:58	2376.15	2802.65	426.50	NWRPO-500-1
23P Deep	III	10/11/2004	7:05	2376.16	2802.65	426.49	NWRPO-500-2
23P Deep	III	10/11/2004	6:45	2376.15	2802.65	426.50	NWRPO-1000-7
23P Deep	III	10/11/2004	6:51	2376.15	2802.65	426.50	NWRPO-1000-6
23P Deep	III	2/14/2005	8:54	2376.18	2802.65	426.47	NWRPO-1000-5
23P Shallow	III	4/23/2002	7:24	2375.94	2802.65	426.71	NWRPO-500-3
23P Shallow	III	5/21/2002	8:11	2375.83	2802.65	426.82	NWRPO-500-3
23P Shallow	III	6/27/2002	5:33	2375.96	2802.65	426.69	NWRPO-500-3
23P Shallow	III	7/25/2002	5:34	2375.97	2802.65	426.68	NWRPO-500-3
23P Shallow	III	8/22/2002	6:07	2375.90	2802.65	426.75	NWRPO-1000-4
23P Shallow	III	9/25/2002	6:36	2376.28	2802.65	426.37	NWRPO-1000-4
23P Shallow	III	10/1/2002	8:50	2376.18	2802.65	426.47	NWRPO-1000-4

Table D-5. Nye County Water Level Measurements through 2/2005 (Continued)

Well NC-EWDP	Phase	Date	Time	Groundwater Elevation (ft amsl)	MP Elevation (ft amsl)	Depth to Water (ft)	Sounder
23P Shallow	III	10/1/2002	14:10	2376.25	2802.65	426.40	NWRPO-1000-4
23P Shallow	III	10/16/2002	13:26	2376.32	2802.65	426.33	NWRPO-1000-6
23P Shallow	III	10/16/2002	13:37	2376.41	2802.65	426.24	NWRPO-1000-4
23P Shallow	III	10/16/2002	13:42	2376.31	2802.65	426.34	NWRPO-1000-5
23P Shallow	III	11/18/2002	9:20	2375.94	2802.65	426.71	NWRPO-1000-5
23P Shallow	III	12/23/2002	12:16	2376.20	2802.65	426.45	NWRPO-1000-5
23P Shallow	III	1/30/2003	9:04	2376.06	2802.65	426.59	NWRPO-1000-5
23P Shallow	III	2/24/2003	7:52	2376.29	2802.65	426.36	NWRPO-1000-5
23P Shallow	III	3/12/2003	7:06	2376.14	2802.65	426.51	NWRPO-1000-5
23P Shallow	III	4/17/2003	7:26	2376.30	2802.65	426.35	NWRPO-1000-5
23P Shallow	III	5/15/2003	7:17	2376.15	2802.65	426.50	NWRPO-1000-5
23P Shallow	III	6/16/2003	7:06	2376.15	2802.65	426.50	NWRPO-1000-5
23P Shallow	III	7/17/2003	5:32	2376.10	2802.65	426.55	NWRPO-1000-5
23P Shallow	III	8/18/2003	5:46	2376.23	2802.65	426.42	NWRPO-1000-5
23P Shallow	III	9/15/2003	6:25	2376.18	2802.65	426.47	NWRPO-1000-5
23P Shallow	III	10/21/2003	6:31	2376.06	2802.65	426.59	NWRPO-1000-5
23P Shallow	III	11/13/2003	6:17	2376.13	2802.65	426.52	NWRPO-1000-5
23P Shallow	III	1/19/2004	9:04	2376.15	2802.65	426.50	NWRPO-1000-5
23P Shallow	III	2/25/2004	6:31	2376.07	2802.65	426.58	NWRPO-1000-5
23P Shallow	III	3/25/2004	6:10	2376.14	2802.65	426.51	NWRPO-1000-5
23P Shallow	III	5/17/2004	6:10	2376.21	2802.65	426.44	NWRPO-1000-5
23P Shallow	III	6/28/2004	5:42	2376.14	2802.65	426.51	NWRPO-1000-5
23P Shallow	III	7/26/2004	5:46	2376.13	2802.65	426.52	NWRPO-1000-5
23P Shallow	III	8/23/2004	8:30	2376.17	2802.65	426.48	NWRPO-1000-5
23P Shallow	III	9/20/2004	6:36	2375.92	2802.65	426.73	NWRPO-1000-5
23P Shallow	III	10/11/2004	6:37	2376.12	2802.65	426.53	NWRPO-1000-5
23P Shallow	III	2/14/2005	8:43	2376.17	2802.65	426.48	NWRPO-1000-5
16P	IV	1/30/2003	14:27	2392.76	2891.57	498.81	NWRPO-1000-5
16P	IV	2/26/2003	6:51	2392.82	2891.57	498.75	NWRPO-1000-5

Table D-5. Nye County Water Level Measurements through 2/2005 (Continued)

Well NC-EWDP	Phase	Date	Time	Groundwater Elevation (ft amsl)	MP Elevation (ft amsl)	Depth to Water (ft)	Sounder
16P	IV	3/11/2003	8:54	2392.94	2891.57	498.63	NWRPO-1000-5
16P	IV	4/15/2003	10:55	2392.78	2891.57	498.79	NWRPO-1000-5
16P	IV	5/14/2003	8:45	2392.92	2891.57	498.65	NWRPO-1000-5
16P	IV	6/14/2003	7:50	2392.80	2891.57	498.77	NWRPO-1000-5
16P	IV	7/20/2003	6:27	2392.86	2891.57	498.71	NWRPO-1000-5
16P	IV	8/17/2003	8:22	2392.91	2891.57	498.66	NWRPO-1000-5
16P	IV	10/20/2003	9:29	2392.77	2891.57	498.80	NWRPO-1000-5
16P	IV	11/14/2003	8:54	2392.82	2891.57	498.75	NWRPO-1000-5
16P	IV	1/16/2004	10:47	2392.93	2891.57	498.64	NWRPO-1000-5
16P	IV	2/24/2004	12:49	2392.78	2891.57	498.79	NWRPO-1000-5
16P	IV	3/24/2004	8:36	2392.90	2891.57	498.67	NWRPO-1000-5
16P	IV	5/16/2004	8:28	2392.99	2891.57	498.58	NWRPO-1000-5
16P	IV	6/25/2004	6:51	2392.92	2891.57	498.65	NWRPO-1000-5
16P	IV	7/23/2004	7:29	2392.96	2891.57	498.61	NWRPO-1000-5
16P	IV	8/20/2004	7:18	2392.94	2891.57	498.63	NWRPO-1000-5
16P	IV	9/17/2004	8:04	2392.96	2891.57	498.61	NWRPO-1000-5
16P	IV	10/10/2004	8:23	2393.04	2891.57	498.53	NWRPO-1000-5
16P	IV	12/16/2004	8:33	2392.79	2891.57	498.78	NWRPO-1000-5
16P	IV	2/24/2005	9:06	2392.91	2891.57	498.66	NWRPO-1000-5
19PB Deep	IV	1/19/2004		2322.10	2690.30	368.20	NWRPO-1000-5
19PB Deep	IV	2/24/2004	11:16	2322.43	2690.30	367.87	NWRPO-1000-5
19PB Deep	IV	3/24/2004	10:06	2322.62	2690.30	367.68	NWRPO-1000-5
19PB Deep	IV	6/25/2004	8:21	2322.80	2690.30	367.50	NWRPO-1000-5
19PB Deep	IV	7/23/2004	8:55	2323.02	2690.30	367.28	NWRPO-1000-5
19PB Deep	IV	8/20/2004	8:50	2322.96	2690.30	367.34	NWRPO-1000-5
19PB Shallow	IV	1/19/2004		2321.06	2690.30	369.24	NWRPO-1000-5
19PB Shallow	IV	2/24/2004	11:06	2320.86	2690.30	369.44	NWRPO-1000-5
19PB Shallow	IV	3/24/2004	9:57	2320.99	2690.30	369.31	NWRPO-1000-5
19PB Shallow	IV	6/25/2004	8:15	2320.90	2690.30	369.40	NWRPO-1000-5

Table D-5. Nye County Water Level Measurements through 2/2005 (Continued)

Well NC-EWDP	Phase	Date	Time	Groundwater Elevation (ft amsl)	MP Elevation (ft amsl)	Depth to Water (ft)	Sounder
19PB Shallow	IV	7/23/2004	8:48	2320.95	2690.30	369.35	NWRPO-1000-5
19PB Shallow	IV	8/20/2004	8:42	2320.90	2690.30	369.40	NWRPO-1000-5
19PB Shallow	IV	12/16/2004	10:01	2320.64	2690.30	369.66	NWRPO-1000-5
19PB Shallow	IV	2/24/2005	7:50	2320.78	2690.30	369.52	NWRPO-1000-5
24P	IV	10/20/2003	12:31	2385.53	2792.28	406.75	NWRPO-1000-5
24P	IV	11/14/2003	7:12	2385.49	2792.28	406.79	NWRPO-1000-5
24P	IV	1/19/2004	7:48	2385.58	2792.28	406.70	NWRPO-1000-5
24P	IV	2/24/2004	11:37	2385.41	2792.28	406.87	NWRPO-1000-5
24P	IV	3/24/2004	9:30	2385.52	2792.28	406.76	NWRPO-1000-5
24P	IV	5/16/2004	9:34	2385.64	2792.28	406.64	NWRPO-1000-5
24P	IV	6/25/2004	7:46	2385.56	2792.28	406.72	NWRPO-1000-5
24P	IV	7/23/2004	8:21	2385.58	2792.28	406.70	NWRPO-1000-5
24P	IV	8/20/2004	8:17	2385.55	2792.28	406.73	NWRPO-1000-5
24P	IV	9/17/2004	9:03	2385.61	2792.28	406.67	NWRPO-1000-5
24P	IV	10/10/2004	9:31	2385.67	2792.28	406.61	NWRPO-1000-5
24P	IV	12/16/2004	9:32	2385.38	2792.28	406.90	NWRPO-1000-5
24P	IV	2/24/2005	7:22	2385.54	2792.28	406.74	NWRPO-1000-5
27P	IV	2/6/2003	10:30	2390.48	2976.10	585.62	NWRPO-1000-4
27P	IV	3/11/2003	8:28	2390.58	2976.10	585.52	NWRPO-1000-5
27P	IV	4/15/2003	10:36	2390.33	2976.10	585.77	NWRPO-1000-5
27P	IV	5/14/2003	8:24	2390.54	2976.10	585.56	NWRPO-1000-5
27P	IV	6/14/2003	7:22	2390.41	2976.10	585.69	NWRPO-1000-5
27P	IV	7/20/2003	6:01	2390.47	2976.10	585.63	NWRPO-1000-5
27P	IV	8/17/2003	8:01	2390.51	2976.10	585.59	NWRPO-1000-5
27P	IV	9/13/2003	8:35	2390.45	2976.10	585.65	NWRPO-1000-5
27P	IV	10/20/2003	9:09	2390.35	2976.10	585.75	NWRPO-1000-5
27P	IV	11/14/2003	8:35	2390.46	2976.10	585.64	NWRPO-1000-5
27P	IV	1/16/2004	10:27	2390.49	2976.10	585.61	NWRPO-1000-5
27P	IV	2/24/2004	12:28	2390.34	2976.10	585.76	NWRPO-1000-5

Table D-5. Nye County Water Level Measurements through 2/2005 (Continued)

Well NC-EWDP	Phase	Date	Time	Groundwater Elevation (ft amsl)	MP Elevation (ft amsl)	Depth to Water (ft)	Sounder
27P	IV	3/24/2004	8:15	2390.48	2976.10	585.62	NWRPO-1000-5
27P	IV	5/16/2004	8:08	2390.60	2976.10	585.50	NWRPO-1000-5
27P	IV	6/25/2004	6:30	2390.50	2976.10	585.60	NWRPO-1000-5
27P	IV	7/23/2004	7:09	2390.53	2976.10	585.57	NWRPO-1000-5
27P	IV	8/20/2004	6:59	2390.49	2976.10	585.61	NWRPO-1000-5
27P	IV	9/17/2004	7:45	2390.54	2976.10	585.56	NWRPO-1000-5
27P	IV	10/10/2004	8:05	2390.60	2976.10	585.50	NWRPO-1000-5
27P	IV	12/16/2004	8:12	2390.32	2976.10	585.78	NWRPO-1000-5
27P	IV	2/24/2005	8:44	2390.50	2976.10	585.60	NWRPO-1000-5
28P	IV	1/30/2003	15:04	2392.34	2770.09	377.75	NWRPO-1000-5
28P	IV	2/26/2003	7:07	2392.76	2770.09	377.33	NWRPO-1000-5
28P	IV	3/11/2003	9:17	2392.88	2770.09	377.21	NWRPO-1000-5
28P	IV	4/15/2003	11:12	2392.67	2770.09	377.42	NWRPO-1000-5
28P	IV	5/14/2003	9:04	2392.83	2770.09	377.26	NWRPO-1000-5
28P	IV	6/14/2003	8:07	2392.68	2770.09	377.41	NWRPO-1000-5
28P	IV	7/20/2003	6:53	2392.76	2770.09	377.33	NWRPO-1000-5
28P	IV	8/17/2003	8:39	2392.82	2770.09	377.27	NWRPO-1000-5
28P	IV	9/13/2003	9:10	2392.78	2770.09	377.31	NWRPO-1000-5
28P	IV	10/20/2003	9:45	2392.72	2770.09	377.37	NWRPO-1000-5
28P	IV	11/14/2003	9:11	2392.76	2770.09	377.33	NWRPO-1000-5
28P	IV	1/16/2004	11:03	2392.90	2770.09	377.19	NWRPO-1000-5
28P	IV	2/24/2004	13:04	2392.67	2770.09	377.42	NWRPO-1000-5
28P	IV	3/24/2004	8:51	2392.81	2770.09	377.28	NWRPO-1000-5
28P	IV	5/16/2004	8:44	2392.92	2770.09	377.17	NWRPO-1000-5
28P	IV	6/25/2004	7:06	2392.79	2770.09	377.30	NWRPO-1000-5
28P	IV	7/23/2004	7:44	2392.87	2770.09	377.22	NWRPO-1000-5
28P	IV	8/20/2004	7:33	2392.84	2770.09	377.25	NWRPO-1000-5
28P	IV	9/17/2004	8:21	2392.87	2770.09	377.22	NWRPO-1000-5
28P	IV	10/10/2004	8:38	2392.99	2770.09	377.10	NWRPO-1000-5

Table D-5. Nye County Water Level Measurements through 2/2005 (Continued)

Well NC-EWDP	Phase	Date	Time	Groundwater Elevation (ft amsl)	MP Elevation (ft amsl)	Depth to Water (ft)	Sounder
28P	IV	12/16/2004	8:49	2392.63	2770.09	377.46	NWRPO-1000-5
28P	IV	2/24/2005	9:21	2392.79	2770.09	377.30	NWRPO-1000-5
29P	IV	10/20/2003	12:45	2377.96	2726.12	348.16	NWRPO-1000-5
29P	IV	11/14/2003	7:27	2377.92	2726.12	348.20	NWRPO-1000-5
29P	IV	1/19/2004	8:04	2377.94	2726.12	348.18	NWRPO-1000-5
29P	IV	2/24/2004	11:51	2377.96	2726.12	348.16	NWRPO-1000-5
29P	IV	3/24/2004	9:46	2377.99	2726.12	348.13	NWRPO-1000-5
29P	IV	5/16/2004	9:51	2378.01	2726.12	348.11	NWRPO-1000-5
29P	IV	6/25/2004	8:01	2377.99	2726.12	348.13	NWRPO-1000-5
29P	IV	7/23/2004	8:35	2378.01	2726.12	348.11	NWRPO-1000-5
29P	IV	8/20/2004	8:31	2378.00	2726.12	348.12	NWRPO-1000-5
29P	IV	9/17/2004	9:16	2378.01	2726.12	348.11	NWRPO-1000-5
29P	IV	10/10/2004	9:44	2378.01	2726.12	348.11	NWRPO-1000-5
29P	IV	12/16/2004	9:47	2377.93	2726.12	348.19	NWRPO-1000-5
29P	IV	2/24/2005	7:37	2377.94	2726.12	348.18	NWRPO-1000-5

Source: Output DTN: SN0702T0510106.007.

MP = measurement point.

Table D-6. Nye County Water Level Measurements for Phase V Wells through 11/2006

Well Name	Phase	Date	Time	Groundwater Elevation (ft amsl)	MP Elevation (ft amsl)	Depth to Water (ft)	Sounder
13P	V	8/17/2005	11:40	2507.94	2940.46	432.52	NWRPO-500-1
13P	V	9/11/2005	6:42	2507.84	2940.46	432.62	NWRPO-1000-5
13P	V	10/10/2005	7:36	2507.69	2940.46	432.77	NWRPO-1000-5
13P	V	10/10/2005	7:44	2507.68	2940.46	432.78	NWRPO-1000-6
13P	V	10/10/2005	7:52	2507.69	2940.46	432.77	NWRPO-1000-7
13P	V	10/10/2005	8:00	2507.70	2940.46	432.76	NWRPO-500-8
13P	V	11/9/2005	9:00	2507.80	2940.46	432.66	NWRPO-500-8
13P	V	12/7/2005	10:28	2507.73	2940.46	432.73	NWRPO-500-8
13P	V	1/21/2006	8:25	2507.65	2940.46	432.81	NWRPO-1000-5
13P	V	4/19/2006	13:51	2507.81	2940.46	432.65	NWRPO-500-8
13P	V	4/19/2006	13:47	2507.79	2940.46	432.67	NWRPO-1000-6
13P	V	6/1/2006	13:54	2507.82	2940.46	432.64	NWRPO-500-8
13P	V	7/3/2006	12:38	2507.81	2940.46	432.65	NWRPO-500-8
13P	V	8/9/2006	15:25	2507.91	2940.46	432.55	NWRPO-500-8
13P	V	9/20/2006	12:34	2507.88	2940.46	432.58	NWRPO-500-8
13P	V	9/27/2006	12:16	2507.73	2940.46	432.73	NWRPO-500-1
13P	V	10/30/2006	13:22	2507.97	2940.46	432.49	NWRPO-500-1
13P	V	11/27/2006	11:56	2508.12	2940.46	432.34	NWRPO-500-8
22PC Deep	V	4/18/2006	12:15	2378.17	2850.59	472.42	NWRPO-500-2
22PC Deep	V	5/30/2006	13:36	2378.26	2850.59	472.33	NWRPO-1000-5
22PC Shallow	V	4/18/2006	12:11	2378.18	2850.61	472.43	NWRPO-500-2
22PC Shallow	V	5/30/2006	13:45	2378.28	2850.61	472.33	NWRPO-1000-5
22PC Shallow	V	9/13/2006	11:27	2378.42	2850.61	472.19	NWRPO-500-8
24PB	V	10/30/2006	15:42	2385.74	2790.57	404.83	NWRPO-500-1
24PB	V	11/27/2006	9:02	2385.57	2790.57	405.00	NWRPO-500-8
32P Deep	V	6/2/2006	13:44	2300.21	2547.29	247.08	NWRPO-1000-7
32P Deep	V	7/7/2006	7:56	2299.93	2547.29	247.36	NWRPO-500-1
32P Deep	V	8/9/2006	14:32	2300.07	2547.29	247.22	NWRPO-500-8
32P Deep	V	10/30/2006	14:54	2300.15	2547.29	247.14	NWRPO-500-1

Table D-6. Nye County Water Level Measurements for Phase V Wells through 11/2006 (Continued)

Well Name	Phase	Date	Time	Groundwater Elevation (ft amsl)	MP Elevation (ft amsl)	Depth to Water (ft)	Sounder
32P Deep	V	11/27/2006	14:15	2300.19	2547.29	247.10	NWRPO-500-8
32P Intermediate	V	6/2/2006	13:40	2299.93	2547.29	247.36	NWRPO-1000-7
32P Intermediate	V	7/7/2006	8:04	2299.84	2547.29	247.45	NWRPO-500-1
32P Intermediate	V	8/9/2006	14:36	2299.82	2547.29	247.47	NWRPO-500-8
32P Intermediate	V	10/30/2006	14:54	2299.97	2547.29	247.32	NWRPO-500-1
32P Intermediate	V	11/27/2006	14:11	2300.08	2547.29	247.21	NWRPO-500-8
32P Shallow	V	6/2/2006	13:30	2302.20	2547.29	245.09	NWRPO-1000-7
32P Shallow	V	7/7/2006	8:12	2301.79	2547.29	245.50	NWRPO-500-1
32P Shallow	V	8/9/2006	14:45		2547.29		NWRPO-500-8
32P Shallow	V	11/27/2006	14:07		2547.29		NWRPO-500-8
33P Deep	V	4/19/2006	12:27	2368.20	2572.18	203.98	NWRPO-1000-6
33P Deep	V	4/19/2006	12:22	2368.20	2572.18	203.98	NWRPO-500-8
33P Deep	V	6/2/2006	14:22	2368.20	2572.18	203.98	NWRPO-1000-7
33P Deep	V	7/3/2006	13:30	2368.17	2572.18	204.01	NWRPO-500-1
33P Deep	V	8/9/2006	13:25	2368.20	2572.18	203.98	NWRPO-500-8
33P Deep	V	10/30/2006	13:13	2368.32	2572.18	203.86	NWRPO-500-1
33P Deep	V	11/27/2006	13:36	2368.40	2572.18	203.78	NWRPO-500-8
33P Intermediate	V	4/19/2006	12:16	2368.31	2572.18	203.87	NWRPO-1000-6
33P Intermediate	V	4/19/2006	12:14	2368.32	2572.18	203.86	NWRPO-500-8
33P Intermediate	V	6/2/2006	14:19	2368.36	2572.18	203.82	NWRPO-1000-7
33P Intermediate	V	7/3/2006	13:38	2368.31	2572.18	203.87	NWRPO-500-1
33P Intermediate	V	8/9/2006	13:32	2368.33	2572.18	203.85	NWRPO-500-8
33P Intermediate	V	10/30/2006	13:11	2368.47	2572.18	203.71	NWRPO-500-1
33P Intermediate	V	11/27/2006	13:34	2368.53	2572.18	203.65	NWRPO-500-8
33P Shallow	V	4/19/2006	11:56	2364.78	2572.18	207.40	NWRPO-1000-6
33P Shallow	V	4/19/2006	12:06	2364.77	2572.18	207.41	NWRPO-500-8
33P Shallow	V	6/2/2006	14:16	2365.10	2572.18	207.08	NWRPO-1000-7
33P Shallow	V	7/3/2006	13:33	2365.05	2572.18	207.13	NWRPO-500-1

Table D-6. Nye County Water Level Measurements for Phase V Wells through 11/2006 (Continued)

Well Name	Phase	Date	Time	Groundwater Elevation (ft amsl)	MP Elevation (ft amsl)	Depth to Water (ft)	Sounder
33P Shallow	V	8/9/2006	13:30	2364.99	2572.18	207.19	NWRPO-500-8
33P Shallow	V	10/30/2006	15:09	2365.03	2572.18	207.15	NWRPO-500-1
33P Shallow	V	11/27/2006	13:32	2365.05	2572.18	207.13	NWRPO-500-8

Source: Output DTN : SN0702T0510106.007.

INTENTIONALLY LEFT BLANK

APPENDIX E
POTENTIOMETRIC SURFACE FOR THE SATURATED ZONE SITE-SCALE FLOW MODEL

E1. PURPOSE

The purpose of this appendix is to describe the potentiometric surface developed for use with the SZ Site-scale flow model described within this report. Also included is the process used to develop or construct the potentiometric surface. The description includes background, software used, inputs, analysis with uncertainty and limitations, and conclusions.

Previous potentiometric surfaces and analyses have been presented by *Water-Level Data Analysis for the Saturated Zone Site-Scale Flow and Transport Model* (USGS 2001 [DIRS 154625], 2004 [DIRS 168473]; BSC 2004 [DIRS 170009]). The initial version of the potentiometric surface (USGS 2001 [DIRS 154625]) was used for the calibration of the SZ site-scale flow model (BSC 2004 [DIRS 170037]).

The USGS (2004 [DIRS 168473]) used updated water-level data for selected wells through the year 2000 as the basis for estimating water-level altitudes and the potentiometric surface in the SZ site-scale flow and transport model domain based on an alternative interpretation of perched water conditions. The updated water-level data presented by the USGS (2004 [DIRS 168473]) include data obtained from the NC-EWDP Phases I and II and data from USW WT-24. That revision developed computer files containing:

- Water-level data within the model area (DTN: GS010908312332.002 [DIRS 163555])
- A table of known vertical head differences (DTN: GS010908312332.003 [DIRS 168699])
- A potentiometric-surface map (DTN: GS010608312332.001 [DIRS 155307]) using an alternative concept from that presented by the USGS (2001 [DIRS 154625]) for the area north of Yucca Mountain.

The water-level data analysis (BSC 2004 [DIRS 170009]) was based on work by the USGS (2004 [DIRS 168473]) and includes an analysis of the impact of more recent water-level data and the impact of adding data from the NC-EWDP Phases III and IV wells. It also expands the discussion of uncertainty in the potentiometric-surface map.

The current potentiometric surface presented in this appendix builds on the potentiometric surface as represented by contour lines presented by the USGS (2004 [DIRS 168473], Figure 6-1) as modified by *Water-Level Data Analysis for the Saturated Zone Site-Scale Flow and Transport Model* (BSC 2004 [DIRS 170009], Figure 6-2), which includes data from two additional recently completed wells, NC-EWDP-24P and NC-EWDP-29P, and is contained in DTN: MO0409SEPPSMPC.000 [DIRS 179336] and illustrated in Figure 6-16.

Output DTN: MO0611SCALEFLW.000 represents the current potentiometric surface and includes representations of the surface in addition to the contours as shown in Figure 6-4.

E2. USE OF SOFTWARE

The potentiometric surface was constructed primarily using EarthVision 5.1 (STN: 10174-5.1-000, [DIRS 167994],) on a Silicon Graphics Octane workstation running IRIX 6.5. EarthVision is a product of Dynamic Graphics, Inc. and is designed for the preparation of three-dimensional geologic surfaces and models. The use of EarthVision to prepare this surface is consistent with the intended use of the software. There are no limitations on the use of this potentiometric surface due to the use of EarthVision.

EarthVision 5.1 can create regularly spaced grids from irregularly spaced data points to create surfaces that represent the top of specific hydrogeological units or the saturated zone. Up to 10,000,000 data points can be used to produce a grid with dimensions up to 1,201 × 1,201 (*GS_EV_5_0.pdf*, pp. 22 and 24). The surface constructed was within the range of these limits.

Several commercially available software packages (exempt per IM-PRO-003) were also used for data handling, formatting, and data visualization in the preparation of the potentiometric surface. These software packages were Microsoft Access (97 and 2000), Microsoft Excel (97 and 2003), AutoCad (2002), EarthVision (7.5.2), and UltraEdit (11.10) by IDM Computer Solutions, Inc. Each of these software packages were used on the Windows 2000 platform. No calculations were performed by these commercial software packages and the only output was in the form of visualizations. AutoCad and EarthVision 7.5.2 were used for data visualization and are therefore exempt per IM-PRO-003. Access, Excel, and UltraEdit were used for formatting data and were also exempt per IM-PRO-003. Each of these exempt software packages is controlled by YMP Software Configuration Management.

E3. INPUTS

The inputs for the construction of the potentiometric surface consist of water level measurements and the contour lines from previous potentiometric surfaces as shown in DTN: MO0409SEPPSMPC.000 [DIRS 179336].

Water level measurements used for the construction of the latest potentiometric surface were obtained from Output DTN: SN0610T0510106.001. In some cases, more than one water-level value is given for a single well and some wells and intervals are not considered appropriate for use in construction of a potentiometric surface. Table A-2 of *Water-Level Data Analysis for the Saturated Zone Site-Scale Flow and Transport Model* (BSC 2004 [DIRS 170009]) was used to determine which wells and intervals were appropriate for use in the construction of the potentiometric surface. For wells or intervals not included in Appendix A of *Water-Level Data Analysis for the Saturated Zone Site-Scale Flow and Transport Model* (BSC 2004 [DIRS 170009]), the value for the uppermost interval found in Output DTN: SN0610T0510106.001 was used.

Contour lines from Figure 6-2 of *Water-Level Data Analysis for the Saturated Zone Site-Scale Flow and Transport Model* (BSC 2004 [DIRS 170009]) and found in DTN: MO0409SEPPSMPC.000 [DIRS 179336] were digitized and included as input data except in the immediate vicinity of the two recently completed wells, NC-EWDP-24P and NC-EWDP-29P.

E4. ANALYSIS

The potentiometric surface discussed herein is intended to be suitable for the needs of the saturated zone site-scale flow model described in this report. The area for which this potentiometric surface was constructed is identical to the area of the Hydrogeologic Framework Model HFM2006 (SNL 2007 [DIRS 174109]) and the SZ site-scale flow model of this report. The area covers about 1,350 km^2 and extends from 533,000 m to 563,000 m (west to east) and 4,046,500 m to 4,091,500 m (south to north), UTM (Zone 11, North American Datum 1927). The resolution, horizontal spacing, of the potentiometric surface was also established to match the Hydrogeologic Framework Model HFM2006 (SNL 2007 [DIRS 174109]) at 125 m.

The minimum tension method, generally recognized as providing geologically reasonable surfaces except where very steep surfaces are encountered (vertical distances many times greater than the horizontal data spacing), was used to construct the potentiometric surface. Control points were used to limit the tendency to overshoot in areas of very steep gradients. Some smoothing was also applied to minimize the effects of uneven data distribution.

The resulting potentiometric surface was checked at the water level measurement locations by determining the absolute value of the difference between the input value and the value indicated by the new potentiometric surface. The median difference was 0.2 m with a standard deviation of 1.9 m. This difference was determined to be suitable for use with the flow model described in this report. The potentiometric surface is intended for use with the SZ site-scale flow model and may not be suitable for other purposes. This surface does not replicate the input data exactly.

The uncertainty in the previously developed potentiometric surface map discussed in Section 6.5 of *Water-Level Data Analysis for the Saturated Zone Site-Scale Flow and Transport Model* (BSC 2004 [DIRS 170009]) is applicable to the current potentiometric surface. Uncertainty within the potentiometric surface is mostly related to the accuracy of the water-level measurements, distribution of data and relative variations of the surface. In areas of limited data and steep gradients, such as in the northwest portion of the model, uncertainty is greater than in the immediate vicinity of the repository. In general, the relatively flat portion of the potentiometric surface located just south of the repository is relatively less uncertain due to more wells located in the area. This area, from the repository extending to the south, is the most likely general direction of groundwater flow and is of more interest than the northwest portion of the model area.

The potentiometric surface intended for use with the SZ site-scale flow model is contained in Output DTN: MO0611SCALEFLW.000.

E5 CONCLUSIONS

The potentiometric surface found in Output DTN: MO0611SCALEFLW.000 has been prepared using the previous potentiometric surface (BSC 2004 [DIRS 170009]) and the most recently available water level information to create a surface suitable for use in the SZ site-scale flow model.

INTENTIONALLY LEFT BLANK

APPENDIX F
CONVERSION OF SURVEY COORDINATES FOR SELECTED NYE COUNTY EARLY WARNING DRILLING PROGRAM BOREHOLES, THROUGH PHASE IV

F1. PURPOSE

The purpose of these calculations is to convert qualified survey coordinates from Nevada State Plan (NSP) to UTM coordinates for selected NC-EWDP boreholes. Qualified borehole coordinates are required to support development of the new site-scale saturated-zone flow model.

The scope of these calculations covers NC-EWDP boreholes, through Phase IV, for which qualified UTM coordinates do not already exist in the Technical Data Management System (TDMS).

This activity is conducted under *Technical Work Plan for Saturated Zone Flow and Transport Modeling* (BSC 2006 [DIRS 177375]). It is a deviation from this TWP insofar as the conversion software used to conduct the activity is not identified in Section 9 of the TWP as software to be used for performing calculations, modeling or analyses for the work covered by the TWP. However, the software used for this activity is qualified, and the software package used to conduct the work was obtained from Software Configuration Management.

F2. QUALITY ASSURANCE

All activities in the governing TWP (BSC 2006 [DIRS 177375]) have been determined to be subject to *Quality Assurance Requirements and Description* (QARD) (DOE 2006 [DIRS 177092]), except for administrative activities. The calculations presented in this report are considered to be an analysis of data to support performance assessment and is therefore subject to the QARD (DOE 2006 [DIRS 177092]). No new data have been collected as part of this work scope. A prerequisite for this task is that all necessary qualified data are obtained from the TDMS.

In addition to the QARD (DOE 2006 [DIRS 177092]), the following procedures are used to perform this task:

- DM-PRO-001, *Document Control*
- DM-PRO-002, *Records Management*
- IM-PRO-002, *Control of the Electronic Management of Information*
- IM-PRO-003, *Software Management*
- RM-PRO-2001, *Document Control*
- SCI-PRO-004, *Managing Technical Product Inputs*
- SCI-PRO-006, *Models*
- TST-PRO-001, *Submittal and Incorporation of Data to the Technical Data Management System*.

Methods used to control the electronic management of data are specified in Section 8.4 of the TWP (BSC 2006 [DIRS 177375]). Specifically, the work described in this report involved the use of a personal computer which was subject to the following requirements:

- Files will be saved to backup disks or backup drives on a weekly basis
- At the completion of the analyses, models, or calculation reports, the developed data files will be transferred to the TDMS in accordance with TST-PRO-001
- Computers and workstations are controlled with passwords, and access to equipment is restricted to YMP trained personnel
- Disks and all other removable backup media will be labeled with the following: generating program, originator, date, document number, and content description.

Electronic files and data transfers will be checked for alteration either visually or by using file comparison software (e.g., signature generation and compare routing) to compare compressed and uncompressed files file-sizes.

The data package submitted to the TDMS will be prepared by outputting the data from the database through a spreadsheet.

The requirements of IM-PRO-002 were met by the following additional measures:

- Computers used for processing and storing information are password-protected
- All files are backed up on magnetic media monthly or more often, as appropriate
- Backup media will be labeled with the date and time of backup, DOE serial number of the computer backed up, system utility used to perform the backup, and format of the magnetic media
- Information transfers from one computer to another are done by magnetic media, Internet, or local network using file transfer protocol or attachments to e-mail
- Where possible, file transfers were verified by visually comparing the name, date, and file size
- ASCII files were also verified by visual comparison of the data.

F3. USE OF SOFTWARE

Software used for performing this calculation was qualified in accordance with LP-SI.12Q-BSC, *Qualification of Software*. The following software package was obtained from the Software Configuration Management Library in Las Vegas, Nevada for this task:

Software:	CORPSCON V.5.11.08
Software Tracking Number (STN):	10547-5.11.08.00 [DIRS 155082]
Status:	Qualified
Software range of use:	State of Nevada
Operating environment:	Dell Precision 420, Pentium III Serial Number JFYRF01 LANL Property Number 1091797 Operated under Windows NT 4.0
Computer location:	EES-6, TA-3, Building 43, Room A2, Los Alamos National Laboratory, Los Alamos NM 87545.

This software was selected because it was qualified and had been used to convert survey data to UTM coordinates for borehole and well locations in this report.

Commercial software (Microsoft Excel) was used without qualification in accordance with Section 2 of IM-PRO-003.

F4. INPUTS

F4.1 DIRECT INPUTS

The following DTNs are directly used to develop the list of well coordinate locations:

- MO0203GSC02034.000. As-Built Survey of Nye County Early Warning Drilling Program (EWDP) Phase III Boreholes NC-EWDP-10S, NC-EWDP-18P, and NC-EWDP-22S - Partial Phase III List. [DIRS 168375]
- MO0206GSC02074.000. As-Built Survey of Nye County Early Warning Drilling Program (EWDP) Phase III Boreholes, Second Set. [DIRS 168378]
- MO0307GSC03094.000. As-Built Survey of Nye County Early Warning Drilling Program Phase IV Boreholes EWDP-16P, EWDP-27P & EWDP-28P. [DIRS 170556]
- MO0312GSC03180.000. As-Built Survey of Nye County Early Warning Drilling Program, Phase IV Boreholes: NC-EWDP-24P & NC-EWDP-29P. [DIRS 174103]
- MO0408GSC04123.000. Nye County Early Warning Drilling Program, Phase IV, As-Built Location of NC-EWDP-19PB Borehole. [DIRS 174102]

F4.2 CRITERIA

The input data are selected to meet the following criteria:

- Acquired survey data are in the TDMS
- Survey data are qualified
- The accuracy and precision of the survey data are sufficient for their intended use in the saturated zone site-scale flow model
- Supporting documentation for the survey data clearly state the data uncertainties, so that these uncertainties can be characterized and propagated through any modeling or other calculations using them, as appropriate.

F4.3 CODES, STANDARDS, AND REGULATIONS

No codes, standards, or regulations are applicable to this task.

F5. ASSUMPTIONS

The input survey data and the coordinate conversion software produce results with adequate accuracy and precision for the intended use in the saturated zone site-scale flow model.

F6. SCIENTIFIC ANALYSIS DISCUSSION

F6.1 CALCULATION

Description and source of mathematical formulations, equations, algorithms, and numerical methods used in the calculation are described in *Software Management Report (SMR) for CORPSCON Version 5.11.08* (LANL 2001 [DIRS 181434]).

The steps taken to convert coordinates, and to verify the conversions, are described below:

1. A formatted data input file (*gscinp.txt*) was prepared for CORPSCON:

NC-EWDP-7SC, 532379.34, 719071.91
NC-EWDP-10P, 576745.41, 720883.49
NC-EWDP-10S, 576716, 720829.32
NC-EWDP-16P, 552178.64, 718826.37
NC-EWDP-18P, 564519.85, 728530.5
NC-EWDP-19IM1, 564093.9, 699185.01
NC-EWDP-19IM2, 564159.05, 699185.13
NC-EWDP-19PB, 564159.18, 699268.66
NC-EWDP-22PA, 573007.77, 711452.61
NC-EWDP-22PB, 573066.18, 711447.98
NC-EWDP-22S, 573003.45, 711393.91
NC-EWDP-23P, 579229.94, 704332.62
NC-EWDP-24P, 564362.13, 711538.96
NC-EWDP-27P, 549794.33, 722157.45
NC-EWDP-28P, 552420.36, 712688.26
NC-EWDP-29P, 564370.14, 703501.85

2. Conversion settings were specified for the input and output CORPSCON files:

	Input Settings	Output Settings
System	2 – State Plane	3 – UTM
Datum	1927 – NAD 27	1927 – NAD 27
Zone	2702 – Nevada Central	11 – 120W to 114W
Units	1 – US Survey Foot	3 – Meter
Vertical Datum	0 - None	0 – None

3. The following output file (*gscout.txt*) was generated by CORPSCON:

```
NC-EWDP-7SC,539632.058,4064316.681
NC-EWDP-10P,553149.116,4064915.731
NC-EWDP-10S,553140.212,4064899.193
NC-EWDP-16P,545665.433,4064262.850
NC-EWDP-18P,549415.690,4067232.928
NC-EWDP-19IM1,549316.995,4058290.464
NC-EWDP-19IM2,549336.848,4058290.570
NC-EWDP-19PB,549336.799,4058316.023
NC-EWDP-22PA,552020.195,4062038.031
NC-EWDP-22PB,552037.998,4062036.683
NC-EWDP-22S,552018.941,4062020.140
NC-EWDP-23P,553923.731,4059875.049
NC-EWDP-24P,549385.644,4062055.183
NC-EWDP-27P,544935.369,4065275.350
NC-EWDP-28P,545745.594,4062392.737
NC-EWDP-29P,549396.599,4059606.163
```

4. The output data were formatted for submission to the TDMS as a DTN (see Section F7).

F6.2 CORROBORATION

Before using the software to convert the borehole coordinates, the output of the CORPSCON conversion routine was first corroborated by executing the validation test case from the Software Management Report (CORPSCON, STN: 10547-5.11.08-00 [DIRS 155082], Section 2). Figure F-1 shows the screen shot of the CORPSCON input and output data used in the successful validation test.

The input DTNs also report acquired survey data in geographic (Latitude-Longitude) coordinates. As a secondary confirmatory action, the coordinates converted from NSP to UTM as described above were compared to those converted from geographic coordinates to UTM. Geographic coordinates were first converted from degree-minute-second format to decimal-degree format using (Equation F-1), producing the results listed in the rightmost columns of Table F-1:

$$\text{decimal degrees} = \text{degrees} + (\text{minutes}/60\ \text{min-deg}^{-1}) + (\text{s}/3{,}600\ \text{s-degree}^{-1}) \quad \text{(Eq. F-1)}$$

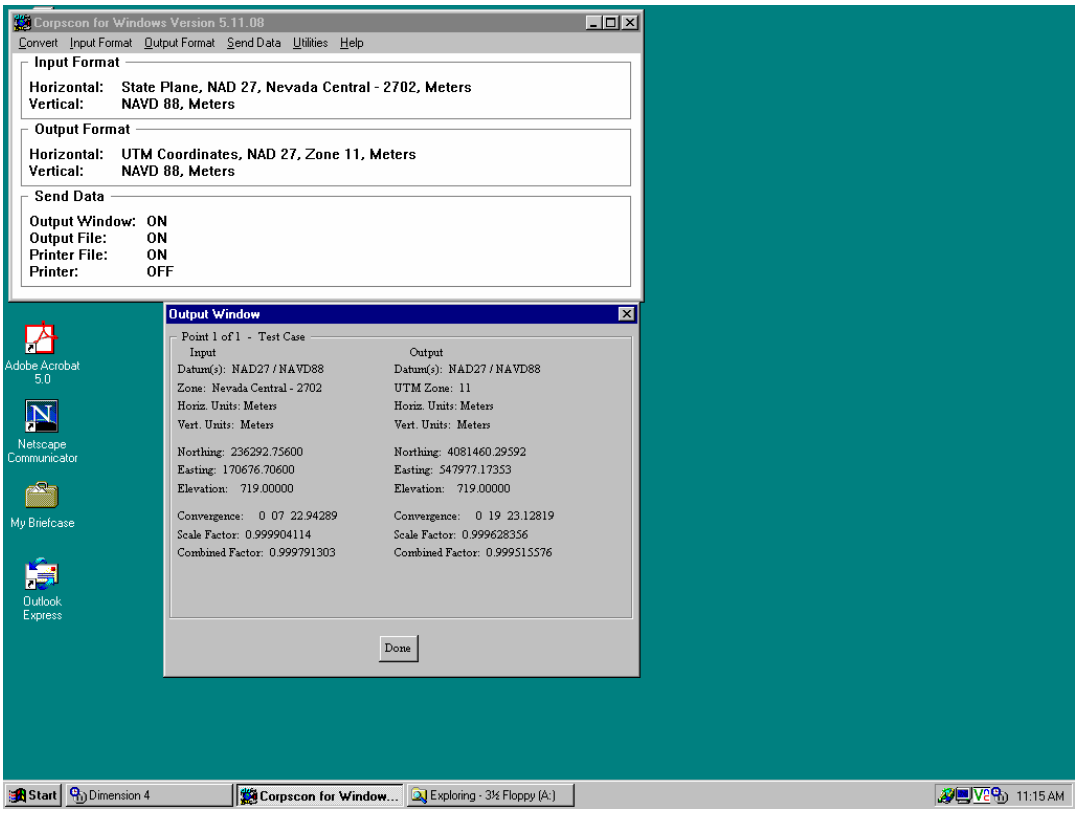

Figure F-1. Screen Shot of the Validation Test Case for CORPSCON Version 5.11.08

Table F-1. Acquired Survey Data used to Create Input File for Verification Calculations

WELL_ID	Source DTN for Geographic Coordinates	Latitude-North (Degree-Min-Sec) (NAD-83)	Longitude-West (Degree-Min-Sec) (NAD-83)	Latitude-North (Decimal degrees) (NAD-83)	Longitude-West (Decimal degrees) (NAD-83)
NC-EWDP-7SC	MO0206GSC02074.000 [DIRS 168378]	36 43 31.812	116 33 25.439	36.72550	116.55707
NC-EWDP-10P	MO0206GSC02074.000 [DIRS 168378]	36 43 48.874	116 24 20.362	36.73024	116.40566
NC-EWDP-10S	MO0203GSC02034.000 [DIRS 168375]	36 43 48.339	116 24 20.725	36.73009	116.40576
NC-EWDP-16P	MO0307GSC03094.000 [DIRS 170556]	36 43 29.089	116 29 22.219	36.72475	116.48951
NC-EWDP-18P	MO0203GSC02034.000 [DIRS 168375]	36 45 04.797	116 26 50.340	36.75133	116.44732
NC-EWDP-19IM1	MO0206GSC02074.000 [DIRS 168378]	36 40 14.615	116 26 56.397	36.67073	116.44900
NC-EWDP-19IM2	MO0206GSC02074.000 [DIRS 168378]	36 40 14.614	116 26 55.597	36.67073	116.44878
NC-EWDP-19PB	MO0408GSC04123.000 [DIRS 174102]	36 40 15.440	116 26 55.593	36.67096	116.44878

Table F-1. Acquired Survey Data used to Create Input File for Verification Calculations (Continued)

WELL_ID	Source DTN for Geographic Coordinates	Latitude-North (Degree-Min-Sec) (NAD-83)	Longitude-West (Degree-Min-Sec) (NAD-83)	Latitude-North (Decimal degrees) (NAD-83)	Longitude-West (Decimal degrees) (NAD-83)
NC-EWDP-22PA	MO0206GSC02074.000[DIRS 168378]	36 42 15.712	116 25 06.581	36.70436	116.41849
NC-EWDP-22PB	MO0206GSC02074.000[DIRS 168378]	36 42 15.665	116 25 05.863	36.70435	116.41830
NC-EWDP-22S	MO0203GSC02034.000 [DIRS 168375]	36 42 15.132	116 25 06.636	36.70420	116.41851
NC-EWDP-23P	MO0206GSC02074.000 [DIRS 168378]	36 41 05.137	116 23 50.412	36.68476	116.39734
NC-EWDP-24P	MO0312GSC03180.000 [DIRS 174103]	36 42 16.775	116 26 52.756	36.70466	116.44799
NC-EWDP-27P	MO0307GSC03094.000 [DIRS 170556]	36 44 02.072	116 29 51.436	36.73391	116.49762
NC-EWDP-28P	MO0307GSC03094.000 [DIRS 170556]	36 42 28.386	116 29 19.390	36.70789	116.48872
NC-EWDP-29P	MO0312GSC03180.000 [DIRS 174103]	36 40 57.297	116 26 52.884	36.68258	116.44802

Source: Output DTN: LA0612RR150304.001.

Conversion settings were then specified for the input and output CORPSCON files:

	Input Settings	Output Settings
System	1 – Geographic	3 – UTM
Datum	1983 – NAD 83(86)	1927 – NAD 27
Zone	NA	11 – 120W to 114W
Units	NA	3 – Meter
Vertical Datum	0 - None	0 – None

NA = not applicable.

Using decimal-degree coordinates in the input file and the above settings, CORPSCON generated the UTM coordinates presented in Table F-2. The difference between the two sets of converted coordinates was calculated using:

$$\text{Difference} = [(\text{UTM-N}_{NSP}\text{-UTM-N}_{GEO})^2 + (\text{UTM-E}_{NSP}\text{-UTM-E}_{GEO})^2]^{0.5} \qquad \text{(Eq. F-2)}$$

where UTM-N_{NSP} and UTM-E_{NSP} are UTM-Northing and UTM-Easting coordinates calculated using Nevada State Plane coordinates for the input data; and UTM-N_{GEO} and UTM-E_{GEO} are UTM-Northing and UTM-Easting coordinates calculated using geographic coordinates for the input data. The consistently small difference of 0.3 m confirms the validity of the conversion process described in Section F6.1.

Table F-2. Comparison of UTM Coordinates Obtained from Conversion of NSP and Geographic Coordinates

	Converted From NSP		Converted From Geographic Coordinates		
Well ID	UTM-Northing (m)	UTM-Easting (m)	UTM-Northing (m)	UTM-Easting (m)	Difference (m)
NC-EWDP-7SC	4064316.68	539632.06	4064316.98	539631.95	0.32
NC-EWDP-10P	4064915.73	553149.12	4064915.88	553148.92	0.25
NC-EWDP-10S	4064899.19	553140.21	4064899.34	553140.01	0.25
NC-EWDP-16P	4064262.85	545665.43	4064263.06	545665.36	0.22
NC-EWDP-18P	4067232.93	549415.69	4067233.04	549415.59	0.15
NC-EWDP-19IM1	4058290.46	549317.00	4058290.76	549316.79	0.36
NC-EWDP-19IM2	4058290.57	549336.85	4058290.84	549336.65	0.34
NC-EWDP-19PB	4058316.02	549336.80	4058316.30	549336.60	0.34
NC-EWDP-22PA	4062038.03	552020.20	4062038.22	552019.98	0.29
NC-EWDP-22PB	4062036.68	552038.00	4062036.88	552037.81	0.28
NC-EWDP-22S	4062020.14	552018.94	4062020.34	552018.73	0.29
NC-EWDP-23P	4059875.05	553923.73	4059875.26	553923.47	0.34
NC-EWDP-24P	4062055.18	549385.64	4062055.40	549385.50	0.26
NC-EWDP-27P	4065275.35	544935.37	4065275.54	544935.33	0.19
NC-EWDP-28P	4062392.74	545745.59	4062392.99	545745.50	0.26
NC-EWDP-29P	4059606.16	549396.60	4059606.42	549396.42	0.31

Source: Output DTN: LA0612RR150304.001.

F7. CONCLUSIONS

Table F-3 summarizes results of this coordinate-conversion calculation.

Table F-3. UTM Coordinates for Selected Nye County EWDP Boreholes, Converted Using CORPSCON V.5.11.08

Borehole Identifier	UTM-Northing (m)	UTM-Easting (m)
NC-EWDP-7SC	4,064,316.68	539,632.06
NC-EWDP-10P	4,064,915.73	553,149.12
NC-EWDP-10S	4,064,899.19	553,140.21
NC-EWDP-16P	4,064,262.85	545,665.43
NC-EWDP-18P	4,067,232.93	549,415.69
NC-EWDP-19IM1	4,058,290.46	549,317.00
NC-EWDP-19IM2	4,058,290.57	549,336.85
NC-EWDP-19PB	4,058,316.02	549,336.80
NC-EWDP-22PA	4,062,038.03	552,020.20
NC-EWDP-22PB	4,062,036.68	552,038.00
NC-EWDP-22S	4,062,020.14	552,018.94
NC-EWDP-23P	4,059,875.05	553,923.73
NC-EWDP-24P	4,062,055.18	549,385.64
NC-EWDP-27P	4,065,275.35	544,935.37
NC-EWDP-28P	4,062,392.74	545,745.59
NC-EWDP-29P	4,059,606.16	549,396.60

Source: Output DTN: LA0612RR150304.001.

INTENTIONALLY LEFT BLANK

APPENDIX G
DISTRIBUTION AND ELEVATIONS OF HYDROGEOLOGIC UNITS IN THE SZ COMPUTATIONAL GRID

G1. PURPOSE

This appendix serves as a visual check of how well the modeled geological units match the HFM. Appendix G presents 23 figures (Figures G-1 through G-23) showing the extent and elevation for each of the 23 units among the 28 hydrogeologic units included in the computational grid. The figures show the distribution of grid nodes for material units 2 through 28, with exception of units 10, 13, 22, and 25, which are not present in the site-scale saturated zone flow model domain. The view is looking down at the top of the unit with North at the top of the page and nodes are colored by their elevation in meters. The white space shows where grid nodes do not exist for a particular unit. The left panel of each figure shows the distribution of units over the full model domain, the right panel shows the resulting distribution when the grid units are truncated by the water table surface (only that portion of the hydrogeologic unit below the water table is illustrated). When the right and left panels are the same, the entire geological unit is saturated (under the water table). The figures differ only when portions of the visualized unit lie above the water table and in these cases, the additional white space in the figure on the right hand side represents only portions of that unit above the water. Along with the figures showing grid node distribution, the number of nodes for the unit is also given in Table 6-5. See the main report for details and text regarding the assignment of the material units.

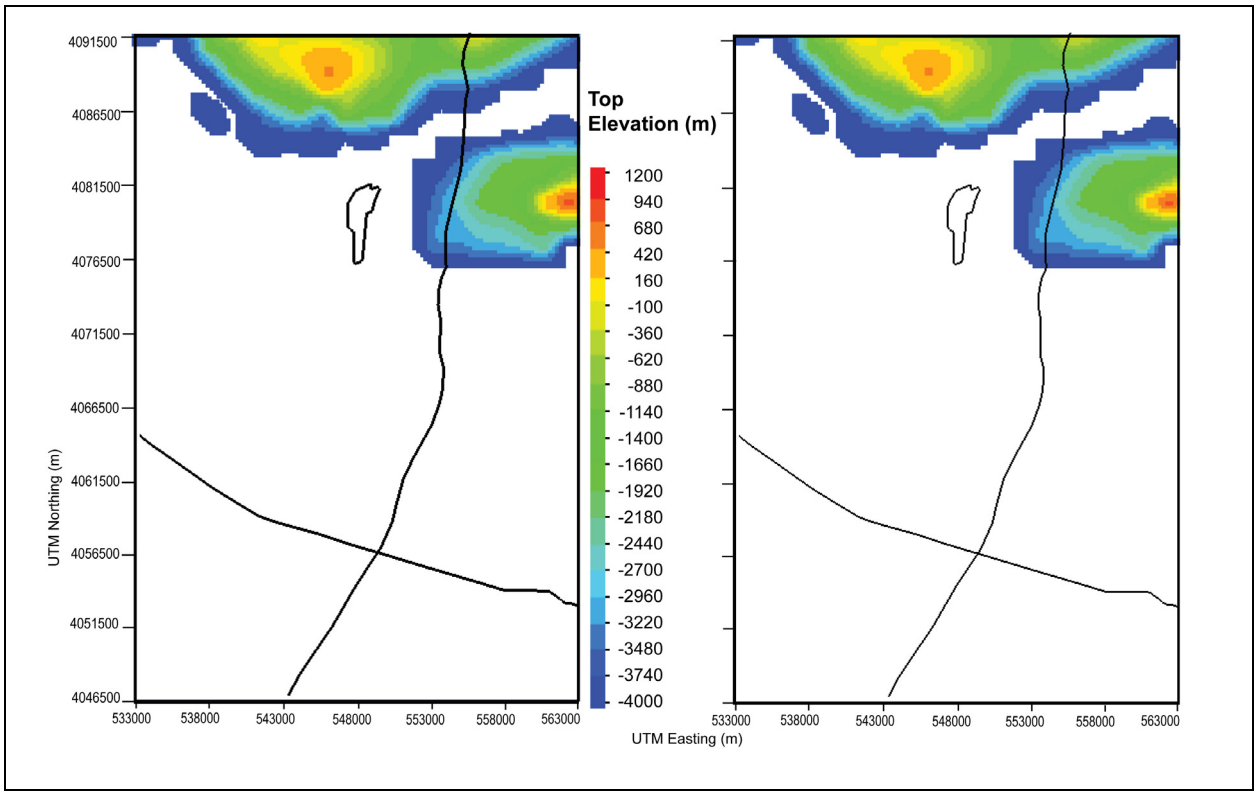

Sources: DTN: MO0610MWDHFM06.002 [DIRS 179352] (HFM2006); SNL 2007 [DIRS 179466] (repository outline).

Output DTNs: MO0611SCALEFLW.000 (potentiometric surface); LA0612TM831231.001.

NOTES: Hydrogeologic properties for unit defined by HFM for computational grid with 20,708 nodes total (left panel) and 20,708 nodes under water table (right panel). Coordinates in UTM, Zone 11, NAD27 meters. Black lines show repository outline, U.S. Highway 95 running East-West, and trace of Fortymile Wash running North-South. Elevation is in meters above mean sea level. For illustration purposes only.

HFM = Hydrogeologic Framework Model; UTM = Universal Transverse Mercator.

Figure G-1. Distribution and Elevations of ICU, Intrusive Confining Unit (2)

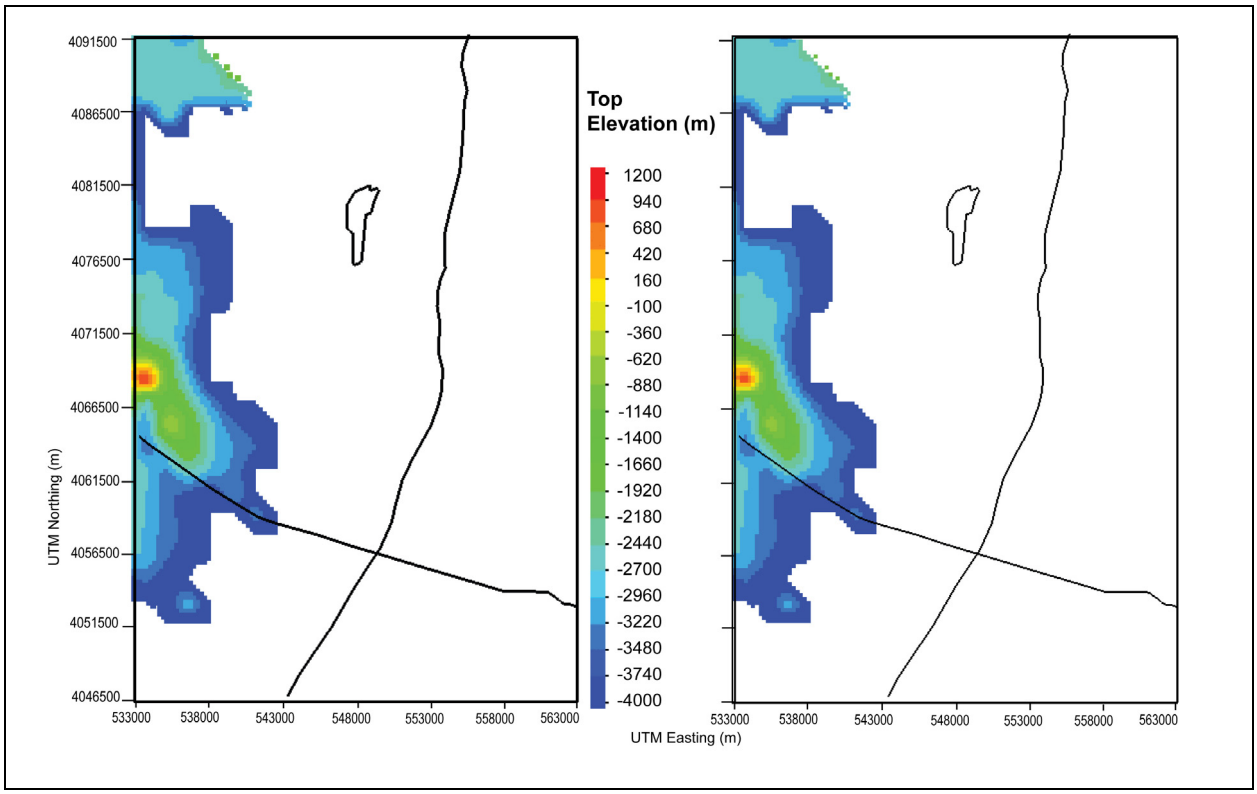

Sources: DTN: MO0610MWDHFM06.002 [DIRS 179352] (HFM2006); SNL 2007 [DIRS 179466] (repository outline).

Output DTNs: MO0611SCALEFLW.000 (potentiometric surface); LA0612TM831231.001.

NOTES: Hydrogeologic properties for unit defined by HFM for computational grid with 10,018 nodes total (left panel) and 10,015 nodes under water table (right panel). Coordinates in UTM, Zone 11, NAD27 meters. Black lines show repository outline, U.S. Highway 95 running East-West, and trace of Fortymile Wash running North-South. Elevation is in meters above mean sea level. For illustration purposes only.

HFM = Hydrogeologic Framework Model; UTM = Universal Transverse Mercator.

Figure G-2. Distribution and Elevations of XCU, Crystalline-Rock Confining Unit (3)

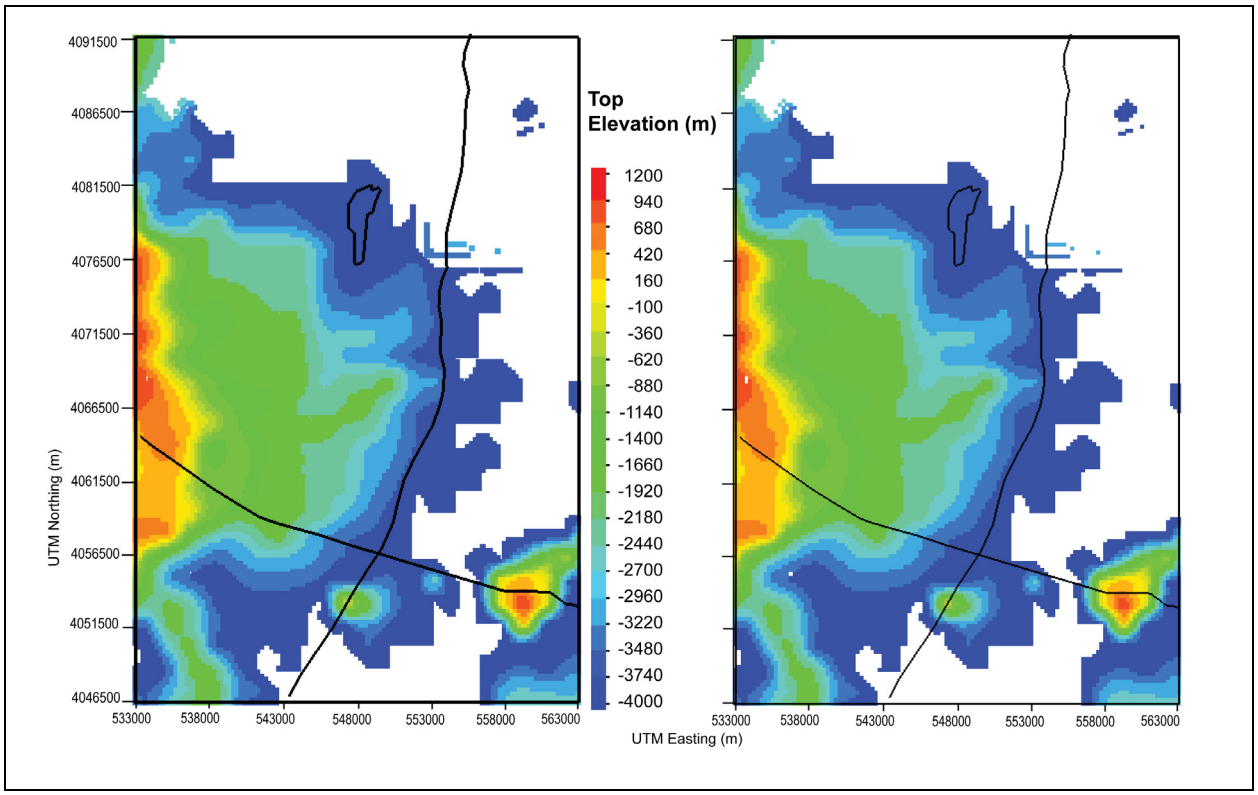

Sources: DTN: MO0610MWDHFM06.002 [DIRS 179352] (HFM2006); SNL 2007 [DIRS 179466] (repository outline).

Output DTNs: MO0611SCALEFLW.000 (potentiometric surface); LA0612TM831231.001.

NOTES: Hydrogeologic properties for unit defined by HFM for computational grid with 52,891 nodes total (left panel) and 52,745 nodes under water table (right panel). Coordinates in UTM, Zone 11, NAD27 meters. Black lines show repository outline, U.S. Highway 95 running East-West, and trace of Fortymile Wash running North-South. Elevation is in meters above mean sea level. For illustration purposes only.

HFM = Hydrogeologic Framework Model; UTM = Universal Transverse Mercator.

Figure G-3. Distribution and Elevations of LCCU, Lower Clastic-Rock Confining Unit (4)

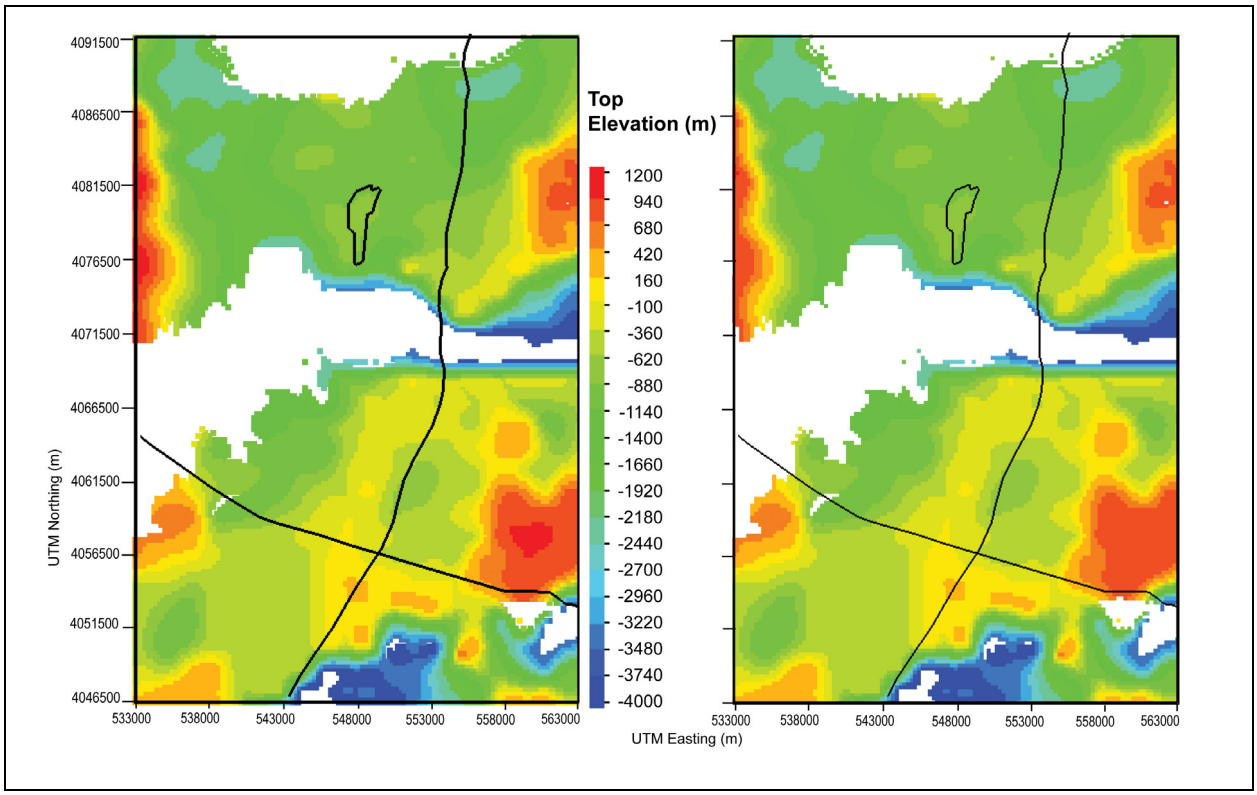

Sources: DTN: MO0610MWDHFM06.002 [DIRS 179352] (HFM2006); SNL 2007 [DIRS 179466] (repository outline).

Output DTNs: MO0611SCALEFLW.000 (potentiometric surface); LA0612TM831231.001.

NOTES: Hydrogeologic properties for unit defined by HFM for computational grid with 135,186 nodes total (left panel) and 131,312 nodes under water table (right panel). Coordinates in UTM, Zone 11, NAD27 meters. Black lines show repository outline, U.S. Highway 95 running East-West, and trace of Fortymile Wash running North-South. Elevation is in meters above mean sea level. For illustration purposes only.

HFM = Hydrogeologic Framework Model; UTM = Universal Transverse Mercator.

Figure G-4. Distribution and Elevations of LCA, Lower Carbonate-Rock Aquifer (5)

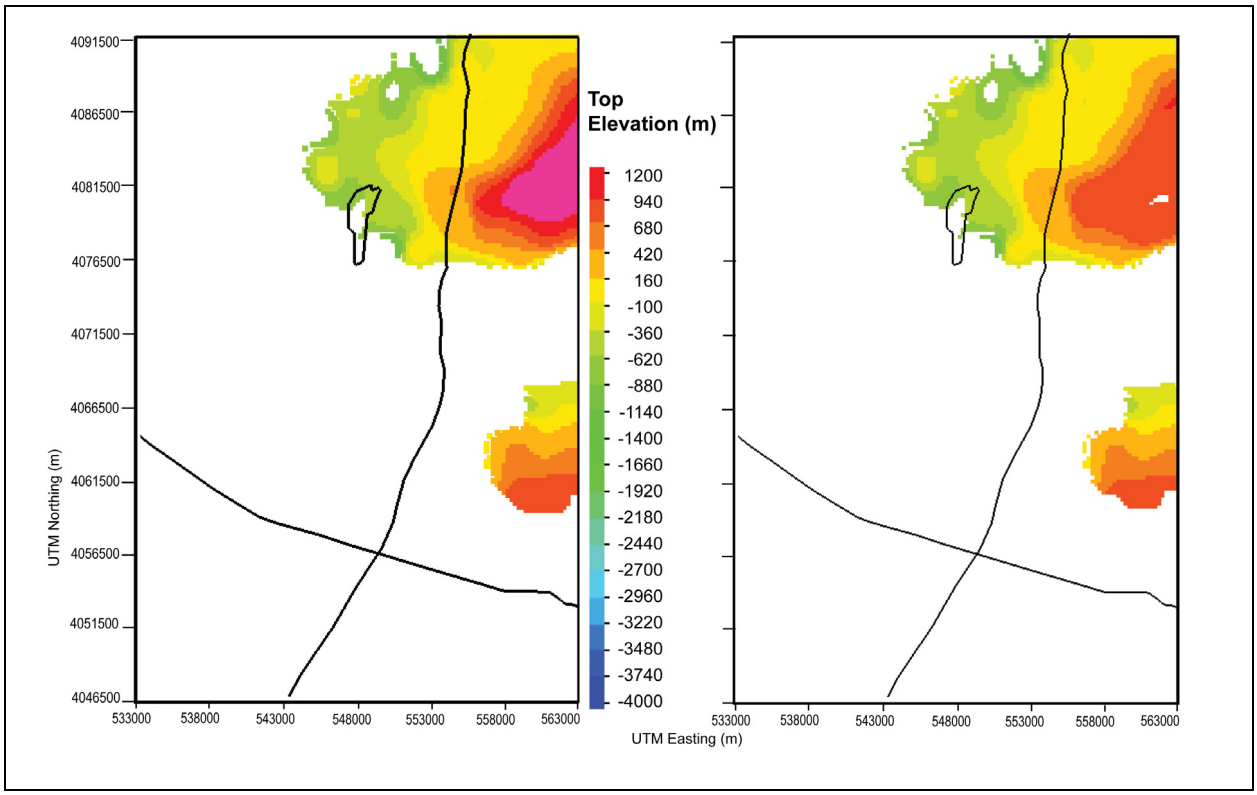

Sources: DTN: MO0610MWDHFM06.002 [DIRS 179352] (HFM2006); SNL 2007 [DIRS 179466] (repository outline).

Output DTNs: MO0611SCALEFLW.000 (potentiometric surface); LA0612TM831231.001.

NOTES: Hydrogeologic properties for unit defined by HFM for computational grid with 40,842 nodes total (left panel) and 33,533 nodes under water table (right panel). Coordinates in UTM, Zone 11, NAD27 meters. Black lines show repository outline, U.S. Highway 95 running East-West, and trace of Fortymile Wash running North-South. Elevation is in meters above mean sea level. For illustration purposes only.

HFM = Hydrogeologic Framework Model; UTM = Universal Transverse Mercator.

Figure G-5. Distribution and Elevations of UCCU, Upper Clastic-Rock Confining Unit (6)

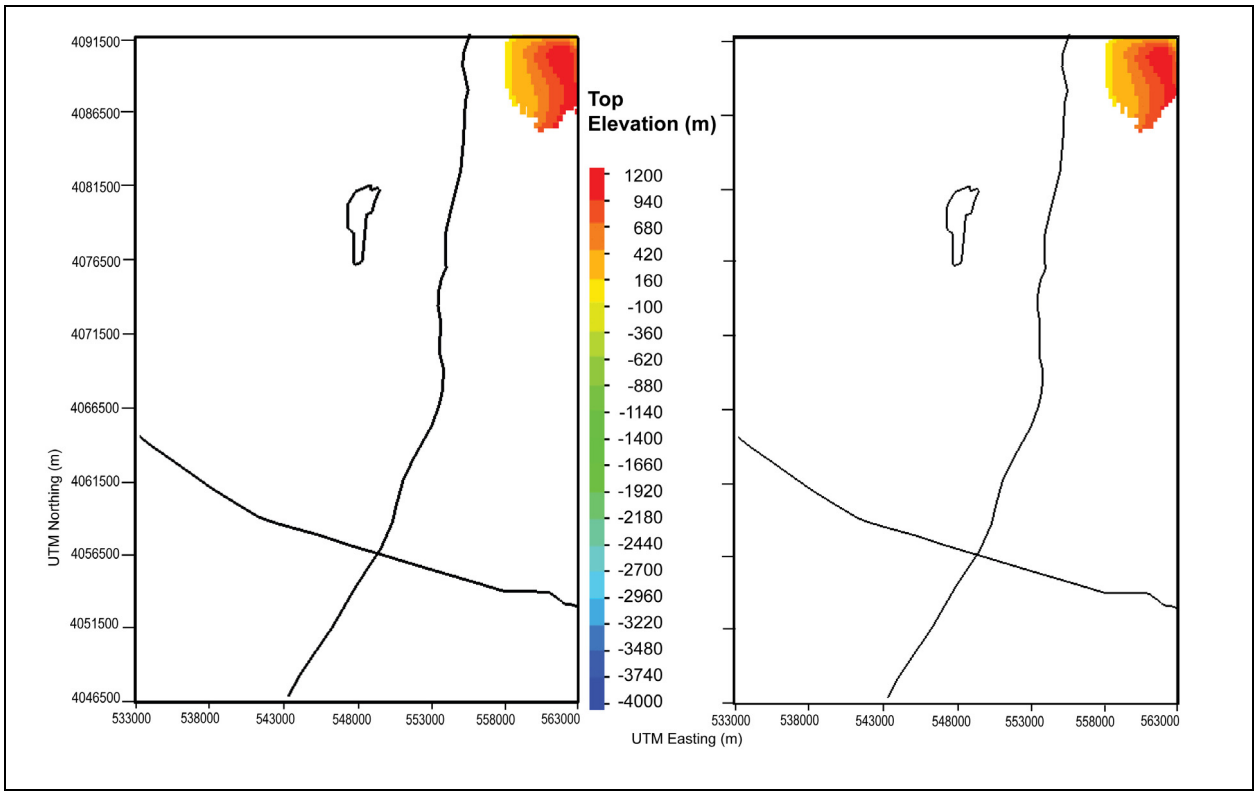

Sources: DTN: MO0610MWDHFM06.002 [DIRS 179352] (HFM2006); SNL 2007 [DIRS 179466] (repository outline).

Output DTNs: MO0611SCALEFLW.000 (potentiometric surface); LA0612TM831231.001.

NOTES: Hydrogeologic properties for unit defined by HFM for computational grid with 4,228 nodes total (left panel) and 4,201 nodes under water table (right panel). Coordinates in UTM, Zone 11, NAD27 meters. Black lines show repository outline, U.S. Highway 95 running East-West, and trace of Fortymile Wash running North-South. Elevation is in meters above mean sea level. For illustration purposes only.

HFM = Hydrogeologic Framework Model; UTM = Universal Transverse Mercator.

Figure G-6. Distribution and Elevations of UCA, Upper Carbonate-Rock Aquifer (7)

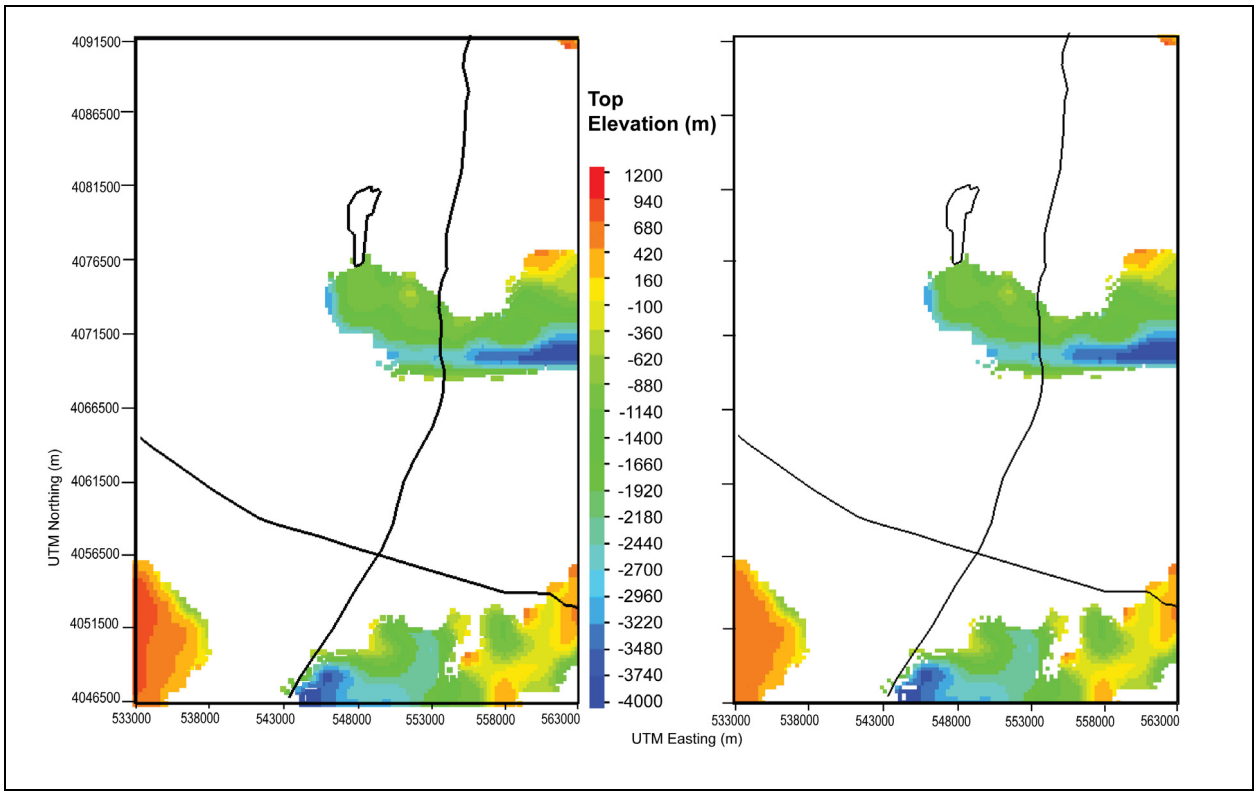

Sources: DTN: MO0610MWDHFM06.002 [DIRS 179352] (HFM2006); SNL 2007 [DIRS 179466] (repository outline).

Output DTNs: MO0611SCALEFLW.000 (potentiometric surface); LA0612TM831231.001.

NOTES: Hydrogeologic properties for unit defined by HFM for computational grid with 17,848 nodes total (left panel) and 17,053 nodes under water table (right panel). Coordinates in UTM, Zone 11, NAD27 meters. Black lines show repository outline, U.S. Highway 95 running East-West, and trace of Fortymile Wash running North-South. Elevation is in meters above mean sea level. For illustration purposes only.

HFM = Hydrogeologic Framework Model; UTM = Universal Transverse Mercator.

Figure G-7. Distribution and Elevations of LCCU-T1, Lower Clastic Confining Unit – Thrust (8)

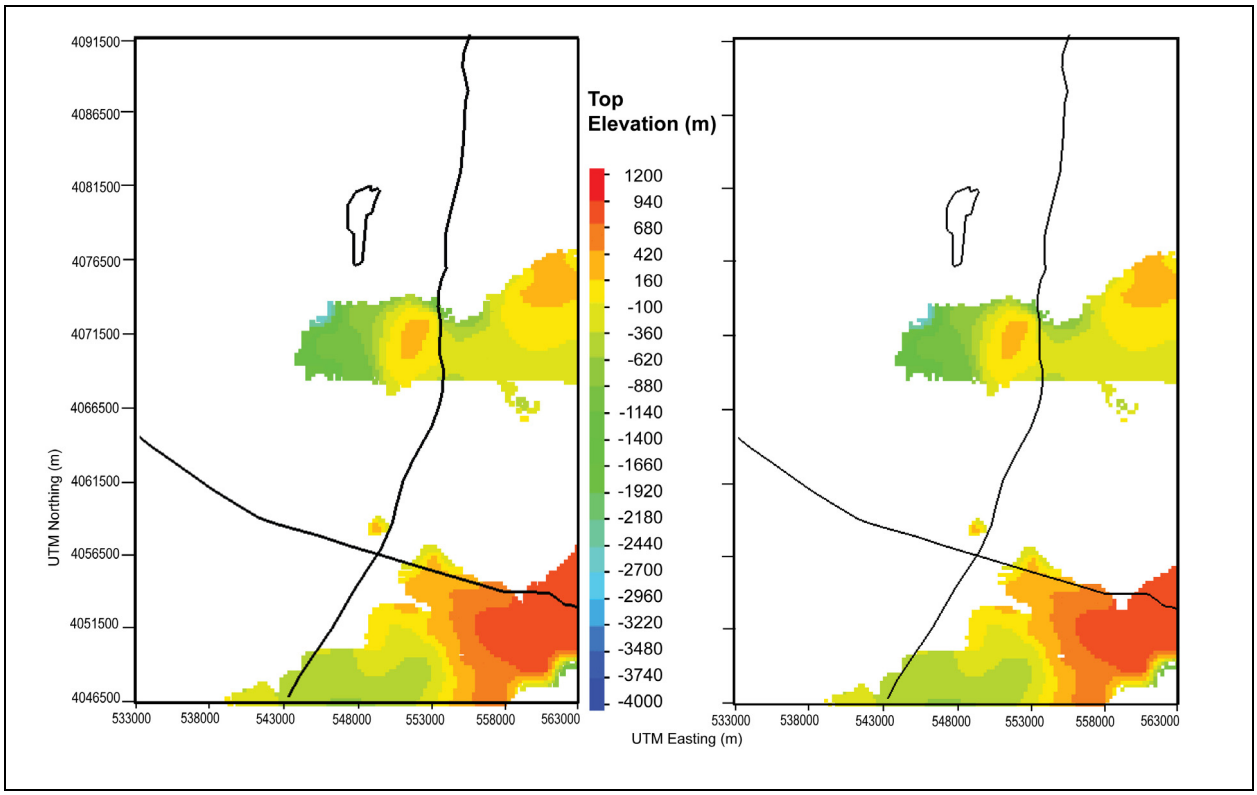

Sources: DTN: MO0610MWDHFM06.002 [DIRS 179352] (HFM2006); SNL 2007 [DIRS 179466] (repository outline).

Output DTNs: MO0611SCALEFLW.000 (potentiometric surface); LA0612TM831231.001.

NOTES: Hydrogeologic properties for unit defined by HFM for computational grid with 31,608 nodes total (left panel) and 28,588 nodes under water table (right panel). Coordinates in UTM, Zone 11, NAD27 meters. Black lines show repository outline, U.S. Highway 95 running East-West, and trace of Fortymile Wash running North-South. Elevation is in meters above mean sea level. For illustration purposes only.

HFM = Hydrogeologic Framework Model; UTM = Universal Transverse Mercator.

Figure G-8. Distribution and Elevations of LCA-T1, Lower Carbonate Aquifer – Thrust (9)

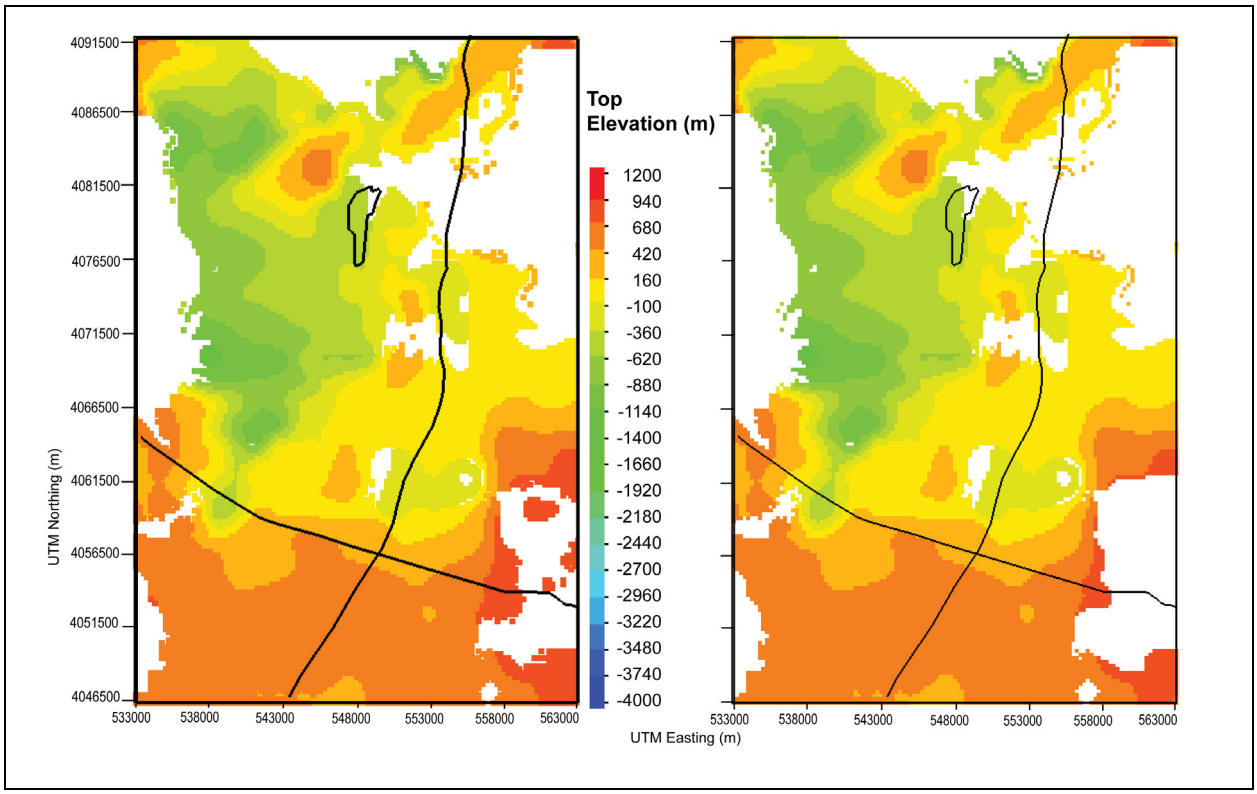

Sources: DTN: MO0610MWDHFM06.002 [DIRS 179352] (HFM2006); SNL 2007 [DIRS 179466] (repository outline).

Output DTNs: MO0611SCALEFLW.000 (potentiometric surface); LA0612TM831231.001.

NOTES: Hydrogeologic properties for unit defined by HFM for computational grid with 78,182 nodes total (left panel) and 76,856 nodes under water table (right panel). Coordinates in UTM, Zone 11, NAD27 meters. Black lines show repository outline, U.S. Highway 95 running East-West, and trace of Fortymile Wash running North-South. Elevation is in meters above mean sea level. For illustration purposes only.

HFM = Hydrogeologic Framework Model; UTM = Universal Transverse Mercator.

Figure G-9. Distribution and Elevations of VSU-Lower, Lower Volcanic and Sedimentary Units (11)

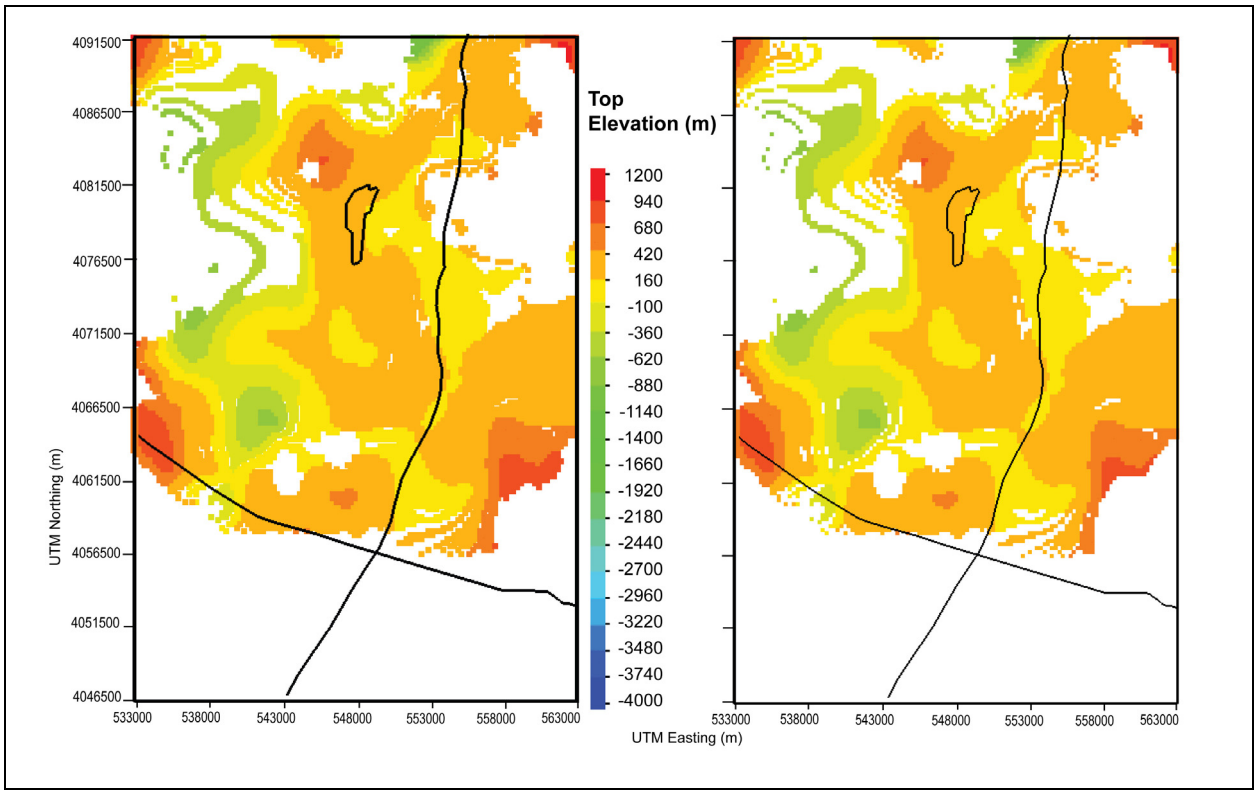

Sources: DTN: MO0610MWDHFM06.002 [DIRS 179352] (HFM2006); SNL 2007 [DIRS 179466] (repository outline).

Output DTNs: MO0611SCALEFLW.000 (potentiometric surface); LA0612TM831231.001.

NOTES: Hydrogeologic properties for unit defined by HFM for computational grid with 27,152 nodes total (left panel) and 26,691 nodes under water table (right panel). Coordinates in UTM, Zone 11, NAD27 meters. Black lines show repository outline, U.S. Highway 95 running East-West, and trace of Fortymile Wash running North-South. Elevation is in meters above mean sea level. For illustration purposes only.

HFM = Hydrogeologic Framework Model; UTM = Universal Transverse Mercator.

Figure G-10. Distribution and Elevations of OVU, Older Volcanic Units (12)

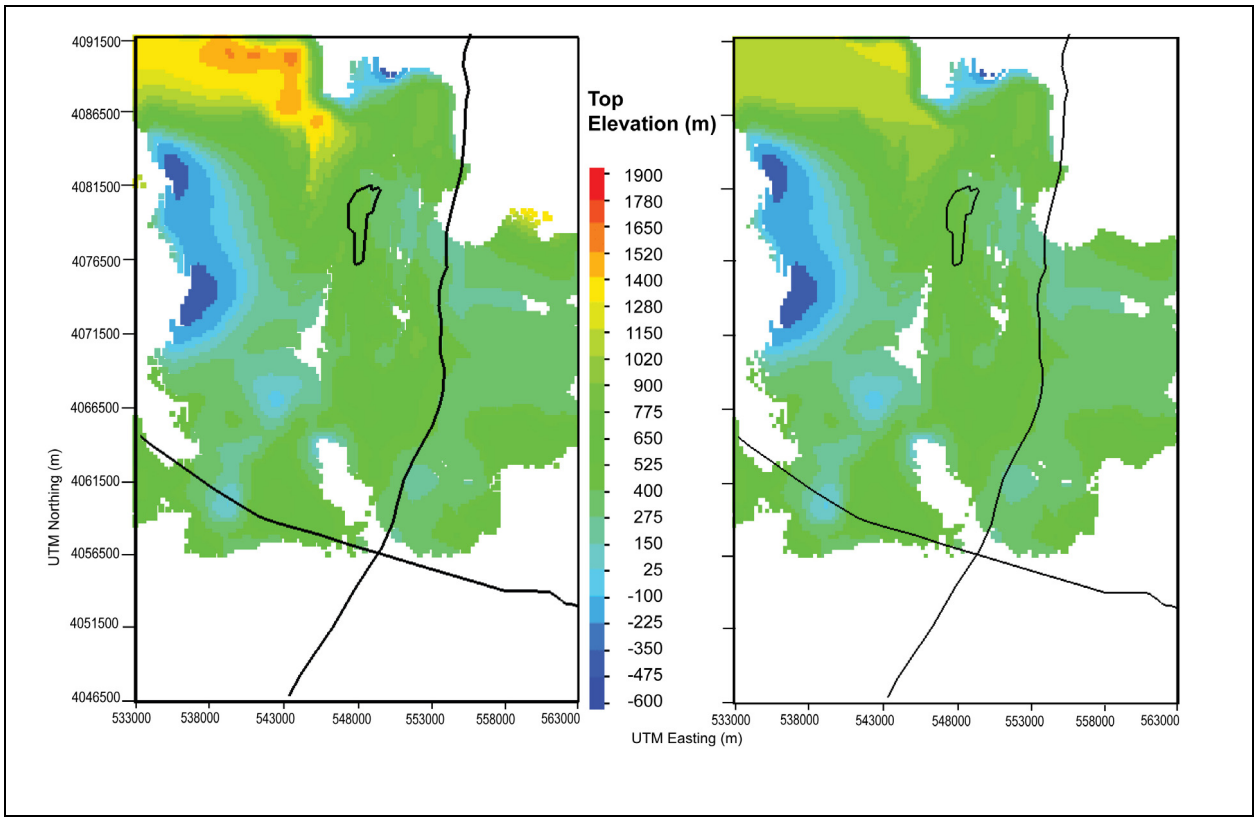

Sources: DTN: MO0610MWDHFM06.002 [DIRS 179352] (HFM2006); SNL 2007 [DIRS 179466] (repository outline).

Output DTNs: MO0611SCALEFLW.000 (potentiometric surface); LA0612TM831231.001.

NOTES: Hydrogeologic properties for unit defined by HFM for computational grid with 98,162 nodes total (left panel) and 93,327 nodes under water table (right panel). Coordinates in UTM, Zone 11, NAD27 meters. Black lines show repository outline, U.S. Highway 95 running East-West, and trace of Fortymile Wash running North-South. Elevation is in meters above mean sea level. For illustration purposes only.

HFM = Hydrogeologic Framework Model; UTM = Universal Transverse Mercator.

Figure G-11. Distribution and Elevations of CFTA, Crater Flat Tram Aquifer (14)

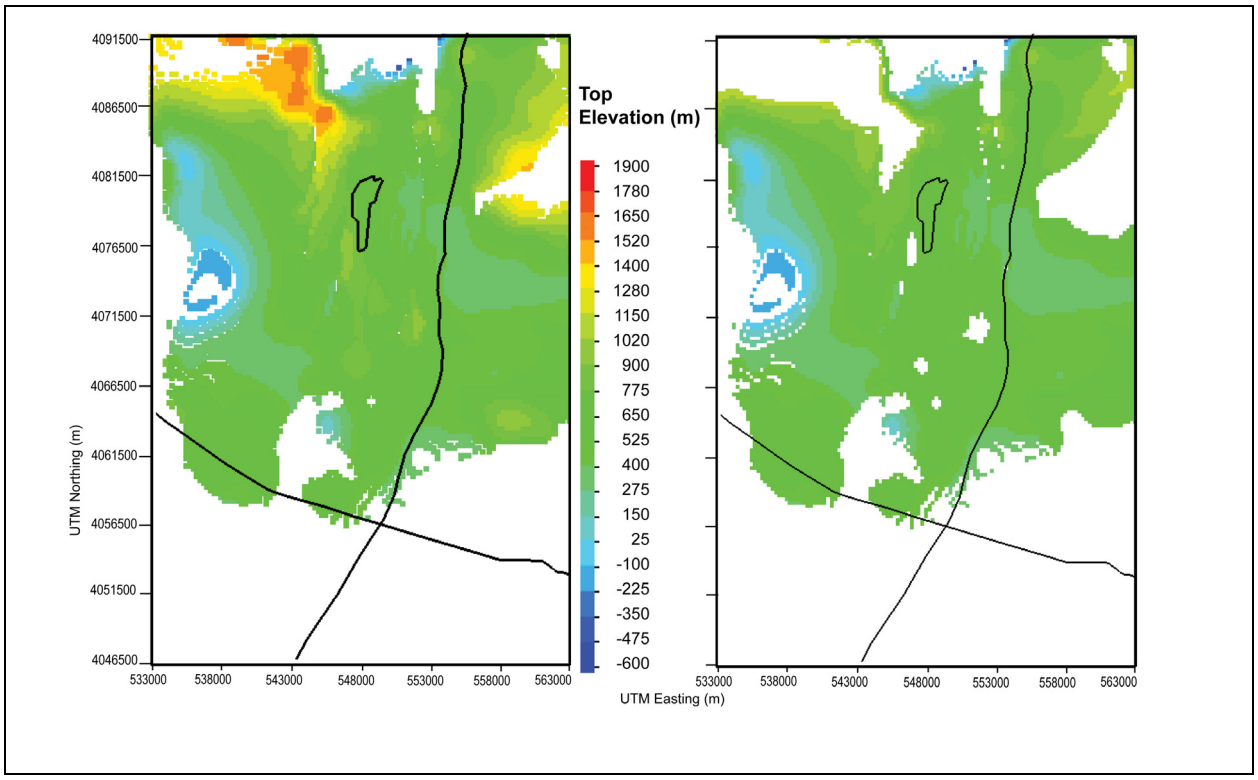

Sources: DTN: MO0610MWDHFM06.002 [DIRS 179352] (HFM2006); SNL 2007 [DIRS 179466] (repository outline).

Output DTNs: MO0611SCALEFLW.000 (potentiometric surface); LA0612TM831231.001.

NOTES: Hydrogeologic properties for unit defined by HFM for computational grid with 73,939 nodes total (left panel) and 67,436 nodes under water table (right panel). Coordinates in UTM, Zone 11, NAD27 meters. Black lines show repository outline, U.S. Highway 95 running East-West, and trace of Fortymile Wash running North-South. For illustration purposes only. Elevation is in meters above mean sea level.

HFM = Hydrogeologic Framework Model; UTM = Universal Transverse Mercator.

Figure G-12. Distribution and Elevations of CFBCU, Crater Flat Bullfrog Confining Unit (15)

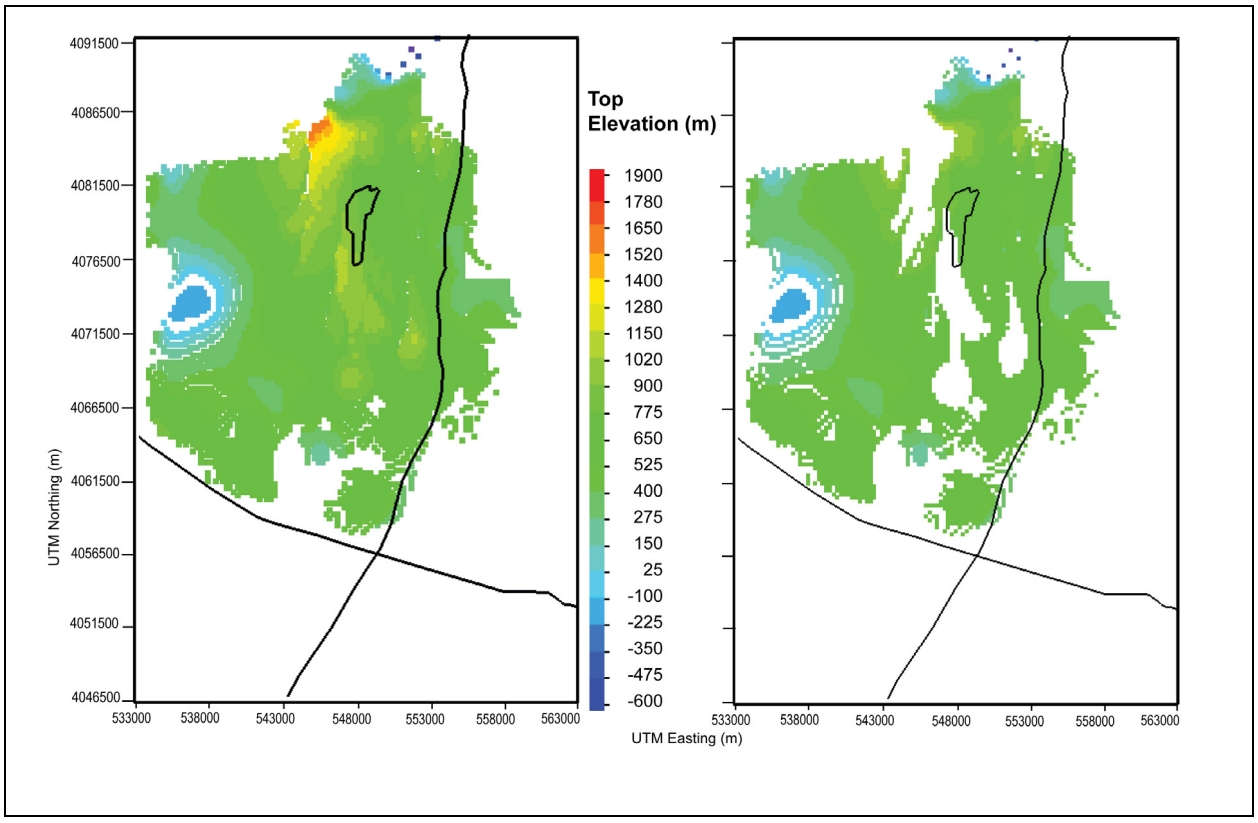

Sources: DTN: MO0610MWDHFM06.002 [DIRS 179352] (HFM2006); SNL 2007 [DIRS 179466] (repository outline).

Output DTNs: MO0611SCALEFLW.000 (potentiometric surface); LA0612TM831231.001.

NOTES: Hydrogeologic properties for unit defined by HFM for computational grid with 23,461 nodes total (left panel) and 20,242 nodes under water table (right panel). Coordinates in UTM, Zone 11, NAD27 meters. Black lines show repository outline, U.S. Highway 95 running East-West, and trace of Fortymile Wash running North-South. Elevation is in meters above mean sea level. For illustration purposes only.

HFM = Hydrogeologic Framework Model; UTM = Universal Transverse Mercator.

Figure G-13. Distribution and Elevations of CFPPA, Crater Flat Prow Pass Aquifer (16)

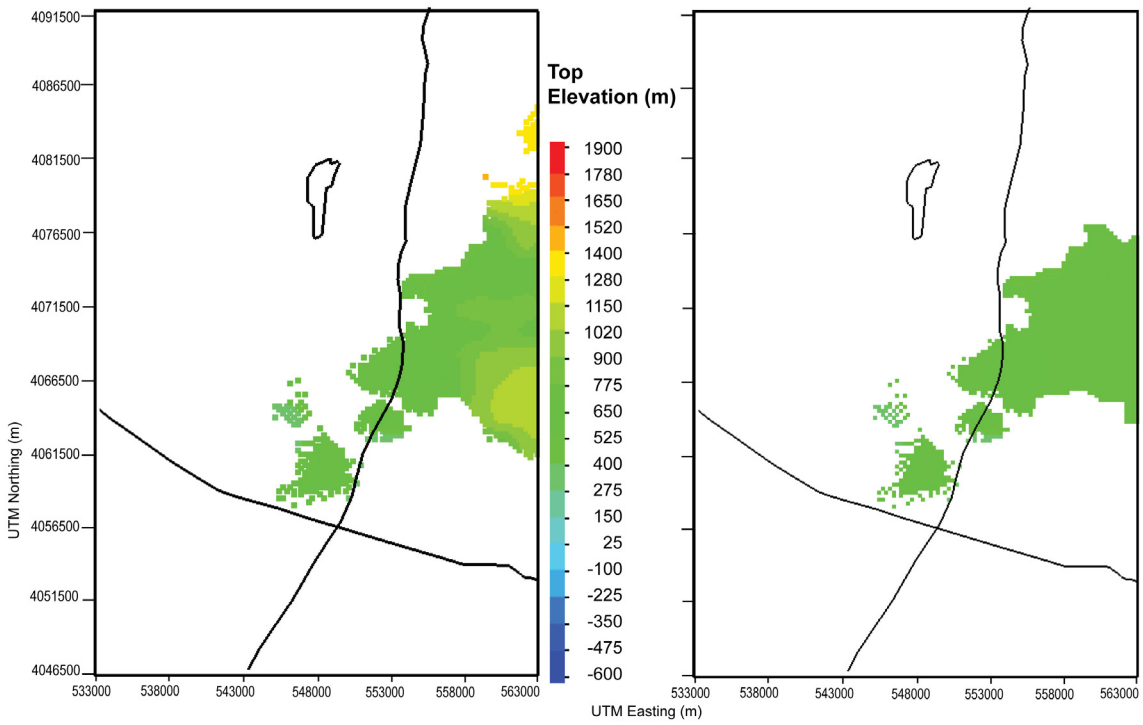

Sources: DTN: MO0610MWDHFM06.002 [DIRS 179352] (HFM2006); SNL 2007 [DIRS 179466] (repository outline).

Output DTNs: MO0611SCALEFLW.000 (potentiometric surface); LA0612TM831231.001.

NOTES: Hydrogeologic properties for unit defined by HFM for computational grid with 21,116 nodes total (left panel) and 14,576 nodes under water table (right panel). Coordinates in UTM, Zone 11, NAD27 meters. Black lines show repository outline, U.S. Highway 95 running East-West, and trace of Fortymile Wash running North-South. Elevation is in meters above mean sea level. For illustration purposes only.

HFM = Hydrogeologic Framework Model; UTM = Universal Transverse Mercator.

Figure G-14. Distribution and Elevations of WVU, Wahmonie Volcanic Unit (17)

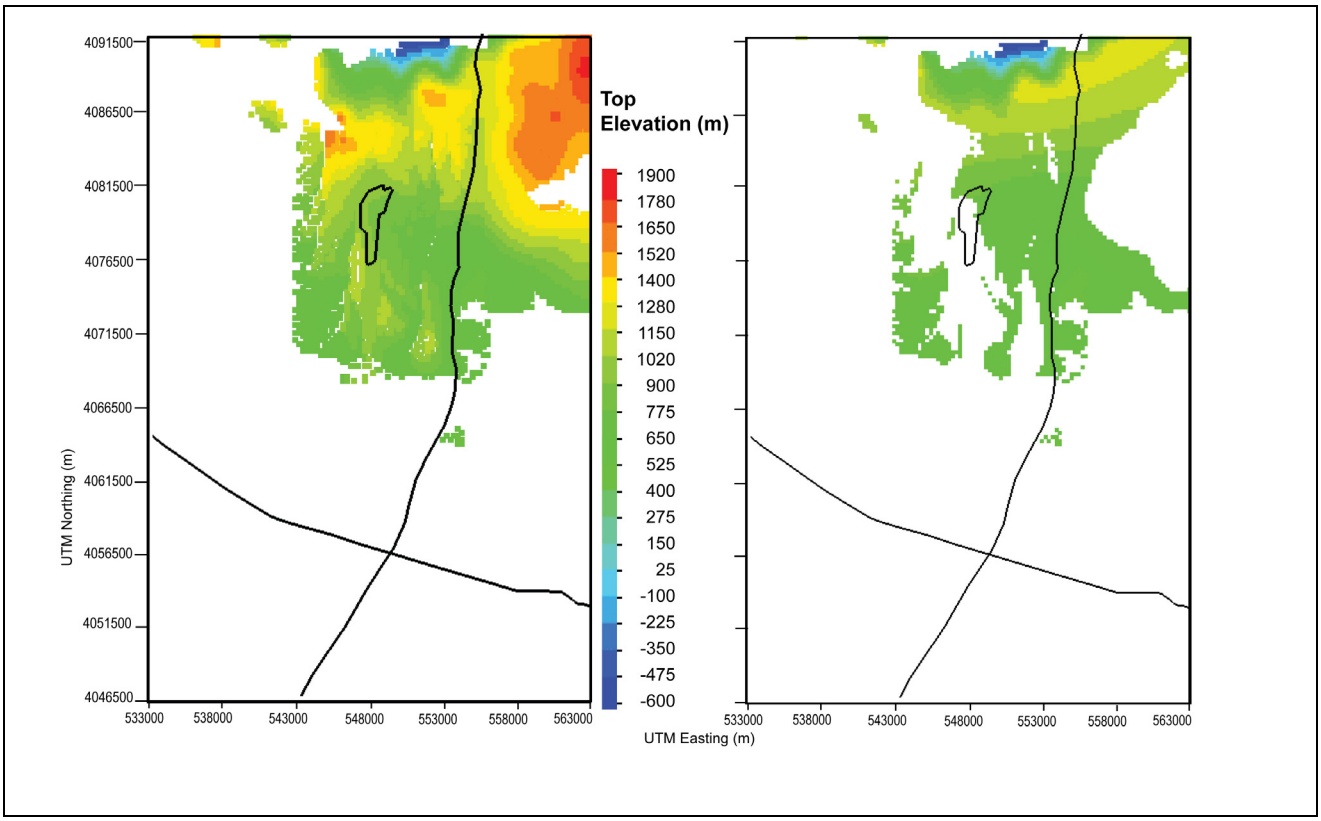

Sources: DTN: MO0610MWDHFM06.002 [DIRS 179352] (HFM2006); SNL 2007 [DIRS 179466] (repository outline).

Output DTNs: MO0611SCALEFLW.000 (potentiometric surface); LA0612TM831231.001.

NOTES: Hydrogeologic properties for unit defined by HFM for computational grid with 47,905 nodes total (left panel) and 29,189 nodes under water table (right panel). Coordinates in UTM, Zone 11, NAD27 meters. Black lines show repository outline, U.S. Highway 95 running East-West, and trace of Fortymile Wash running North-South. Elevation is in meters above mean sea level. For illustration purposes only.

HFM = Hydrogeologic Framework Model; UTM = Universal Transverse Mercator.

Figure G-15. Distribution and Elevations of CHVU, Calico Hills Volcanic Unit (18)

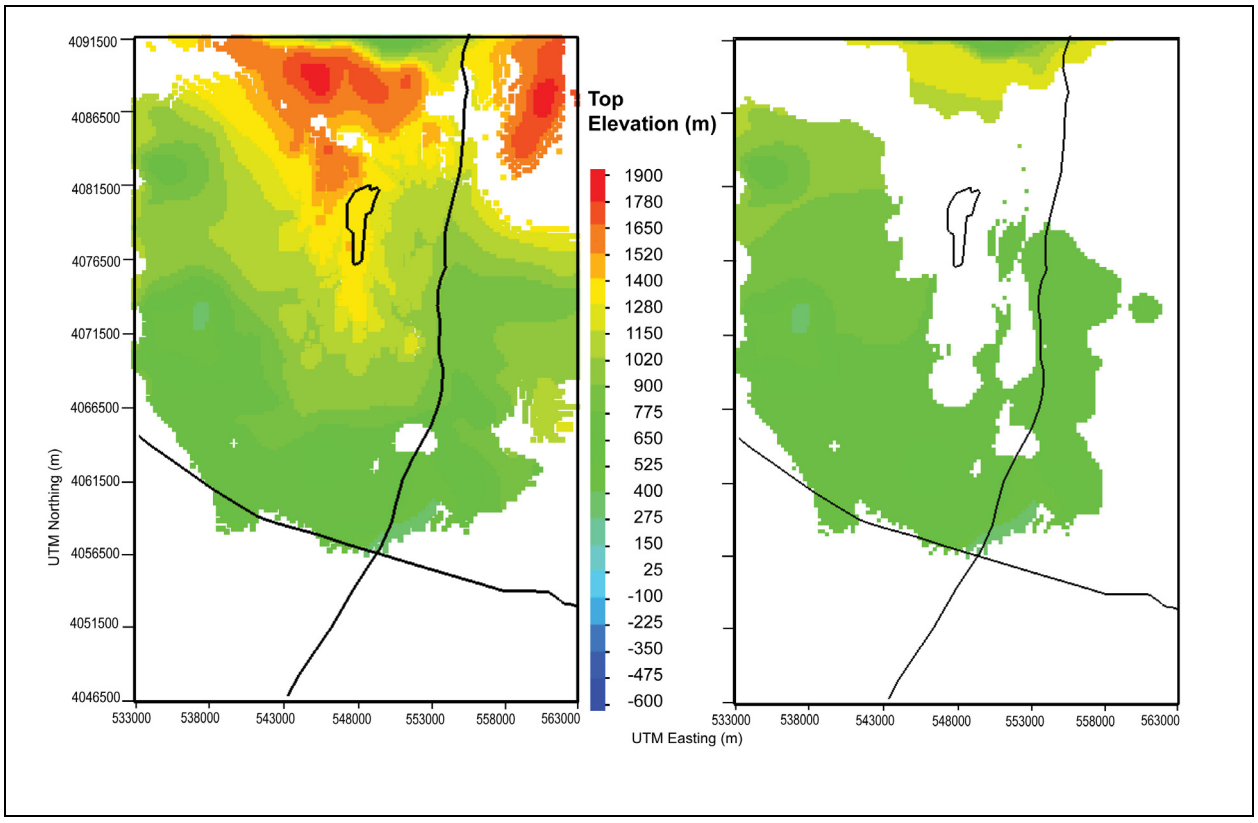

Sources: DTN: MO0610MWDHFM06.002 [DIRS 179352] (HFM2006); SNL 2007 [DIRS 179466] (repository outline).

Output DTNs: MO0611SCALEFLW.000 (potentiometric surface); LA0612TM831231.001.

NOTES: Hydrogeologic properties for unit defined by HFM for computational grid with 143,658 nodes total (left panel) and 94,149 nodes under water table (right panel). Coordinates in UTM, Zone 11, NAD27 meters. Black lines show repository outline, U.S. Highway 95 running East-West, and trace of Fortymile Wash running North-South. Elevation is in meters above mean sea level. For illustration purposes only.

HFM = Hydrogeologic Framework Model; UTM = Universal Transverse Mercator.

Figure G-16. Distribution and Elevations PVA, Paintbrush Volcanic Aquifer (19)

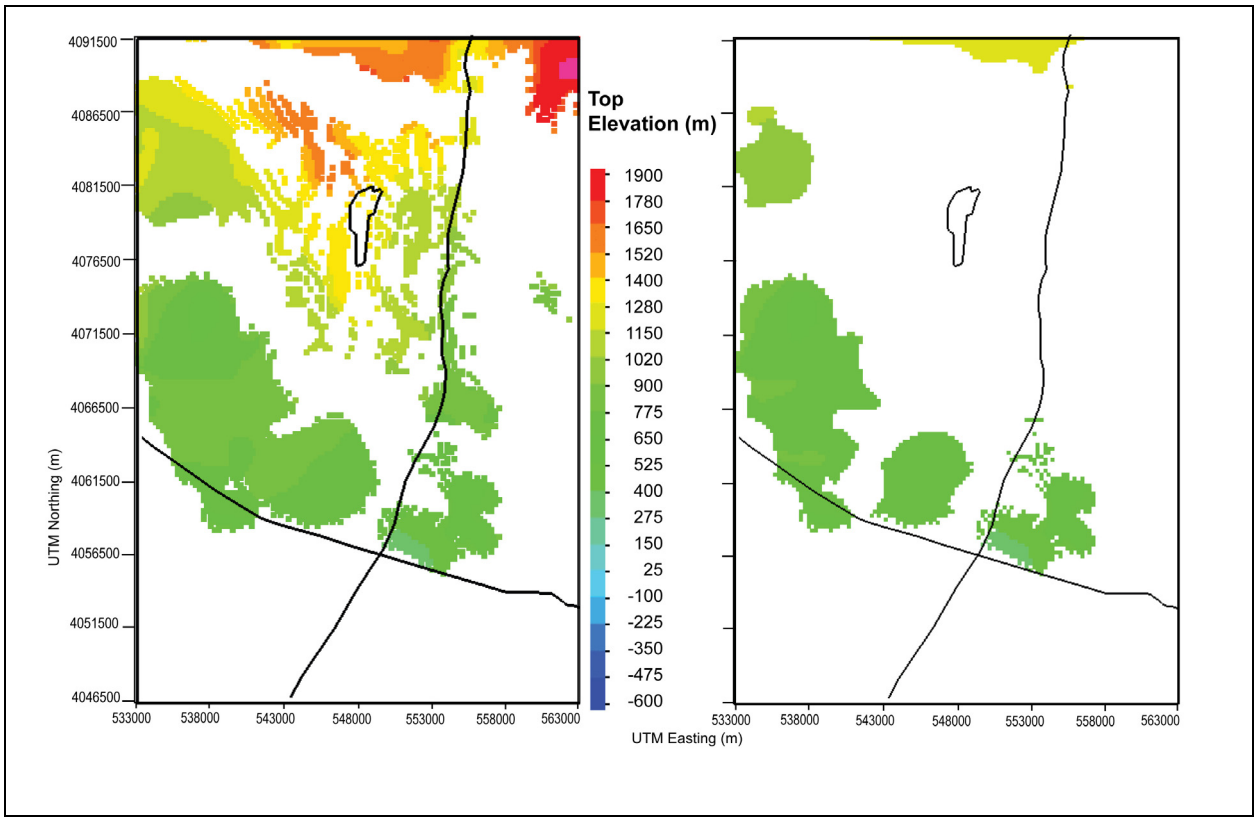

Sources: DTN: MO0610MWDHFM06.002 [DIRS 179352] (HFM2006); SNL 2007 [DIRS 179466] (repository outline).

Output DTNs: MO0611SCALEFLW.000 (potentiometric surface); LA0612TM831231.001.

NOTES: Hydrogeologic properties for unit defined by HFM for computational grid with 27,940 nodes total (left panel) and 18,131 nodes under water table (right panel). Coordinates in UTM, Zone 11, NAD27 meters. Black lines show repository outline, U.S. Highway 95 running East-West, and trace of Fortymile Wash running North-South. Elevation is in meters above mean sea level. For illustration purposes only.

HFM = Hydrogeologic Framework Model; UTM = Universal Transverse Mercator.

Figure G-17. Distribution and Elevations of TMVA, Timber Mountain Volcanic Aquifer (20)

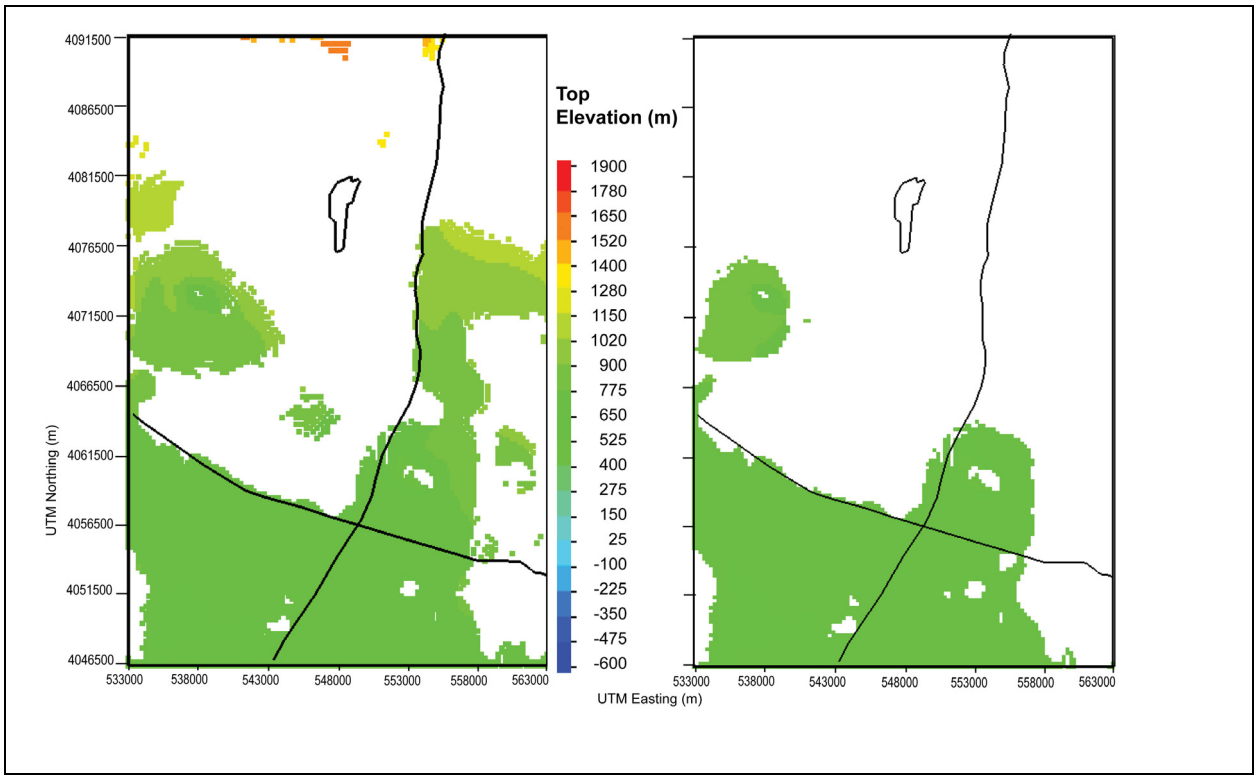

Sources: DTN: MO0610MWDHFM06.002 [DIRS 179352] (HFM2006); SNL 2007 [DIRS 179466] (repository outline).

Output DTNs: MO0611SCALEFLW.000 (potentiometric surface); LA0612TM831231.001.

NOTES: Hydrogeologic properties for unit defined by HFM for computational grid with 53,911 nodes total (left panel) and 42,717 nodes under water table (right panel). Coordinates in UTM, Zone 11, NAD27 meters. Black lines show repository outline, U.S. Highway 95 running East-West, and trace of Fortymile Wash running North-South. Elevation is in meters above mean sea level. For illustration purposes only.

HFM = Hydrogeologic Framework Model; UTM = Universal Transverse Mercator.

Figure G-18. Distribution and Elevation of VSU, Volcanic and Sedimentary Unit (Upper) (21)

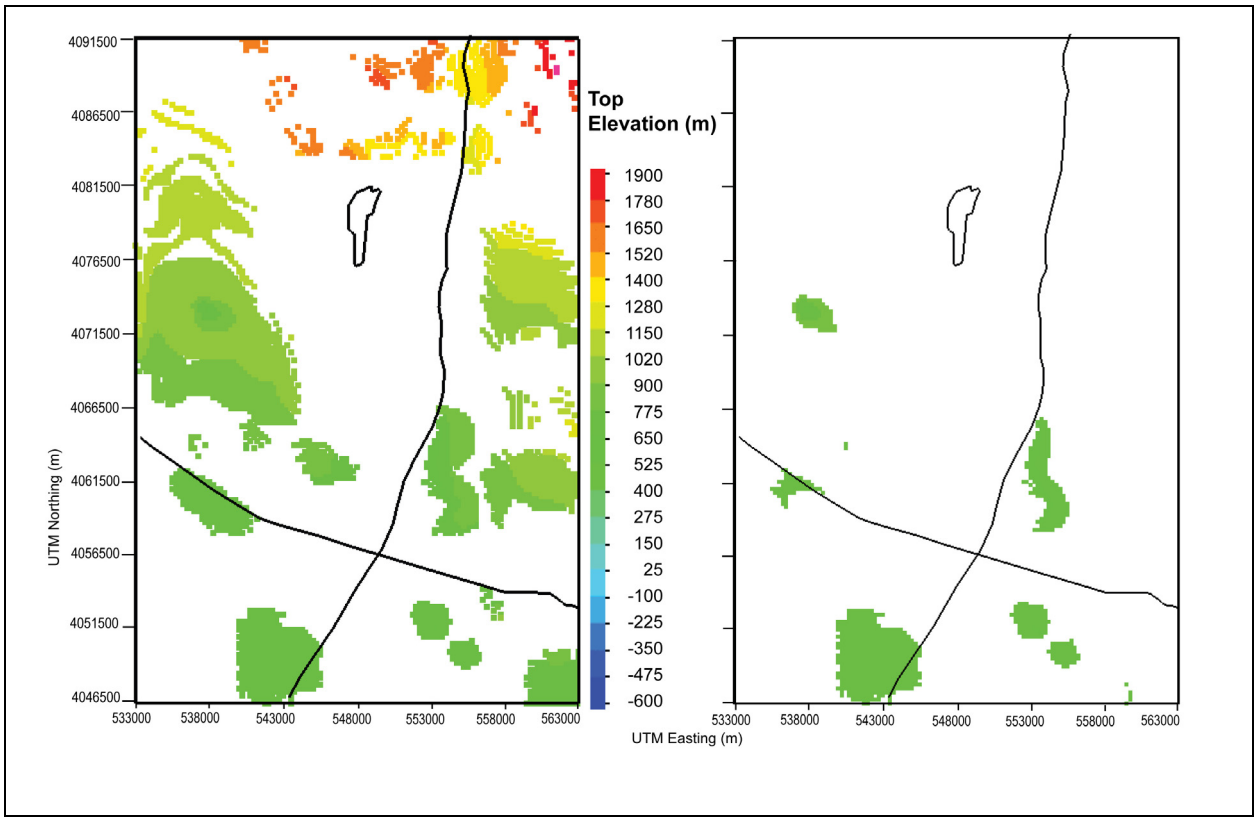

Sources: DTN: MO0610MWDHFM06.002 [DIRS 179352] (HFM2006); SNL 2007 [DIRS 179466] (repository outline).

Output DTNs: MO0611SCALEFLW.000 (potentiometric surface); LA0612TM831231.001.

NOTES: Hydrogeologic properties for unit defined by HFM for computational grid with 8,608 nodes total (left panel) and 2,751 nodes under water table (right panel). Coordinates in UTM, Zone 11, NAD27 meters. Black lines show repository outline, U.S. Highway 95 running East-West, and trace of Fortymile Wash running North-South. Elevation is in meters above mean sea level. For illustration purposes only.

HFM = Hydrogeologic Framework Model; UTM = Universal Transverse Mercator.

Figure G-19. Distribution and Elevations of LFU, Lava Flow Unit (23)

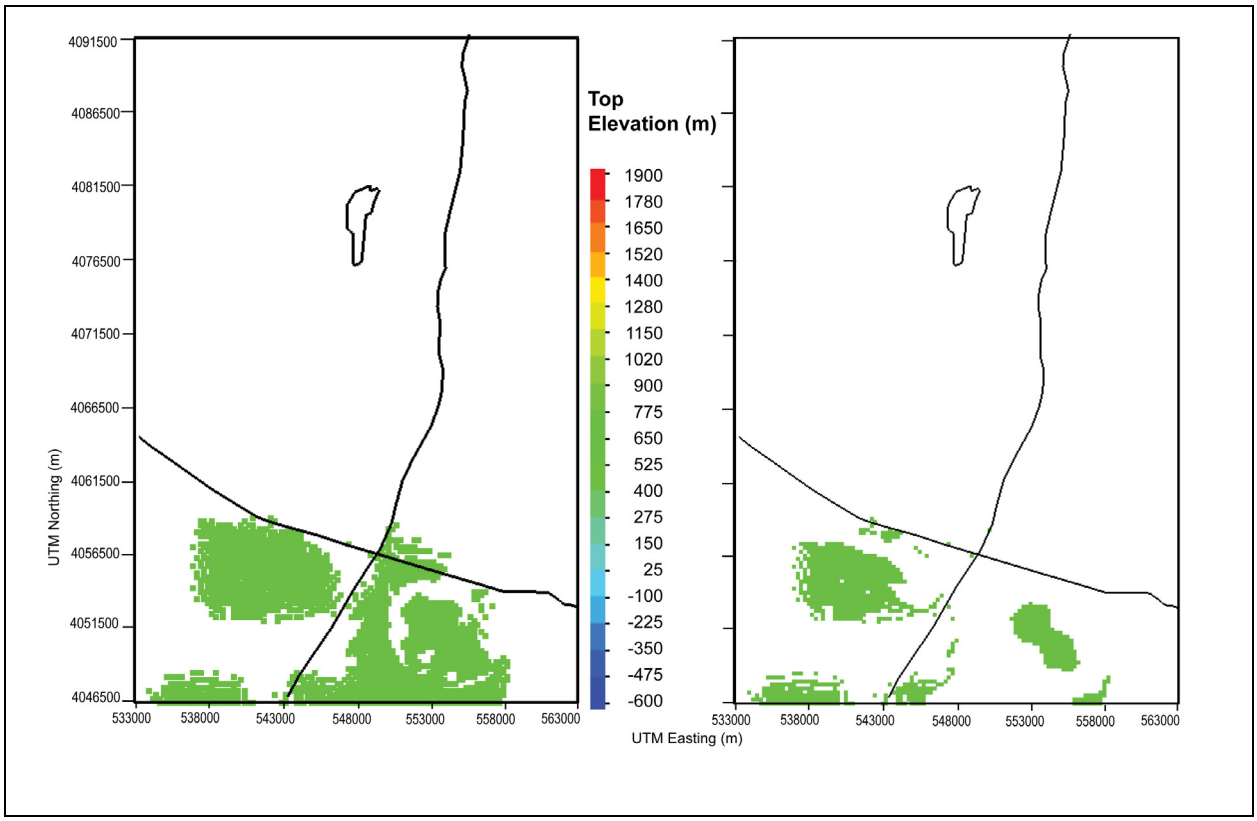

Sources: DTN: MO0610MWDHFM06.002 [DIRS 179352] (HFM2006); SNL 2007 [DIRS 179466] (repository outline).

Output DTNs: MO0611SCALEFLW.000 (potentiometric surface); LA0612TM831231.001.

NOTES: Hydrogeologic properties for unit defined by HFM for computational grid with 3,289 nodes total (left panel) and 1,387 nodes under water table (right panel). Coordinates in UTM, Zone 11, NAD27 meters. Black lines show repository outline, U.S. Highway 95 running East-West, and trace of Fortymile Wash running North-South. Elevation is in meters above mean sea level. For illustration purposes only.

HFM = Hydrogeologic Framework Model; UTM = Universal Transverse Mercator.

Figure G-20. Distribution and Elevations of LA, Limestone Aquifer (24)

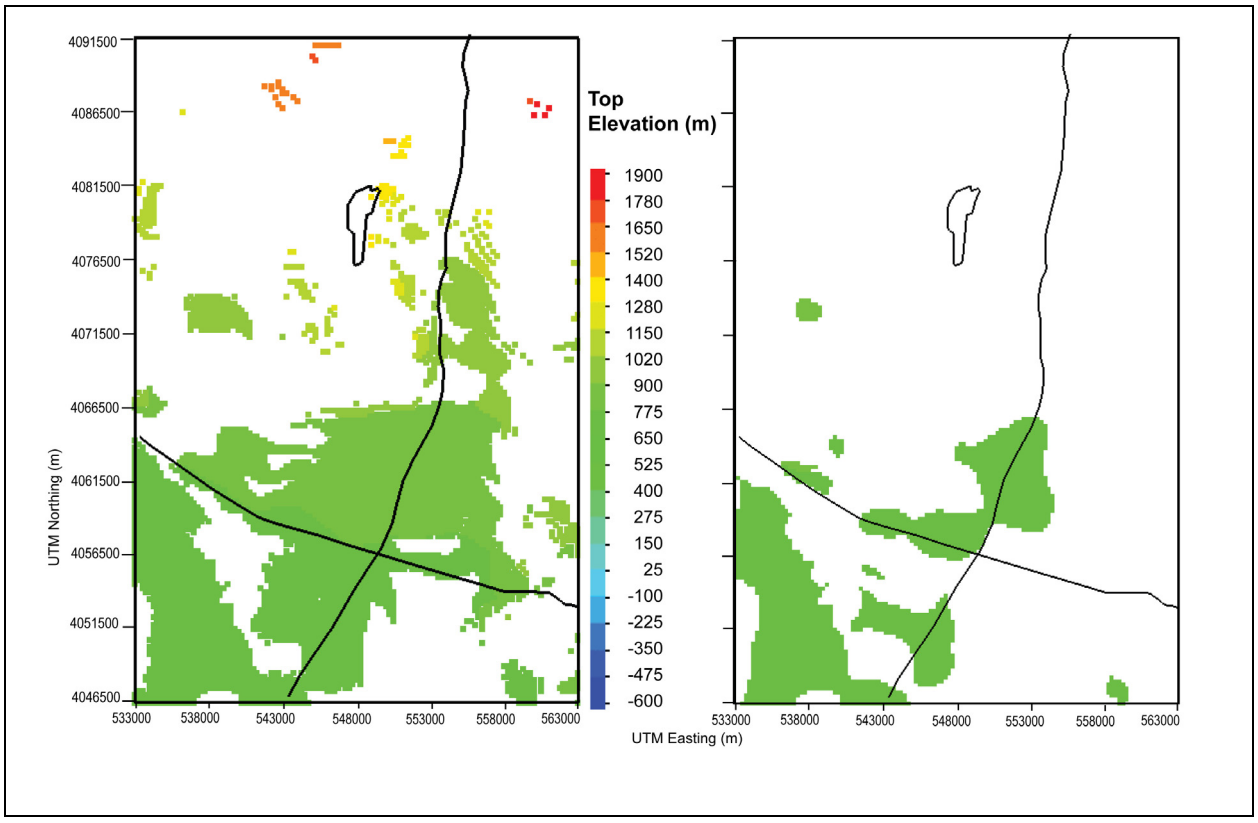

Sources: DTN: MO0610MWDHFM06.002 [DIRS 179352] (HFM2006); SNL 2007 [DIRS 179466] (repository outline).

Output DTNs: MO0611SCALEFLW.000 (potentiometric surface); LA0612TM831231.001.

NOTES: Hydrogeologic properties for unit defined by HFM for computational grid with 24,148 nodes total (left panel) and 10,637 nodes under water table (right panel). Coordinates in UTM, Zone 11, NAD27 meters. Black lines show repository outline, U.S. Highway 95 running East-West, and trace of Fortymile Wash running North-South. Elevation is in meters above mean sea level. For illustration purposes only.

HFM = Hydrogeologic Framework Model; UTM = Universal Transverse Mercator.

Figure G-21. Distribution and Elevations of OAA, Older Alluvial Aquifer (26)

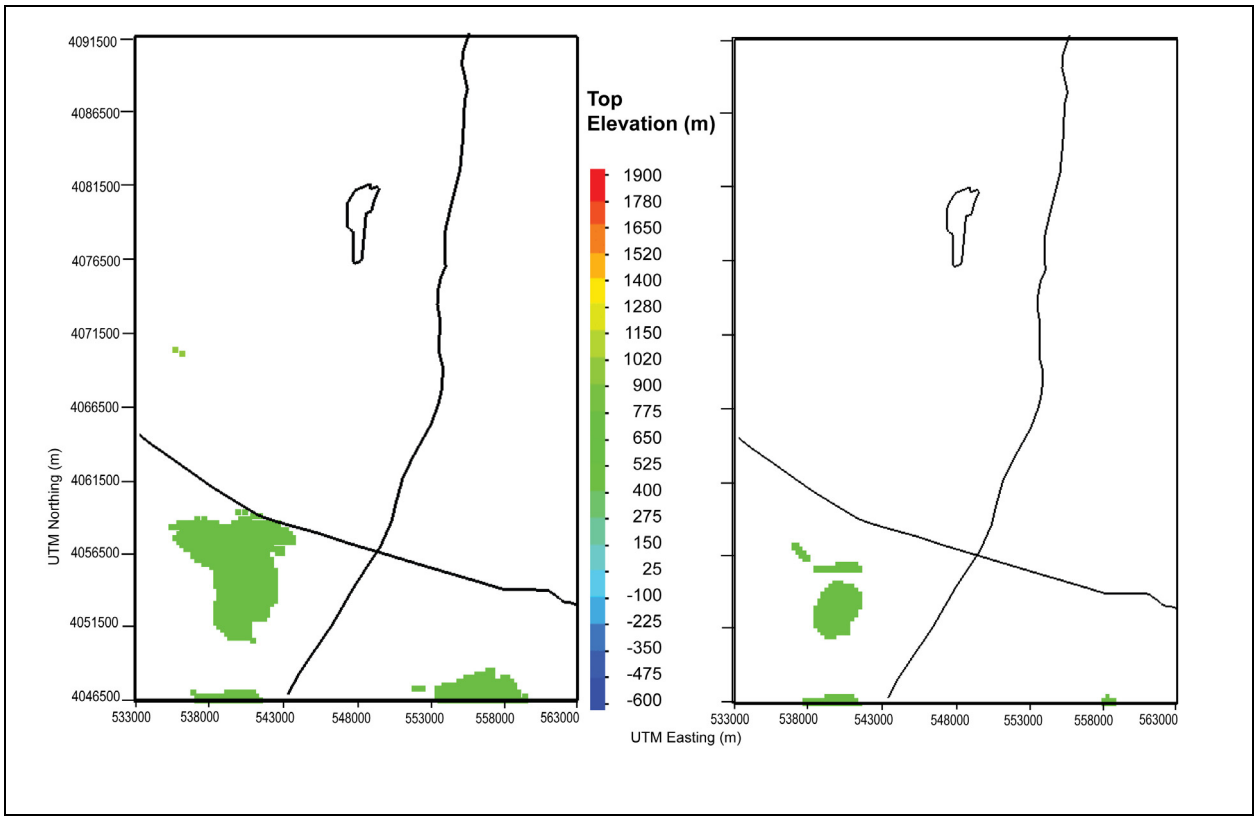

Sources: DTN: MO0610MWDHFM06.002 [DIRS 179352] (HFM2006); SNL 2007 [DIRS 179466] (repository outline).

Output DTNs: MO0611SCALEFLW.000 (potentiometric surface); LA0612TM831231.001.

NOTES: Hydrogeologic properties for unit defined by HFM for computational grid with 1,580 nodes total (left panel) and 247 nodes under water table (right panel). Coordinates in UTM, Zone 11, NAD27 meters. Black lines show repository outline, U.S. Highway 95 running East-West, and trace of Fortymile Wash running North-South. Elevation is in meters above mean sea level. For illustration purposes only.

HFM = Hydrogeologic Framework Model; UTM = Universal Transverse Mercator.

Figure G-22. Distribution and Elevations of YACU, Young Alluvial Confining Unit (27)

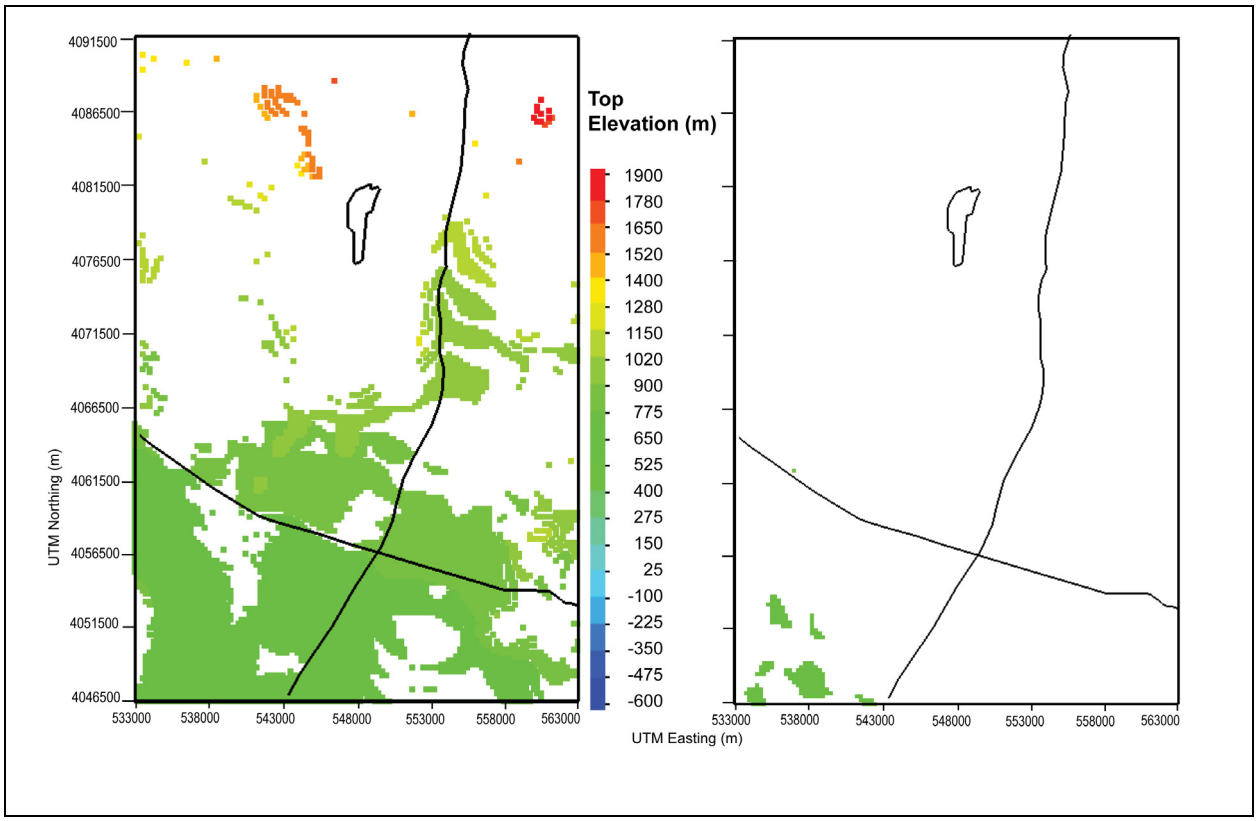

Sources: DTN: MO0610MWDHFM06.002 [DIRS 179352] (HFM2006); SNL 2007 [DIRS 179466] (repository outline).

Output DTNs: MO0611SCALEFLW.000 (potentiometric surface); LA0612TM831231.001.

NOTES: Hydrogeologic properties for unit defined by HFM for computational grid with 9,965 nodes total (left panel) and 197 nodes under water table (right panel). Coordinates in UTM, Zone 11, NAD27 meters. Black lines show repository outline, U.S. Highway 95 running East-West, and trace of Fortymile Wash running North-South. Elevation is in meters above mean sea level. For illustration purposes only.

HFM = Hydrogeologic Framework Model; UTM = Universal Transverse Mercator.

Figure G-23. Distribution and Elevations of YAA, Young Alluvial Aquifer (28)

APPENDIX H
REGULARIZED INVERSION AS A BASIS FOR MODEL CALIBRATION AND PREDICTIVE UNCERTAINTY ANALYSIS: AN EXPLANATION

H1. INTRODUCTION

Models are calibrated so that they make better predictions than if they were not calibrated. Unfortunately, calibrated model predictions can still be wrong. Furthermore, it is now being fully understood that a calibrated model can make even worse predictions than it did before calibration. With traditional approaches to model calibration, there is no way to find out: (1) whether a calibrated model's predictions are better than those before calibration, (2) if the predictions are better how much better they are, and (3) if their predictions are wrong how wrong they are. Traditional approaches to calibration are not able to ensure that calibrated models minimize "potential predictive wrongness" while quantifying the remaining uncertainty in the potential predictive wrongness.

The traditional approach to model calibration follows the tenet of the "principal of parsimony" espoused in many modeling texts and guidelines. First, the dimensionality of the calibration problem is reduced to facilitate a tractable model (i.e., few enough parameters are used to ensure their unique estimability) given the dataset available for calibration. The parameters values are then estimated through implicitly or explicitly maximizing some goodness-of-fit criterion. When the fit is judged to be "sufficient" (usually through minimization of an objective function), the model is deemed to be "calibrated" and therefore suitable for the making of predictions – predictions that may lay the groundwork for performance assessment calculations.

If automatic parameter estimation software is used in the calibration process, some estimates of parameter uncertainty are available. Estimates of the uncertainty of key model predictions can then be made based on the dependence of these predictions on the estimated parameters and their uncertainties.

The objective of this appendix is to show that calibrating a model and exploring the potential error of model predictions based on the theory of mathematical regularization, used in portions of this report, are better than methods based on the traditional approach to model calibration and predictive error analysis based on the principle of parsimony, which is not always effective or accurate. This same theory of mathematical regularization is regularly applied in many other branches of science where the analysis of costly and important data demands that maximum information be extracted (e.g., geophysical exploration and medical imaging). For example, a kidney is not defined prior to processing the data contained within a medical image; instead the location of the kidney "emerges" as a natural part of the data interpretation process. The same process should be used in groundwater data interpretation (which is what model calibration is) now that software that implements these methods efficiently in the groundwater modeling context are available. Public domain software that implements modern calibration and predictive uncertainty analysis based on regularized inversion is now available through the PEST package and its supporting utilities (Doherty 2003 [DIRS 178642], 2004 [DIRS 178643], 2006 [DIRS 178613]; PEST 2003 [DIRS 161564]). The groundwater industry will have to cross the same threshold that has been crossed in other industries, through application of regularized inversion as a methodology for model calibration and uncertainty analysis as a matter of course.

H2. TRADITIONAL MODEL CALIBRATION

Even with automatic optimization software, the task of calibrating a model can be unsatisfying and frustrating. Often a complex model of the groundwater system is developed. Its level of complexity is based on intuition and should be commensurate with available data available. This is an important point: whenever a model is built, it is based on some preconceived notion underpinning its construction related to the predictions it must make. Decisions regarding many aspects of the construction of that model must, of course, be made for the purpose of enhancing (and certainly not eroding) the model's ability to make that prediction.

Model complexity should be commensurate with the predictions it makes; no processes salient to those predictions should be omitted if the integrity of those predictions would be eroded by their omission. The same thing holds for parameters; no parameter salient to model prediction should be dropped or otherwise lumped into other parameters. Following the principle of parsimony, the dimensionality of the calibration is reduced to a tractable level, perhaps at the expense of compromising prediction validity by draping this simplistic parameterization scheme (based on a relatively small number of parameters) over what are often a set of complex processes. Then, with a certain sense of disquiet, it is assumed that values (that the model must employ for a vast number of parameter types and boundary conditions) have merit only because they are "reasonable." Next, a calibration methodology is defined that requires that the values of only a few parameters (normally defined to encompass considerable portions of the model domain) be estimated on the basis of field measurements. Hence, huge simplifications inevitably compromise a model's ability to estimate reality (e.g., assuming that large areas of the model domain subtended by artificial, rectilinear boundaries are homogeneous or that neighboring nodes within a geological unit possess exactly the same hydraulic properties). The fact that significant heterogeneity exists within a study area is ignored because unique assignment of values to the parameterization associated with this possible heterogeneity is simply beyond the reach of a limited calibration dataset.

Clearly heterogeneity is a foregone conclusion in subsurface formations even if ignoring heterogeneity during model calibration is justified on the basis that parameters pertaining to this heterogeneity cannot be estimated. Unfortunately, it is not equally justifiable that heterogeneity be ignored when the model is used to make a prediction. If a prediction is sensitive to actual system heterogeneity – heterogeneity that, of necessity, "falls between the cracks" of the calibration process – then that prediction may be seriously in error, despite the fact that the model may be "well calibrated" (i.e., a good fit between model outputs and field observations was obtained on the basis of a parameter simple enough to allow unique estimation of parameters, but which possesses just enough complexity to obtain this good fit).

Similar considerations apply to assumptions made for parameters with "fixed values" (e.g., vertical anisotropy). A good fit between model outputs and historical measurements of system state with these parameters fixed at "reasonable" values does not prove that these values are correct because it is quite possible that other reasonable values could also have been provided for these parameters. In fact, it is likely that adjustable parameters assigned "calibrated" values are (to some degree) incorrect to compensate for erroneous values assigned to fixed parameters. Despite the fact that the model may be "well-calibrated," a prediction will be in error if it is

sensitive either to an erroneously assigned fixed parameter, or to any parameter whose value has been misestimated to compensate for the erroneous value assigned to the fixed parameter.

As well as the above conceptual problems, the traditional approach to model calibration is fraught with practical difficulties. For example, parameter zonation will often start with a geological map; however such maps have varying accuracy and varying degrees of hydrogeologic relevance. Even where a map is available, ability to infer the disposition of geological units with depth is often limited. Furthermore, the salience of structural features such as faults or gravel beds (whose existence or whereabouts are estimated) to groundwater and contaminant movement is often difficult to judge. Nevertheless, model calibration is still based on a simplified zonation pattern, often with only a subset of zone-based parameters actually estimated. Hence, one of two things invariably occurs. On the one hand, it may become obvious that the zonation scheme is not properly reflective of subsurface hydraulic property spatial variability due to an inability to obtain a good fit between model outputs and site data. More zones may be needed or zone boundaries may need adjustment – both of which require that subjective and unsatisfying decisions be made on where to place rectilinear zone boundaries, and both inciting the modeler to wonder how sensitive different predictions may be to *ad hoc* decisions to emplace particular boundaries here and not there. On the other hand, where geological data are plentiful, and where groundwater head data are scarce (as is often the case where deep groundwater and contaminant movement is simulated as part of waste disposal and other studies), too many zones may have been introduced to allow unique assignment of parameter values through the calibration process. In this case, the modeler must decide which zones should be eradicated through amalgamation with neighboring zones, and/or which zonal hydraulic properties should be fixed at questionable values. Both of these procedures will effect model predictions, leaving the modeler with the sure knowledge that these predictions are in error. However, ability to assess the possible magnitude of this error is entirely lacking with this approach to parameter definition and estimation.

H3. TWO INESCAPABLE FACTS AND TWO FUNDAMENTAL PRINCIPLES

Some important facts must be acknowledged. And then, taking these as the starting point, an alternative approach to model parameterization and calibration based on these two fundamental principles is developed:

1. If a model is to be "calibrated" then its parameterization must be simplified so that the "inverse problem" (the calibration process) of assigning values to model parameters on the basis of an (often limited) calibration dataset has a unique solution. Traditionally, such simplification is undertaken prior to model calibration through adoption of a simplified parameter scheme as discussed above (e.g., an effective permeability applied to an entire geologic unit). However, as will be described below, other approaches to calibration are needed so that simplifications undertaken during the calibration process itself are far less subjective. Nevertheless, the fact remains that pursuit of the "calibrated model" requires sufficient parameterization simplification to yield a (simplification-dependent) unique set of estimated parameters. Because it is impossible to infer parameterization detail to the same level that hydraulic property detail really exists, the cost of obtaining a calibrated model is therefore a parameter field that *must be* locally in error, even if it is roughly correct in an average sense. See

Moore and Doherty (2006 [DIRS 178403]), and papers cited therein, for a more complete discussion of this topic.

2. Parameter error leads to predictive error. Furthermore, to the extent that a prediction depends on hydraulic property heterogeneity that "falls between the cracks" of the calibration process, the potential magnitude of its error grows. In general, predictions different from those comprising the calibration dataset (e.g., specific discharge predictions and hydraulic head calibration data) are more likely to be in error because they may depend on hydraulic properties that were fixed or grossly averaged over the model domain due to a paucity of information on these properties within the calibration dataset. Unfortunately, this introduces a contradiction because the reason for employing a complex physically based model in the first place is because predictions of just these types (different from the dataset) need to be made (otherwise the prediction would simply be directly measured at the site).

Armed with these facts, two fundamental criteria are defined that can, and should, enlighten the pursuit of a good strategy for model calibration:

1. The calibration process should aim to provide a model with a set of parameters that allows it to make predictions with minimized potential error.

2. The extent of this potential error should be quantified.

An approach to model calibration that goes a long way towards achieving these two fundamental objectives is outlined below.

H4. REGULARIZED INVERSION

"Regularization" is a word that mathematicians use to describe the parameter simplification process necessary to achieve a unique solution to an inverse problem (such as that of model calibration). In general, with fewer available data, more regularization must be undertaken (and hence a greater degree of parameter simplification). Regularization can be implemented using manual parsimonizing methods such as zonal definitions. As demonstrated below, parameter parsimony can also be implemented mathematically such that it is optimized to the calibration dataset and hence extracts maximum information from that dataset. This satisfies the first of the above principles.

The point of departure of calibration methods based on regularized inversion from traditional approaches is that the former are designed for the estimation of many parameters (possibly numbering in the hundreds or even thousands) rather than just a few. Thus we introduce to the model domain a parameterization density that is commensurate with whatever hydrogeological or process complexity that it is necessary for model prediction accuracy. It should be noted that this does not eliminate parameter error (and hence model predictive error) because parameter simplification in one form or another is an unavoidable precursor to model calibration. What it does provide however, is the ability to *quantify* potential parameter and predictive error. Because parameter complexity is not sustainable in a model due to inherent limitations in the calibration dataset, this complexity can be readily reintroduced where predictive "wiggle room"

is tested as part of a predictive error analysis procedure. Thus, the second of the above principles is respected.

Parameters whose values are estimated through regularized inversion can be defined on the basis of a large number of small zones of piecewise constancy, through devices such as pilot points (Doherty 2003 [DIRS 178642], 2004 [DIRS 178643]), through local or global basis functions, through combinations of these, or using other methodologies. The point is that if potential variability of hydraulic properties over a certain area is relevant to a prediction, such variability should be recognized in the model's parameterization (and thus included in the calibration and subsequent predictive error analysis). Inclusion in the calibration process ensures that maximum information is extracted from a calibration dataset; inclusion in the predictive error analysis ensures that the level of potential error associated with important model predictions is quantified. To the extent that simplification is required to achieve a unique solution to the inverse problem, mathematical regularization ensures that the calibration dataset is used optimally. Essentially, this produces "smoothed" or "blurred" parameter fields that are no "smoother" and no more "blurred" than necessary. To the extent that a prediction depends on hydraulic property detail that cannot be represented in these smoothed fields, the effect of smoothing on potential predictive error is quantified. Meanwhile, agonizing decisions such as how to supplement, reduce, or adjust an often artificial rectilinear zonation scheme do not need to be made, thus making calibration a far less subjective process.

Some may complain that the use of so many parameters may lead to "over-fitting" to a calibration dataset, pointing out that a close fit between model outputs and historical measurements can indeed be obtained when many parameters are estimated, but that predictive error may be consequently increased. The reader can be assured that this is easily avoided because regularized inversion, no matter how it is implemented, allows the modeler to vary the extent to which improved model-to-measurement fit is traded against the potential for model predictive error. In fact, because the potential for such error can now be quantified, it can also be minimized once the level of measurement noise and the level of geological heterogeneity are estimated.

H5. REGULARIZATION METHODS

H5.1 GENERAL

A brief description of some regularization methodologies is now presented while a few mathematical details are provided in Section H8. The reader is referred to literature cited herein for more details. Note that all methodologies described herein are available through the PEST suite of software (Watermark Computing 2004 [DIRS 178612]; Doherty 2006 [DIRS 178613]).

Two broad approaches to regularized inversion have been applied to groundwater model calibration: "Tikhonov" and "subspace" methodologies. Each has its advantages and disadvantages; however, certain hybrid schemes are able to combine the strengths of both of these without compromising computational efficiency. Complex models with long run times can be assigned thousands of parameters while their calibration can be achieved within a number of model runs less than twice the number of parameters actually used in the model. Linear and nonlinear predictive error analysis can then be undertaken with similar computational efficiency.

H5.2 TIKHONOV METHODS

Tikhonov regularization is implemented by reformulating the inverse problem of model calibration as a constrained minimization problem. First, a "preferred condition" is defined for all parameters used in the model. This can comprise preferred values for these parameters or preferred relationships between them (e.g., estimated or measured hydraulic property homogeneity). A set of parameter values is sought that achieves a certain (user-specified) level of model-to-measurement fit; this level of fit is set in accord with expected levels of measurement noise. Uniqueness is achieved by finding values for parameters that achieve this fit with minimal departure from the preferred parameter condition. If preferred parameter conditions are sensibly defined on the basis of site characterization studies, a realistic set of parameters is thereby achieved.

H5.3 SUBSPACE METHODS

The use of subspace methods recognizes the fact that most calibration datasets are best equipped to provide unique estimates of combinations of parameters and not individual parameters. Mathematical tools (singular value decomposition) determine what these combinations are and how many such combinations are estimable while inestimable parameter combinations retain their original values. By working with parameter combinations rather than individual parameters (combinations that are orthogonal in parameter space), the dimensionality of the "calibration solution space" (i.e., the number of parameter combinations that are actually estimated) can be optimized in accord with the level of measurement noise. That is, these combinations are assembled to provide optimal "receptacles" for the information content of the calibration dataset. If initial parameter estimates provided to the inversion process are based upon site characterization studies, then the fact that parameter combinations comprising the inestimable "calibration null space" (which is orthogonal to the calibration solution space) remain unchanged during calibration ensures reasonable parameter values in the calibrated model. The optimal dimensionality of the calibration solution and null spaces depends on the level of model-to-measurement fit desired, which should be set in accordance with measurement noise.

H5.4 HYBRID METHODS

There is no reason why both Tikhonov and subspace methods cannot be used in the same regularized calibration process as is done using the "SVD-assist" scheme implemented in PEST (Doherty 2006 [DIRS 178613]). Not only does this scheme combine the strengths of both of these methods; it carries another significant advantage. Through predefinition of estimable parameter combinations (using singular value decomposition or some related methodology), and through maintenance of these combinations through the calibration process as "super parameters," the number of effective parameters is reduced to one comprising the optimal dimensionality of the calibration solution space. The number of model runs required per calibration iteration is thereby reduced to the number of super parameters employed in the inversion process, as derivatives are computed with respect to these super parameters rather than with respect to individual model parameters. As Tonkin and Doherty (2005 [DIRS 178576]) show, the model run efficiency of the calibration process may be increased enormously.

H5.5 DISCUSSION

Regardless of the regularization method used, the advantages of developing many parameters to characterize hydraulic property complexity and heterogeneity over a model domain, rather than just a few parameters, are considerable. The parameter estimation process is free to be maximally responsive to the calibration dataset, introducing heterogeneity to estimated spatial parameter fields where the data suggest that such heterogeneity exists, or producing smooth or uniform parameter fields where there are no data to suggest otherwise. Thus, heterogeneity exists within the calibrated model "where it has to exist" because regularized inversion will introduce heterogeneity only where it is stipulated by the data. However, because model representation of heterogeneity may be considerably smoothed compared to what actually exists, parameter and predictive error may still abound. The question remains: how is predictive error quantified?

But before answering, it is important to point out that regularized inversion based on large numbers of parameters does not preclude the use of zones inspired by geological mapping. In fact, both of these parameterization schemes can comfortably coexist within the same model domain. Regularization allows all known geologic zones to be retained, even if unique estimates of the hydraulic properties associated with each zone cannot be extracted from the calibration dataset. Zones can also be combined with the use of finer scale parameterization devices such as pilot points. Furthermore, during the regularized inversion process (model calibration), heterogeneity can be preferentially introduced at zone boundaries, while the introduction of intrazonal heterogeneity is restricted only to those locations necessitated by the data.

H6. PREDICTIVE ERROR ANALYSIS

Because hydraulic properties in any real-world system are much more complex and heterogeneous than the calibrated model parameter fields that represent them, model parameters cannot help but be locally in error. So, too, will be many model predictions, particularly those that depend on hydraulic property detail. Thus, as has already been discussed, an unavoidable consequence of building and calibrating a model is the introduction of parameter and predictive error with most of this error arising from differences between model and real-world hydraulic property fields. These differences represent the hydraulic property detail that "slips between the cracks" of the calibration process.

Where the number of parameters used in a model is commensurate with potential hydraulic property complexity, predictive error can be quantified. Through site characterization studies, or simply through geological insight, information will always be available on the range of hydraulic properties that may exist within a study site or region, and on the degree of spatial correlation that these properties may show. Sometimes this information may be encapsulated in geostatistical descriptors such as a variogram. Regardless, reasonable estimates of hydraulic property variability can always be made; after all, a geologist will quickly identify aspects of model parameterization that seem unbelievable. These ideas can be approximately encapsulated in a spatial covariance matrix of hydraulic properties, which provides both a brief statistical summary of the innate variably of hydraulic properties in a study area and the likely continuity of these properties. Often, such a matrix can be built easily for most sites. Its approximate nature does not matter because approximation infers uncertainty. High uncertainty infers potentially

high hydraulic property variance, which is justifiably translated into potentially high levels of model predictive uncertainty if hydraulic property details are inestimable through the calibration process and predictions of interest are sensitive to them. Using basic matrix manipulation methods, such a probabilistic description of the "heterogeneity that may exist" within the subsurface, when compared with the "heterogeneity which must exist" as represented by the calibrated model parameter field, allows a probabilistic description of model predictive error to be developed, based on the difference between the two.

Subspace regularization methods provide particularly useful insights into the sources of model predictive error. As already stated, certain combinations of parameters are estimable through the calibration process; however, these estimates are contaminated by measurement noise in the calibration dataset. This is one source of potential predictive error. The other source of error arises from inestimable parameter combinations comprising the calibration null space. Thus, to the extent that a prediction depends on the null space (orthogonal) combinations of parameters, its potential error is in no way decreased during the calibration process. The potential wrongness of model predictions that depends on these parameter combinations is thus a function of the innate variability of system hydraulic properties described by the user-supplied covariance matrix. Total predictive error is computed by combining this term (null space error) with the measurement noise term (see Moore and Doherty 2005 [DIRS 178402] for more details).

Model predictive error analysis is a routine adjunct to regularized inversion using the PEST suite of software. Linear analysis (in which the action of the model on its parameters is approximated by a sensitivity matrix of appropriate dimensions) yields: (1) approximations to true predictive error variance, (2) contributions made by different parameter types to the potential error of key model predictions, and (3) optimization of yet-to-be-acquired data (based on the premise that the best data reduce predictive error variance the most). Such analysis is far superior to methods such as OPR-PPR that ignore the role of extra data in increasing the dimensionality of the calibration solution space, and hence can lead to erroneous conclusions regarding the relative benefits of future site characterization efforts.

Nonlinear predictive error analysis is more computationally expensive than linear analysis, but is more accurate. Moore (2006 [DIRS 178788]) shows how the constrained predictive maximization/minimization methodology of Vecchia and Cooley (1987 [DIRS 178577]) can be extended to the realm of regularized inversion based on large numbers of parameters. Despite the potentially large number of parameters involved in such a maximization/minimization process, it can nevertheless be efficiently undertaken if parameter variation is restricted to a "predictive subspace" encompassing only linear combinations of parameters to which the prediction of interest is most sensitive. Meanwhile, calibration constraints (which ensure that the model remains calibrated) and reality constraints (which ensure that parameters remain realistic) are applied to all model parameters, regardless of whether they belong to the predictive solution or null spaces.

"Calibration-constrained Monte Carlo" analysis is rapidly and cheaply implemented as another adjunct to regularized inversion. Information forthcoming from the regularized inversion process facilitates generation of stochastic parameter fields that minimally affect the calibrated status of a model. By adding these parameter variations to the calibrated parameter field (using precalculated sensitivities to eliminate the need for extra model runs and by correcting for

model-to-measurement misfit incurred by model nonlinearity through minor adjustment of parameter combinations comprising the calibration solution space), a suite of parameter fields that calibrate the model while encompassing the innate complexity of hydraulic property reality is generated. Model predictions made with all fields span the variance of that prediction.

H7. CONCLUSIONS

This appendix outlines the advantages of model calibration through regularized inversion over traditional methodologies based on the use of a small number of parameters in accordance with the "principle of parsimony." In fact, all calibration requires parameter simplification and parsimonizing. However, where regularization is undertaken by mathematical means, such simplification is optimally tuned to the calibration dataset, thus extracting maximum information from that dataset. This results in a calibrated parameter field that is indeed a simplified or smoothed version of reality, but are no simpler and no smoother than necessary. Furthermore, the difference between the heterogeneity that *must* exist to explain the data, and that which *may* exist in accordance with geological considerations, is explicitly accommodated in a predictive error analysis process during the regularized calibration process. As a result of this, the two basic principles of model calibration espoused above are respected (see Section H3).

In addition to its mathematical superiority, regularized inversion has other benefits. In most cases, it is far easier to implement than traditional parameter estimation. A modeler need no longer agonize over whether an artificial parameterization scheme is appropriate or not, or wonder whether it needs to be made more or less parsimonious. Model parameterization is now a far simpler matter, based on the tenet that "if it may affect the prediction, then include it as a parameter" (the same rule that applies to processes simulated by the model). Problems of parameter identifiability simply disappear because irrelevant parameters are combined during regularization. Thus, a modeler can never contrive too many parameters because the complexity of the estimated parameter field will be reduced to the level sustainable by the calibration dataset. Good fits between model outputs and field data can be achieved on the basis of aesthetically pleasing and geologically reasonable parameter fields, unencumbered by artificialities (such as geologically unsupported rectilinear zones arbitrarily emplaced at locations) contrived to lead to a better fit between model outputs and field measurements. Overall, a modeler will be satisfied that data have been treated with respect, and endowed with a worth equal to its cost because maximum information is extracted from it to make predictions whose potential wrongness is minimized.

H8. POST SCRIPTUM: SOME THEORY

H8.1 GENERAL

The purpose of this section is to briefly present some equations that underpin the points raised in a more qualitative manner in the above discussion. For simplicity, model linearity is assumed although extension of this theory to nonlinear systems is found in see many of the references previously cited.

Let the vector, $\mathbf{h}$, represent a set of system state measurements (dataset, e.g., groundwater heads), and let the vector, $\boldsymbol{\varepsilon}$, represent the noise associated with these measurements. Let the matrix, $\mathbf{X}$,

represent the action of the model (under calibration conditions) on a set of parameters **p**. Then, ignoring offsets:

$$\mathbf{h} = \mathbf{X}\mathbf{p} + \boldsymbol{\varepsilon}. \quad \text{(Eq. H-1)}$$

The noise, **ε**, associated with a particular set of measurements cannot be known. However, it is assumed that statistical structure is encapsulated in a known covariance matrix, $C(\boldsymbol{\varepsilon})$.

Let, s (a scalar), represent a model prediction of interest whose sensitivities to model parameters **p** is described by the vector, **y**. Then, for a linear model:

$$s = \mathbf{y}^T\mathbf{p}, \quad \text{(Eq. H-2)}$$

where the superscript T indicates the transpose. If the covariance matrix, $C(\mathbf{p})$, provides a stochastic description of innate parameter variability (taking account of the conditioning provided by direct or indirect measurements of hydraulic properties already available prior to the calibration process), then the variance σ_s^2 of the uncertainty associated with the model prediction, s, is:

$$\sigma_s^2 = \mathbf{y}^T C(\mathbf{p})\mathbf{y}. \quad \text{(Eq. H-3)}$$

Equation H-3 also characterizes the "error variance" of s. For an uncalibrated model, "uncertainty" and "error variance" are equivalent.

H8.2 OVER-DETERMINED PARAMETER ESTIMATION

Suppose that the system represented by **X** is a simple one, requiring only a few parameters for its characterization. Suppose further that these parameters are uniquely estimable on the basis of the calibration dataset comprising **h**. If measurement noise, **ε**, has a Gaussian distribution, then the best estimate, $\underline{\mathbf{p}}$, of the parameter set, **p**, can be computed using the equation:

$$\underline{\mathbf{p}} = \left(\mathbf{X}^T\mathbf{Q}\mathbf{X}\right)^{-1}\mathbf{X}^T\mathbf{Q}\mathbf{h}, \quad \text{(Eq. H-4)}$$

obtained by minimizing the following objective function:

$$\boldsymbol{\Phi} = (\mathbf{h} - \mathbf{X}\mathbf{p})^T\,\mathbf{Q}(\mathbf{h} - \mathbf{X}\mathbf{p}), \quad \text{(Eq. H-5)}$$

where **Q** is:

$$\mathbf{Q} = C^{-1}(\boldsymbol{\varepsilon}). \quad \text{(Eq. H-6)}$$

The prediction, as calculated by the calibrated model, is:

$$\underline{s} = \mathbf{y}^T\underline{\mathbf{p}}. \quad \text{(Eq. H-7)}$$

Model predictive error is thus:

$$s - \underline{s} = \mathbf{y}^T \left(\mathbf{p} - \underline{\mathbf{p}} \right) = \mathbf{y}^T \left[\mathbf{p} - \left(\mathbf{X}^T \mathbf{Q} \mathbf{X} \right)^{-1} \mathbf{X}^T \mathbf{Q} \mathbf{h} \right]. \quad \text{(Eq. H-8)}$$

Substituting Equation H-1 for **h** into Equation H-8 yields:

$$s - \underline{s} = -\mathbf{y}^T \left(\mathbf{X}^T \mathbf{Q} \mathbf{X} \right)^{-1} \mathbf{X}^T \mathbf{Q} \boldsymbol{\varepsilon}, \quad \text{(Eq. H-9)}$$

the variance of which is [recalling Equation H-6]:

$$\sigma^2_{s-\underline{s}} = \mathbf{y}^T \left(\mathbf{X}^T \mathbf{Q} \mathbf{X} \right)^{-1} \mathbf{y}. \quad \text{(Eq. H-10)}$$

In this case too, predictive error and predictive uncertainty are equivalent. Equation H-10 proves that the stochastic distribution of model predictive error (as encapsulated in its variance, $\sigma^2_{s-\underline{s}}$) is ultimately calculable from the stochastic distribution of measurement noise as encapsulated in **Q** through Equation H-6.

H8.3 UNDER-DETERMINED PARAMETER ESTIMATION

Suppose that the $\mathbf{X}^T\mathbf{QX}$ matrix of equation 4 cannot be inverted, or that it is so ill-conditioned that estimates of predictive error variance calculated using Equation H-10 exceed those calculated using Equation H -3. In the former case a generalized inverse of $\mathbf{X}^T\mathbf{QX}$ may be used in Equation H-4 to minimize **Φ** of Equation H-5. Thus:

$$\mathbf{p} = \left(\mathbf{X}^T \mathbf{Q} \mathbf{X} \right)^{-} \mathbf{X}^T \mathbf{Q} \mathbf{h}, \quad \text{(Eq. H-11)}$$

where the "–" rather than "−1" suffix indicates the generalized rather than unique matrix inverse. Because a rank-deficient matrix possesses an infinite number of generalized inverses, it is no longer possible to obtain a unique solution to the inverse problem solely through minimization of **Φ** (thus maximizing model-to-measurement goodness of fit). In fact, in most cases it is not appropriate to minimize this function at all because this will probably result in greater predictive error variance than that calculated using Equation H-3. Hence, definition of a set of "calibrated parameters," **p**, is a more difficult process and it must be undertaken carefully to avoid excessive transferal of measurement noise to the estimated parameter field (and to predictions that depend on it). In fact, as stated in the body of this document, the set of parameters, **p**, that should ideally be selected as the "calibrated parameter set" is that which minimizes the potential error of key model predictions. This will probably differ from the parameter set calculated through Equation H-11, because that parameter set allows a sufficient fit between model outputs and field data. This fit has as much information as possible extracted from calibration dataset, but it is not "over fitted" where estimated parameters and model predictions are not unduly contaminated by measurement noise. Moore and Doherty (2005 [DIRS 178402]) demonstrate how such a parameter set can be calculated.

In general, a calibrated parameter set, **p**, is computed from field measurements, **h**, as:

$$\underline{\mathbf{p}} = \mathbf{G}\mathbf{h}. \quad \text{(Eq. H-12)}$$

The nature of the matrix, **G**, depends on the type of regularization used during model calibration. Use of Tikhonov regularization yields:

$$\mathbf{G} = \left(\mathbf{X}^T\mathbf{Q}\mathbf{X} + \beta^2\mathbf{Z}^T\mathbf{R}\mathbf{Z}\right)^{-1}\mathbf{X}^T\mathbf{Q}, \quad \text{(Eq. H-13)}$$

where **Z** is a matrix of "regularization constraints" on parameter values which collectively stipulate a "preferred parameter condition." **R** is a suitable "regularization weight matrix." The "regularization weight factor," β^2, is calculated during the calibration process as that which leads to a user-specified level of model-to-measurement fit when the calibrated parameter field, **p**, is employed by the model.

When singular value decomposition is used, **G** is given by:

$$\mathbf{G} = \left(\mathbf{V}_1\mathbf{E}_1^{-1}\mathbf{V}^T\right)\mathbf{X}^T\mathbf{Q}, \quad \text{(Eq. H-14)}$$

where $\mathbf{V}_1$ is an orthogonal matrix whose columns are the eigenvectors of the $\mathbf{X}^T\mathbf{Q}\mathbf{X}$ matrix which span the calibration solution space and $\mathbf{E}_1$ is a diagonal matrix whose elements comprise corresponding eigenvalues of $\mathbf{X}^T\mathbf{Q}\mathbf{X}$. The calibration null space is spanned by vectors comprising the columns of another orthogonal matrix $\mathbf{V}_2$ (which is also orthogonal to $\mathbf{V}_1$). Eigenvalues of $\mathbf{X}^T\mathbf{Q}\mathbf{X}$ associated with the $\mathbf{V}_1$ eigenvectors are higher than those associated with the $\mathbf{V}_2$ eigenvectors (many of which can be zero). Ideally, the cutoff point between the two is selected by the user as that for which predictive error variance is reduced to a minimum. Alternatively, it is selected on the basis that model-to-measurement misfit is commensurate with measurement noise.

For hybrid regularization schemes that combine Tikhonov and subspace methods, the equations for **G** are slightly more complex; the reader is referred to *Addendum to the PEST Manual* (Doherty 2006 [DIRS 178613]) for details.

H8.4 MODEL PREDICTIVE ERROR ANALYSIS

Substitution of Equation H-1 into Equation H-12 yields:

$$\mathbf{p} = \mathbf{G}\mathbf{X}\mathbf{p} + \mathbf{G}\boldsymbol{\varepsilon} = \mathbf{R}\mathbf{p} + \mathbf{G}\boldsymbol{\varepsilon}, \quad \text{(Eq. H-15)}$$

where **R** in Equation H-15 is often referred to as the "resolution matrix." If no measurement noise accompanies the calibration dataset, the elements of each row of this matrix represent "averaging weights" through which the individual estimated parameters comprising the elements of **p** are computed from their real-world counterparts comprising the elements of **p**. A "perfect" resolution matrix would be the identity matrix, **I**, because then all model parameters would be equal to the real-world hydraulic properties that they represent. However, where calibration is under-determined, **R** is rank-deficient (a reflection of the fact that the inverse problem of model

calibration is ill-posed), and hence cannot be the identity matrix. The best that can be hoped for is that its diagonal elements dominate other row elements, thereby ensuring that each estimated parameter is more reflective of its real-world counterpart than it is of other model parameters. Unfortunately, off-diagonal elements are often high when calibrating real-world models against real-world datasets. Recall that a calibrated parameter assigned to a point or to an area of limited spatial extent within the domain of a calibrated model is actually a spatial integration of real-world hydraulic properties over a much larger area. Furthermore, this averaging process will often cross parameter boundaries where more than one type of parameter comprises **p**. The averaging process described by the resolution matrix, **R**, is responsible for smoothing of parameter fields assigned to a calibrated model during the regularized inversion process. As discussed previously, parameter simplification through spatial integration of heterogeneous real-world hydraulic properties is also partly responsible for model predictive error. Unfortunately, however, it is an unavoidable consequence of the quest for uniqueness in the calibrated model.

On the basis of Equation H-15, parameter error is described by:

$$\mathbf{p} - \underline{\mathbf{p}} = (\mathbf{I} - \mathbf{R})\mathbf{p} - \mathbf{G}\boldsymbol{\varepsilon}. \quad \text{(Eq. H-16)}$$

Predictive error is then given by:

$$s - \underline{s} = \mathbf{y}^T(\mathbf{p} - \underline{\mathbf{p}}) = \mathbf{y}^T(\mathbf{I} - \mathbf{R})\mathbf{p} - \mathbf{y}^T\mathbf{G}\boldsymbol{\varepsilon}. \quad \text{(Eq. H-17)}$$

Because **p** and **ε** are never known (only $\underline{\mathbf{p}}$, **R**, and **G** are known), model predictive error cannot be known. However, if $C(\mathbf{p})$ and $C(\boldsymbol{\varepsilon})$ are known (or guessed), model predictive error variance can be computed using the equation:

$$\sigma^2_{s-\underline{s}} = \mathbf{y}^T(\mathbf{I} - \mathbf{R})C(\mathbf{p})(\mathbf{I} - \mathbf{R})^T\mathbf{y} + \mathbf{y}^T\mathbf{G}C(\boldsymbol{\varepsilon})\mathbf{G}^T\mathbf{y}. \quad \text{(Eq. H-18)}$$

Equation H-18 forms the basis of linear model predictive error variance analysis. It is apparent that model predictive error is dependent not just on one, but on two stochastic distributions, viz. $C(\boldsymbol{\varepsilon})$, which characterizes measurement noise, and $C(\mathbf{p})$, which characterizes real-world hydraulic property variability. Thus, there are two contributors to model predictive error that arise from 1) differences between hydraulic properties represented in the calibrated model and those that exist in reality, and 2) the fact that parameter estimation takes place on the basis of a dataset contaminated by measurement noise. The first term of Equation H-18 represents the contribution to model predictive error variance made by the calibration null space (anecdotally, this is often the dominant contributor to predictive error), while the second constitutes the contribution to predictive error variance made by the calibration solution space. Note that, as is obvious from Equation H-10, the first term is ignored in traditional model calibration and predictive error analysis.

It is important to note that *a priori* simplification of parameters employed by a model of a complex system, undertaken to formulate an over-determined inverse problem, does not eliminate the first term of Equation H-18 (Moore and Doherty 2006 [DIRS 178403]). Such a process is indeed a form of regularization and, as such, can be ascribed a resolution matrix (normally a less-than-optimal resolution matrix). Strictly speaking, Equation H-10 can only be

used for computation of predictive error variance at study sites where the earth is as simple as the model or when a correction is made to the computed predictive error variance to accommodate a priori regularization undertaken in this manner (Cooley 2004 [DIRS 178650]; Cooley and Christensen 2006 [DIRS 178598]). However, while such a strategy can indeed accommodate the contribution made to potential model predictive error due to parsimonized reality (thus satisfying the second of the precepts outlined in Section H.3), it does not necessarily result in minimization of that potential error (thus violating the first of these precepts).

H8.5 MODEL PREDICTIVE UNCERTAINTY ANALYSIS

Equation Equation H-18 allows computation of "potential model predictive wrongness," that is, the variance of $s - \underline{s}$. Model predictive uncertainty is a slightly different concept, requiring a Bayesian approach for its computation.

Combining Equations H-1 and H-2 into a single equation yields:

$$\begin{bmatrix} s \\ \mathbf{h} \end{bmatrix} = \begin{bmatrix} \mathbf{y}^T & \mathbf{0} \\ \mathbf{X} & \mathbf{I} \end{bmatrix} \begin{bmatrix} \mathbf{p} \\ \boldsymbol{\varepsilon} \end{bmatrix}. \tag{Eq. H-19}$$

Using standard matrix relationships for propagation of covariance:

$$\begin{aligned} C\left(\begin{bmatrix} s \\ \mathbf{h} \end{bmatrix}\right) &= \begin{bmatrix} \mathbf{y}^T & \mathbf{0} \\ \mathbf{X} & \mathbf{I} \end{bmatrix} \begin{bmatrix} C(\mathbf{p}) & \mathbf{0} \\ \mathbf{0} & C(\boldsymbol{\varepsilon}) \end{bmatrix} \begin{bmatrix} \mathbf{y} & \mathbf{X}^T \\ \mathbf{0} & \mathbf{I} \end{bmatrix} \\ &= \begin{bmatrix} \mathbf{y}^T C(\mathbf{p}) \mathbf{y} & \mathbf{y} C(\mathbf{p}) \mathbf{y}^T \\ \mathbf{X} C(\mathbf{p}) \mathbf{y} & \mathbf{X} C(\mathbf{p}) \mathbf{X}^T + C(\boldsymbol{\varepsilon}) \end{bmatrix}. \end{aligned} \tag{Eq. H-20}$$

Now suppose that an arbitrary vector $\mathbf{x}$ is partitioned into two separate vectors $\mathbf{x}_1$ and $\mathbf{x}_2$. That is:

$$\mathbf{x} = \begin{bmatrix} \mathbf{x}_1 \\ \mathbf{x}_2 \end{bmatrix}. \tag{Eq. H-21}$$

Let $C(\mathbf{x})$, the covariance matrix of $\mathbf{x}$, be correspondingly partitioned as:

$$C(\mathbf{x}) = \begin{bmatrix} \mathbf{C}_{11} & \mathbf{C}_{12} \\ \mathbf{C}_{21} & \mathbf{C}_{22} \end{bmatrix}. \tag{Eq. H-22}$$

Suppose further that the elements of $\mathbf{x}_2$ are known. Then, if there is correlation between at least some members of $\mathbf{x}_2$ and some members of $\mathbf{x}_1$ (this resulting in non-null $\mathbf{C}_{12}$ and $\mathbf{C}_{21}$ submatrices), the conditioned $\mathbf{C}_{11}$ matrix $\mathbf{C}_{11}^{'}$ is calculable as:

$$\mathbf{C}_{11}^{'} = \mathbf{C}_{12} - \mathbf{C}_{12}\mathbf{C}_{22}^{-1}\mathbf{C}_{21}, \tag{Eq. H-23}$$

provided **x** has a multi-Gaussian probability distribution. Applying this to Equation H-20, the conditional variance of the prediction *s* given the acquisition of calibration data, **h**, is:

$$\sigma_s^2 = \mathbf{y}^T C(\mathbf{p})\mathbf{y} - \mathbf{y}^T C(\mathbf{p})\mathbf{X}^T \left[\mathbf{X}C(\mathbf{p})\mathbf{X}^T + C(\boldsymbol{\varepsilon})\right]^{-1} \mathbf{X}C(\mathbf{p})\mathbf{y}. \qquad \text{(Eq. H-24)}$$

σ_s^2 of Equation H-24 is the variance of uncertainty of the prediction, *s*. Using methodologies such as those described by Kitanidis (1996 [DIRS 178599]), calibration can be undertaken in such a manner that σ_s^2 and $\sigma_{s-\underline{s}}^2$ are equal (thus ensuring that $\underline{s}$ provides us with a minimum error variance prediction of system behavior). In practice, if regularized inversion is properly undertaken, the difference between σ_s^2 and $\sigma_{s-\underline{s}}^2$ is normally small. Furthermore, where parameter and calibration datasets are large, regularized inversion based on the methods briefly outlined above, are made unconditionally numerically stable and computationally inexpensive, no matter how ill-posed the inverse problem is.

Versions of PEST from 11.1 onwards provide utility software to compute both model predictive error variance and model predictive uncertainty based on Equations H-18 and H-24, respectively.

INTENTIONALLY LEFT BLANK

APPENDIX I
PREDICTIVE ERROR ANALYSIS THROUGH CONSTRAINED PREDICTION MAXIMIZATION/MINIMIZATION

I1 THEORY – OVER DETERMINED CASE

Vecchia and Cooley (1987 [DIRS 178577]) present a method for exploration of the confidence interval of a prediction made by a calibrated model, which accommodates the fact that the relationships between model outputs and parameters may not be linear. The methodology is based on a constrained optimization technique. The prediction of interest is maximized or minimized while parameters are constrained such that the model remains in a calibrated state at a certain confidence level. This confidence level is then equated to the confidence level of the prediction. Confidence is assessed in terms of the rise in the objective function that is incurred through maximizing or minimizing the prediction (and thereby incurring alterations to parameter values such that they no longer minimize that function). The relationship between objective function rise and parameter/predictive confidence interval is assessed in terms of the stochastic distribution that is assumed to pertain to measurement noise, together with a multiplier for this distribution (the so-called "reference variance") that is estimated through the calibration process.

Figure I-1 shows this process schematically. The dashed lines show contours of a prediction as a function of two parameters; let it be supposed that the value of the prediction increases to the upper right of this figure. The full line is a single contour of the objective function. The minimum of this objective function (which defines the values of parameters which calibrate the model) is within this contour. The contour itself defines the value of the objective function at which the model is no longer calibrated at a certain confidence level. The "critical points" A and B define locations in parameter space (and hence parameter values) at which the prediction of interest is minimized and maximized respectively at the same confidence level as that which applies to the contour. The difference between the corresponding model predictions defines the confidence interval of the prediction.

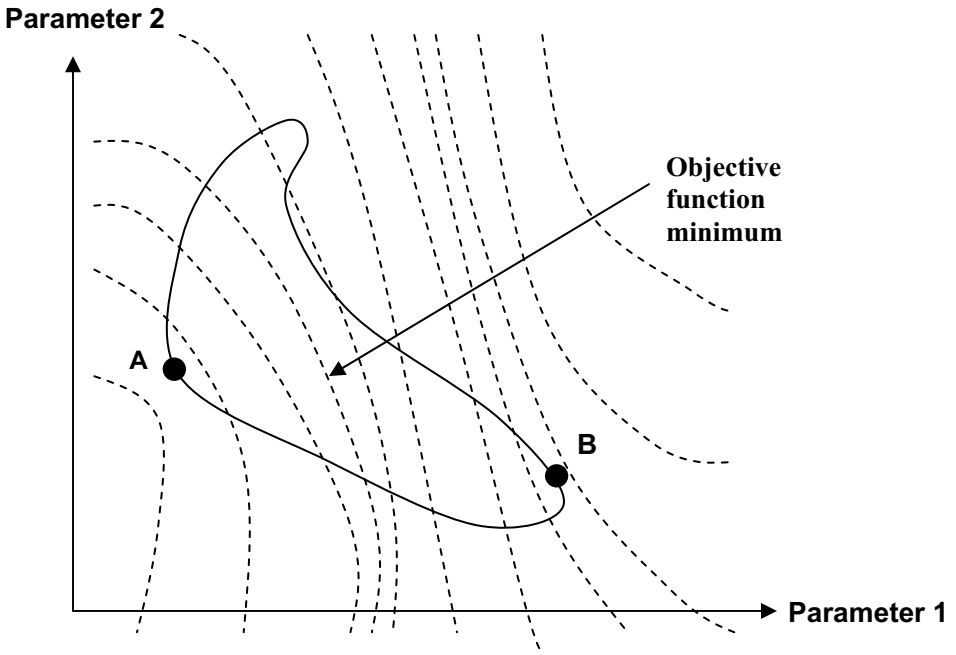

Figure I-1. Points in Parameter Space Corresponding to Maximum/Minimum Values of a Prediction at a Certain Confidence Level

Let δ refer to the difference between the objective function at the contour depicted in Figure I-1 and the minimized objective function. At a confidence level of 1 – α, δ is given by:

$$\delta = m\sigma_r^2 F_\alpha (m, n-m), \quad \text{(Eq. I-25)}$$

where $F(.,.)$ signifies an F distribution, n is the number of observations comprising the calibration dataset and m is the number of parameters being estimated. The reference variance σ_r^2 is given by:

$$\sigma_r^2 = \frac{\Phi_{\min}}{n-m}, \quad \text{(Eq. I-26)}$$

where $\Phi_{\min}$ is the minimized objective function as achieved through the calibration process. The objective function is defined as the sum of weighted squared differences between model outputs and field measurements. Derivation of Equation I-1 assumes that n is reasonably large.

For a linear model, the constrained maximization/minimization problem through which the points A and B of Figure I-1 must be obtained can be formulated as follows.

Find a parameter set **p** such as to maximize (minimize) $\mathbf{y}^T\mathbf{p}$ subject to:

$$(\mathbf{h} - \mathbf{X}\mathbf{p})^T \mathbf{Q} (\mathbf{h} - \mathbf{X}\mathbf{p}) = \Phi_0, \quad \text{(Eq. I-27)}$$

where

$$\Phi_0 = \Phi_{\min} + \delta. \quad \text{(Eq. I-28)}$$

In Equation I-3, **X** is the matrix representing the relationship between model outputs, **h**, and parameters, **p**, under calibration conditions, **y** encapsulates the sensitivity of a prediction s to the parameters **p**, and **Q** is the observation weight matrix, which is assumed to be inversely proportional to the measurement noise covariance matrix C(**ε**). Φ_0 is the objective function pertaining to a certain level of confidence as described by Equation I-1.

It can be shown that the solution to this problem is given by:

$$\mathbf{p} = \left(\mathbf{X}^T\mathbf{Q}\mathbf{X}\right)^{-1}\left(\mathbf{X}^T\mathbf{Q}\mathbf{h} - \frac{\mathbf{y}}{2\lambda}\right), \quad \text{(Eq. I-29)}$$

where λ is defined by:

$$\left(\frac{1}{2\lambda}\right)^2 = \frac{\Phi_0 - \mathbf{h}^T\mathbf{Q}\mathbf{h} + \mathbf{h}^T\mathbf{Q}\mathbf{X}\left(\mathbf{X}^T\mathbf{Q}\mathbf{X}\right)^{-1}\mathbf{X}^T\mathbf{Q}\mathbf{h}}{\mathbf{y}^T\left(\mathbf{X}^T\mathbf{Q}\mathbf{X}\right)^{-1}\mathbf{y}}. \quad \text{(Eq. I-30)}$$

Note that solution of the calibration problem through which parameters corresponding to Φ_{min} are computed, is achieved through an equation of somewhat similar form to Equation I-5, viz.:

$$\mathbf{p} = \left(\mathbf{X}^T\mathbf{Q}\mathbf{X}\right)^{-1}\mathbf{X}^T\mathbf{Q}\mathbf{h}. \quad \text{(Eq. I-31)}$$

When predictive analysis is carried out for a nonlinear model, the same equations are used. However in this case, **X** is replaced by the model Jacobian matrix, **J**, and a parameter upgrade vector is calculated instead of a solution vector. The solution process is then an iterative one in which the true solution is approached by repeated calculation of an upgrade vector based on repeated linearization of the problem through determination of a Jacobian matrix that is updated every iteration. For further details see Vecchia and Cooley (1987 [DIRS 178577]).

I2 UNDER-DETERMINED CASE

Use of the above theory assumes that the inverse problem of model calibration is unique; that is, it assumes that all contours about the minimum of the objective function are closed. Unfortunately, this is not the case for the SZ flow model, where the same objective function can be obtained using many different sets of parameters.

Fortunately, as Doherty (2006 [DIRS 178613]) and Moore (2006 [DIRS 178788]) show, the theory can be extended to the case of under-determined parameter estimation without too much difficulty.

For underdetermined parameter estimation there is no unique solution to Equation I-7. Hence, some form of regularisation must be introduced to the inverse problem. This often takes the form of a subspace method such as truncated singular value decomposition, or a Tikhonov method in which an optimal parameter set is defined as that which departs minimally from a preferred parameter condition. In either case, an optimised parameter set $\underline{\mathbf{p}}$ is computed as:

$$\underline{\mathbf{p}} = \mathbf{G}\mathbf{h}. \quad \text{(Eq. I-32)}$$

Now if the action of the model can be replaced by its linear matrix approximation, **X**, then (assuming zero offsets for simplicity):

$$\mathbf{h} = \mathbf{X}\mathbf{p} + \boldsymbol{\varepsilon}, \quad \text{(Eq. I-33)}$$

where **p** in Equation I-9 signifies the set of "real" system parameter values (can never be known), and **h** is, once again, the calibration dataset.

Thus:

$$\underline{\mathbf{p}} = \mathbf{R}\mathbf{p} + \mathbf{G}\boldsymbol{\varepsilon}, \quad \text{(Eq. I-34)}$$

where **R** is the "resolution matrix." Where noise is zero or minimal, each row of this matrix represents averaging weights through which calibrated parameter values contained in $\underline{\mathbf{p}}$ are obtained as functions of real parameter values contained in **p**. For under-determined inversion, **R** is always a rank-diminished matrix. Its null space defines the subspace of parameter space

from which any parameter realisation can be added or subtracted from the true set of parameters **p**, and that will still result in the same calibrated parameter set **p**. This space spans the "details that fit between the cracks" of the calibration process – these being parameter combinations that it is impossible to infer on the basis of the calibration dataset.

To the extent that a prediction of interest depends on parameter combinations occupying the "calibration solution space" (the orthogonal compliment to the calibration null space), constraints on this prediction are enforced by the fact that the model must remain calibrated. In fact, if a prediction depends only on these parameter combinations, then the above theory for over-determined predictive confidence interval determination could be employed subsequent to parameter reformulated as linear combinations of native model parameters lying entirely within the calibration solution space. Though some account would need to be taken of the fact that any kind of parsimonizing (including the projection of parameters onto the calibration solution space) incurs some degree of structural noise (see, for example, Moore and Doherty 2006 [DIRS 178403]), this could be simply accommodated by appropriate redefinition of measurement weights encapsulated in the **Q** matrix as proportional to the inverse covariance matrix of this noise as shown by Cooley (2004 [DIRS 178650]).

If a prediction is at least partially sensitive to linear combinations of parameters which occupy the calibration null space, the problem becomes a little more difficult, for separate constraints must be employed on these null space parameter combinations as a prediction is maximized or minimized. Suppose that singular value decomposition of the resolution matrix **R** yields:

$$\mathbf{R} = \mathbf{U}\mathbf{S}\mathbf{V}^T. \qquad \text{(Eq. I-35)}$$

Suppose also that the orthogonal matrix, **V**, can be represented as:

$$\mathbf{V} = [\mathbf{V}_1\ \mathbf{V}_2], \qquad \text{(Eq. I-36)}$$

where the columns of $\mathbf{V}_2$ represent orthogonal axes spanning the calibration null space, this corresponding to zero and near-zero values of the diagonal singular value matrix **S**. Define:

$$\begin{aligned} \mathbf{p}_1 &= \mathbf{V}_1\mathbf{V}_1^T\mathbf{p}, \\ \mathbf{p}_2 &= \mathbf{V}_2\mathbf{V}_2^T\mathbf{p}. \end{aligned} \qquad \text{(Eq. I-37)}$$

Then $\mathbf{p}_2$ represents the projection of the (unknown) real-world parameters **p** onto the calibration null space while $\mathbf{p}_1$ represents the projections of these same parameters onto the calibration solution space.

As a prediction is either maximized or minimized to determine its confidence interval, constraints on $\mathbf{p}_1$ are exerted through the necessity for the model to remain calibrated, just as for over-determined parameter estimation. Constraints on $\mathbf{p}_2$ however must be exerted in other ways, for these have no effect on the calibrated status of the model. Constraints on these parameters must, in fact, be "reality constraints;" that is, the parameters must remain realistic at a certain level of confidence. This level of confidence must be assessed in terms of their assumed probability distribution.

Let C(**p**) be a covariance matrix which describes the stochastic character of parameters represented in a model. Diagonal elements of this matrix describe the innate variability of individual parameters; off-diagonal elements described spatial parameter correlation. Based on $\mathbf{p}_2$ in Equation I-13, the stochastic nature of $\mathbf{p}_2$ projections onto the calibration null space can then be described by:

$$\mathrm{C}(\mathbf{p}_2) = \mathbf{V}_2\mathbf{V}_2^T\mathrm{C}(\mathbf{p})\mathbf{V}_2\mathbf{V}_2^T. \qquad \text{(Eq. I-38)}$$

The maximization/minimisation problem through which predictive confidence limits in the over-determined case are computed can now be formulated as follows.

Find a parameter set **p** such as to maximize (minimize) $\mathbf{y}^T\mathbf{p}$ Equation I-14 subject to:

$$(\mathbf{h}-\mathbf{X}\mathbf{p})^T\mathbf{Q}(\mathbf{h}-\mathbf{X}\mathbf{p}) + \mathbf{p}^T\mathbf{V}_2\mathbf{V}_2^T\mathbf{C}_2^{-1}(\mathbf{p})\mathbf{V}_2\mathbf{V}_2^T\mathbf{p} = \Phi_0, \qquad \text{(Eq. I-39)}$$

where Φ_0 is chosen on the basis of a desired level of confidence. The objective function defined by Equation I-15 includes both of the above-mentioned constraints on parameter values, viz. those on calibration solution space projections enforced by the necessity for the model to remain calibrated (the first term), and those on calibration null space parameter projections, enforced by the necessity for parameters to remain realistic (the second term). With definition of this new objective function, maximization/minimization of the prediction *s* can be implemented using the same maximization/minimization algorithm as that described above.

In practice, it is better to work with parameter and model output differences than native parameter values when implementing the above procedure. Thus, **p** now represents differences between parameters obtained through the maximization/minimization process and those which are assumed to calibrate the model in Equation I-8. The objective function under calibration conditions with this new formulation is thus zero. If measurement noise and parameters are assumed to be describable by multi-Gaussian stochastic distributions, and if **Q** is formulated $\mathrm{C}^{-1}(\boldsymbol{\varepsilon})$ (where C(**ε**) is the covariance matrix of measurement noise), values for Φ_0 at different confidence levels are expressible as the square of normal deviates. For example, setting Φ_0 to 4 (square of 2) and maximizing and then minimizing the prediction *s*, results in definition of the 95.4% confidence interval for that prediction.

Approximations employed in this approach include the following:

1. Measurement noise is assumed to be represented by a user-supplied C(**ε**) covariance matrix. In practice most "measurement noise" is actually structural noise. Furthermore, as stated above, some of this structural noise is regularisation-induced. The latter can be computed (using, for example, paired stochastic model runs as described by Cooley (2004 [DIRS 178650]) and accommodated through appropriate definition of **Q**. However, if there are many parameters involved in the parameter estimation process, and if the fit between model outputs and field measurements is reasonably good, it may be possible to ignore the structural component of this term. In the case of the Yucca Mountain model this will probably not be the case. (It must be said, however, that the structural noise term is universally ignored elsewhere, in both general and academic groundwater modelling practice.)

2. The magnitude of structural noise associated with the calibration dataset (whether this be parsimonization-induced or a result of other model inadequacies) is normally assessed through the calibration process using a "reference variance" term. However, the estimation of this quantity has uncertainty associated with it. It is shown in most textbooks on parameter estimation that, even if measurement noise possesses a Gaussian distribution, parameter and predictive probabilities acquire a Student-t distribution for their characterization because of this. This will apply to the first term of Equation I-15 but not the second. Thus, use of the square of a normal variate for the total objective function as a means of assessing confidence will be somewhat in error.